

DOI: 10.31891/2079-1372

THE INTERNATIONAL SCIENTIFIC JOURNAL

***PROBLEMS
OF
TRIBOLOGY***

Volume 30

No 1/115-2025

МІЖНАРОДНИЙ НАУКОВИЙ ЖУРНАЛ

ПРОБЛЕМИ ТРИБОЛОГІЇ

PROBLEMS OF TRIBOLOGY

INTERNATIONAL SCIENTIFIC JOURNAL

Published since 1996, four time a year

Volume 30 No 1/115-2025

Establishers:

Khmelnyskyi National University (Ukraine)
Lublin University of Technology (Poland)

Associated establisher:

Vytautas Magnus University (Lithuania)

Editors:

O. Dykha (Ukraine, Khmelnytskyi), **M. Pashechko** (Poland, Lublin), **J. Padgurskas** (Lithuania, Kaunas)

Editorial board:

V. Aulin (Ukraine, Kropivnitskiy),
B. Bhushan (USA, Ohio),
V. Voitov (Ukraine, Kharkiv),
Hong Liang (USA, Texas),
E. Ciulli (Italy, Pisa),
V. Dvoruk (Ukraine, Kiev),
M. Dzimko (Slovakia, Zilina),
M. Dmitrichenko (Ukraine, Kiev),
L. Dobzhansky (Poland, Gliwice),
J. Zubrzycki (Poland, Lublin),
G. Kalda (Ukraine, Khmelnytskyi),
T. Kalaczynski (Poland, Bydgoszcz),
M. Kindrachuk (Ukraine, Kiev),
Jeng-Haur Horng (Taiwan),
L. Klimenko (Ukraine, Mykolaiv),
K. Lenik (Poland, Lublin),

O. Mikosianchyk (Ukraine, Kiev),
R. Mnatsakanov (Ukraine, Kiev),
J. Musial (Poland, Bydgoszcz),
V. Oleksandrenko (Ukraine, Khmelnytskyi),
M. Opielak (Poland, Lublin),
G. Purcek (Turkey, Karadeniz),
V. Popov (Germany, Berlin),
V. Savulyak (Ukraine, Vinnytsa),
A. Segall (USA, Vancouver),
M. Stechyshyn (Ukraine, Khmelnytskyi),
M. Chernets (Poland, Lublin),
V. Shevelya (Ukraine, Khmelnytskyi),
Zhang Hao (China, Peking),
M. Śniadkowski (Poland, Lublin),
D. Wójcicka-Migasiuk (Poland, Lublin)

Executive secretary: O. Dytynuik

Editorial board address:

International scientific journal "Problems of Tribology",
Khmelnyskyi National University,
Instytutska str. 11, Khmelnytskyi, 29016, Ukraine
phone +380975546925

Indexed: CrossRef, DOAJ, Ulrichsweb, ASCI, Google Scholar, Index Copernicus

E-mail: tribology@khmnu.edu.ua

Internet: <http://tribology.khnu.km.ua>

ПРОБЛЕМИ ТРИБОЛОГІЇ

МІЖНАРОДНИЙ НАУКОВИЙ ЖУРНАЛ

Видається з 1996 р.

Виходить 4 рази на рік

Том 30

№ 1/115-2025

Співзасновники:

Хмельницький національний університет (Україна)
Університет Люблінська Політехніка (Польща)

Асоційований співзасновник:

Університет Вітовта Великого (Литва)

Редактори:

О. Диха (Хмельницький, Україна), М. Пашечко (Люблін, Польща),
Ю. Падгурскас (Каунас, Литва)

Редакційна колегія:

В. Аулін (Україна, Кропивницький),
Б. Бхушан (США, Огайо),
В. Войтов (Україна, Харків),
Хонг Лян (США, Техас),
Е. Чіуллі (Італія, Піза),
В. Дворук (Україна, Київ),
М. Дзимко (Словакія, Жиліна)
М. Дмитриченко (Україна, Київ),
Л. Добжанський (Польща, Глівіце),
Я. Зубжицький (Польща, Люблін),
Г. Калда (Україна, Хмельницький),
Т. Калачинські (Польща, Бидгощ),
М. Кіндрачук (Україна, Київ),
Дженг-Хаур Хорнг (Тайвань),
Л. Клименко (Україна, Миколаїв),
К. Ленік (Польща, Люблін),

О. Микосянчик (Україна, Київ),
Р. Мнацаканов (Україна, Київ),
Я. Мушял (Польща, Бидгощ),
В. Олександренко (Україна, Хмельницький),
М. Опеляк (Польща, Люблін),
Г. Парсек (Турція, Караденіз),
В. Попов (Германія, Берлін),
В. Савуляк (Україна, Вінниця),
А. Сігал (США, Ванкувер),
М. Стечишин (Україна, Хмельницький),
М. Чернець (Польща, Люблін),
В. Шевеля (Україна, Хмельницький)
Чжан Хао (Китай, Пекин),
М. Шнядковський (Польща, Люблін),
Д. Войцицька-Мігасюк (Польща, Люблін),

Відповідальний секретар: О.П. Дитинюк

Адреса редакції:

Україна, 29016, м. Хмельницький, вул. Інститутська 11, к. 4-401
Хмельницький національний університет, редакція журналу "Проблеми трибології"
тел. +380975546925, E-mail: tribology@khmnu.edu.ua

Internet: <http://tribology.khnu.km.ua>

Зареєстровано Міністерством юстиції України

Свідоцтво про держреєстрацію друкованого ЗМІ: Серія КВ № 1917 від 14.03. 1996 р.
(перереєстрація № 24271-1411 ПП від 22.10.2019 року)

Входить до переліку наукових фахових видань України
(Наказ Міністерства освіти і науки України № 612/07.05.19. Категорія Б.)

Індексується в МНБ: CrossRef, DOAJ, Ulrichsweb, ASCI, Google Scholar, Index Copernicus

Рекомендовано до друку рішенням вченої ради ХНУ, протокол № 10 від 13.03.2025 р.

© Редакція журналу "Проблеми трибології (Problems of Tribology)", 2025



CONTENTS

A.H. Dovhal, O.M. Biliakovych, L.B. Pryimak. Lifetime improvement of contact brush units of automotive power machines. Part 1.....	6
R. E. Kostunik, A. L. Maystrenko, A. S. Vasylichuk, D.S. Kustovskyi. Analysis of damage to ceramic balls in hybrid rolling friction pairs.....	12
Yu. Ye. Meshkov, M. S. Dmitriev. Improvement of physical and mechanical characteristics of gearbox shafts using the oxycarbonitriding method.....	23
O. Milanenko, A. Savchuk, O. Kushch, A. Bobro, V. Petrekutsy, O. Vansovskyi. Interrelation of the volume temperature of modified oils and local temperatures in the friction contact zone under extreme operating conditions.....	31
M.S. Stechyshyn, O.V. Dykha, D.V. Zdorenko, E.G. Oleksandrenko. Wear resistance of structural steels carbonitrided by the separate method.....	38
R. M. Marchuk, R. G. Mnatsakanov, O. P. Yashchuk, O. I. Kushch, D. V. Nyshchuk. Influence of tribotesting on microhardness of polymers.....	47
O.V. Dykha, V.O. Dytyniuk, O.S. Kovtun, V.O. Fasolia, M.V. Hetman. Improving the wear resistance of guides: tribological analysis, surface texture and lubricants.....	51
I.V. Morshch. Analysis of the causes of damage to centrifugal pumps during operation and methods of their elimination.....	60
A.M. Krasota, I.V. Shepelenko, M.V. Krasota. Physical and chemical processes in the application of antifriction coatings by the friction-mechanical method.....	66
A. Gupka, I. Yarema, I. Hevko, R. Leshchuk, V. Kobelnyk, V. Buhovets, T. Pyndus. Research on thermoplastics under impact-abrasive wear.....	74
V.V. Shchepetov, N.M. Fialko, S.S. Bys. Tribotechnical properties of coatings based on magnesium compounds.....	85
O.V. Bereziuk, V.I. Savulyak, V.O. Kharzhevskiy, Ye.S. Harbuz. Improved mathematical model of the operation of hydraulic drives of garbage truck mounted sweeping equipment with regard to the wear of a cylindrical brush.....	92
D.D. Marchenko, K.S. Matvyeyeva. Research on the technological process of restoration with electrodiffusion strengthening of the working surfaces of the segments of the headers of combine harvesters.....	100
A.V. Voitov, V.I. D'yakonov, Y.O. Gradiskiy. Selection of informative acoustic emission parameters for determining the wear rate of woodworking equipment in transient modes.....	108
V.V. Aulin, A.A. Tykhyi, O.D. Derkach, S.V. Lysenko, D.O. Makarenko. Strengthening of tribocoupling parts of transport and agricultural machines with fullerene materials.....	116
Rules of the publication	122



ЗМІСТ

Довгаль А. Г., Білякович О. М., Приймак Л. Б. Поліпшення ресурсу контактних щіткових вузлів автомобільних електромашин. Ч.1.....	6
Костюник Р.Є., Майстренко А.Л., Васильчук О.С., Кустовский Д.С. Аналіз пошкоджень керамічних куль в гібридних парах тертя коченню.....	12
Мешков Ю. С., Дмитрієв М. С. Покращення фізико-механічних характеристик валів коробок передач за допомогою методу оксикарбонітування.....	23
Міланенко О., Савчук А., Куц О., Бобро А., Вансовський О. Взаємозв'язок об'ємної температури модифікованих олив і локальних температур у зоні контакту тертя в екстремальних умовах експлуатації.....	31
Стечишин М.С., Диха О.В., Здоренко Д.В., Олександренко Є.Г. Зносостійкість карбоазотованих роздільним способом конструкційних сталей.....	38
Марчук Р.М., Мнацаканов Р.Г., Ящук О.П., Куц О.І., Нищук Д.В. Вплив триботестування на мікротвердість полімерів.....	45
Диха О.В., Дитинюк В.О., Ковтун О.С., Фасоля В.О., Гетьман М.В. Підвищення зносостійкості напрямних: трибологічний аналіз, текстура поверхні та мастильні матеріали.....	51
Морщ І. В. Аналіз причин пошкоджень відцентрових насосів в процесі експлуатації та способи їх усунення.....	60
Красота А.М., Шепеленко І.В., Красота М.В. Фізичні та хімічні процеси при нанесенні антифрикційних покриттів фрикційно-механічним методом.....	66
Гупка А., Ярема І., Гевко І., Лещук Р., Кобельник В., Буховець В., Пиндус Т. Дослідження термопластів при ударно-абразивному зношуванні.....	74
Щепетов В.В., Фіалко Н.М., Бись С.С. Триботехнічні властивості покриттів на основі сполук магнію.....	85
Березюк О.В., Савуляк В.І., Харжевський В.О., Гарбуз Є.С. Удосконалена математична модель роботи гідроприводів навісного підмітального обладнання сміттевоза із урахуванням зносу циліндричної щіткоюююююю.....	92
Марченко Д.Д., Матвєєва К.С. Дослідження технологічного процесу відновлення із електродифузійним зміцненням робочих поверхонь сегментів жаток зернозбиральних комбайнів.....	100
Войтов А.В., Д'яконов В.І., Градиський Ю.О. Вибір інформативних параметрів акустичної емісії для визначення інтенсивності зносу деревообробного обладнання в перехідних режимах.....	108
Аулін В.В., Тихий А.А., Деркач О.Д., Лисенко С.В., Макаренко Д.О. Зміцнення трибоспряження деталей транспортних і сільськогосподарських машин фулероїдними матеріалами.....	116
Вимоги до публікацій	122



Lifetime improvement of contact brush units of automotive power machines. Part 1

A.H. Dovhal*, O.M. Biliakovych, L.B. Pryimak

Kyiv Aviation Institute, Kyiv, Ukraine

*E-mail: andrii.dovhal@npp.nau.edu.ua

Received: 15 November 2024; Revised: 15 December 2024; Accept: 05 January 2025

Abstract

Lifetime improvement of contact brush units of automotive power machines is suggested. Particularities of mass transfer of aluminium electrode on copper substrate is researched. The structure of aluminium electrospark coating on copper substrate is investigated. The fine dispersed eutectic structure with copper-aluminium solid solutions of electrospark coating is detected. This structure is suitable for good coating conductance and well coating adhesion for high speed application under electric current like a contact brush unit of alternators or commutator unit of power starters.

Keywords: AC power machines, alternator, vehicle starter, contact brush unit.

Introduction and review of publications

The automotive electric equipment involves the electric machines (starter, alternator) incorporating the brush unit and hybrid drive vehicles as well. It has the friction joint of conducting copper and graphite brush. Work efficiency and lifetime of these machines strongly depend on the contact quality and general state of this friction joint. Wear products of graphite and copper results in short-circuiting of the starter plated commutator or alternator slip ring thus reducing its performance during the ICE start procedure and battery recharge process. So the wear resistance of these elements is of great importance for proper brush adlining and power power transfer through it as well.

Great interest rose in development and improvement of electric equipment parts made of copper and aluminium. These two metals are used in power equipment, and their chemical interaction is very interested for development of superficial strengthening technique.

Thus in the research [1] the paper presents a study of surface layers produced by electrospark deposition (ESD) using copper electrode on aluminium. The layers were investigated with metallographic methods. Microscopic examination was carried out to examine the structure of formed layers. Image analysis methods were used to observe the cross-section of the layer. For diffusion observations, ESD analyzes were performed on the cross-section of the produced layer. Scanning electron microscope (SEM) and energy-dispersive X-ray spectroscopy (EDX) analysis was conducted to characterize the microstructure and composition of the coating. Also the tribological tests were made on the T-01 M type Ball-on-Disk testing machine. The research carried out for a sliding distance of 1000 m with load 10 N. The results of investigations showed that there is a possibility of obtaining the satisfying quality superficial layer on the aluminium using copper electrode. So these elements are suitable for electrospark coatings of good wear resistance.

The publicaion [2] is about good adhesion of copper to aluminium under electrospark alloying. So, there replacement of ferrous metals with lighter non-ferrous ones, in particular with aluminum and its alloys, is of great importance for reducing the specific material consumption of products. Modification of aluminum alloy D16 with combined electro spark coating VK8 + Cu is considered. Based on the method of finite element analysis of the Nastran software complex, an optimal coating continuity was determined at the level of 55-65%, which provides efficient workability of the coating via reducing the residual stresses in the base and tangent stresses in the plane of adhesive contact, optimization of the coating continuity, distribution of contact loads, and formation of optimal surface geometry. The results of modeling the stress-strain state of the coating-base at a coating continuity of 60% and a normal load of 600 N indicate a 30 MPa increase in equivalent stresses in a unit element of the coating and a decrease of this parameter by 100 MPa in the base as compared with an unmodified D16 surface, indicating the



localization of normal stresses mainly in the combined coating. It was experimentally established that at a combined coating continuity of 60%, reduction of D16 wear by 2 times and decrease in the average power of acoustic emission by 1.33 times are provided, which testifies to the efficient structural adaptability of the coating-base under friction. The mechanisms of increasing the wear resistance of the VK8+Cu coating according to the rheological-kinetic model, which reflects the correlation between processes of fracture and deformation under friction, are considered. It is determined that the high wear resistance of the combined coating is due to the combination of rheological properties of hard alloy VK8 with a fracture toughness of $13.2 \text{ MPa}\cdot\text{m}^{1/2}$ and plastic copper material with a fracture toughness of $100 \text{ MPa}\cdot\text{m}^{1/2}$, which contributes to the efficient relaxation of stresses under friction. So, this research additionally proves good adhesion of discrete electrospark coating of copper to aluminium alloy.

Antifriction alloys are also friendly for copper structure as stated in article [3]. The running-in coatings on the surface of tin bronze that was formed by electro spark alloying (ESA) applying the antifriction material of silver, copper, Babbitt B83 and graphene oxide (GO). The analysis of deposition on mass transfer, roughness, thickness and tribological properties of the running-in coatings were investigated by electronic scales, 3D optical profilometers, scanning electron microscopy (SEM), energy dispersion spectrum (EDS), metallographic microscopy and tribometer. The results show that the running-in coatings are dense, grains refined, uniformly distributed and metallurgical fusion with the substrate. The test results of different running-in coatings were summarized and analyzed, and the best industrial application scheme is determined. The base material, coating material, processing technology and coating technology of bearing bush which affect the product quality are analyzed. A new environmental protection technology of constructing running-in coatings of tin bronze bearing bush is put forward, and the technical design, manufacture, processing, installation and trial operation are described in detail. The industrial application adopts a new electro spark alloying of running-in coating technology on the tin bronze bearing Bush to realize the advantages of good surface comprehensive performance, excellent antifriction performance, strong fatigue resistance, high reliability, good durability. So, the running-in coating can be formed on the surface for better contact properties.

Good adhesion ability of copper bond to Ti and Mo during electrospark alloying is stated in work [4]. The article focuses on the laser treatment impact on strength of electric-spark deposited coatings. The coating microstructure, microhardness, and corrosion resistance are analyzed to evaluate the coating properties. Experiments have been carried out with Mo and Ti coatings deposited onto the substrate of steel 45 followed with a laser fusion treatment carried out in BLS 720 installation with neodymium (ND) glass. So, the electrospark copper coating can be easily mixed with different metal additives for structural improvement.

The structural phase content of copper electrospark coatings was comprehensively studied in research [5]. Antifriction materials, such as silver, copper, Babbitt B83, and graphene oxide (GO), were used to prepare running-in coatings on the surface of bronze QSn10-1 by electro-spark deposition (ESD). The analyses of mass transfer, roughness, thickness, morphology, composition, nanoindentation, and tribological properties of the coatings were investigated. The results showed that the running-in coatings were dense with refined grains that were uniformly distributed and in a metallurgical bond state with the tin bronze substrate. At optimum process parameters, the mass transfer was 244.2 mg, the surface roughness was $15.9 \mu\text{m}$, and the thickness of the layers was $160 \mu\text{m}$. The diffraction peaks clearly indicated the phases corresponding to α -Sn, SbSn, Cu_6Sn_5 , and Cu, and a phase of Ag_3Sn appeared. The modulus and the hardness of the running-in coatings were 24.9% and 14.2% of the substrate, and the deformation ratio of the coatings was 10.2% higher than that of the substrate. The friction coefficient of the running-in coatings was about 0.210 after the running-in stage, which was 64.8% of that of the substrate (0.324). The main wear mechanism of the running-in coatings under optimal process parameters is plastic deformation, scratching, and slight polishing. The running-in coating deformation under the action of high specific loads provides the automatic adjustment of parts and compensation for manufacturing errors. So these coatings will work in the antifriction range.

Copper and aluminium electrospark interaction was comprehensively studied in paper [6]. There the layer-by-layer electrospark deposition of Cu, In, Pb, Cd, and Sn group metals and Ti, V, and W metals, as well as their carbides and hard metals of WC type, onto metallic surfaces is studied. This technique improves the quality and wear resistance of the surface layer compared to coatings without a sublayer. The sintered electrode materials containing 1030 wt.% of the (NiCrSiB)-WC6 alloy allow electrospark coatings with thickness up to $100 \mu\text{m}$ and microhardness 12.3–14.2 GPa to be formed. The wear resistance and service life of these coatings are substantially higher than of those made of standard hard metal WC6. Among the NiCrAl alloys, the best effectiveness in worn-part recovery is shown by the alloy from the ternary eutectic region (50.3 wt.% Ni, 40.2 wt.% Cr, 9.5 wt.% Al), which may provide coating thickness up to 1.0 mm. The novel coating technique and proposed electrode materials increase the resistance of cutting tools and life of equipment parts. So good electrospark adhesion of copper and aluminium additives can improve even hard loaded cutting tools.

The copper alloy electrospark coatings were investigated in research [7]. There was specified about that electrospark deposition (ESD) technology is a new method for repairing and strengthening the surface of metal materials. This method has the advantages of simple equipment, convenient operation and wide application range. The alloyed coating has higher wear resistance, good corrosion resistance, excellent friction performance and other special properties, so it has better practical value and wide application prospect. The paper introduces the characteristics and principle of electro-spark deposition technology, analyzes the research status of this technology

and points out the future development direction of this technology. And there the wear scars of the tin bronze substrate after tribological testing were investigated by scanning electronic microscopy.

Even small content of aluminium provides strong adhesion of electrospark copper coating to titanium, as stated in scientific work [8]. Nowadays, copper-titanium coatings have invited extensive attention of researchers in the surface modification of industrial and biomedical materials due to their excellent mechanical properties and biocompatibility. For the first time, the electrospark deposition technique was used for Cu-Ti coatings deposition on the Ti_6Al_4V alloy by processing in a mixture of copper and titanium granules at a copper concentration from 10 to 90 at.%. It is revealed that both cathode mass gain and coatings thickness rise with the copper concentration increase in the mixture of granules. According to EDS analysis, the copper concentration in the coating linearly grew with a growth of its content in the granule mixture. According to the data of X-ray analysis, intermetallic compounds were found in the structure of the coatings: $CuTi_3$, $CuTi$, Cu_4Ti_3 , and Cu_3Ti . The detected phases provide the coating microhardness up to 6.7 GPa. Polarization tests in 3.5% NaCl solution showed corrosion resistance growth with a copper content decrease in Cu-Ti coatings. The oxidation resistance at a temperature of 900 °C grows with an increasing copper concentration in the coating structure. Cu-enriched sublayer is formed on upper layers of Ti_6Al_4V alloy after Cu-Ti coating oxidation at 900 °C. The wear rate of the coated samples as a function of copper concentration had the form of a parabola with a minimum for the coating made in an equimolar mixture of copper and titanium. The use of electrospark Cu-Ti coatings makes it possible to increase the wear resistance of the Ti_6Al_4V alloy surface up to 11 times.

Copper can be used as sublayer or additive for electrospark deposition of refractory compounds, as stated in paper [9]. In order to improve the lifespan of spot-welding electrodes used for welding zinc coated steel sheets, titanium diboride was deposited onto their surface after precoating nickel as an intermediate layer. The microstructures and phase compositions of TiB_2 and Ni coatings were characterized by SEM and XRD. The coating hardness was measured using a microhardness tester. The results indicate that a satisfactory TiB_2 coating is obtained as a result of the intermediate nickel layer acting as a good binder between the TiB_2 coating and the copper alloy substrate. Owing to its capacity of deforming, the precoated nickel layer is dense and crack free, while cracks and pores are observed in the TiB_2 coating. The hardness of the TiB_2/Ni coating decreases with the increase of voltage and capacitance because of the diffusion of copper and nickel and the oxidation of the coating materials. Because of the good thermal and electrical conductivities and high hardness properties of TiB_2 , the deformation of the electrode with TiB_2/Ni coating is reduced and its spot-welding life is by far prolonged than that of the uncoated one. So the adhesion of electrospark copper additives is sufficient for different applications.

Formerly the electrospark coating on aluminium substrate were researched [10]. The problems of resource extension and recovery of the piston–cylinder parts of internal combustion engines are considered. A method for modelling working conditions of pair ‘groove–ring’ of motors is developed, and durability of aluminium Al-25 alloy with electrospark coatings of different composition paired with a chromium alloyed steel under high-temperature fretting process is carried out. Optimum modes of hardening treatment for piston ring grooves of pistons of internal combustion engines are determined. But the mass transfer during electrospark alloying is about possibility of creation of aluminium coating on copper substrate.

Problem statement and objective

Thus present objective of this study is development of strengthening technique of friction joint of brush unit ‘copper-graphite’ under working current flow and technique. Namely this paper is dedicated for research of coating structure.

Methods

For experimental purposes the samples of M1E electric conductive copper (content: 99,96% Cu, 0,002 Ni, 0,005 Fe, 0,004 S, 0,002 Sn, 0,005 Pb, 0,004 Zn, 0,002 Sb – initial structure of which is indicated on fig. 1.) were fabricated in dimensions of hole disks $16 \times 6 \times 2,5$ mm in order to provide the least friction contact area for experiment acceleration.

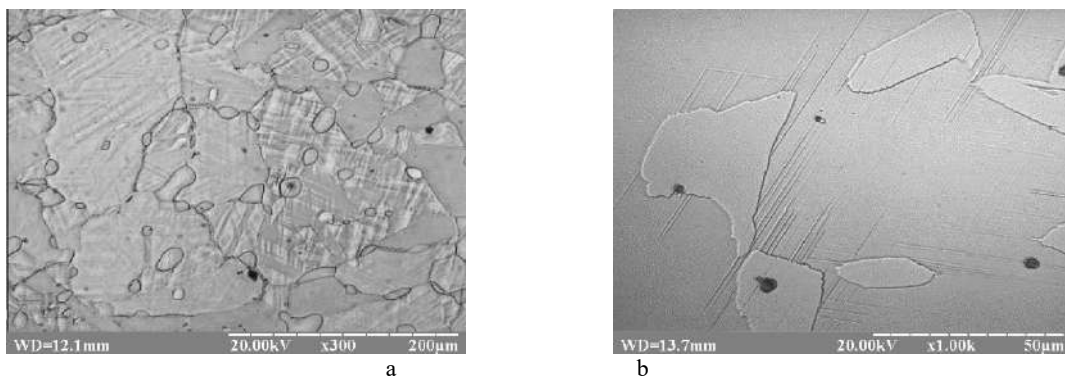


Fig. 1. SEM images of initial structure of electric conductive copper M1E: a) under 300 electronic zoom; b) under 1000 electronic zoom

As the friction counterbody the conventional alternator brush made of graphite ГЭ-1, (contains 0.05% Cu, ash content 10-14 %) was used. Copper samples were strengthened by electro-spark alloying on unit ALIER-52 on 6-7 modes by aluminum electrode made of rod aluminum (АД31Е (1310Е, 6101) containing 97.68% Al, 0,5 % Fe, 0,7% Si, 0,03% Mn, 0,03% Cr, 0,1% Cu, 0,06% B, 0,8% Mg, 0,1% Zn. The 6 mode of ALIER-52 installation provides the following electrospark alloying descriptions: impulse duration was 700 microseconds, amplitude value of current impulse was 200 A; the impulse energy was 2,52 Joiles; coating thickness was 0,3 mm. On the 7th mode the coating appears to be overburnt and dirty by soot and ash, and thus extremely porous. At that the electrode weight change Δa and cathode specimen of 1 cm² area weight change Δc were continuously monitored in a 1 minute period. According to aquired data the kinetic diagrams of electrode weight change was plotted. However the kinetic volume diagrams are more informative, so as the density of copper is twice bigger than aluminium one, so the kinetic volume diagrams were used for coating formation analysis (fig. 2. a). Mass transfer factor ($K_t = (\sum \Delta c / \sum \Delta a) \cdot 100\%$) was calculated as well (fig. 2. b).

Main results

The coating formation kinetics is on fig. 2. This diagram is about that the aluminium electrospark coating is deposited on the 6th mode of installation only in first two minutes (fig. 2., a) than the mass transfer is changing into reverse direction - the copper is transferred on aluminium electrode, so the copper substrate erosion takes place. Mass transfer factor during this time is about 200% (fig. 2. b).

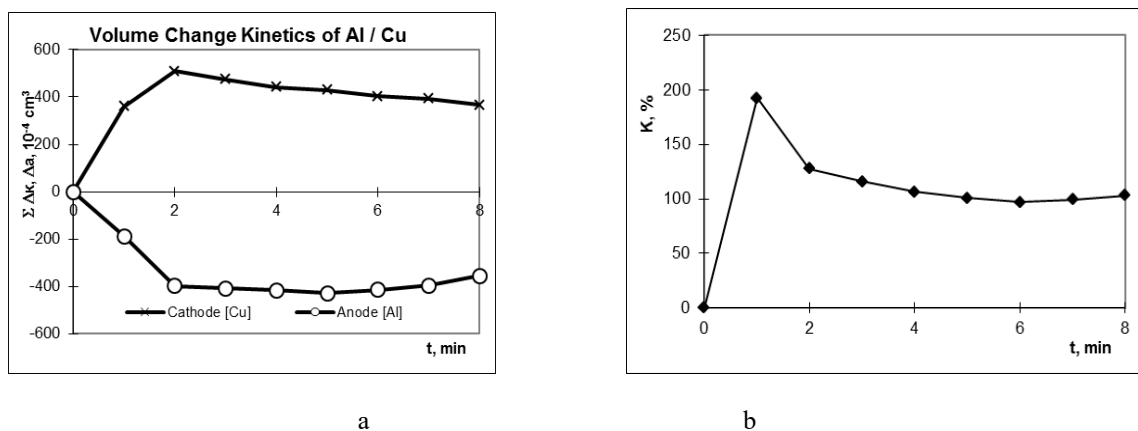


Fig. 2. The volume change kinetics (a) and mass transfer factor (b) of aluminium electrospark coating on copper surface

On preliminary cleaned surface from oxides the electrospark coating has been deposited of thickness 150 micrometers per one cycle of electrospark alloying. Its total thickness is indicated on fig. 3. It is the modified superficial layer of 2-3 millimeters thick.

The coating structure is the matrix with black inclusions of copper oxide and aluminium oxide which will probably weaken the coating strength and worsen its electric conductivity (fig. 3.).

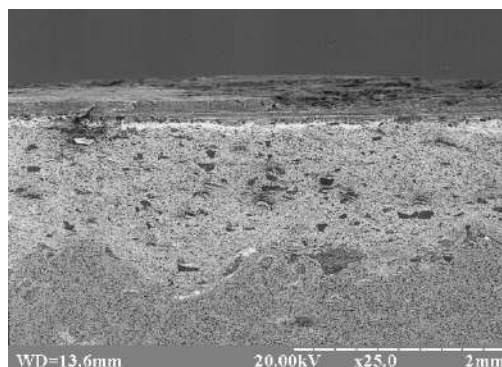


Fig. 3. SEM image of electrospark coating on the electric conductive copper by aluminium electrode under 25 zoom

The strengthening phase (matrix) in copper is the gamma-phase solid solution of aluminum in copper. It is well conductive for current and heat from the surface. Enriching the superficial content of aluminum the delta-phase solid solution of aluminum in copper, which hardness and melting temperature is less and bigger conductivity close to aluminum. Profound electronic microscopic research and X-ray phase research detected these two solid solutions (gamma – is dark grey and delta – is light grey) create the eutectic structure under electrospark fusion as indicated on fig. 4. The black dots on all structures (fig. 1., 3.-4.) are the carbon containing contaminations not relating to research procedure. It was only the lack of samples fabrication.

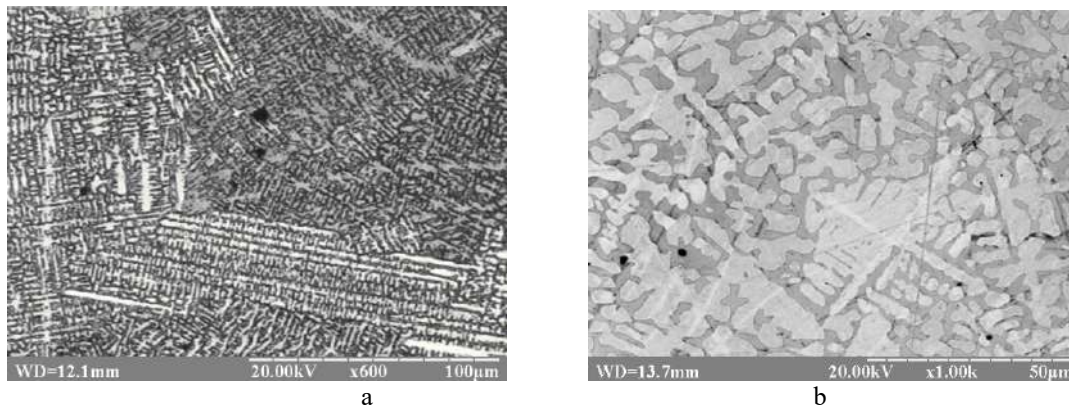


Fig. 4. SEM electronic images of matrix structure of electrospark coating on copper substrate by aluminium electrode: a) under 600 zoom; b) under 1000 zoom

The coated and uncoated samples were tested on the friction test bench M-22ПВ under “pin-on-shaft” layout. Conventional vehicle alternator brush unit has been used in a friction test bench, so the load was equal to brush spring force. Friction speed was about 1,5-2 m/s that complies the test bench shaft rotation speed about 2000-2400 rpm. In order to simulate the brush unit work the 24 V DC voltage was applied to friction contact and linear wear rate was detected. Wear mechanism and friction surfaces will be investigated in following research.

Conclusions

So using electrospark alloying technique the wearproof coating has been acquired with good adhesion to substrate. The structure of this coating is eutectic of gamma-phase solid solution of aluminum in copper and delta-phase solid solution of aluminum in copper. This fine eutectic structure has satisfactory conductivity for power transfer purposes.

Thus the technique researched is suitable and can be recommended for improvement of brush units of vehicle alternators and starters, DC engines collectors for electric power vehicles, hybrid vehicles and quadcopters as well.

References

1. S. Spadlo, P. Młynarczyk Selected Properties of the Micro Electrical Discharge Alloying Process Using Copper Electrode on Aluminum, *Transportation Research Procedia*. 40 (2019) 96–101.
2. T.M.A. Al-Quraan, V.V. Tokaruk, O.A. Mikosianchyk, R.G. Mnatsakanov, N.M. Kichata, N.O. Kuzin Influence of Continuity of Electric Spark Coatings on Wear Resistance of Aluminum Alloy. *Tribology in Industry* Vol. 43, No. 4 (2021) 603-614.
3. Zhang Zhengchuan, Ie. Konoplianchenko, V. Tarelnyk, Liu Guanjun, Du Xin, Ju Yao, Song Zhaoyang Industry Application of the Coatings On the Bearing Bush By Electro Spark Alloying Technology. *Науковий вісник ІФНТУНГ*. No. 1(52) (2022) 15-23.
4. N. Radek, Ju. Shalapko, M. Kowalski Investigations of the Cu-Mo and Cu-Ti electrospark coatings after laser treatment. *Vestnik Dvigatelistroyeniya*. 1 (2009) 143-149.
5. Zhengchuan Zhang, Ie. Konoplianchenko, V. Tarelnyk, Guanjun Liu, Xin Du, Hua Yu The Characterization of Running-In Coatings on the Surface of Tin Bronze by Electro-Spark Deposition Coatings 12. 930. (2022) 1-16.
6. V. B. Tarelnyk, A. V. Paustovskii, Yu. G. Tkachenko, E. V. Konoplianchenko, V. S. Martsynkovskiy, B. Antoszewski Electrode materials for composite and multilayer electrospark-deposited coatings from Ni–Cr and WC–Co alloys and metals *Powder Metallurgy and Metal Ceramics*, Vol. 55, Nos. 9-10, January, 2017. 585-595.
7. Zhang Zhengchuan, Liu Guanjun, Ie. Konoplianchenko, V. Tarelnyk, Ge Zhiqin, Du Xin A Review of the electro-spark deposition technology. *Вісник Сумського національного аграрного університету. Серія «Механізація та автоматизація виробничих процесів»*, випуск 2 (44), (2021). 45-53.
8. Burkov A.A., Chigrin P.G., Dvornik M.I. Characteristics of Cu-Ti electrospark coatings on titanium alloy Ti6Al4V. Preprint research paper. Electronic copy available at: <https://ssrn.com/abstract=4373155>
9. LUO Cheng, XIONG Xiang, DONG Shi-jie TiB₂/Ni coatings on surface of copper alloy electrode prepared by electrospark deposition. *Transaction of Nonferrous Metals Society of China*. 21. (2011). 317-321.
10. M. F. Dmitrichenko, V. V. Varyuhno, A. V. Kulinich, A. G. Dovgal, and V. P. Koba, Extension of Resource of Power-Plants’ Parts of Aviation Ground Equipment under Operating Conditions, *Metallofiz. Noveishie Tekhnol.*, 39, No. 1: (2017) 69–81.

Довгаль А. Г., Білякович О. М., Приймак Л. Б. Поліпшення ресурсу контактнo-щіткових вузлів автомобільних електромашин. Ч.1.

Запропоновано поліпшення ресурсу контактнo-щіткових вузлів автомобільних електромашин. Досліджено особливості масопереносу алюмінієвого електроду на мідну підкладку. Досліджена структура електроіскрових покриттів на мідній підкладці. Виявлена дрібнодисперсна евтектична структура різних твердих розчинів алюмінію у міді електроіскрового покриття. Ця структура придатна для гарної провідності покриття а також хорошої адгезії покриття для високошвидкісного застосування під електричним струмом подібно до контактнo-щіткового вузла генераторів та колекторних вузлів електричних стартерів.

Ключові слова: електромашини змінного струму, генератор, автостартер, контактнo-щітковий вузол.



Analysis of damage to ceramic balls in hybrid rolling friction pairs

R. E. Kostunik¹, A. L. Maystrenko^{2*}, A. S. Vasylychuk², D.S. Kustovskiy²

¹*Kyiv Aviation Institute, Kyiv, Ukraine*

²*V.M. Bakul Institute of Superhard Materials, National Academy of Sciences of Ukraine*

**E-mail: almaystrenko46@gmail.com*

Received: 25 November 2024; Revised: 25 December 2024; Accept: 15 January 2025

Abstract

Most bearings are currently made primarily from steel, but they fail relatively quickly under high loads, temperatures, as well as abrasive, corrosive, chemical and other types of wear. Replacing steel balls with ceramic balls, i.e. creating hybrid bearings, in many cases allows achieving significantly higher performance and expanding the range of functionality of the devices in which they are used. For example, hybrid ball bearings take advantage of ceramic rolling elements with high quality surface treatment of steel rings, which allows for longer service life and better performance at high rotational speeds. As practice shows, hot-pressed silicon nitride (Si_3N_4) is the main material used to create hybrid bearings with ceramic rolling elements, although there is also interest in materials such as boron carbide (B_4C), silicon carbide (SiC) and aluminium oxide (Al_2O_3). However, there are no publications devoted to the analysis of the causes of formation and accumulation of damage to ceramic balls in hybrid rolling friction pairs. Therefore, the aim of the study is to determine the mechanism of formation and development of surface damage in ceramic balls of hybrid rolling friction pairs. As a result of the study, a technological cycle of electric sintering of ceramic ball blanks from Si_3N_4 under high pressure up to 4 GPa was created, which made it possible to compact the monophasic ceramic material to a practically poreless state. The technology of precision diamond processing of ceramic balls with a diameter of 12.7 mm is described. The paper presents the results of tribological tests of a hybrid rolling friction pair " Si_3N_4 ceramic balls - steel SHKH-15". For the first time, the mechanism of damage to the surface layers of ceramic balls in the form of the formation of surface fatigue microcracks, which lead to the formation of pitting and delamination of the surface layer, was investigated. For the first time, Walner lines were found on the pitting surfaces, which proves the fatigue mechanism of their formation and development.

Keywords: Electric sintering of ceramics, silicon nitride, diamond processing of ceramic balls, hybrid ball bearing, fatigue cracks, rolling friction, wear, pitting.

Introduction

Most bearings are currently made primarily of steel, but they fail relatively quickly under high loads, temperatures, as well as abrasive, corrosive, chemical and other types of wear. Replacing steel balls with ceramic balls, i.e. creating hybrid bearings, in many cases allows achieving significantly higher performance and expanding the range of functionality of the devices in which they are used [1-3]. For example, hybrid ball bearings take advantage of the advantages of ceramic rolling elements with high quality surface treatment of steel rings, which allows for longer service life and better performance at high rotational speeds. As practice shows, hot-pressed silicon nitride (Si_3N_4) is the main material used to create hybrid bearings with ceramic rolling elements, although there is also interest in materials such as boron carbide (B_4C), silicon carbide (SiC) and aluminium oxide (Al_2O_3). A number of well-known companies manufacture and operate ceramic or hybrid rolling bearings [1-3]. However, there are no publications devoted to the analysis of the causes of formation and accumulation of damage to ceramic balls in hybrid rolling friction pairs. Therefore, the aim of the study is to determine the mechanism of formation and development of surface damage in ceramic balls of hybrid rolling friction pairs.

Sintering of ceramic materials under high pressure.

The hybrid rolling friction pair under study consists of ceramic balls made of Si_3N_4 and steel rings (counterbodies) made of bearing steel SHKH-15 [4] (analogue of AISI 52100). For wear-resistant ceramic



elements based on silicon nitride in hybrid ball bearings, one of the important requirements is high ceramic density, which is possible only in the absence of residual porosity, so hot pressing, hot isostatic pressing, as well as SPS and its modifications are used for their sintering [5,6]. A number of effective methods have been developed in the field of electric discharge sintering: the SPS (Spark Plasma Sintering) method and its analogue FAST (Field Assisted Sintering Technology), as well as EDS (Electric Discharge Compaction). The rapid heating of the powder briquette is realised by means of a high-frequency pulse discharge and the resulting plasma effect in the spark discharge. The main disadvantages are the relatively low pressing pressure of 100-500 MPa [6,7] and the uneven distribution of electric current in the sintered briquette. In addition, the level of applied pressure during hot pressing in graphite moulds is limited due to the relatively low strength and plastic deformation of graphite components at high temperatures. Typically, the billet is heated during sintering by induction heating of a graphite mould or by passing an electric current through the graphite components of the mould, as well as by resistive heating by passing an electric current of industrial frequency directly through the billet [8-10].

Electric sintering of ceramics under high pressure, which was implemented using the well-known principle of resistive heating of the briquette, but at a much higher pressure [8-10]. As a result of the high pressure and short duration of the sintering process, grain size growth is practically not observed. Due to the fact that ceramic balls made of silicon nitride are loaded in bearings under high contact stresses, we need to obtain a sintered porous billet with a density close to the theoretical one. These conditions can be met by using the process of resistive electro-sintering of ceramic material at high pressure (ESR) [10]. At the Bakul Institute of Materials Science, a high-pressure apparatus for the spontaneous synthesis of superhard materials and electric sintering of ceramic products was developed [9,11], which makes it possible to sinter conductive and non-conductive powder compositions at high pressures (4-8 GPa). In this setup, the sample is pre-pressed into a container made of lithographic stone, loaded with pressure, and an electric current is passed through the sample. The design of the unit allows for the consolidation of ceramic materials at pressures up to 4-5 GPa and temperatures up to 2000°C [9,11]. The proposed method is relatively cheap and simple compared to other alternative existing technologies.

For the manufacture of ceramic balls, silicon nitride powder was used, which was obtained by the method of spontaneously combustion synthesis (SCS). The average size of the initial powder was $\langle D \rangle = 4.8 \mu\text{m}$, and the phase composition was Si_3N_4 1160 - 89%, Si_3N_4 0360 - 9%, SiO_2 - 2%.

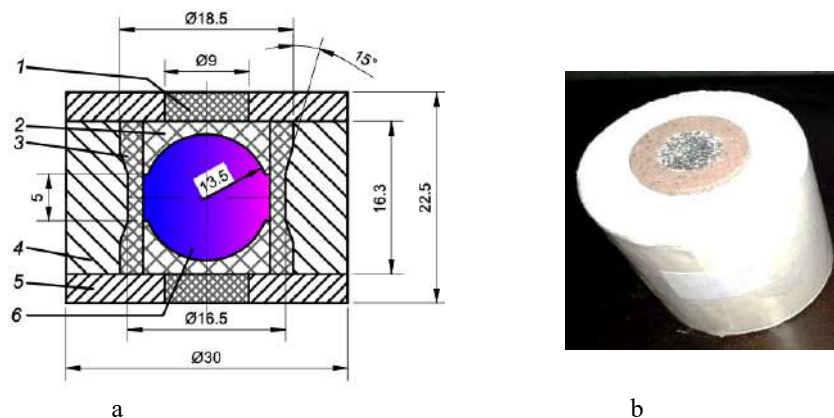


Fig. 1. Schematic of the layout of the reaction vessel for sintering ceramic ball blanks in a high-pressure apparatus: 1 - graphite disc; 2 - graphite moulder; 3 - heater with TRG; 4,5 - container of silicate (pyrophyllite $\text{Al}_2[\text{Si}_4\text{O}_{10}](\text{OH})_2$); 6 - ball blank from Si_3N_4 powder; - (a); general view of the assembled container for sintering ceramic ball blanks from silicon nitride - (b)

For sintering ceramic ball blanks with a diameter of 12.7 mm, a high-pressure apparatus [11] based on a hydraulic press mod. DO-043 with a force of 20 MN and an electronic control system (software unit) for the sintering process.



Fig. 2. General view of sintered ceramic ball blanks

The materials and dimensions of the components of the reaction cell were preliminarily calculated in order to obtain a temperature distribution during billet sintering with a minimum temperature gradient along the diameter [9]. The layout of the reaction vessel for sintering ceramic ball blanks under high pressure is shown in Fig. 1,a. Cold pressing of ceramic ball briquettes was performed in steel moulds under a pressure of 180-200 MPa. After cold briquette pressing, the billets had a diameter of 15.4 mm and a total height of 19 mm. The compressed briquettes were placed in a container of a high-pressure apparatus. The sintering temperature of the billets was 1650°C, the pressure was 4 GPa, and the duration was $\tau = 4$ min. After sintering, the diameter of the billets was reduced to 13.5 mm and their height to 13.44 mm (Fig. 2).

All sintered billets were tested, as a result of which the average values of the ceramic material density, elastic and shear moduli, Poisson's ratio and Vickers hardness (HV) were determined on the basis of a sample of 30 samples - (Table 1).

Table 1
Physical and mechanical properties of Si₃N₄ ceramic balls (ESWT) and steel SHKH-15 used in the study of wear of a hybrid rolling friction pair

Characteristics	Steel SHKH -15 [4] (AISI 52100) [12,13]	Si ₃ N ₄ (ESWT) [14]
Density, g/cm ³ (10 ⁻³ m)	7.812	3.187
Elastic modulus E, GPa	211	289
Shear modulus G, GPa	80	119
Poisson's ratio	0.28	0.26
Critical stress intensity factor K _{1c} , MPa.m ^{1/2}	15.4–18.7	5.0
HV hardness at 20 °C	-	27.4

Manufacturing precision ceramic balls by diamond processing

Samples of precision ceramic balls were made from sintered Si₃N₄ billets (ESWT). At the preliminary stage, the workpieces were ground according to the scheme between two discs, one of which (upper) is a diamond wheel, and on the plane of the second (lower), located eccentrically, freely rotating balls had a circular feed. At the next stage, the precision balls were ground between two discs in a V-shaped annular groove in several stages with a consistent decrease in the diamond slurry grain size from ASM 28/20 to ASM 1/0 [17]. Thus, the test samples of balls with a diameter of 12.7 mm had a deviation from the spherical shape of 0.4 μm and a surface roughness of Ra 0.025 (accuracy class G16 according to ISO 3290-2:2014) [17,18] - Fig. 3.

Evaluation of the surface texture and condition of the near-surface layer of Si₃N₄ ceramic balls after diamond processing

The amplitude parameters Sa, Sq, Sp, Sv, St, Ssk, Sku were chosen to quantify the surface roughness of ceramic balls [18]. The surface topography of the balls was recorded using a non-contact interference 3D profilograph "Micron-alpha" based on an optical microscope II-4 by processing a sequence of interference patterns. The measurement area was 250 × 190 μm. The measurements were repeated 3-5 times in different areas. The calculation of roughness parameters was performed in the software environment "3D Surface Texture Mountains Map". The average values of the amplitude parameters of the surface roughness of Si₃N₄ ceramic balls are given in Table 2.

Table 2
Amplitude parameters of the surface roughness of a Si₃N₄ ceramic ball (ESWT) with a diameter of 12.7 mm after diamond processing

Sa ,mkm	Sq ,mkm	Sp ,mkm	Sv ,mkm	St ,mkm	Ssk	Sku	Sz ,mkm
0.0379	0.0572	0.2827	0.2712	0.5292	0.361	8.5975	0.4787



Fig. 3. General view of ceramic balls with a diameter of 12.7 mm after diamond processing

The manufactured balls were also cut along their diametrical cross-section to analyse the presence of microcracks in the surface layers after diamond processing, which was necessary to determine the subsequent evolution of damage as a result of the operation of the hybrid rolling friction pair. Examination of the near-surface layer of the ball's diameter cross-section using a Carl ZEISS EVO 50 XVP scanning electron microscope showed the absence of microcracks in the near-surface layer of the ceramic ball.

Tribological tests of ceramic balls for wear in a hybrid rolling friction pair

In order to determine the wear resistance of balls in the Si_3N_4 ceramic - SHKH-15 steel system under lubrication with an oil-vapour-gas mixture (TC-1 and MC-8p oil), a rapid test method was developed taking into account the geometric and kinematic parameters of the test assembly on the laboratory device for unidirectional three-point rolling friction KIIGA-1m (Fig. 4) [19,24].

The test assembly of the device simulates the geometry of the contact of rolling friction of balls on a steel support (Fig. 4), which allows simulating the friction processes of a real tribosystem of a deep groove ball bearing. The balls were centred using the standard raceway of the steel bearing ring, and the upper ring was mounted with a flat working surface.

For a comparative assessment of the wear resistance of the model thrust ball bearing and testing of the test methodology, serial balls of ball bearing 8211 (steel SHKH-15 (AISI 52100)) with a diameter of 12.7 mm not lower than the fourth degree of accuracy and prototypes of ceramic balls made of silicon nitride with a diameter of 12.7 mm were used. The initial friction conditions were determined by preliminary tests of serial steel and ceramic balls, namely: engine spindle speed - 1500 rpm; total maximum test time excluding periodic stops (every 15 minutes) to control the wear of the sample material; axial load under dry friction and in lubricant - 490 N; wear criterion for the steel sample - depth of the raceway; wear criterion for the test balls - loss of ball material weight.

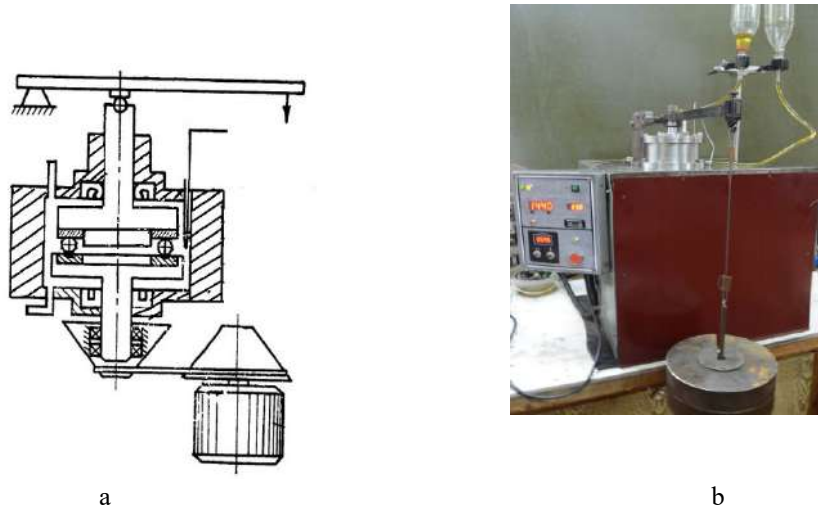


Fig. 4. Scheme of testing a hybrid rolling friction pair [19] - (a); General view of the setup for tribological testing of ceramic balls - (b)

A stationary thrust ball bearing ring 8211 made of steel SHKH -15 was mounted on the holder, with the standard raceway facing outwards. At the bottom of the chamber, namely on its lower surface, a movable sample (lower thrust ball bearing ring, steel SHKH -15) was mounted up the previously finished working surface, on which a separator with test ball samples was installed. After that, the separator was centred relative to the centre of rotation by positioning the balls in accordance with the raceway of the standard ball bearing ring pre-installed on the holder's seating surface. The chamber was filled with lubricant, and the necessary calibrated weights were placed on the lever of the loading system. The total time for the tribological tests was up to 6 hours. The wear rate of the lower steel ring was based on the linear wear of the ball bearing working surface and the weight loss of the test balls measured by profiling.

Determination of the contact pressure in the contact zone between the ball and the steel base

It is known that the wear rate of the friction pair components depends not only on the kinematic operating conditions of the rolling friction unit, but also on the level of contact pressure. For this purpose, the level of contact stresses in the contact area of a ceramic ball with a steel ring groove was estimated (Fig. 5). A ball of radius is located in a cylindrical groove (trough) with radius $r > R$ under a load $P = 490$ N:

$$\frac{1}{R_1} = \frac{1}{R} - \frac{1}{r}, \quad \frac{1}{R_2} = \frac{1}{R}.$$

The X-axis is directed perpendicular to the cylinder face. Due to the fact that the ball is in contact with the surface of the counterbody on a cylindrical surface rather than a plane, the contact patch is elliptical. The line of action of the compressive force is P normal to the elliptical area of the contact patch and passes through its centre.

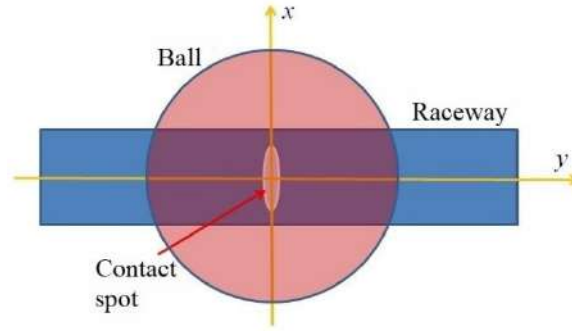


Fig. 5. Diagram of the formation of a contact spot of a ceramic ball on the surface of a groove in a steel support ring

The eccentricity $e = \sqrt{1 - (b/a)^2}$ of the elliptical contact patch with the $a > b$ axes is the solution of the transcendental equation [20]

$$\frac{R_2}{R_1} = \frac{(1 - e^2)[K(e) - E(e)]}{E(e) - (1 - e^2)K(e)},$$

where $K(e)$ and $E(e)$ are complete elliptic integrals of the first and second kind, respectively. A more convenient transcendental equation for analysis with respect to $\chi = a/b$ is:

$$\chi_{n+1} = \left[\frac{R_1 R_D(0, \chi_n^{-3/2}, \chi_n^{1/2})}{R_2 R_D(0, \chi_n^{3/2}, \chi_n^{-1/2})} \right]^{2/3},$$

where $R_D(p, q, r) = \frac{3}{2} \int_0^\infty \frac{dt}{[(t+p)(t+q)(t+r)^3]^{1/2}}$

is the elliptic Carlson integral of the second kind [21]. It is solved by the iteration method [22] with the initial approximation:

$$\chi_0 = \left(\frac{R_1}{R_2} \right)^{2/3}.$$

The semi-axes of the ellipse:

$$a = \left[\frac{PR_1}{\pi E^*} R_D(0, (b/a)^2, 1) \right]^{1/3}, \quad b = \left[\frac{PR_2}{\pi E^*} R_D(0, (a/b)^2, 1) \right]^{1/3},$$

where $E^* = \left(\frac{1 - \nu_1^2}{E_1} + \frac{1 - \nu_2^2}{E_2} \right)^{-1}$.

Pressure distribution over the contact patch:

$$p = \frac{3P}{2\pi ab} \sqrt{1 - \frac{x^2}{a^2} - \frac{y^2}{b^2}}.$$

Pressure in the centre of the spot:

$$p_0 = \frac{3}{2} p_m = \frac{3}{2} \frac{P}{\pi ab},$$

where p_m is the average pressure.

In the contact area along the axis along the axis x ($y = 0$):

$$\frac{\sigma_x}{p_0} = -2\nu\gamma - (1 - 2\nu) \frac{b}{ae^2} \left[\left(1 - \frac{b\gamma}{a} \right) - \frac{x}{ae} \operatorname{arth} \left(\frac{ex}{a + b\gamma} \right) \right],$$

$$\frac{\sigma_y}{p_0} = -2\nu\gamma - (1 - 2\nu) \frac{b}{ae^2} \left[\left(\frac{a\gamma}{b} - 1 \right) + \frac{x}{ae} \operatorname{arth} \left(\frac{ex}{a + b\gamma} \right) \right],$$

where $\gamma = \sqrt{1 - x^2/a^2 - y^2/b^2}$ i $\operatorname{arth}(x) = \frac{1}{2} \ln \left(\frac{1+x}{1-x} \right)$ is the hyperbolic arctangent.

In the centre of the spot we have [23]

$$\frac{\sigma_x}{p_0} = -2\nu - (1 - 2\nu) \frac{b}{a+b}, \quad \frac{\sigma_y}{p_0} = -2\nu - (1 - 2\nu) \frac{a}{a+b}, \quad \frac{\sigma_z}{p_0} = -1.$$

Outside the contact spot, we have only shear stress:

$$\begin{aligned} \frac{\sigma_x}{p_0} &= -2\nu\gamma - (1-2\nu)\frac{b}{ae^2} \left[\left(1 - \frac{b\gamma}{a}\right) - \frac{y}{ae} \operatorname{arctg}\left(\frac{aey}{b(a\gamma+b)}\right) \right], \\ \frac{\sigma_y}{p_0} &= -2\nu\gamma - (1-2\nu)\frac{b}{ae^2} \left[\left(\frac{a\gamma}{b} - 1\right) + \frac{y}{ae} \operatorname{arctg}\left(\frac{aey}{b(a\gamma+b)}\right) \right], \\ \frac{\sigma_x}{p_0} = -\frac{\sigma_y}{p_0} &= -(1-2\nu)\frac{b}{ae^2} \left[1 - \frac{x}{ae} \operatorname{arth}\left(\frac{ex}{a}\right) - \frac{y}{ae} \operatorname{arctg}\left(\frac{aey}{b^2}\right) \right], \\ \frac{\tau_{xy}}{p_0} &= -(1-2\nu)\frac{b}{ae^2} \left[\frac{y}{ae} \operatorname{arth}\left(\frac{ex}{a}\right) - \frac{x}{ae} \operatorname{arctg}\left(\frac{aey}{b^2}\right) \right]. \end{aligned}$$

Table 3

The size of the contact spot and stresses in its centre for groove radii in a steel ring $r = 6.5405$ mm and a ceramic ball $R = 6.35$ mm under a total load $P = 490$ N on 3 balls simultaneously (i.e. 163.3 N each)

r / R	a , mm ($10^{-3} M$)	b , mm ($10^{-3} M$)	S , mm^2 ($10^{-6} M^2$)	p_0 , GPa
1.030	0.655	0.068	0.140	0.714

It is expected that close values of r and R correspond to a larger contact patch and, consequently, a lower stress level. Thus, the contact pressure in the center of the contact patch can reach 0.714 GPa, which is twice the contact fatigue limit for ceramics of this type [15].

Characterization of ceramic ball surfaces after tribological tests

Quantitative analysis of the parameters of the topography of the surfaces of ceramic balls after tribological tests was also carried out using a noncontact interference 3D profiler “Micron-alpha”. The determined average values of the results of calculating the parameters of surface roughness of the spent ceramic balls made of Si_3N_4 are given in Table 4.

Table 4

Parameters of the surface condition of a ceramic ball $\varnothing 12.7$ mm made of Si_3N_4 after tribological tests

S_a , mkm	S_q , mkm	S_p , mkm	S_v , mkm	S_t , mkm	S_{sk}	S_{ku}	S_z , mkm
0.1176	0.1986	0.752	0.9276	1.68	0.2640	4.1740	1.4680

Table 4 shows that due to the friction of a ball in a hybrid rolling pair, damage is formed on its surface, resulting in an increase in its roughness by 3.1 times in the S_a parameter and by 3.37 times in the S_q parameter, which is confirmed by the damage observed in the near-surface layer of balls (Figs. 9-10).

Analysis of the results

Based on the tribological tests performed, the total mass loss of three ceramic and steel balls as a result of their wear when rolling on a steel ring was determined (Fig. 6) and the wear intensity of a flat steel ring (steel SHKH-15) was determined (Fig. 7) [24].

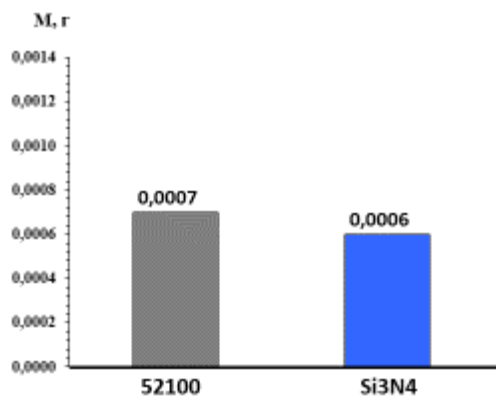


Fig. 6. Total mass loss of three balls made of Si_3N_4 ceramics and SHKH-15 steel under friction under conditions of lubrication with an oil-vapor-gas mixture

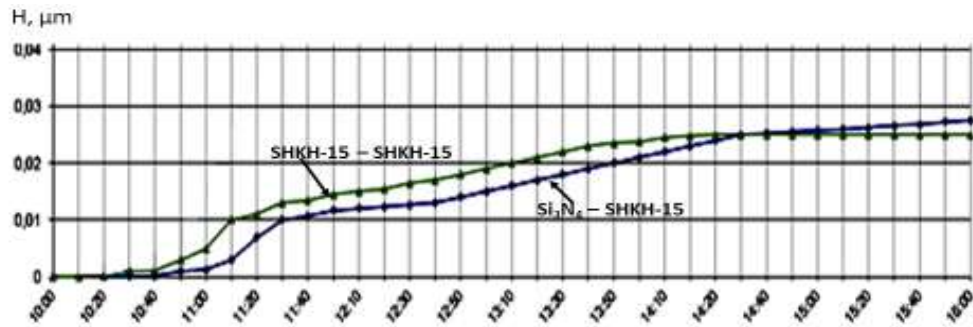


Fig. 7. Graph of wear intensity of a flat sample (steel SHKH-15) over time under rolling friction ceramic and steel balls in an oil-vapor-gas mixture

Analysis of the surface condition of ceramic balls after tribological tests

Pitting corrosion is accompanied by the formation of pits on the surfaces of the friction pair components, which start from the surface. This is a special case of fretting corrosion, which is formed during the cyclic mutual movement of two surfaces in contact. Contact fatigue includes two subcategories: subsurface and surface fatigue. The formation of subsurface fatigue cracks [25] is caused by the cyclic loading of the contacting surfaces, in fact, in the studied case, it is the local cyclic loading of a $\varnothing 12.7$ mm ball with steel rings at a shaft rotation speed of 1500 rpm, i.e., $510 \cdot 10^3$ rpm/h. The number of cycles of contact loading is (at a cycle asymmetry factor of $R=0$), excluding slippage, $1020 \cdot 10^3$ contacts of the ball with the surfaces of the rings, which leads to a change in the material structure and leads to the formation of microcracks. Microcracks are formed in the near-surface layer, often in foreign inclusions in the material, and extend to the surface in the form of chips.

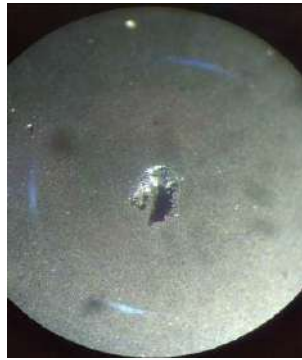
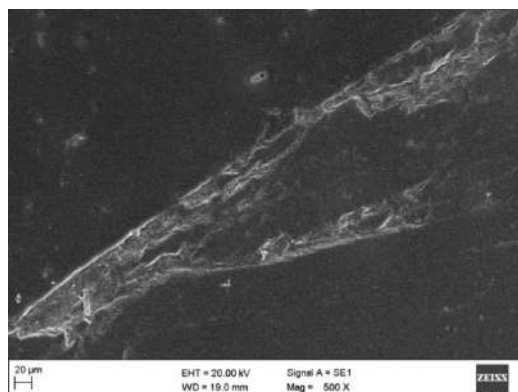
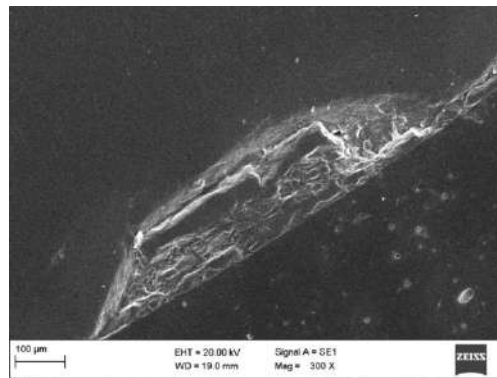


Fig. 8. General view of the pitting formed on the surface of a ceramic ball of Si_3N_4 with a diameter of 12.7 mm after 6 hours of loading in a hybrid rolling friction pair

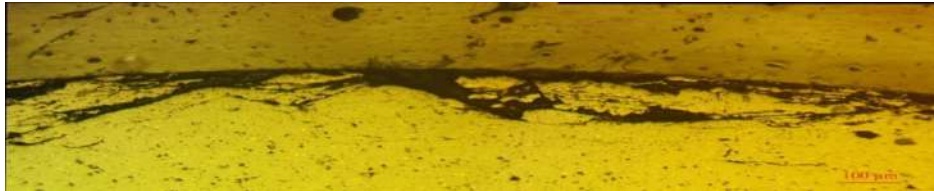
The level of fatigue strength of ceramics of this type reaches the number of load cycles $\leq 10^7$ according to estimates in [15] 350-400 MPa and in [26] 300-450 MPa, which are 2-3 times lower than those in the studied rolling friction pair (see Table 3). That is, this leads to a high probability of the formation of localized cracks of contact fatigue, the signs of which are shown in Fig. 9.

Thus, during cyclic loading of ceramic balls in a hybrid rolling friction pair, as a result of contact fatigue, damage in the form of microcracks is formed and accumulated in the surface layer, which are oriented relative to the contacting surface at an angle of 250-300 (Fig. 9). Their further development leads to the formation of surface pits, i.e., pitting with distinct Wallner curves that reflect the process of fatigue crack propagation (Fig. 10 b, c), according to the kinetic diagram of fatigue crack propagation in Si_3N_4 ceramics [15].



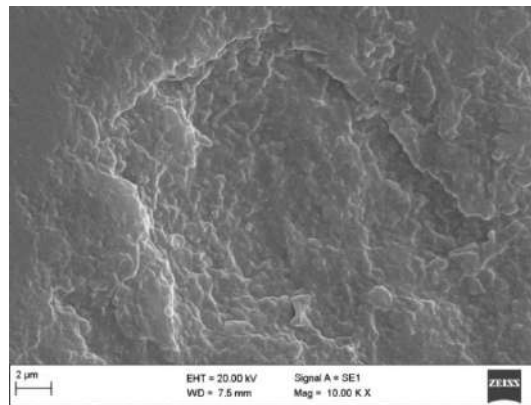


b

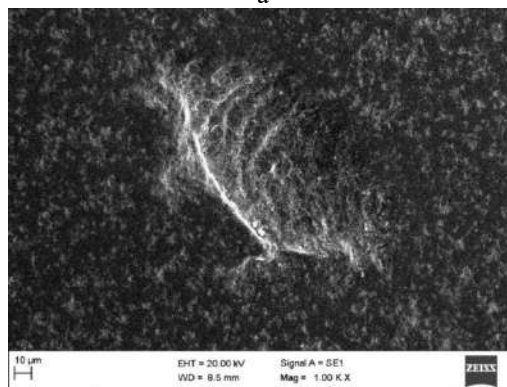


c

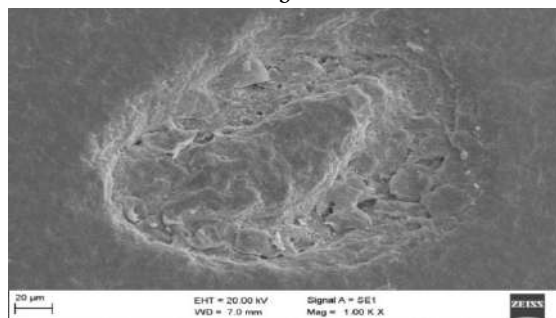
Fig. 9. Damage to the surface layer of the grinded section of a Si₃N₄ ceramic ball as a result of of contact fatigue in a hybrid rolling friction pair



a



b



c

Fig. 10. Pitting on the surfaces of Si₃N₄ ceramic balls

A similar phenomenon of surface damage formation in the form of pitting is also observed on steel rails under the conditions of wheel rolling on the rail surface with a high probability of formation of such defects of contact-fatigue origin [27]. This paper theoretically determines the characteristic angle of formation and propagation of surface cracks in rail heads (10° - 40°), which is the main factor in the formation of typical surface contact-fatigue damage such as pitting. The contact pressure of a stamp (ball or wheel model) on a half-plane is modelled by unidirectional repeated translational movement along the edge of the half-plane of the Hertzian contact forces with a tangential component.

Thus, comparing the values of K_{th} given in Table 5, it becomes clear why pitting occurs in a ceramic ball rather than in a steel ring, since the values of K_{th} for Si_3N_4 ceramics are almost 2 times lower than for steel SHKH-15 (Table 5).

Table 5

Comparative characteristics of the kinetic diagram of fatigue crack propagation in the materials of the studied rolling friction pair

Materials of friction pair	Density ρ , g/cm ³ (10^{-2} M)	Elastic modulus E, GPa	Threshold value of the intensity factor at the beginning of fatigue crack growth K_{th} , MPa.M ^{1/2}	Critical stress intensity factor K_{Ic} , MPa.M ^{1/2}
Si_3N_4 [14-16, 26,28]	3.187	289	2.5 - 3.0	5.0
Steel SHKH-15 [12,13]	7.812	211	5.0 - 6.0	15.4-18.7

Conclusions

For the first time, the possibility of sintering ceramic ball blanks from Si_3N_4 at a pressure of 4 GPa with a density close to the theoretical one was shown. The total mass loss of three Si_3N_4 ceramic balls during tribological tests based on 6 hours in an oil-vapour-gas mixture was 0.0006 mg.

It is shown that the formation and development of surface damage in ceramic balls of hybrid rolling friction pairs is determined by the level of acting contact cyclic stresses, which are the main factor influencing the formation and development of surface fatigue cracks.

For the first time, it is shown that damage to the surface layer of a ceramic ball made of silicon nitride is caused by contact fatigue during cyclic loading of the ball in the process of rolling along the annular groove of the steel counterbody of a hybrid bearing, in the form of delamination and crushing of the surface layer to a depth of 120-150 μ m, resulting in the formation of pitting corrosion pits on the surface of ceramic balls. Moreover, pitting is formed in ceramic balls because the threshold value of the stress intensity factor at the beginning of fatigue crack growth K_{th} in ceramics is 2 times lower than in steel SHKH-15.

References

1. Yoshikiyo Yukawa. Trends and Future Prospects for Rolling Bearing Technologies. Koyo Engineering Journal . English Edition. 2001. No. 159E.
2. Gregory A. Zimmerman. The Sky is the Limit . SKF, Evolution. 2016.
3. Gloeckner P., Rodway C. The Evolution of Reliability and Efficiency of Aerospace Bearing Systems . Engineering. 2017. Vol. 9. - pp. 962–991.
4. GOST 801-78. "Ball-bearing steel. Technical conditions. Moscow. 1978
5. Kislyy, P. / Boron carbide (Kislyy, P. , Kuzenkova, M. , Bodnaruk, N. and Grabchuk, B. Kyiv: Naukova dumka, 1988. - 216 p. (in Russian)
6. Groza J./Sintering activation by external electrical field . Groza J., Zavaliangos A. Materials Science and Engineering A. – 2000. – 287, №2. – pp. 171–177.
7. Salvatore Grasso / Highly Transparent Pure Alumina Fabricated by High-Pressure Spark Plasma Sintering. Salvatore Grasso, Byung-Nam Kim, Chunfeng Hu, Giovanni Maizza, and Yoshio Sakka. J. Am. Ceram. Soc., 93 [9].- 2010.- pp. 2460–2462.
8. Patent Ukraine No. 2064367(RF). Installation for hot pressing of products from high resistive composite materials", Pereyslov, V., Bologova, L., Kulich, L., Simkin, E., Maystrenko, A. 27.07.1996. - № 21.
9. V. A. Dutka / Modeling the Temperature Field in a High-Pressure Apparatus during the Sintering of Large-Sized Products Based on Boron Carbide. V. A. Dutka, A. L. Maystrenko, O. I. Borymskyi, V. G. Kulich and T. O. Kosenchuk . Journal of Superhard Materials. - 2020, Vol.42, No. 4. - pp. 240–250.
10. A. L. Maystrenko./ Electrosintering of ceramic materials . A. L. Maystrenko, O. I. Borymskyi, V. G. Kulich, V. A. Dutka , D.O. Stratiychuk. Kyiv: Naukova dumka. – 2022. - 297 p. (in Ukraine).
11. N. V. Novikov /Steel high pressure apparatus for synthesis of superhard materials . N. V. Novikov, A. I. Prikhna, A. I. Borimsky. High Pressure Research and Industry VIII AIRAPT Conf., Upsala, Aug. 17–22, 1981. – Upsala, 1982. – 2. – pp. 790–792.

12. J.A. Rescalvo Santiago. Fracture and fatigue crack growth in 52100, m-50 and 18-4-1 bearing steels .Submitted in partial fulfillment of the requirements for the degree of doctor of philosophy. Massachusetts Institute of Technology. June 1979. -197 p.
13. Beswick J. M. Fracture and fatigue crack propagation properties of hardened 52100 steel. Metallurgical Transactions A, vol. 20, 1989. - pp. 1961–1973.
14. Maystrenko, A./ Treschinostoykost kristalicheskikh i kompozitsionikh sverkhverdikh materialov. Novikov, N., Maystrenko, A., Physicochemical mechanics of materials (PCMM), 1983.-No4, pp. 46-53. (in russian)
15. Robert O. Ritchie / Cyclic Fatigue of Ceramics: A Fracture Mechanics Approach to Subcritical Crack Growth and Life Prediction . Robert O. Ritchie and Reinhold H. Dauskardt. Journal of The Ceramic Society of Japan . - 99 [10] . -1991. - pp.1047-1062.
16. Mehanika razrushenia i prochnost materialov, V.4. Ustalost i tsiklicheskay reshinosoykost konstruktcionikh materialov. Kyiv. Naukova dumka. 1990. (in russian)
17. Sokhan' S./ Diamond Grinding of Ceramic Balls with a Circular Feed. Voznyi V., Sorochenko V., Hamaniuk M., Journal of Superhard Material.-2023.-vol. 45, No 4. pp. 293–305.
18. ISO 3290-2:2014(en). Rolling bearings - Balls - Part 2: Ceramic balls <https://www.iso.org/obp/ui/ru/#iso:std:iso:3290:-2:ed-2:v1:en>
19. Aksenov A.F. Trenie i iznashivanie metalov v uglevodorodnykh zhidkostyakh [Aksenov A.F. Friction and wear of metals in hydrocarbon liquids. - M.: Mashinostroenie] - 1977. – 152 c. (in russian)
20. Lurie A. I. Prostranstvennyye zadachi teorii uprugosti [Spatial Problems of Theory of Elasticity]. Moscow, Gostekhizdat. -1955.(in russian)
21. Carlson B. C. Computing elliptic integrals by duplication. Numerische Mathematik, 33. - 1979. - pp.1-16.
22. Greenwood J. A. Hertz Theory and Carlson Elliptic Integrals . J. Mech. Phys. Solids, 119 (2018) - pp.240-249.
23. Johnson K. L. Contact Mechanics. Cambridge University Press, 1985.
24. A. L. Maystrenko / Rolling Friction of Hybrid Ceramic–Steel Pairs under Different Lubrication Conditions. A. U. Stelmakh, b, R. E. Kostunik, V. A. Radzievskiy , A. L. Maystrenko, S. V. Sokhan , V. G. Kulich . Journal of Friction and Wear. - 2020, Vol. 41, No. 5, pp. 432–442.
25. ISO 15243 Rolling bearings — Damage and failures — Terms, characteristics and causes Roulements — Détérioration et défaillance — Termes, caractéristiques et causes. – 2017.- Geneva, Switzerland
26. J.K. Tien / Fatigue and Creep Behavior of Si3N4 and SiC for Gas Turbine Applications. J.K. Tien, R. M. Arons , L. Roth. FP-1060 Research Project 271 Final Report, Prepared by Columbia University. Henry Krumb School of Mines Metallurgy Division New York, New York 10027 .- May 1979.
27. O. P. Datsyshyn / Pitting formation during fretting fatigue. O. P. Datsyshyn, O. S. Kalahan, V. M. Kadira, R. B. Shchur Physicochemical Mechanics of Materials. - 2004.-№2. - p.7-19.
28. Carrasquero-Rodríguez Edwuin / Determination of fracture toughness and elastic module in materials based silicon nitride /Carrasquero-Rodríguez Edwuin , Jaime Moisés , Romero-Romero Byron Ramiro , Luis Marcelo . Ingeniería Investigación y tecnología, vol. XX (núm.4), oct.-diciem. 2019: - pp.1-13. <https://.orcid.org/0000-0003-1047-398X>

Костюник Р.Є., Майстренко А.Л., Васильчук О.С., Кустовский Д.С. Аналіз пошкоджень керамічних куль в гібридних парах тертя кочення

Вперше описаний технологічний цикл електроспінання керамічних заготовок куль з Si₃N₄ під високим тиском до 4 ГПа. Описана технологія прецизійної алмазної обробки керамічних куль діаметром 12.7 мм. В статті наведені результати трибологічних випробувань гібридної пари тертя кочення «керамічні кулі Si₃N₄ – сталь 52100». Вперше досліджено механізм пошкодження поверхневих шарів керамічних куль у вигляді формування поверхневих мікротріщин втоми, які приводять до утворення пітінга та відшарування приповерхневого шару. Вперше визначені лінії Вальнера на поверхнях утвореного пітінгу, що доводить втомний механізм їх утворення й розвитку.

Ключові слова: електроспінання кераміки при високому тиску, нітрид кремнію, алмазна обробка керамічних куль, гібридний шарикопідшипник, тертя кочення, зношування, пітінг



Improvement of physical and mechanical characteristics of gearbox shafts using the oxycarbonitriding method

Yu. Ye. Meshkov*, M. S. Dmitriev

Kherson National Technical University, Kherson, Ukraine

**E-mail: mieshkov.yuri@gmail.com*

Received: 15 December 2024; Revised: 10 January 2025; Accept: 30 January 2025

Abstract

The article investigates the issue of promising methods for improving steels by modifying surface layers with the application of protective coatings. Priority areas of scientific research in the field of mechanical engineering have been identified for the development of new methods and technologies for increasing the wear resistance of steel surfaces by applying modified diffusion coatings. It has been shown that the key problem in optimizing the processes of saturation of metals and alloys with one element is cementation, nitriding, alitization, chromium plating, etc. Saturation with two or more elements is used very limitedly. The features of chemical-thermal treatment of steel are considered, with the help of which we have the opportunity to obtain a material characterized by increased characteristics and properties (surface hardness, corrosion resistance, wear resistance). Based on the identified features of coatings in terms of composition, structure, and properties, chemical-thermal treatment methods can be promising when operating them under wear conditions. However, the proposed innovative metallization method – oxycarbonitriding – can compete with these technologically complex processes. It was established that combined chemical-thermal treatment, including nitriding and oxidation, allows to significantly increase the corrosion resistance of the material, the longer the oxycarbonitriding process time, the thicker the oxycarbonitrided layer, but at the same time the absolute deformation value increases, which must be considered when processing precision surfaces. Promising directions for further scientific research in this field are identified.

Key words: modification, surface layers, chemical-thermal treatment, saturation of metals and alloys, diffusion coatings, corrosion resistance, wear resistance.

Introduction

There is no doubt about the prospects for the development of such defining branches of production as mechanical engineering, chemical, radio engineering, space, energy and nuclear engineering. Therefore, today the task of developing new methods and technologies for increasing the wear resistance of steel surfaces by applying modified diffusion coatings remains relevant.

The destruction of machine parts, tools and other products in the vast majority of cases begins with the surface, and it is to the surface layers that the above requirements apply. The reduction in wear resistance leads to billions of dollars in losses annually, and solving this problem is an important task. The main loss is not the loss of metal as such, but the enormous cost of products. That is why the annual losses of industrially developed countries are so large. Real losses cannot be determined by assessing only direct losses, which include the cost of the destroyed structure, the price of changing equipment, and the costs of measures to improve wear resistance. Indirect losses are even greater. This is simple equipment when replacing corroded parts and assemblies, disruption of technological processes.

Economic losses from metal corrosion are enormous. According to estimates of experts from different countries, these losses in industrially developed countries amount to from 2 to 4% of the gross national product. At the same time, metal losses, which include the mass of metal structures, products, and equipment that have failed, amount to from 10 to 20% of annual steel production [1]. In this regard, bulk alloying of alloys is usually uneconomical, and in many cases even impossible due to the almost complete loss of their plasticity and toughness



[1]. Therefore, in recent years, increasing attention of researchers and manufacturers has been paid to various methods of surface hardening. One of the main methods of surface hardening is chemical-thermal treatment.

Problem statement

Currently, the processes of saturation of metals and alloys with one element are quite widely used: cementation, nitriding, alitization, chromium plating, etc. Saturation with two or more elements is used very limitedly. It is quite obvious that multicomponent saturation allows to significantly change the properties of surface layers [1].

Analysis of recent research and publications

One of the most promising methods for improving steels is the modification of surface layers by applying protective coatings. The principle of combining high hardness, wear resistance, corrosion-oxidation resistance and chemical inertness to active environmental reagents with strength and wear resistance is most successfully implemented on 12X18N10T steel and is reflected in many works of modern scientists.

In work [2], a classification of coating methods is given according to the nature of the interaction between the base material being processed and the saturating element, as well as the possibilities of obtaining coatings. Each of the technological methods for coating has its own advantages and disadvantages.

There is a significant number of scientific works on the classification of chemical-thermal treatment. Thus, in work [3], an overview of existing methods of combined strengthening treatment of steel machine parts is given, the main methods of combined treatment of structural and tool steels are considered.

Chemical-thermal treatment is based on solid-phase, liquid-phase and gas-phase saturation of the surfaces of parts. Diffusing elements can saturate the surface of the part directly, without intermediate reactions, with a preliminary chemical reaction at the interface of the processed material and the coating or in the volume of the starting reagents. chemical-thermal treatment can be implemented by saturating nickel and nickel alloys with both metals and nonmetals. As a result, diffusion coatings are formed. The rate of formation, kinetics of coating growth, its structure and properties are largely determined by the process temperature, saturation time, diffusion parameters of the saturating components in the material and, finally, significantly depend on the chemical composition, structure and properties of the latter. During chemical-thermal treatment, the change in the chemical and phase composition, structure and properties of the surface layers is carried out at elevated temperatures.

The following processes occur in this case [3]:

- formation of active atoms of saturating elements and their transfer to the processed surface;
- adsorption (chemisorption) of active atoms by the processed surface;
- diffusion movement of adsorbed atoms into the product and the resulting diffusion redistribution of elements of the base alloy.

Diffusion saturation of the surface zones of nickel and nickel alloys with metals and nonmetals leads to the formation of coatings consisting either of solid solutions of saturating elements in the original alloys, or of chemical compounds. Due to this, it becomes possible to obtain protective coatings on the surface of products with different composition and operational properties. The optimal choice of a saturating element for a particular base material provides a high level of adhesion, practically unattainable with other types of processing (plasma, gas-thermal). Diffusion coatings during HTO are applied, as a rule, under isothermal conditions in artificially created saturating environments.

As noted in many works [4-7], chemical-thermal treatment of steel is of certain scientific and practical interest. As a result of this treatment, we have the opportunity to obtain a material characterized by increased characteristics and properties (surface hardness, corrosion resistance, wear resistance). It has been established that during titanization of samples from annealed steel 12X18H10T, multilayer coatings of Fe_2Ti , $\text{Ti}_4\text{Fe}_2\text{O}$, TiN , TiC are formed [5]. In addition, it has been shown that the TiN layer acts as a barrier, significantly reduces the content of iron, nickel and chromium in the coating, and also significantly inhibits the diffusion of titanium and aluminum into the base. The microhardness of TiN layers in complex compounds is 20.5...23.0, and the diffusion zone of the compounds is 5.5...12.5 GPa. The researchers concluded that, in terms of composition, structure, and properties, titanizing of 12X18H10T steel can be recommended for use as heat- and corrosion-resistant, antifriction [6].

Preliminary nitriding of 12X18H10T steel also has positive results. It was established [7] that as a result of titanizing of pre-nitrided steel, a multilayer coating with the participation of Fe_2Ti , $\text{Ti}_4\text{Fe}_2\text{O}$, TiN , CrN compounds is formed on the treated surface. The results of the work confirm the prospects of using titanizing and nitriding when operating under high temperatures, aggressive environments, and harsh friction conditions [7].

Complex saturation of 12X18H10T steel with chromium and titanium was implemented under reduced pressure [7]. The possibility of forming a chromium-alloyed coating with a barrier layer based on titanium nitride TiN on 12X18H10T steel is shown, the presence of which causes a decrease in the concentration of iron and titanium on the outer side of the coating, an increase in the concentration of aluminum, a decrease in the thickness of the zone of compounds and solid aluminum solution in the base.

Boration of 12Kh18N10T steel is considered in [8]. The introduction of copper or its alloys into the composition of the saturating powder media makes it possible to intensify the boration of 12X18H10T steel without deteriorating the operational properties of boride coatings while simultaneously reducing their fragility.

Single-component chromium plating of 12X18H10T steel [8] is implemented for products operating under friction conditions. In order to increase the saturation rate and wear resistance, copper powder was added to the composition of the carburizer.

Presentation of the main material

Thus, known methods of applying multicomponent coatings in terms of composition, structure, and properties can be promising when used in wear conditions. However, the proposed innovative metallization method - oxycarbonitriding can be a worthy competitor to these technologically complex processes.

More details about the surface hardening method "oxycarbonitriding" and the processes that occur in the metal can be found in well-known scientific studies. First of all, this method can be compared with long-known surface treatment methods, such as: nitriding and carbonitriding. These methods and their combinations are increasingly gaining popularity in the areas of restoration and improvement of wear resistance, by changing surface layers with minimal changes in size, while providing the material with resistance to corrosion and wear with insignificant roughness values.

In work [9], the change in the size of parts during various types of chemical-thermal treatment is investigated, how the environment and temperature affect the process of surface saturation with carbon. Fig. 1 shows the difference in hardness.

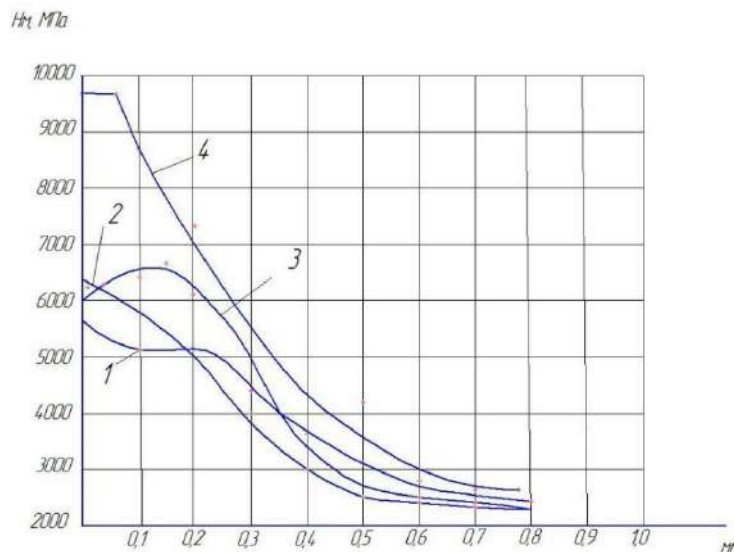


Fig. 1. Microhardness of restored parts by different methods of chemical-thermal treatment. 1) nitriding; 2) carbonitriding; 3) oxynitriding; 4) rotary chrome plating.

Processing of parts by oxycarbonitriding (Fig. 1, curve 3) was performed at temperature regimes of 590 – 610°C and provides sufficient microhardness of surface layers at a depth of 0.1-0.2mm, which is 6370-6770MPa, and the total depth of the hardened layer varies within 0.25-0.35mm. The recorded changes in the dimensions of the parts of the plunger pairs of fuel pumps are 20-45µm, which is an advantage for high-precision parts that have worn out and lost their working dimensions.

More details about oxycarbonitriding are given in [10]. The author, using foreign literature and various methods of carrying out the selected process, highlights their positive aspects, which are combined into one process, and positively affects the corrosion resistance index and the friction coefficient, which under different loads is a constant value and is within the limits of $0.03 < f < 0.004$ after 40 hours of operation.

According to electrochemical studies conducted by Ebersbach and co-authors [11], nitriding in a gas environment leads to a 10-fold reduction in the corrosion rate in a sodium chloride solution (concentration 0.9M). Additional oxidation of the nitrided layer provides an even more significant effect, reducing the corrosion rate by two orders of magnitude, additionally reducing the rate of through corrosion by hundreds of times.

When nitriding iron in ammonia, the formation of a diffusion layer occurs in accordance with the phase diagram of the iron-nitrogen system (Fe-N). This diagram shows the dependence of the phase states of iron on the nitrogen content and temperature, which allows us to determine the conditions for the formation of iron nitrides (such as ϵ -Fe₂-3N and γ '-Fe₄N). Typically, the process occurs at elevated temperatures in an ammonia environment, where ammonia dissociates, releasing atomic nitrogen, which penetrates the metal. This process improves the hardness, wear resistance and corrosion resistance of the material due to the formation of a strengthened diffusion layer. The formation of oxynitride surface layers is carried out by oxidation of nitride layers. In the temperature range 450–700°C, the affinity of metals for oxygen significantly exceeds their affinity for nitrogen.

This causes exchange reactions during the oxidation of nitrided layers, when oxygen partially replaces nitrogen in the surface nitride layer.

Thermodynamic calculations confirm this: iron nitrides interact with oxygen more actively than pure iron. For example, the isobaric-isothermal potential of the oxide formation reaction at 500°C is 209–293 kJ/mol for Fe, and 878–1463 kJ/mol for Fe₄N.

It is important that the high affinity of nitrides for oxygen ensures the formation of optimal oxide structures. In nitrides, the solubility of oxygen is three orders of magnitude higher than in pure iron (at 700°C – 3% versus 0.009% for α -Fe), which contributes to the formation of oxides of the first type, which are solid solutions of oxygen. Oxynitride zones have greater plasticity than Fe₂O₃ oxide films, and at the same time demonstrate similar anti-adhesive properties. As Mittermeyer and Collin [12] established, further oxidation of nitrided surfaces contributes to filling the pores of the α -phase with oxygen. Combined chemical-thermal treatment, which includes nitriding and oxidation, allows to significantly increase the corrosion resistance of the material.

Previously, to carry out the process of improving the working surfaces of gearbox shafts, samples from steel 35XIT DSTU 7806:2015 identical to the part were used. To understand how the microstructure of the metal changed after the heat treatment process, it was decided to first consider the structure before the chemical-thermal treatment. To begin with, microsections were made from the prepared samples, an example of which is shown in Fig. 2.

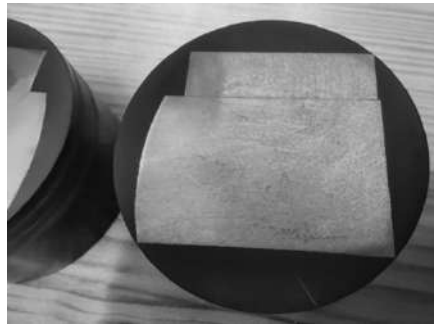


Fig. 2. Photo of a manufactured and prepared microsection of 35XIT steel

The placement of samples in the microsection is chosen in such a way as to be able to study the microstructure of the longitudinal or cross-section. Where the larger piece is the cross-section, and the smaller and narrow piece is the longitudinal. The section of samples for microsections is necessarily performed by cold methods without exceeding the temperature of critical points to preserve the structure, for example, water jet or saw cutting with cooling. Fig. 3 shows the microstructure of steel before the oxycarbonitriding process at a magnification of $\times 100$ in the longitudinal section. The microstructure of steels before heat treatment ideally consists of ferrite and pearlite. But in practice, the ideal structure cannot be achieved due to foundry production technologies and equipment. In 35XIT steels, ferrite has the form of a mesh, the thickness of which in different batches may not differ significantly. Based on practice, the finer the mesh, the worse the processing and roughness. Also, inclusions are observed in the steel, previously it is residual unformed ferrite, in the form of clusters that have a hardness of 332 HV, and in general the hardness of this steel does not exceed 202 HV. The samples show a ferrite-pearlitic structure, a uniform distribution of the ferrite mesh with occasional enlargements of pearlite cells. The measured pearlite to ferrite ratio is 65:35 and there is a reduction in ferrite in the ratio of 75:25 according to DSTU 8233-56. The size of pearlite grains is on average 60-80 μm , and with uniform enlarged grains 150-200 μm .

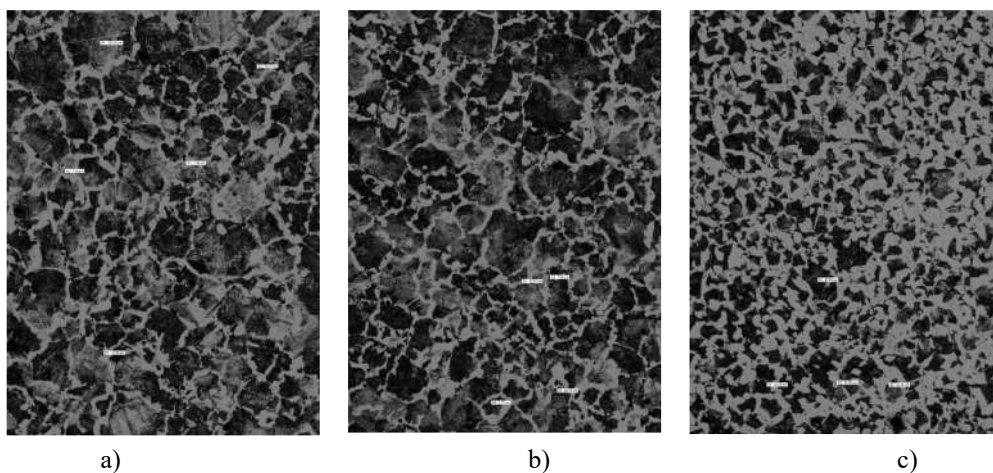


Fig. 3. View of the microstructure of the samples in cross section

When examining the microstructure, a certain regularity of the appearance of the microstructure was noticed, which consists in the fact that an increased amount of ferrite (light mesh) is located along the edge of the rolling roller along the entire length. So, in Fig. 3a and 3b, the structure of the central region is shown, and in Fig.

3c - closer to the edges. When studying the microstructure of longitudinal section samples, sulfide inclusions were found, which accumulate in the form of stripes along the length of the rolled product. In a vertical section, the inclusions have a round shape. These inclusions are poorly visible, so it is necessary to focus the microscope lens below the pearlite grains and ferrite mesh, because they are etched deeper. Therefore, for objective vision, it is necessary to adjust the focus specifically for these inclusions, as shown in Figs 3a; 3b. It was also found that sulfide inclusions are etched faster than the base metal. To check for inclusions in a particular area of the microsection, there is a special mode of the microscope camera that shows the surface relief (Fig. 4 c). The etched pearlite zones are shown by the arrow number 1, and sulfide inclusions are shown by the arrow number 2. They are also visible in unetched areas (Fig. 5 c).

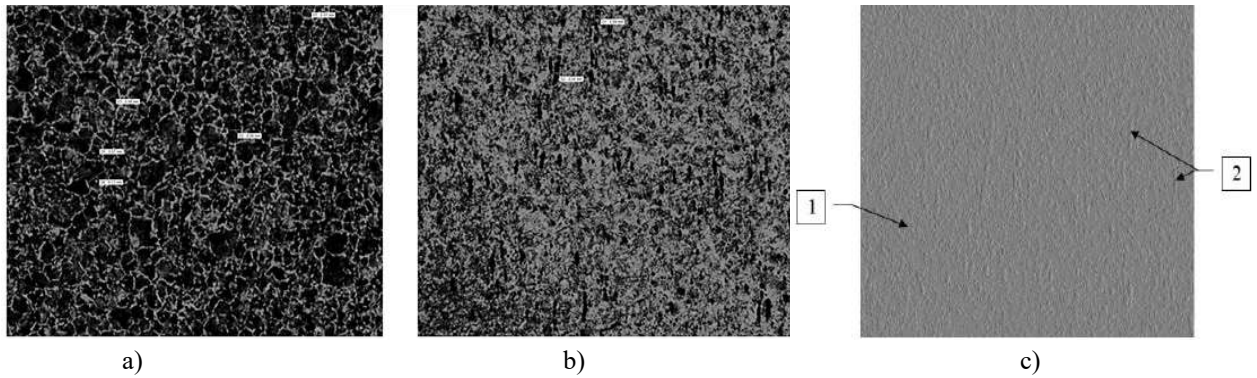


Fig. 4. Example of microstructure in different modes with magnification $\times 25$: a) focus on ferrite network; b) focus on sulfide inclusions; c) view of the structure in relief.

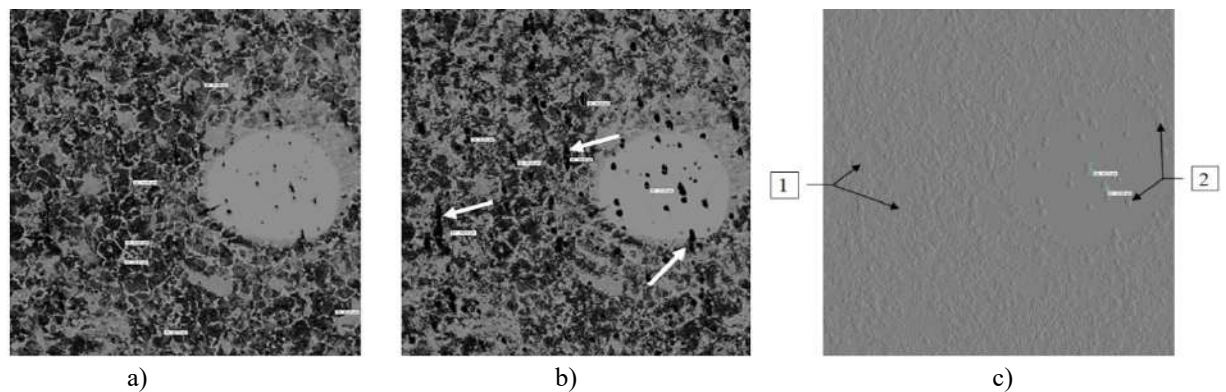


Fig. 5. Example of microstructure in different modes with magnification $\times 50$: a) focus on ferrite network; b) focus on sulfide inclusions; c) view of the structure in relief.

Analyzing longitudinal cross-section samples from different batches, an accumulation of residual ferrite is observed, which certainly has a negative impact on mechanical and heat treatment in the future. This defect is shown by arrows in Fig. 6, which has the form of large accumulations ranging in size from 50 to 600 μm .

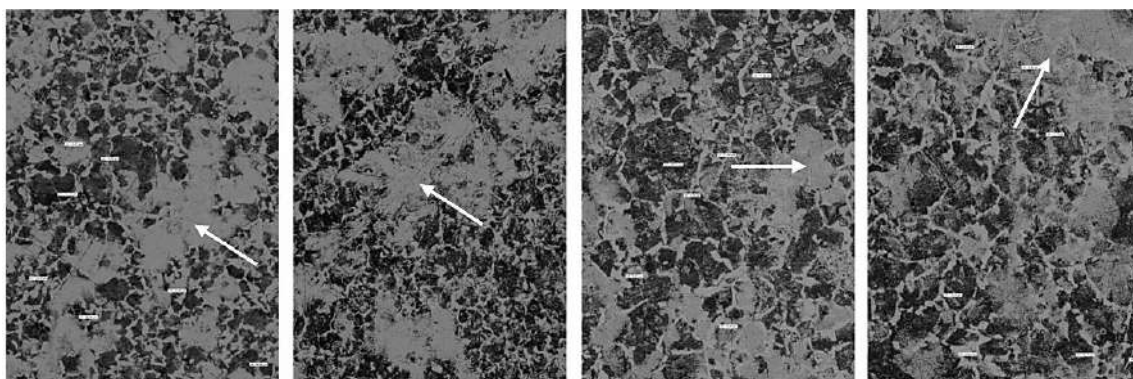


Fig. 6. Appearance of the microstructure of 35XIT steel with defects, $\times 100$

After applying the oxycarbonitriding method, grinding of the metal structure, burnout and a decrease in the number of sulfide inclusions are observed. As expected, a white oxycarbonitride layer is observed on the surface of the part, which is indicated by an arrow (Fig. 7 b).

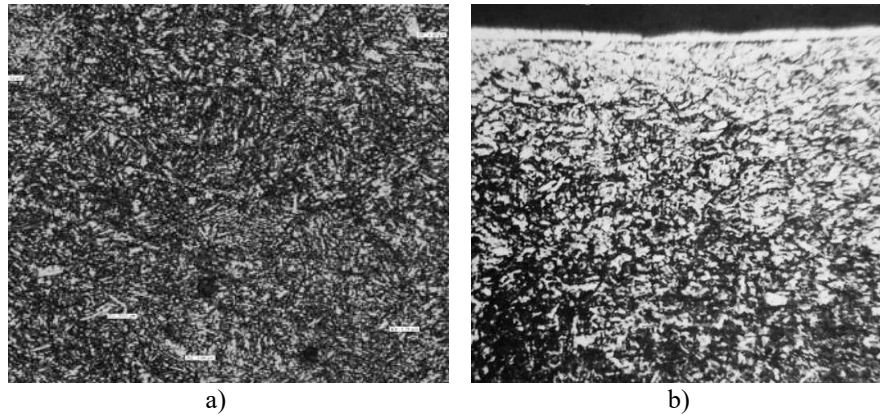


Fig. 7. Image of the microstructure after heat treatment. a) microstructure in depth; b) surface microstructure with oxycarbonitride layer

The hardness of the samples was measured by the Rockwell method. The hardness of the upper layer was set within 50-58 HRC, and the hardness of the inner layers was on average 30 HRC. The thickness of the formed oxycarbonitride layer was 0.12-0.20 mm.

When studying the deformation effect on the cylindrical part, a PMT-3 microhardness tester was used. Absolute deformation (δD) was determined according to formula 1. With a duration of chemical-thermal treatment of about 8 hours, the absolute deformation value is 0.024 mm. at $\varnothing 49$ mm.

$$\delta D = \frac{D_2 - D_1}{2} \quad (1)$$

where: D_1 is the diametrical size before oxycarbonitriding;

D_2 is the diametrical size after oxycarbonitriding.

The absolute deformation value was calculated at least in three places of one diametrical size. It was experimentally established that the absolute deformation value increases by 0.003 mm for each subsequent hour of the surface hardening process. Therefore, the longer the oxycarbonitriding process time, the thicker the oxycarbonitriding layer, but the absolute deformation value increases, which must be taken into account when processing precision surfaces. After the chemical-thermal treatment processes, local chemical analysis of the samples was carried out in a special laboratory. Measurements of chemical inclusion values were carried out at seven points on each sample. An example of one of the samples is shown in Fig. 8.

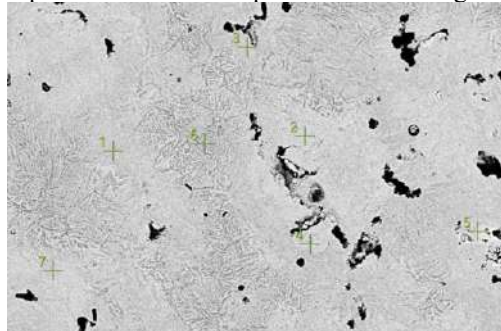


Fig. 8. Steel microstructure with measurement points

After the measurement, the obtained values were averaged and grouped into Table 1.

Table 1

Values of chemical inclusions of steel 35XFT DSTU 7805:2015.

Element	Value in %						
	Point 1	Point 2	Point 3	Point 4	Point 5	Point 6	Point 7
C	4.8	4.2	4.8	4.9	5.8	3.5	4.9
O	0.0	0.0	0.0	0.0	0.6	0.0	0.0
Si	0.4	0.5	0.5	0.3	0.3	0.5	0.5
Cr	0.9	0.8	0.9	0.7	0.7	1.0	0.9
Mn	0.6	0.6	0.6	0.6	0.4	0.5	0.7
Fe	92.7	91.8	92.6	85.0	74.4	93.7	92.5
Ni	0.3	0.3	0.3	0.3	0.3	0.4	0.3
Cu	0.3	1.8	0.3	8.0	17.3	0.3	0.3
Mo	0.1	0.0	0.0	0.1	0.1	0.0	0.0

As can be seen from Table 1, the chemical elements are not evenly distributed in the samples. Thus, at point 5, the maximum value of carbon is observed - 5.8% and copper - 17.3%, the smallest amount of iron is 74.4%, manganese - 0.4%, chromium - 0.7%, silicon - 0.3%. The smallest amount of carbon is observed at point 6 - 3.5%, but the largest amount of iron is present - 93.7% and nickel - 0.4%.

Conclusions

In this work, the material of the part modified by the oxycarbonitriding method was studied. A study was conducted to change the structure and metal, what defects are observed. The parameters of the oxycarbonitriding process were studied, and experimentally established which ones are necessary for the selected part. A wear-resistant oxycarbonitriding layer with a thickness of 0.12-0.2 mm was obtained, which has a hardness of about 60 HRC on the surface. A chemical analysis of the samples was also carried out and non-uniformity of the location was revealed. After conducting the chemical-thermal treatment, dimensions were obtained that will correspond to the tolerances on the drawing.

Prospects for further research.

One of the priority areas of using such technologies is to improve the operating characteristics of cutting tools, friction pairs of machine parts, gearbox shafts operating under extreme mechanical and temperature loads.

CCHT technology is environmentally friendly and can in most cases replace galvanic coatings (oxidation, zinc plating, chrome plating, cadmium plating, etc.), which can provide a cost reduction of 35 - 40%.

References

1. Khyzhnyak V. G., Loskutova T. V., Datsyuk O. E., Khyzhnyak O. V.. Multicomponent diffusion coatings based on titanium, aluminum and silicon on nickel. Scientific Bulletin of the National Technical University of Ukraine "Kyiv Polytechnic Institute". 2015. No. 1. P. 79-84
2. Cutting theory and tools: textbook / N. R. Veselovska et al. Vinnytsia: 2018. 297 p.
3. Pogrebna N. E., Kutsova V. Z., Kotova T. V. Methods of strengthening metals: textbook. Dnipro: NMetAU, 2021. 89 p.
4. M. V. Arshuk, A. V. Mykytchyk, V. G. Khyzhnyak, M. V. Karpets., Titanium-aluminide coatings on steel 12X18N10T with a barrier layer of titanium nitride. NTUU "Kyiv Polytechnic Institute" International Center for Electron Beam Technologies of the E. O. Paton Institute of Electrical Engineering of the National Academy of Sciences of Ukraine, Kyiv. 2011. 50 p.
5. V.G. Khizhnyak, M.V. Arshuk, T.V. Loskutova, M.V. Karpets., Diffusion coatings with the participation of titanium and aluminum on nitrided steel 12X18N10T. NTUU "KPI". Kiev, 2011. P. 118-122.
6. V.G. Khizhnyak, M.V. Arshuk, M.V. Karpets. Physics and chemistry of solids. T.12, No. 3. NTUU "KPI", Kyiv, 2011 P. 757-761.
7. Chemical-thermal treatment of titanium alloys. Surface solid-solution modification: monograph / V. M. Fedirko et al.; FMI NASU. Kyiv: Nauk. Dumka, 2020. 183p.
8. Alloy steels and alloys with special properties. Textbook. Kutsova V.Z., Kovzel M.A., Nosko O.A. Dnipropetrovsk: NMetAU, 2008. 348 p.
9. Effectiveness of methods for restoring parts of plunger pairs of fuel pumps of diesel engines of agricultural machinery. P. S. Popyk, L. L. Rogovsky, O. M. Vechera, O. G. Polishchuk. Machinery & Energetics. 2019. P. 115–120.
10. Pisarenko V. G. Combined chemical-thermal treatment as an effective way to increase the durability of precision mechanics parts. Problems of Tribology. Vinnytsia, 2011. P. 75–78.
11. Spies, H. -J; Winkler, H. -R; Langenhan, B: On the corrosion and wear behavior of E-nitrides on steel. Harterei – Tech. Mitt. 44 (1989) 2, P. 75-82.
12. Ohsawa, M: The current state of Nitriens in vehicle construction in Japan. Harterei – Tech. Mitt. 34 (1979) 2, P 3-10.

Мешков Ю. Є., Дмитрієв М. С. Покращення фізико-механічних характеристик валів коробок передач за допомогою методу оксикарбонітрування

У статті досліджується питання перспективних методів удосконалення сталей модифікуванням поверхневих шарів з нанесенням захисних покриттів. Визначені пріоритетні напрями наукових досліджень в галузі машинобудування з розробки нових методів та технологій з підвищення зносостійкості поверхонь сталей за рахунок нанесення модифікованих дифузійних покриттів. Показано, що ключовою проблемою в оптимізації процесів насичення металів і сплавів одним елементом являється цементація, азотування, алітування, хромування і т.д. Насичення двома чи декількома елементами застосовують дуже обмежено. Розглянуто особливості хіміко-термічної обробки сталі, за допомогою якої маємо можливість отримати матеріал, який характеризується підвищеними характеристиками та властивостями (поверхневою твердістю, стійкістю до корозії, зносостійкістю). Виходячи з визначених особливостей покриттів за складом, будовою, властивостями методи хіміко-термічної обробки можуть бути перспективними при їх експлуатації в умовах зношування. Однак, гідну конкуренцію цим технологічно складним процесам може скласти запропонований інноваційний метод металізації – оксикарбонітрування. Встановлено що комбінована хіміко-термічна обробка, що включає азотування і окиснення, дозволяє значно підвищити корозійну стійкість матеріалу, чим більший час процесу оксикарбонітрування тим товстіший оксикарбонітридний шар, але при цьому збільшується значення абсолютної деформації, що потрібно враховувати при обробці точних поверхонь. Визначені перспективні напрямки подальших наукових досліджень в зазначеній галузі.

Ключові слова: модифікування, поверхневі шари, хіміко-термічна обробка, насичення металів і сплавів, дифузійні покриття, стійкість до корозії, зносостійкість



Interrelation of the volume temperature of modified oils and local temperatures in the friction contact zone under extreme operating conditions

O. Milanenko*, A. Savchuk, O. Kushch, A. Bobro, V. Petrekutsy, O. Vansovskyi

National Transport University of Ukraine, Kyiv, Ukraine

**E-mail: milanmasla@gmail.com*

Received: 25 December 2024; Revised: 20 January 2025; Accept: 30 January 2025

Abstract

A methodology has been developed that allows, using the temperature criterion, to determine the thermomechanical stability of oils and, thus, to analyze the modification of oils to improve the lubrication efficiency and wear resistance of friction pairs of conformal internal combustion engine units operating under extreme conditions. The correlation relationship between the temperature in the local frictional contact zone and the bulk temperature of the modified oil was determined with an increase in the maximum contact stress during the running-in period with a corresponding shift of the correlation linear dependences towards high temperatures. Under conditions of operation up to 15 cycles, increased thermomechanical stability of the modified oil was established in comparison with the standard oil, which confirms the optimal structural adaptability of the modified layers to extreme operating conditions.

Key words: conformal friction assembly, thermomechanical stability, wear resistance, oil modification, extreme operating conditions, temperature in the friction contact, oil temperature, thermal method.

Introduction

From the point of view of energy efficiency and national security, at strategic enterprises of the oil and gas, thermal power and aerospace complexes, in the production of high-speed transport, agricultural and military hybrid equipment, predicting the effectiveness of lubrication and wear resistance of the friction pairs, especially for friction units operating under extreme operating conditions, is a necessary direction to increase reliability and extend the service life in a wide range of changes in contact loads, speeds, temperatures, impacts, etc.

Extreme operating conditions for friction units will arise in case of insufficient lubrication (lubrication starvation), when the lubricant does not have time to regularly enter the contact zone due to several reasons: 1) non-stationary friction conditions in the “stop-and-go” mode; 2) loss of mechanical stability of the lubricant due to the manifestation of non-Newtonian properties at high shear rates under low-temperature start-up conditions; 3) insufficient structural adaptability of the modified layers under conditions of boundary lubrication at local temperatures in the friction contact zone.

For extreme conditions of operation of an internal combustion engine (ICE)'s the conformal friction assembly under sliding friction, an important aspect is the temperature factor, namely, it is important to compare the average local temperature in the friction contact zone and the critical local temperature, which will be determined by thermomechanical stability under conditions of plastic-deformed contact in the boundary lubrication mode, for example, in the zone of the upper dead center (UDC) along the piston stroke of an ICE.

The purpose of the work

To develop a methodology that will allow, by means of a correlation assessment between the volumetric and local temperatures in the friction contact zone, to determine the thermomechanical stability of modified and standard oils under all other operating conditions and, thus, to analyze the modification of oils according to the appropriate temperature criterion to improve the lubrication efficiency and wear resistance of the friction pairs of an ICE's the conformal friction assembly in extreme operating conditions.



Methodical support for determination of thermomechanical stability of the oils in an ICE's the conformal friction assembly under non-stationary friction conditions

The basic principle of choosing a tribological test scheme with consideration of the temperature factor under unsteady-state friction conditions is to maximize the approximation to the actual operating conditions of the studied tribological couplings. To do this, it was necessary to ensure that the nature of the movement of the samples, sliding values and speeds, as well as the materials of the friction pairs, which simulate the conditions of friction units in the "stop-end-go" mode, were consistent. When choosing a schematic diagram for studying the processes of friction and wear of moving joints in lubricants, it was necessary to take into account the qualitative picture obtained on the samples observed when the conditions of intensive wear of friction pairs of an ICE's the conformal friction assembly are realized, namely, when the compression ring - inner wall of the working cylinder contacts with full contact of the contact surfaces under conditions of pure sliding friction.

The studies were carried out on a modernized universal automated friction test bench (UAFTB) based on the SMC-2 friction machine (Fig. 1), which is based on the method of measuring the voltage in the normal glow discharge (NGD) mode [1], which is based on the theory of the occurrence of a glowing gas discharge in a lubricant (oil) associated with the formation of gas bubbles.

The chosen research scheme (see Fig. 1) has the following advantages:

- the possibility of changing the temperature in the range from minus 20°C to 150°C, which does not affect the value of the voltage drop;
- the voltage drop almost does not depend on the properties and composition of oils, since the discharge occurs in gas;
- moisture content and wear products, as well as the properties of the metal surfaces of friction pairs, do not affect the voltage value;
- the ability to measure separately the thickness of lubricating layers of different origin, which is ideal for mixed friction conditions.

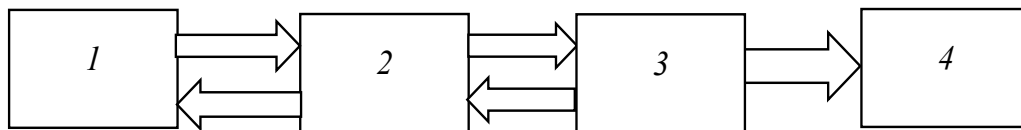


Fig. 1. Block diagram of the UAFTB: 1 - Friction machine SMC-2; 2 - 4: Automated control unit with software (ACUS), which includes: 2 - Strain gauge unit; 3 - Analog-to-digital converter (ADC); 4 - PC software

According to the kinematic diagram, the SMC-2 friction machine (Fig. 2) is a single-contact unit consisting of a pad-roller sample mounting unit for clean sliding conditions in a non-stationary friction mode (Fig. 3).



Fig. 2. General view of the UAFTB



Fig. 3. Pad-roller tribopair at the SMC-2

For the exchange of parametric information between the primary transducer (strain gauge) and the PC (see Fig. 1), a programmable complex is used, which includes an analog-to-digital converter (ADC) "eZtrend V5" by Honeywell, designed to switch analog signals and convert them into digital code. The program implements the hardware launch of the ADC. The ADC request is executed before the converter is ready. For hardware startup of the ADC at different intervals, a timer is used, which is part of the universal programmable complex.

Measurement and control of the volumetric temperature is carried out using a digital thermostat TR-3 with built-in temperature sensors and a measuring range from minus 20°C to 150°C. Forced heating of the oil to the set temperature is carried out using a heating element - a heating element. Low temperature conditions are ensured by the circulation of carbon dioxide from the Dewar tank (see Fig. 2). To investigate the relationship between the volumetric temperature of the oil under study, measured by a thermocouple, and the local temperature in the local friction contact zone, we used the thermal imaging method of measuring the field of local temperatures using different modes of loading in the contact.

The thermal imaging method allows us to study the change in local temperatures of friction units in the friction contact zone and beyond using a modern portable thermal imager TESTO-875-2i (Fig. 4).



Fig. 4. General view of the portable thermal imager "TESTO-875-2i"

The technical characteristics of the portable thermal imager of this brand are as follows:

- detector 160 x 120 pixels, uncooled microbolometer;
- thermal sensitivity - 0.08 °C;
- spectral range 8...14 microns;
- 3.5" LCD display, 320 x 240 pixels;
- image viewing - infrared and real (digital camera);
- temperature measurement range (- 20 ... + 280 °C);
- measurement error - 2°C;
- minimum focal length - 0.4 m;
- 2GB memory card (approximately 1000 images);
- power supply from lithium batteries;
- operating ambient temperature - from (-15°C) to (+50°C);
- battery life - 4 hours;
- weight about 900 g.

Results of studying the thermomechanical stability of oils in the friction contact zone of an ICE's the conformal friction assembly

As the lubricant under study, we used a modified motor oil with the addition of a mixture of fullerenes with a concentration of the 2% according to the preliminary results obtained in [2, 3]. Temperature studies were conducted in 2 stages:

Stage 1 - thermal imaging measurement of the temperature fields of the local roller contact zone and the volumetric temperature for the modified oil under atmospheric conditions – $T = 291\text{ K}$ at the maximum contact stress in the contact, $\sigma_{max} = 55\text{ MPa}$. The temperature regime of heating was as follows: $T = 303\text{K}; 313\text{K}; 318\text{K}; 338\text{K}; 348\text{K}; 353\text{K}; 363\text{K}$ respectively.

Stage 2 - thermal imaging measurement of the temperature fields of the local contact zone of the roller and the volumetric temperature for the modified oil under atmospheric conditions – $T = 291\text{K}$ at the maximum contact stress in the contact, $\sigma_{max} = 68\text{ MPa}$.

The temperature regime of heating was as follows: $T = 303\text{K}; 313\text{K}; 318\text{K}; 338\text{K}; 348\text{K}; 353\text{K}; 363\text{K}$ respectively. The initial operating period was reproduced for different shaft rotation cycles: 5 cycles, 10 cycles, and 15 cycles, respectively.

The results of the thermal imaging tests are presented in the form of thermograms for the maximum contact stresses in the contact $\sigma_{max} = 55\text{ MPa}$ (Fig. 5 a, b) and $\sigma_{max} = 68\text{ MPa}$ (Fig. 6 a, b) at $T = 348\text{K}$ and $T = 363\text{K}$, respectively.

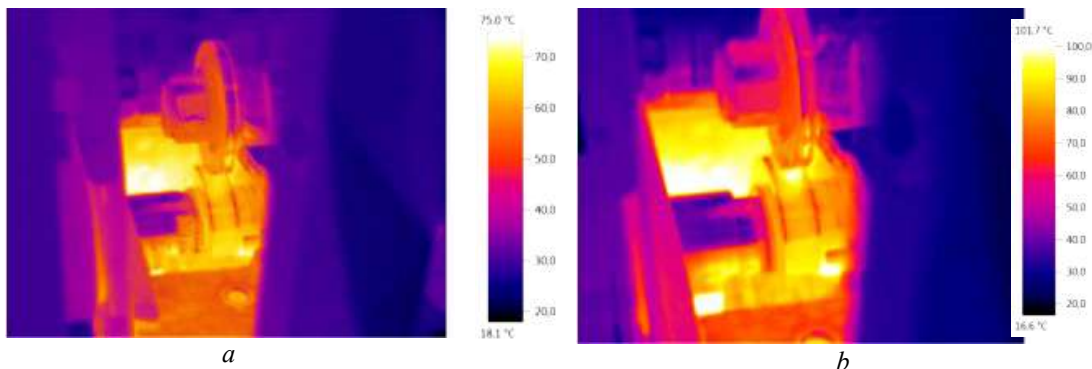


Fig. 5. Thermogram of the temperature fields of the contact zone: for the initial operating period at $\sigma_{max} = 55\text{ MPa}$ during heating to $T = 348\text{K}$ (a) and $T = 363\text{K}$ (b), respectively

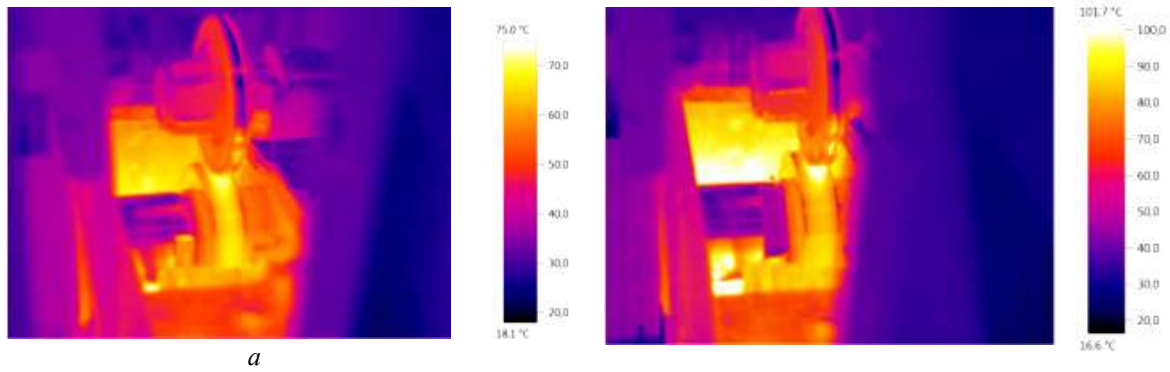


Fig. 6. Thermogram of the temperature fields of the contact zone: for the initial operating period at $\sigma_{max} = 68$ MPa during heating to $T = 348K$ (a) and $T = 363K$ (b), respectively

Below, we present the results of the studies in tabular form (Table 1) and graphical interpretation of the results (Fig. 7) at the maximum contact stress in the contact, $\sigma_{max} = 55$ MPa for the initial operating period.

According to the results in Fig. 7, a correlation was established between the temperature of the roller in the local friction contact zone and the volumetric temperature of the modified oil for the initial operating period at $\sigma_{max} = 55$ MPa, which ranges from 6% to 34% as the temperature increases in the studied range. Moreover, the temperature of the roller increases linearly, reaching a maximum temperature of $T = 380K$ at the end of the operating time, at which the temperature difference between the oil and the roller is equal on average to $\Delta T = 25K$.

The following research results are presented in tabular form (Table 2) and in the form of a graphical interpretation of the results (Fig. 8) at the maximum contact stress in the contact $\sigma_{max} = 68$ MPa for the initial operating period.

Table 1

Results of correlation between the roller's local temperature and the modified oil's volumetric temperature at the maximum contact stress in the contact, $\sigma_{max} = 55$ MPa

Object of research	№, cycles	Correlation between roller temperature and oil temperature, taken from the thermogram, °C						
		Oil heating temperature by thermocouple, °C						
		30	40	45	65	75	85	90
Oil	5	45.3	48.2	48.5	62	73.5	71.9	80.4
Oil	10	46.3	49	52.8	67.2	73.2	77	78.4
Oil	15	43.8	47.2	55.4	63.6	70.3	80.9	81.9
Roler	15	47.6	48	76.1	85	90.2	100	107

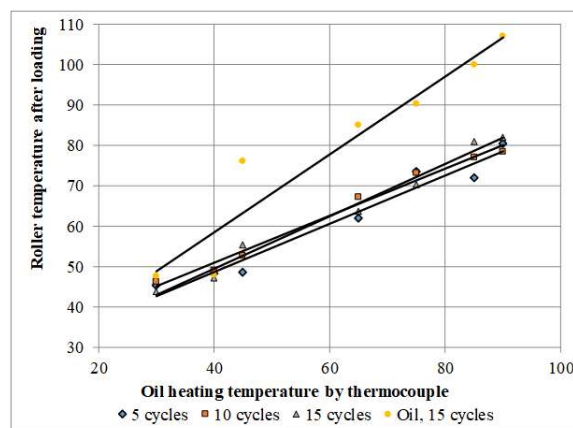


Fig. 7. The correlation between the local temperature of the roller in the contact zone and the volumetric temperature of the modified oil during the initial operating period at $\sigma_{max} = 55$ MPa

According to the results of Fig. 8, a correlation was established between the temperature of the roller in the local contact zone and the volumetric temperature of the modified oil for the initial operating period at $\sigma_{max} = 68$

MPa, which ranges from 4% to 58% as the temperature increases in the studied range. Moreover, the temperature of the roller increases linearly, reaching a maximum temperature of $T = 382.4K$ at the end of the operating time, at which the temperature difference between the oil and the roller is equal on average to $\Delta T = 40K$.

Thus, the results of the correlation between the local temperature of the roller in the local contact zone and the volumetric temperature of the modified oil, for the initial operating period with an increase in the maximum contact stress σ_{max} from 55 MPa to 68 MPa, extends the spread of the correlation linear dependences towards high temperatures by an average of $\Delta T = 15K$, which determines the importance of taking into account the increase in the local temperature of the roller in the local friction contact zone relative to the oil volume temperature with increasing load (maximum contact stress).

In order to determine the thermomechanical stability, it is necessary to know the average temperature in the local contact zone, taking into account the correlation between the volume temperature of the modified oil and the local temperature in the friction contact zone, where the temperature fields (changes in the special temperature point) are determined by the thermal imaging method for the roller-pad friction pair ("roller" - made of Steel 40H, "pad" - made of bronze BrOCS 4-4-17) during the period from startup to 15 cycles in the non-stationary sliding friction mode at different warm-up temperatures: $T = 298K$; 303K; 313K; 338K; 348K, respectively.

By the thermal imaging method of research, the fields of local temperatures in the friction contact zone of the roller (changes in the special point of the corresponding temperature) were determined in the form of thermograms (Fig. 9, where it is shown for $T = 298 K$) and changes in local temperatures in the friction contact zone of the roller were determined (Fig. 10, a-d) relative to the volumetric temperature of the studied modified oil measured by a thermocouple, taking into account the correlation performed during the period from startup to 15 cycles in the unsteady-state mode of sliding friction at different heating temperatures.

Table 2

**Results of correlation between the roller's local temperature and the modified oil's volumetric temperature
at the maximum contact stress in the contact, $\sigma_{max} = 68 MPa$**

Object of research	№. cycles	Correlation between roller temperature and oil temperature. taken from the thermogram. °C						
		Oil heating temperature by thermocouple. °C						
		30	40	45	65	75	85	90
Oil	5	38.2	45.9	47.4	56.1	55.9	68.5	69.1
Oil	10	35.3	43.5	48.1	50.5	64.2	67.1	69.6
Oil	15	35.3	42.4	49.9	59.4	55.9	71.5	68.6
Roler	15	35.3	44.5	76.1	83.7	89.3	99.3	109.4

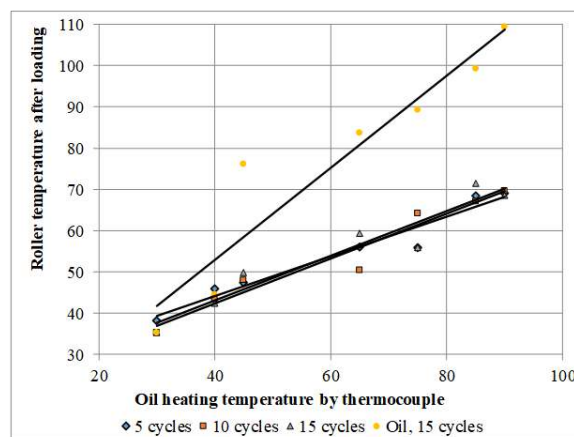


Fig. 8. The correlation between the local temperature of the roller in the contact zone and the volumetric temperature of the modified oil during the initial operating period at $\sigma_{max} = 68 MPa$

Based on the results of the fields of local temperatures (thermograms) of the roller surface (see Fig. 10 a-d), special points of local temperature in the friction contact zone were determined, taking into account the preliminary correlation between the local temperature of the roller surface and the volumetric temperature measured by the thermocouple for the studied oils: modified oil and standard oil selected for comparison during the operating period.

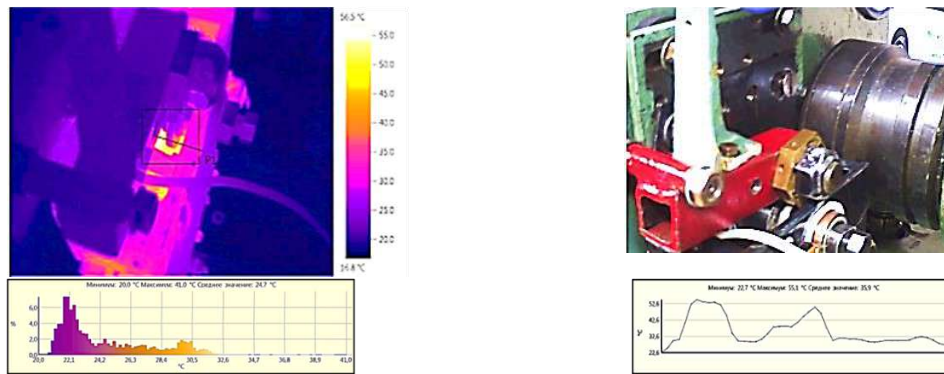


Fig. 9. Thermogram of a special point of local temperature in the friction contact zone of the roller at $T = 298K$ during the initial operating period

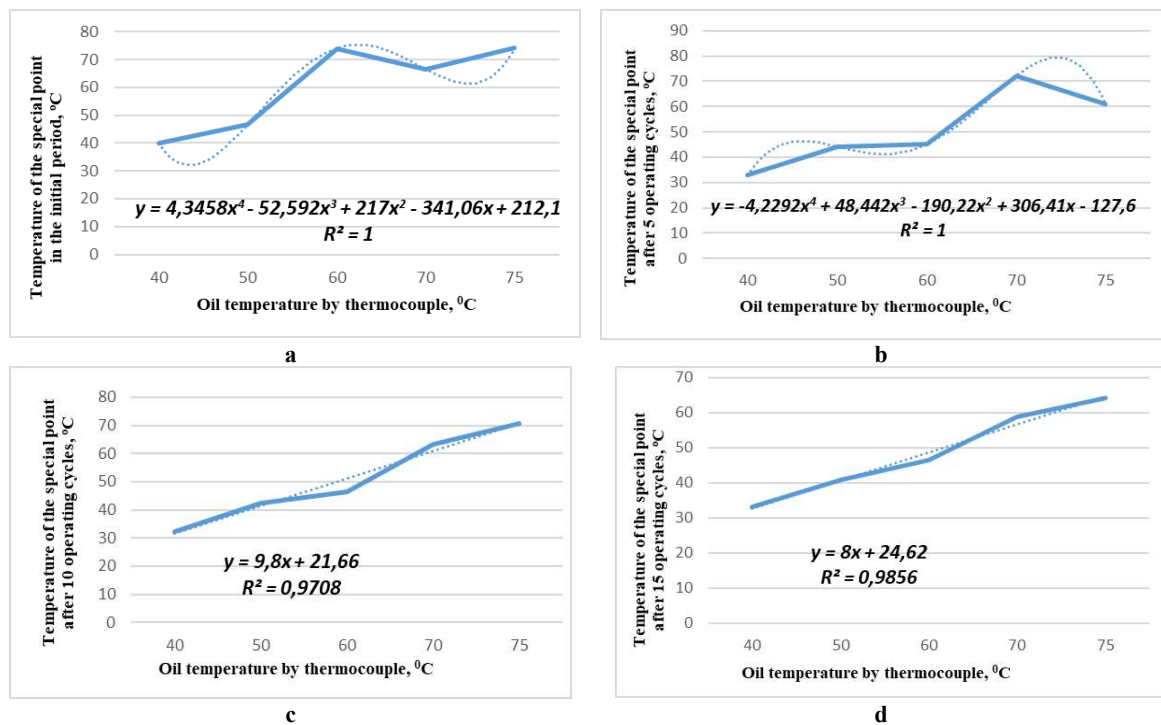


Fig. 10.- Change of the local temperature feature point regarding the previous correlation: in the initial operating period (a), after 5 (b), -10 (c), -15 (d) operating cycles

According to the equations (see Fig. 10 a - d), it was determined that under the conditions of operating time up to 15 cycles, the condition for the temperature criterion is met: $T_{critical} < T_{average}$ for both oils, but for the modified oil, an increased thermomechanical stability was established, on average by $\Delta T = 23K$, which confirms the better structural adaptability of the modified layers of the corresponding modified oil to extreme operating conditions.

Conclusions

The correlation between the temperature in the local friction contact zone and the volumetric temperature of the modified oil was determined when the maximum contact stress was increased to $68 MPa$ during the running-in period with a corresponding shift of the correlation linear dependencies towards high temperatures by $\Delta T = 15K$. Under the conditions of operating up to 15 cycles, the thermomechanical stability of the modified oil was found to be increased compared to the standard oil, on average by $\Delta T = 23K$, which confirms the optimal structural adaptability of the modified layers to extreme operating conditions.

References

1. Rayiko M. Some Aspects of Boundary Lubrication in the Local Contact of Friction Surfaces / Rayiko M., Dmytrychenko N. - Wear. – 1988. – vol. 126. – P. 69–78.
2. Dmitrichenko N.F. Improving the efficiency of lubricants by introducing friction modifiers for tracked vehicles under stationary conditions of friction / N.F. Dmitrichenko, A.A. Milanenko, A.N. Savchuk, O.N. Bilyakovich, Y.A. Turitsa, M.V. Pavlovskiy, S.I. Artemuk // Journal of Friction and Wear. - 2016. - Volume 37(5). – P. 441-447.

3. Dmytrychenko M.F. Influence of the active metal surface on the polymerization of hydrocarbon components of oil and fullerene C_{60} / M.F. Dmytrychenko, O.M. Bilyakovich, A.M. Savchuk, Y.O. Turitsa, O.A. Milanenko // Systems and means of motor transport. Selected problems: Monografia. - Politechnika Rzeszowska. – 2018. - №14 (Seria: Transport). – P.47-52.

Міланенко О., Савчук А., Куш О., Бобро А., Вансовський О. Взаємозв'язок об'ємної температури модифікованих оливи і локальних температур у зоні контакту тертя в екстремальних умовах експлуатації

Розроблено методику, яка дозволяє за допомогою температурного критерію, визначати термомеханічну стійкість оливи і, таким чином, аналізувати модифікування оливи щодо підвищення ефективності мащення і зносостійкості пар тертя конформних вузлів ДВЗ, які працюють в екстремальних умовах роботи.

Визначено кореляційний взаємозв'язок між температурою в локальній зоні фрикційного контакту і об'ємною температурою модифікованої оливи при збільшенні максимального контактного напруження до 68 МПа в період припрацювання з відповідним рознесенням кореляційних лінійних залежностей в бік високих температур на $\Delta T = 15 \text{ К}$. В умовах напрацювання до 15 циклів, встановлена збільшена термомеханічна стійкість модифікованої оливи в порівнянні зі штатною оливою, в середньому на $\Delta T = 23 \text{ К}$, що підтверджує оптимальну структурну пристосовуваність модифікованих шарів до екстремальних умов роботи.

Ключові слова: конформні вузли, термомеханічна стійкість, ефективність мащення, зносостійкість пар тертя, модифікування оливи, структурна пристосовуваність, температура контакту, температура оливи, тепловізійний метод.



Wear resistance of structural steels carbonitrided by the separate method

M.S. Stechyshyn, O.V. Dykha*, D.V. Zdorenko, E.G. Oleksandrenko

Khmelnytskyi national University, Ukraine

**E-mail: tribosensor@gmail.com*

Received: 05 Decemberr 2024; Revised 22 January 2025; Accept 28 January 2025

Abstract

The article investigates the influence of technological modes of separate carbonitriding of carbon steels on the thickness and microhardness of the hardened layer. Two hardening variants were investigated: first, carburizing of surfaces was carried out in argon-propane, and then nitriding in argon-nitrogen mixtures and vice versa. As the conducted studies have shown, the variant of the hardening technological process significantly affects the physical and mechanical characteristics of the hardened layer. In all two variants of the technological process, the hardened layer consists of a surface carbonitride zone and a diffusion zone of internal nitriding, but the properties of these zones are different in different variants of the technological process. Thus, when hardening steels according to the first mode, the thickness of the carbonitride zone is maximum, and the internal nitriding zone has a small thickness. This is explained by the fact that the carbonitride layer created on the steel surface at the first stage of processing performs the function of shielding the surface from the penetration of nitrogen ions into the surface layer of the metal. When hardening according to the second mode, the carbonitride zone has a slightly smaller thickness, but a more developed internal nitriding zone. In addition, carbonitriding according to the first mode leads to the formation of carbonitride inclusions in the diffusion zone in the form of a mesh, which significantly reduce the plasticity of the layer and under dynamic loads are centers of microcrack nucleation. It has also been established that a carbonitride ϵ – phase is formed on the surface of steels, which consists of carbonitrides of the type $\text{Fe}_2(\text{N,C})$, $\text{Fe}_3(\text{N,C})$, $\text{Fe}_4(\text{N,C})$. The carbonitride zone has high hardness, high corrosion resistance, and increased wear resistance. The thickness of the carbonitride zone reaches a thickness of up to 25 microns. Under the carbonitride zone is the internal nitriding zone, which has a large thickness and is the main part of the carbonitrided layer. The internal nitriding zone consists of a nitrogenous solid solution of the base metal, its nitrides and nitrides of alloying elements. The dependences of thickness and microhardness on the technological parameters of carbonitriding of carbon steels obtained in the work: temperature, saturation time, composition of the gas medium, its pressure allow them to be optimized depending on the requirements of further operation.

Keywords: carbon steels, wear resistance, carbonitration, medium pressure, thickness of the hardening layer

Introduction

Machine parts and tools that operate under conditions of intensive wear are widely used in technology. Increasing their service life will significantly reduce operating and repair costs, which will provide a significant economic effect. Known hardening technologies require further processing of parts and tools, require significant energy resources and are in most cases environmentally harmful. The developed technology significantly reduces energy consumption, is environmentally friendly, and allows you to predict the operational properties of the processed parts.

A significant disadvantage of almost all types of chemical-thermal treatment, and especially furnace nitriding, is the need to heat the products to high temperatures and hold them at these temperatures for a long time, which leads to significant energy consumption. In addition, after nitriding, residual tensile stresses are formed in the "coating-base" system, which reduce the performance of the product. Such coatings cannot work in heavily loaded friction units. At high local loads, the nitrided layer is pushed through, since it lies on a soft base, the microhardness of which is significantly lower than the microhardness of the layer itself. This is due to the fact that



the technological process of nitriding involves preparatory heat treatment of steel: quenching with high tempering at a temperature of 800-860 K, which coincides with the temperature of furnace nitriding.

There is a known method of strengthening such coatings, which, after the process of furnace nitriding in an ammonia environment at a temperature of 800-860 K with a holding time of 15...20 hours, is subjected to laser treatment, which is performed after nitriding discretely by points with a treatment area of 20-35% of the total area of the steel product, with a power of 105 -108 W/cm². As a result of such treatment, the microhardness of discrete areas of steel was: 20MnCr5G- 6500 MPa, 37Cr4 - 8200 MPa, 41CrAlMo7- 8900 MPa [1].

The disadvantage of this method is the duration of the furnace nitriding process (10...15 hours), high energy consumption, explosiveness and environmental hazard of the process, expensive equipment, and its absence on the Ukrainian market.

It is known that the technology of hydrogen-free glow discharge nitriding (GHND) can be used in all industries where there is a need to increase the service life of parts that operate under conditions of intensive wear, cavitation-erosion and corrosive effects of the external environment on them [2, 3]. This ensures increased wear resistance [4], surface strength [5], corrosion resistance [6], reliability and durability of the machined parts [7].

In addition, glow discharge nitriding is characterized by the lowest energy consumption among all known processes of this class - 100...130 kWh/t. For comparison, the corresponding indicator for hardening varies within 1250...1450 kWh/t, for annealing - 300...1500 kWh/t, normalizing - 600...1400 kWh/t, cyanidation - 1050...1600 kWh/t, for laser hardening it is 230 kWh/t, gas nitrocarburization - 600 kWh/t, liquid - 800 kWh/t, gas nitriding - 450 kWh/t. Another extremely important advantage of ATP is the practical absence of deformation of products, which eliminates the need for further surface finishing. It is obvious that both of these facts significantly reduce the cost of the processed part [8].

A significant advantage of the proposed technology compared to domestic and world analogues is the rejection of the use of hydrogen-containing gas media traditionally used in GLOW DISCHARGE NITRIDING - ammonia and a mixture of nitrogen and hydrogen. The presence of hydrogen in the glow discharge stimulates hydrogen embrittlement. Another serious drawback associated with the use of hydrogen-containing media is the environmental hazard of the process [7, 8].

Goal and problem statement

To investigate the influence of technological parameters of separate carbonitriding of carbon steels (temperature, pressure, propane content in the propane-argon mixture, saturation time, sequence of nitriding and carburizing) to find their optimal characteristics that ensure the operational requirements for the hardened surfaces of parts.

Research methodology

The technological parameters of the carbonitriding process in a glow discharge significantly affect the physical and mechanical characteristics, structure, phase composition, and wear resistance of the carbonitride layer, therefore, studying this influence is an important task.

The research was conducted on steel grades: AISI 3415, T8, 37Cr4, 45, 105WC6. The task of the research was to determine the dependence of the characteristics of the carbonitridated layer (depth, hardness, structure, phase and chemical composition) on the main parameters of the technological process (pressure, composition of the saturating medium, temperature and duration of the process). As working gases, mixtures of nitrogen and argon (75% N₂ + 25% Ar) and propane C₃H₈ were used, the saturation temperature varied from 480 °C to 600 °C, the pressure of the gas mixture in the process of diffusion saturation was from 80 Pa to 400 Pa, the duration of the process was from 20 min to 240 min.

In the process of research, methods of metallography, X-ray diffraction and chemical analysis were used, as a result of which the following characteristics of the carbonitridated layer were determined: structure and thickness based on microscopes MMP-2P, "Neophot-21"; microhardness using a PMT-3 microhardness tester; phase composition based on an X-ray device DRON-3M.

In order to conduct experiments rationally and obtain reliable information, mathematical methods of planning experiments (first- and second-order plans) and statistical methods of processing experimental results were used.

Studies of the influence of technological parameters of the nitriding process on the operational characteristics of nitrided samples showed that all dependencies are nonlinear. The use of first-order mathematical models to describe these processes is possible only in a narrow range of changes in variable factors, when the function in a given area can be approximated with sufficient accuracy by a straight line. Therefore, when solving the forecasting problem, the method of planning experiments - the Hartley second-order plan - was used to mathematically describe these dependencies and conduct rational research [9]. Hartley plans differ from other second-order plans in their high efficiency. For example, in a four-factor experiment, 25 experiments must be conducted using an orthogonal central-compositional plan, 31 experiments using a uniform rotatable central-compositional plan, and 17 experiments using a Hartley compositional plan. However, processing the results of the experiments requires the use of software.

Studies of the carbonitriding process in a glow discharge were carried out on an experimental setup that provides hardening of both samples and industrial parts with a diameter of up to 400 mm and a length of up to 1000 mm.

Experimental studies of samples for wear resistance were carried out on a universal machine for testing friction materials model 2168UMT. The counterbody material is steel ShKh15 with a base hardness of HRC61; pressure in the contact zone $P = 16$ MPa; sliding speed $v = 0.1$ m/s; the controlled parameter is linear wear h , which was determined as a change in the linear size of the sample measured normal to the friction surface as a result of passing a section with a length l . The test was carried out in the dry friction mode, which is typical for many parts of agricultural machinery.

Presentation of research materials

To find the optimal amount of propane in the saturating medium and the pressure in the discharge chamber, a number of technological modes of hardening of AISI 3415, 105WC6 and 37Cr4 steels were carried out. Technological parameters of the process of forming a carbide layer in a glow discharge: process temperature $T = 580$ °C, hardening duration $\tau = 240$ min, the pressure in the chamber varied from 67 Pa to 333 Pa, the propane content in the saturating medium in a volume fraction from 3% to 15% (hereinafter, the abbreviated notation of the composition of the gas mixture will be used in the text, for example, 15% C3H8).

In the process of studying samples of AISI 3415, 105WC6 and 37Cr4 steels, the dependences of the surface microhardness of the carbide layer on the technological parameters of the hardening process - pressure in the discharge chamber and propane content were obtained. Data on the microhardness of hardened steels are given in Table 1. The dependences of microhardness on the parameters of carbonitriding are shown in Figures 1 and 2.

Table 1

Microhardness of AISI 3415, 105WC6 and 37Cr4 steels hardened in a glow discharge in a carbon environment

Mode	Technological parameters of the mode				Microhardness H100, MPa					
	p, Pa	% C3H8	I, A	U, B	AISI 3415		105WC6		37Cr4	
					To	After	To	After	To	After
1	333	9.0	6.8	315	2420	6500	3000	4350	2970	4700
2	266	9.0	6.7	380	2700	7300	3150	4800	3000	5500
3	200	9.0	5.6	410	2850	6800	2550	5300	2860	4750
4	133	9.0	4.6	550	2450	5650	2800	4500	2600	3800
5	67	9.0	3.6	970	2650	5000	3000	3750	2800	3600
6	266	15.0	6.6	360	2600	5500	3050	3900	2930	4100
7	266	12.0	6.5	400	2800	6700	3080	4550	2700	5150
8	266	9.0	6.7	380	2750	7300	3050	4800	2950	5500
9	266	6.0	6.1	450	2800	6250	3180	4280	3050	5000
10	266	3.0	6.3	420	2700	5500	3000	3500	2950	3600

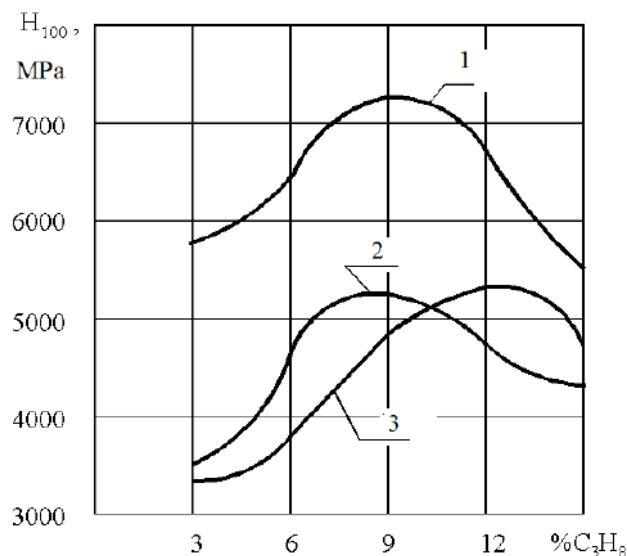


Fig. 1. Dependence of the microhardness of the carbide layer on the propane content in the saturating medium: 1- AISI 3415; 2- Steel 37Cr4; 3- Steel 105WC6

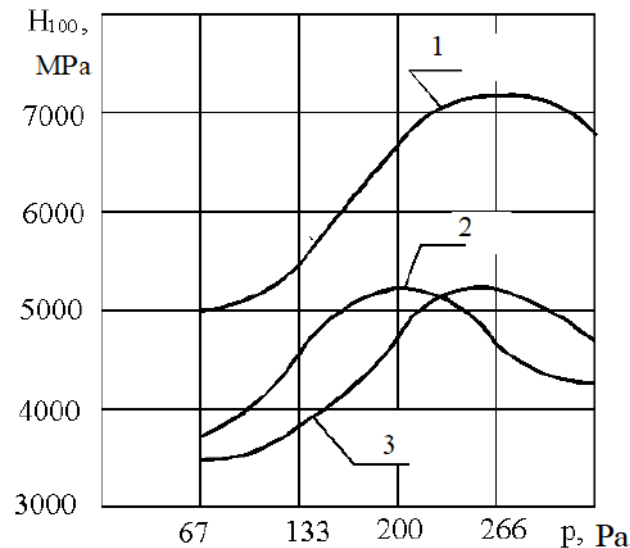


Fig. 2. Dependence of the microhardness of the carbide layer on the pressure in the discharge chamber: 1- AISI 3415; 2- Steel 37Cr4; 3- Steel 105WC6

Previous studies of the influence of the propane content in the medium and the pressure in the discharge chamber have shown that for all the studied steels there are optimal values of the propane content in the saturating medium (from 9% to 12%) and the pressure in the discharge chamber (from 266 Pa to 300 Pa), at which the surface microhardness will be maximum. With an increase in the propane content in the saturating medium, the surface of the samples is covered with soot, which complicates the penetration of saturating gases into the metal surface and the formation of a hardened layer.

The influence of the technological process of carbonitriding on the physical-mechanical and tribological characteristics of AISI 3415, 105WC6 and 37Cr4 steels are researched. Hardening was carried out using two variants of the technological process:

1. Carbon saturation ($\tau = 120$ min, medium – 88% Ar + 12% C₃H₈) + nitrogen saturation ($\tau = 120$ min, medium – 25% Ar + 75% N₂).

2. Nitrogen saturation ($\tau = 120$ min, environment – 25% Ar + 75% N₂) + carbon saturation ($\tau = 120$ min, environment – 88% Ar + 12% C₃H₈).

The process temperature and pressure in the discharge chamber in all two variants of the hardening process remained unchanged. The results of studies of the surface microhardness, the thickness of the hardened layer and the thickness of the carbonitride zone of the hardened steels are given in Table 2. The microstructures of steels for different variants of hardening processes are shown in Fig. 3. As the conducted researches showed, the variant of technological process of hardening significantly influences physical and mechanical characteristics of the hardened layer. In all two variants of technological process the hardened layer consists of a surface carbonitride zone and a diffusion zone of internal nitriding, but the properties of these zones at different variants of technological process are different. Thus, at hardening of steels according to the first mode.

Table 2
Characteristics of carbonitrided layer of steels, hardened in glow discharge depending on the variant of technological process

Mode	Parameters strengthening	Steel grade	Microhardness H100, MPa		Layer thickness, μm	Carbonitrided zone, μm
			to	after		
1	$\tau = 120$ min, 88% Ar + 12% C ₃ H ₈ $\tau = 120$ min, 25% Ar + 75% N ₂ T = 580 °C, p = 266 Pa	AISI 3415	2700	7800	48	20
		105WC6	3000	7200	45	13
		37Cr4	2950	7350	40	25
2	$\tau = 120$ min, 25% Ar + 75% N ₂ $\tau = 120$ min, 88% Ar + 12% C ₃ H ₈ T = 580 °C, p = 266 Pa	AISI 3415	2800	8200	100	15
		105WC6	3180	7240	65	12
		37Cr4	3050	7900	80	20

$\tau = 120$ min, environment (88% Ar + 12% C₃H₈); $\tau = 120$ min, environment (25% Ar + 75% N₂), $T = 580$ °C, $p = 266$ Pa) the thickness of the carbonitride zone is maximum, and the internal nitriding zone has a small thickness. This is explained by the fact that the carbonitride layer created on the steel surface at the first stage of processing performs the function of shielding the surface from the penetration of nitrogen ions into the surface layer of the metal (Fig. 3a, 4a, 5a).

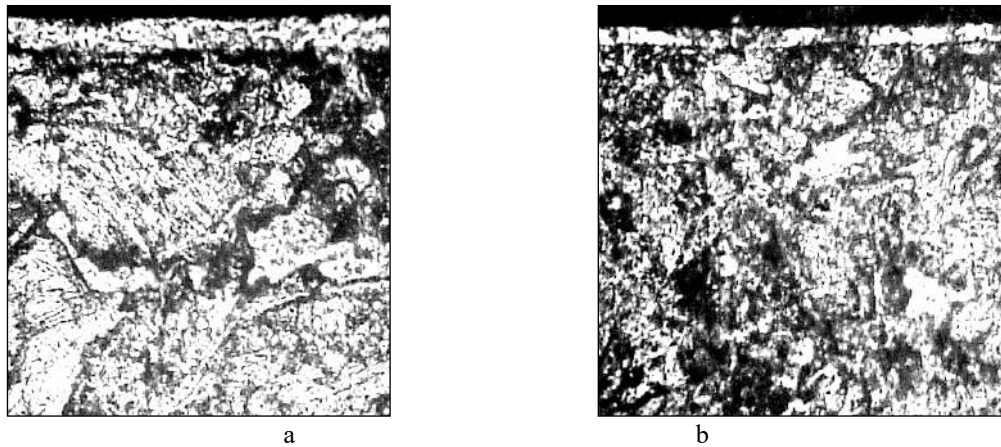


Fig. 3. Microstructure of AISI 3415 steel: a – mode 1, b – mode 2

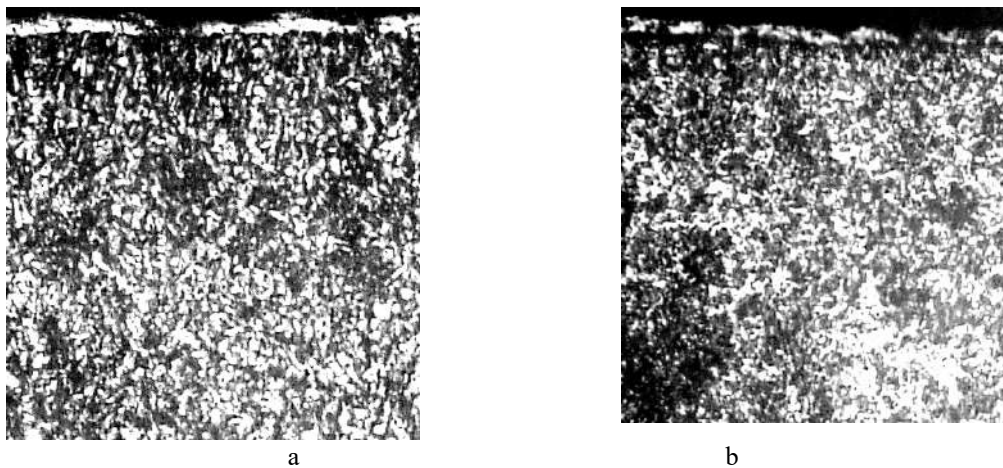


Fig. 4. Microstructure of 37Cr4 steel: a – mode 1, b – mode 2

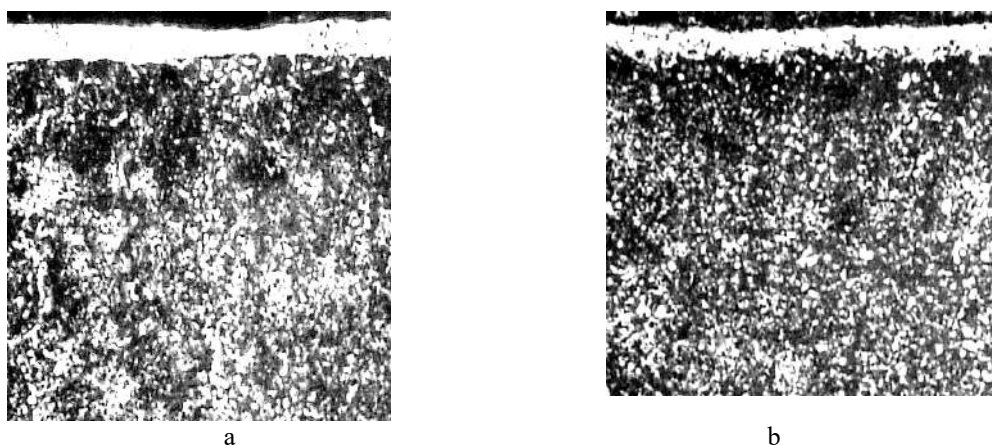


Fig. 5. Microstructure of 105WC6 steel: a – mode 1, b – mode 2

When hardening in the second mode $\tau = 120$ min, environment (25% Ar + 75% N₂); $\tau = 120$ min, environment (88% Ar + 12% C₃H₈), $T = 580$ °C, $p = 266$ Pa) the carbonitride zone has a slightly smaller thickness, but a more developed zone of internal nitriding (Fig. 3b, 4b, 5b).

Carbonitriding in the first mode leads to the formation of carbonitride inclusions in the diffusion zone in the form of a mesh, which significantly reduce the plasticity of the layer and, under dynamic loads, become centers of microcrack nucleation.

The results of experimental studies of the microhardness and thickness of the carbonitrided layer of AISI 3415, 105WC6 steels, 45, 37Cr4 and U8 steels for 20 modes according to the Hartley plan were obtained in the work and the dependences of the change in the microhardness H100 of the samples on the depth h of the carbonitrided layer at different technological modes were constructed. From these dependences it follows that when carbonitriding in a glow discharge, as a rule, the highest hardness is obtained on the surface of the part. The latter is explained by the fact that a carbonitride ϵ – phase is formed on the surface of the part, which consists of carbonitrides of the type Fe₂(N,C), Fe₃(N,C), Fe₄(N,C). The carbonitride zone has high hardness, high corrosion resistance, and increased wear resistance. The thickness of the carbonitride zone reaches a thickness of up to 25 μm . Below the carbonitride zone is the internal nitriding zone, which has a large thickness and is the main part of the carbonitrided layer. The internal nitriding zone consists of a nitrogenous solid solution of the base metal, its nitrides and nitrides of alloying elements.

The dependences of thickness and microhardness on the technological parameters of carbonitriding of carbon steels obtained in the work: temperature, saturation time, composition of the gas medium, its pressure allow them to be optimized depending on the requirements of further operation. Thus, previously conducted studies on the wear resistance during dry friction of carbonitrided steel 45 by the developed method showed that to achieve 100 μm of wear, a friction path of 560 km is required, and for the traditional method, 410 km. That is, we have an increase in wear resistance by 1.36 times. It should be noted that with an increase in the content of carbon (steel U8) and alloying elements (steels 37Cr4, AISI 3415, 105WC6) the effect of increasing wear resistance also increases. The developed method of carbonitriding of carbon steels is protected by a patent of Ukraine [10].

Conclusions

Thus, carbonitriding in a glow discharge allows you to change the structure of the hardened layer by changing the technological parameters of the saturation process and, as a result, change its operational properties. Thus, the increase in wear resistance during dry friction of carbonitrided steel 45 by the developed method increases by 1.36 times compared to the known method.

References

1. Method of discrete processing of nitrided steel products [Patent No. 45549 class C23C8/80 dated 10. 11. 2009. Authors: Kindrachuk Myroslav Vasilyevich, Dukhota Oleksandr Ivanovych, Shevchenko Oleksiy Leonidovich, Tisov Oleksandr Viktorovich, Holovko Leonid Fedorovych, Korbut Yevhen Valentinovich, Kindrachuk Vitaliy Myroslavovich.
2. Stechyshyna N.M. Corrosion and mechanical wear resistance of food production equipment parts: monograph / N.M. Stechyshyna, M.S. Stechyshyn, N.S. Mashovets. – Khmelnytskyi: KhNU, 2022.-181p.
3. M. Stechyshyn, M. Macko, O. Dykha, S. Matiukh, J. Musial. Tribotechnologies of strengthening and wear modeling of structural materials. Bydgoszcz: Foundation of Mechglow discharge nitridingonics Development, 2023. 196p.
4. Stechyshyn M. Wear resistance of nitrogenated structural steel with limitand dry friction / M. Stechyshyn, V Oleksandrenko, M. Lukyanyuk // Actual problems of modern science. Monograf: Bydgoszcz, Poland - 2021. - R. 733-740.
5. Stechyshyn M.S. Strength and Plasticity of the Surface Layers of Metals Nitrided in Glow Discharge./ Stechyshyn, M.S., Stechyshyna, N.M., Martynyuk, AV, Lukyanyuk, MM // Materials Science: Springer (USA). - 2018. - 54 (5). - PP. 55-60.DOI: 10.1007/s11003-018-0156-5.
6. M. S. Stechyshyn, NM Stechyshyna, VS Kurskoi. Corrosion and Electrochemical Characteristics of the Metal Surfaces (Nitrided in Glow Discharge) in Model Acid Media March 2018, Volume 53, Issue 5, pp 724.
7. Kaplun V. G., Kaplun V. G. Ionic nitriding in anhydrous media: monograph. Khmelnytskyi: KhNU, 2015. 315 p.
8. Shepherd I. M. Theory and practice of hydrogen-free nitriding in a glow discharge. Kharkiv: National scientific center "Kharkov Physical and Technical Institute", 2006. 364 p.
9. Skyba M.E. Planning of experimental studies of the process of carbonitriding in a glow discharge / M.E. Skyba, M.S. Stechyshyn, M.M. Luk'yanuk, N.M. Stechyshyna, // Problems of friction and wear – Kyiv: NAU, 2020, No. 1(86). – P.78-86.
10. Patent 157997 Ukraine, MPK C23C8/02 (2024.01). Method of separate hydrogen-free carbonitriding in a glow discharge of structural steels / Stechyshyn M.S., Dykha O.V., Stechyshyna N.M., Oleksandrenko E.G. ; applicant and patent owner Khmelnytskyi National University. – u202402891; appl. 30.05.2024; publ. 18.12.2024, bull. No. 51/2024 – 4 p. <https://sis.nipo.gov.ua/uk/search/detail/1833248/>

Стечишин М.С., Диха О.В., Здоренко Д.В., Олександренко Є.Г. Зносостійкість карбоазотованих роздільним способом конструкційних сталей

У статті досліджено вплив технологічних режимів роздільного карбоазотування вуглецевих сталей на товщину та мікротвердість зміцненого шару. При цьому досліджувалося два варіанта зміцнення: спочатку проводилося науглецьовування поверхонь в аргоно-пропановій, а далі азотування в аргоно-азотній сумішах і навпаки. Як показали проведені дослідження, варіант технологічного процесу зміцнення значно впливає на фізико-механічні характеристики зміцненого шару. У всіх двох варіантах технологічного процесу зміцнений шар складається із поверхневої карбонітридної зони та дифузійної зони внутрішнього азотування, але властивості цих зон при різних варіантах технологічного процесу різні. Так, при зміцненні сталей по першому режиму товщина карбонітридної зони максимальна, а зона внутрішнього азотування має невелику товщину. Це пояснюється тим, що створений на поверхні сталі карбонітридний шар на першому етапі обробки виконує функцію екранування поверхні від проникнення в поверхневий шар металу іонів азоту. При зміцненні по другому карбонітридна зона має дещо меншу товщину, але більш розвинену зону внутрішнього азотування. Крім того, карбоазотування за першим режимом приводить до утворення в дифузійній зоні карбонітридних включень у вигляді сітки, які значно знижують пластичність шару і при динамічних навантаженнях являються центрами зародження мікротріщин. Встановлено також, що на поверхні сталей утворюється карбонітридна ϵ – фаза, яка складається із карбонітридів типу $Fe_2(N,C)$, $Fe_3(N,C)$, $Fe_4(N,C)$. Карбонітридна зона має велику твердість, високу корозійну стійкість, підвищений опір зносу. Товщина карбонітридної зони досягає товщини до 25 мкм. Під карбонітридною зоною розташована зона внутрішнього азотування, яка має велику товщину і є основною частиною карбоазотованого шару. Зона внутрішнього азотування складається із азотистого твердого розчину основного металу, його нітридів та нітридів легуючих елементів. Отримані в роботі залежності товщини та мікротвердості від технологічних параметрів карбоазотування вуглецевих сталей: температури, часу насичення, складу газового середовища, його тиску дозволяють їх оптимізувати залежно від вимог подальшої експлуатації. Розроблений спосіб карбоазотування вуглецевих сталей захищено патентом.

Ключові слова: вуглецеві сталі, зносостійкість, карбоазотування, тиск середовища, товщина шару зміцнення



Influence of tribotesting on microhardness of polymers

R. M. Marchuk^{1*}, R. G. Mnatsakanov¹, O. P. Yashchuk¹, O. I. Kushch², D. V. Nyshchuk¹

¹*Kyiv Aviation Institute, Ukraine*

²*National Transport University, Ukraine*

*4629663@stud.kai.edu.ua

Received 25 December 2024; Revised 22 January 2025; Accept 10 February 2025

Abstract

This study investigates the microhardness of the polymeric material Zedex zx-100k and other polymers following tribological testing at different sliding speeds. The primary objective of this research is to select polymers for potential use in composite materials. Microhardness was determined using a PIMT-3 microhardness tester by indenting diamond indenters into samples in various zones – on the initial surface of the material and in the wear area. The results obtained allow evaluating the influence of sliding speed on the change in microhardness of the polymeric material and its behavior under wear conditions. Additionally, the results enable comparison of different polymers tested on a tribometric setup with subsequent assessment of their physical characteristics.

The research highlights the importance of understanding the tribological properties of polymers, as these materials are increasingly being used in various industrial applications due to their favorable characteristics, such as low weight, cost-effectiveness, and chemical resistance. The selection of suitable polymers for composite materials is crucial for enhancing the performance and durability of products in which these materials are used.

Moreover, the study provides insights into the mechanisms of wear and the role of microhardness in the wear resistance of polymers. By analyzing the behavior of polymers under different sliding speeds, the research contributes to the development of more effective materials for engineering applications where high wear resistance is required. The findings suggest that optimizing the sliding speed can significantly impact the wear resistance and longevity of polymer-based components.

In conclusion, this study offers a comprehensive analysis of the microhardness of polymers subjected to tribological testing, providing valuable data for the selection and optimization of materials in composite applications. The methodology and results discussed in the paper can serve as a basis for further research aimed at improving the performance of polymeric materials in demanding operational environments.

Key words: polymers, microhardness, wear resistance, tribological properties, composite materials.

Introduction and statement of the research problem

This study examines the hardness of polymeric materials, which is defined as the ability of a material to resist localized surface deformation under indentation [1]. The hardness of a material can be interpreted in different ways depending on its properties. For example, if hardness is viewed as resistance to touch, steel is harder than rubber. However, if hardness is understood as the ability of a material to resist permanent deformation, then rubber can be considered harder than most metals because its range of elastic deformation is much wider.

Metals, despite having high elastic moduli, have a limited elastic range [2]. Therefore, during hardness testing, the deformation of metals mostly goes beyond the elastic range and turns into plastic deformation. In the case of polymers, the situation is even more complicated. Polymers can exhibit both elastic and plastic properties depending on their composition, operating conditions, and temperature [3]. For example, some polymers can change their hardness in the area of contact with other materials, which can be considered a surface hardening effect similar to the scaling in metals. This feature is important for assessing the wear resistance of polymers under different sliding conditions.

The study of microhardness of polymers has been of interest due to the need for a deeper understanding of their behavior under load, as the viscoelastic properties of plastics significantly affect test results. Since plastics exhibit both elastic and viscoelastic properties, testing their hardness requires taking into account phenomena such as creep under load and time-dependent recovery after load removal. It is known that the term “hardness” covers



many different aspects: scratch hardness, rebound, deformation, etc. In the case of viscoelastic materials, such as polymers, hardness properties can change depending on the time of loading, which necessitates the selection of a well-defined test method for accurate comparisons [4].

From a practical point of view, microhardness testing of polymeric materials has significant potential as a non-destructive method for assessing the quality of polymeric products [5]. For example, microhardness results can correlate with parameters such as polymer morphology, density, orientation effects, and even mechanical properties during molding. In addition, microhardness results can help in the study of stress, polymerization, water dissipation, and durability parameters of polymer coatings, which is particularly valuable for understanding the long-term stability of polymers in service [6].

Materials and methods of research

In this study, the following polymeric materials produced by the Röchling Group were selected: Sustamid 6G OL yellow, Sustamid 66 gray, Sustadur PET white, Sustapeek GF30, Sustamid 6 black, Sustapei transparent, Sustadur GLD white, Zedex zx-100k.

All samples were subjected to standard preparation prior to testing, including dirt removal and degreasing to prevent the influence of foreign substances on the results of microhardness measurements.

The Sustamid 6, Sustapei, Sustamid 6G OL, Sustapeek GF30, Sustadur GLD, Sustamid 66 and Sustadur PET materials were tested at a sliding speed of 2.8 m/s, which provided standardized conditions for evaluating their characteristics.

After the initial series of tests on a tribometric machine [7] under the same conditions, it was determined that the Zedex zx-100k material showed the best results and was selected for further experiments. This material was additionally tested at three sliding speeds: 1.4, 2.8, and 5.5 m/s.

The hardness of the tested samples was evaluated using a PMT-3 microhardness tester with a diamond indenter. The indenter has the shape of a tetrahedral diamond pyramid with an angle of 136 degrees at the top, which ensures high accuracy of indentation and measurement of the microhardness of polymers.

The microhardness tests were performed both for the original surface that was not subjected to friction and for the surface in the friction track zone, which allowed comparing the effect of the tribological experiment on changes in microhardness. The load applied during indentation was 0.39 N for all samples.

The main indentation hardness tests can be divided into two categories:

1. Tests that evaluate the residual strain after application and removal of the indenter (such tests are typically used for metals, as they measure the hysteresis or elastic function).
2. Tests that evaluate the load and strain characteristics, which are used for polymers because they measure the elastic modulus function.

The method of the second category was used to test polymers, since it allows taking into account the peculiarities of viscoelastic deformation of polymers, ensuring the accuracy of the assessment of their microhardness under loading conditions. [8].

The friction tests were performed using a counterpart made of 30KhGSA steel, which had the following characteristics: HRC = 43 and Ra = 0.37 μm . The contact surface of the polymers interacted with the steel counterbody during friction, which allowed for standardized loading conditions for each sample and ensured comparability of results.

The process of assessing the microhardness of polymers requires taking into account their viscoelastic properties, as polymers tend to deform significantly under load. To reduce the influence of viscoelastic deformation and ensure the stability of the results, the measurements were performed a short time after the indenter was inserted. The experiments took into account the change in microhardness of the samples in the friction zone, which may be due to the phenomenon of sticking, characteristic of polymers under specific loading conditions. This allows for a deeper understanding of the mechanism of behavior of polymeric materials under friction and wear.

Purpose

The aim of the study is to analyze in detail the changes in the microhardness of polymeric materials under different sliding speed conditions, using Zedex zx-100k as a base material for testing. In the course of the study, the microhardness of polymer samples is evaluated before and after tribometric loading, which allows establishing the regularities of changes in the physical and mechanical properties of the material under the influence of various operating conditions. Particular attention is paid to the change in microhardness in the contact zone, which is an important indicator for assessing the wear resistance and durability of polymeric materials.

Results

The study evaluated the changes in the microhardness of various polymeric materials after testing on a tribometric setup. An important aspect was the comparison of the microhardness values on the original surface and on the friction track, which made it possible to assess the trend of changes in the microhardness of the material after the experiment. The Sustapeek GF30 material (Fig. 1), like other samples, was measured on the PMT-3 installation using a diamond indenter, which allows obtaining accurate hardness results that are important for understanding the wear resistance and mechanical stability of polymers.

Table 1 shows the results of changes in the microhardness of polymeric materials. The deviation values show the difference between the original surface and the contact zone where friction was observed. Negative values (weakening) indicate a loss of hardness after friction, which may indicate a decrease in the material's strength under load. For example, the Sustamid 6 material has a significant weakening, with a deviation of -1296.8, which may indicate a decrease in its resistance to prolonged friction.

Particular attention was paid to the Zedex material, which was tested in three sliding speed regimes to investigate the effect of different operating conditions. Samples Zedex No. 1 (5.5 m/s), Zedex No. 2 (2.8 m/s) and Zedex No. 3 (1.4 m/s), conventionally numbered to simplify the analysis, show different hardening rates with increasing sliding speed, which may be useful for further optimization of the material depending on the conditions of use.



Fig. 1. Image of the microhardness tester imprint on the surface of Sustapeek GF30 material.

In the process of studying the microhardness of polymers after friction with a metal counterbody, one can observe the phenomena of mechanical destruction and thermal destruction of polymeric materials, which have a key impact on the parameters of the contact zone. Mechanodegradation occurs due to the influence of mechanical load, which leads to the destruction of molecular bonds and a decrease in the integrity of the polymer structure. This destruction is associated with microscopic deformations and cracks that gradually accumulate on the polymer surface, especially in areas of high pressure, such as the contact zone with a metal counterbody. Mechanodestruction is an important wear factor because it leads to degradation of physical properties such as hardness and, ultimately, to a reduction in material life.

In addition to mechanical degradation, thermal degradation of polymeric materials occurs under friction at high speeds. It is caused by a significant increase in the temperature in the contact zone, when it sometimes exceeds the operating range of the material. When critical temperature values are reached, some polymers begin to lose structural stability, which can lead to softening, loss of stiffness, or even chemical degradation. Thermal degradation can lead to partial melting or oxidation of the surface layers of the polymer, which reduces its mechanical strength. It is this fracture mechanism that explains the microhardness deviation value for Zedex #1, which showed the least tendency to harden after testing at the highest quench rate.

Table 1

Results of Changes in Microhardness of Polymeric Materials

Material	Microhardness H ₄₀ , MIIa				Weight wear, g
	The original surface	The friction track	ΔH		Δm
Sustamid 6	1830.1	533.3	1296.8	weakening	0.3147
Sustapei	996.5	337.7	658.8	weakening	0.1800
Sustamid 6G OL	1313.6	1037.9	275.7	weakening	0.1996
Sustapeek GF30	738.9	500.3	238.6	weakening	0.1232
Sustadur GLD	658.8	569.7	89.2	weakening	0.0836
Sustamid 66	398.9	328.4	70.4	weakening	0.1178
Sustadur PET	260.6	798.8	538.2	strengthening	0.0458
Zedex zx-100k (№1)	158.4	214.1	55.7	strengthening	0.0354
Zedex zx-100k (№2)	158.4	293.5	135.0	strengthening	0.0184
Zedex zx-100k (№3)	158.4	305.4	147.0	strengthening	0.0094

The increase in the microhardness of polymers under tribotechnical loading can be explained by both mechanical and morphological factors. First, the mechanical strengthening of the surface layer due to local deformation from friction leads to its compaction and orientation of molecules in the direction of the load. This contributes to the creation of a denser and more stable structure, which has a positive effect on microhardness. This effect often occurs as a result of slandering, which, although typical for metals, can also occur in polymeric

materials under certain conditions. The results of the studies of weight wear and microhardness of materials are shown in Figure 2. The graphs demonstrate the relationship between the mechanical properties of materials and their resistance to wear.

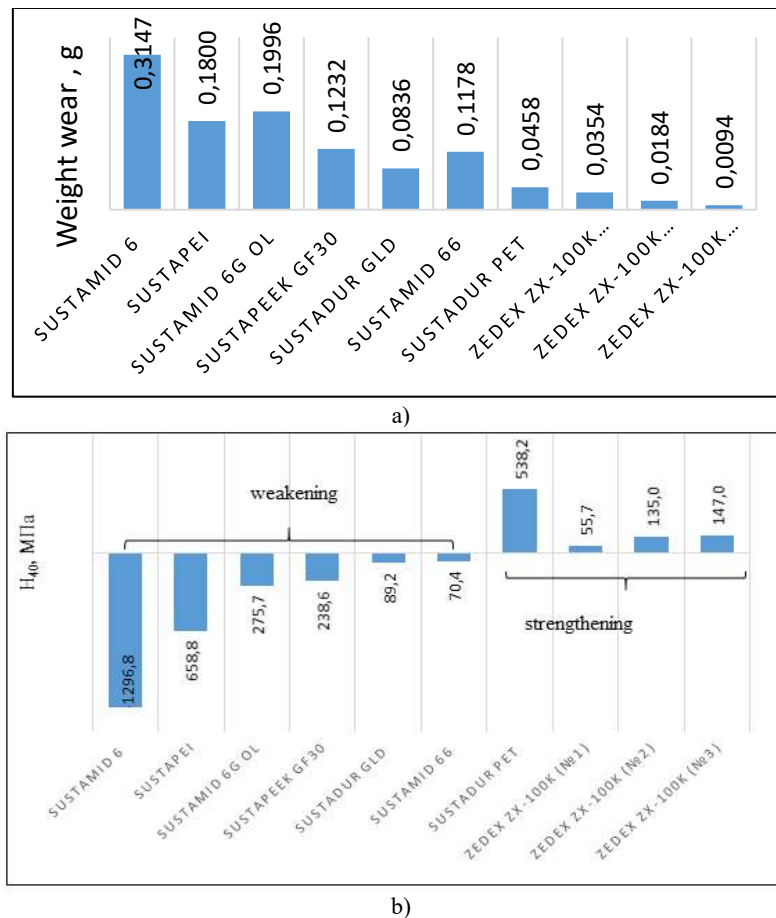


Fig. 2. Comparison of weight wear (a) and microhardness (b) of materials: results of experimental studies.

Second, morphological changes that occur in the surface layers of polymers during friction play an important role. Increased temperature and mechanical loading can promote partial crystallization of the polymer, which leads to the formation of a more structured, oriented microstructure. This is especially true for partially crystalline polymers [9], which are capable of changing their morphology under heating conditions. Such structural changes increase the material's resistance to external influences and contribute to the growth of microhardness.

Conclusions

The study has shown that the polymeric material Zedex zx-100k (No. 1) has a positive tendency to strengthen even at high sliding speeds. Despite the recorded destruction of the surface in the contact zone, a slight strengthening of the material was observed after the test was completed. This indicates the ability of Zedex zx-100k to withstand significant loads and maintain its structural integrity, which is an important factor for its use in composite materials operating in harsh environments.

Comparison of the microhardness of polymers allows us to determine the optimal operating conditions for each material. In particular, an increase in hardness in the friction zone indicates the ability of polymeric materials to adapt structurally in response to mechanical loading, which is a promising factor for their selection as matrices in composite materials. The decision to choose Zedex zx-100k for a more in-depth analysis was justified, as this material proved to be resistant to deformation and showed a tendency to increase microhardness after testing on a tribometric machine.

In addition, it was noted that the processes of mechanical degradation and thermal degradation play a key role in the behavior of polymers during operation. The temperature rise in the contact zone sometimes exceeded the operating range of the materials, which caused structural changes in the surface layers of polymers. Accordingly, the selection of polymeric materials based on their temperature and mechanical characteristics is important to increase their durability and stability. Careful selection of materials can help to minimize the negative impact of destructive processes on polymer parts operating in harsh environments.

Thus, the results of the study confirm the prospects of using polymeric materials, in particular Zedex zx-100k, in composites subjected to significant loads. This opens up new opportunities for improving polymer composites that can adapt to operating conditions and demonstrate increased wear resistance and strength.

References

1. Tabor D. *The Hardness of Metals*. Oxford, 2000; online edn, Oxford Academic, 31 Oct. 2023). <https://doi.org/10.1093/oso/9780198507765.001.0001> [English]
2. Belenkiy L. M., Raskin Y. N., Vuillemin J. *Effective plating in elastic–plastic range of primary support members in double-skin ship structures*. *Marine Structures*. 2007. Vol. 20, Is. 3. P. 115-123. <https://doi.org/10.1016/j.marstruc.2007.06.002> [English]
3. Baltá Calleja FJ, Fakirov S. *Microhardness determination in polymeric materials*. In: *Microhardness of Polymers*. Cambridge Solid State Science Series. Cambridge University Press; 2000. P.11-45. <https://doi.org/10.1017/CBO9780511565021> [English]
4. Wodtke M., Wasilczuk M. Evaluation of apparent Young's modulus of the composite polymer layers used as sliding surfaces in hydrodynamic thrust bearings. *Tribology International*. 2016. Vol. 97. P. 244-252. <https://doi.org/10.1016/j.triboint.2016.01.040> [English]
5. Lopez J. Microhardness Testing of Plastics: Literature Review. *Polymer Testing*. 1993. 12. P.437-458. [English]
6. Goyal R. K., Tiwari N., Negi Y. S. Microhardness of PEEK/ceramic micro- and nanocomposites: Correlation with Halpin–Tsai model. *Materials Science and Engineering A*. 2008. 491(1-2). P. 230-236. DOI: [10.1016/j.msea.2008.01.091](https://doi.org/10.1016/j.msea.2008.01.091) [English]
7. Marchuk R. M., Mnatsakanov R. G. Analysis of Basic Functional Parameters of Surface Microrelief Roughness of Polymers. *Problems of Friction and Wear*, 2024, 2(103), pp. 130-138. [https://doi.org/10.18372/0370-2197.2\(103\).18695](https://doi.org/10.18372/0370-2197.2(103).18695) [Ukrainian]
8. Crawford R. J. Microhardness testing of plastics. *Polymer Testing*. 1982. 3(1). P. 37-54. [https://doi.org/10.1016/0142-9418\(82\)90011-3](https://doi.org/10.1016/0142-9418(82)90011-3) [English]
9. Мікульонюк І. О. Технологічні основи перероблення полімерних матеріалів [Електронний ресурс]: навч. посіб., 2-ге вид., переробл. та доповн.; КПІ ім. Ігоря Сікорського.– Київ : КПІ ім. Ігоря Сікорського, 2020. 292 с. <https://ela.kpi.ua/server/api/core/bitstreams/a01b3f86-c11f-49e8-8dc5-49c03b765a0e/content> [Ukrainian]

Марчук Р. М., Мнацаканов Р.Г., Ящук О. П., Куш О. І., Нищук Д. В. Вплив триботестування на мікротвердість полімерів

У цьому дослідженні вивчається мікротвердість полімерного матеріалу Zedex zx-100k та інших полімерів після триботестування за різних швидкостей ковзання. Основна мета цього дослідження – відібрати полімери для потенційного використання в складі композиційних матеріалів. Мікротвердість визначали за допомогою мікротвердоміра ПМТ-3. Отримані результати дозволяють оцінити вплив швидкості ковзання на зміну мікротвердості полімерного матеріалу та його поведінку в умовах зносу. Крім того, результати дозволяють порівняти різні полімери, що тестувалися на трибометричній установці, із подальшою оцінкою їх фізичних характеристик.

Дослідження підкреслює важливість розуміння трибологічних властивостей полімерів, оскільки ці матеріали дедалі більше використовуються у різних промислових галузях завдяки їхнім сприятливим характеристикам, таким як низька вага, економічна ефективність та хімічна стійкість. Вибір відповідних полімерів для композитних матеріалів є ключовим для покращення продуктивності та довговічності виробів, у яких ці матеріали використовуються. Крім того, дослідження надає розуміння механізмів зношування та ролі мікротвердості у зносостійкості полімерів. Аналізуючи поведінку полімерів за різних швидкостей ковзання, дослідження сприяє розробці більш ефективних матеріалів для інженерних застосувань, де вимагається висока зносостійкість. Результати показують, що оптимізація швидкості ковзання може суттєво вплинути на зносостійкість та тривалість служби полімерних компонентів.

У підсумку, це дослідження пропонує комплексний аналіз мікротвердості полімерів після триботестування, надаючи цінні дані для вибору та оптимізації матеріалів у композитних застосуваннях. Методологія та результати, обговорені у статті, можуть слугувати основою для подальших досліджень, спрямованих на покращення характеристик полімерних матеріалів у складних експлуатаційних умовах..

Ключові слова: полімери, мікротвердість, зносостійкість, трибологічні властивості, композиційні матеріали



Improving the wear resistance of guides: tribological analysis, surface texture and lubricants

O.V. Dykha^{*}, V.O. Dytyniuk, O.S. Kovtun, V.O. Fasolia, M.V. Hetman

Khmelnytskyi national University, Ukraine

**E-mail: tribosenator@gmail.com*

Received: 15 Decemberr 2024; Revised 10 February 2025; Accept: 28 February 2025

Abstract

The article considers the main failure modes of guides, in particular wear and contact fatigue, which depend on friction between contact surfaces. The influence of tribological parameters, in particular surface roughness and lubricating structures, on the operational characteristics of linear guides is studied. Particular attention is paid to the dynamic behavior of guides, which determines the accuracy and stability of mechanical systems. To predict wear, mathematical models based on the Archard and Hertz theories were used, which allow estimating load distribution and contact deformations. The influence of lubricants, in particular molybdenum disulfide and hexagonal boron nitride, on reducing the friction coefficient and improving antifriction properties was separately studied. The prospects for using new materials, such as cubic boron nitride, to increase the wear resistance of guides are considered. Methods for optimizing the load between rolling elements, which contributes to increasing the durability of guides, are proposed. The results obtained can be used to improve the designs of high-precision mechanical systems and reduce operating costs.

Keywords: wear, friction, contact fatigue, stiffness, lubricating structures, guideway dynamics, load optimization

Introduction

Guideways are one of the key components of mechanical systems that ensure the accuracy and stability of movement in various technical devices. They are widely used in industrial machines, lathes, conveyor systems, and other high-precision mechanisms. One of the main issues that arises during the operation of guideways is wear, which largely depends on the friction between the contact surfaces. As a result of prolonged use, guideways can experience significant deformation, reducing their efficiency and requiring frequent maintenance or replacement.

One of the key factors affecting wear is the surface texture of the contacting elements, as well as the choice of lubricating materials. Inadequate surface roughness parameters and improper lubricant selection can increase the friction coefficient, which, in turn, accelerates wear. However, optimizing the surface texture and using specialized lubricating materials can significantly reduce this effect. Therefore, one of the priority areas of research is the analysis of the impact of various factors on the tribological characteristics of guideways, which allows the development of new methods for improving their wear resistance.

In particular, studies have shown that using composite lubricants containing molybdenum disulfide, hexagonal boron nitride, and other promising additives can significantly improve friction and wear resistance of guideways. At the same time, optimizing the geometry of the contact surfaces and controlling the lubrication process are necessary to achieve maximum efficiency of mechanical systems.

Thus, the problem of wear resistance of guideways and optimizing their characteristics is relevant and requires further scientific development, which will contribute to increasing their lifespan and improving the reliability of mechanical systems.

Main material

The most common failure modes of the guide are wear and contact fatigue, which are significantly affected by the friction properties of the contact surfaces. In the paper [1], the parameters of the three-dimensional rough surface are investigated for the evaluation of the guide. First, an effective three-dimensional surface model is



achieved using the wavelet transform method and reverse engineering software. Second, the influence of the parameters of the functional surface on the friction force, average pressure and friction coefficient is studied using the computational fluid dynamics modeling method, and a regression model is built to predict the friction force. Third, the combinations of optimal surface parameters are analyzed considering the friction index and the simulation results are compared. The results show good agreement between the experimental results and the simulation. This study provides theoretical guidance for the fabrication of the guide.

Roller linear guide is a type of precision linear motion component that is widely used [2]. Stiffness and wear directly affect the performance and service life of roller linear guides. Therefore, the study of stiffness and wear is important for optimizing the design and improving the performance of roller linear guides. The study analyzes the contact mechanics between the roller and the raceway and the deformation of the roller. Using Archard's wear theory, the wear process of roller linear guides is analyzed. A calculation model of the slider movement, which is related to the wear loss of the slider's raceway during its reciprocating motion under load, is developed to predict the wear of roller linear guides. The effectiveness of the proposed models in predicting the contact stiffness and wear is verified through simulation and experiments on a specialized test system.

Guides adapt to the movement of tools or workpieces, and their dynamic behavior and associated sliding effects have a great influence on accuracy, stability, and productivity [3]. During machining, guides are subjected to oscillatory excitations due to cutting forces, which requires consideration of their pre-slip behavior along with the sliding characteristics to compensate for the associated tracking errors by the position control system. The study [3] considers the friction effects in the pre-slip and sliding modes of lubricated linear roller guide systems to provide an accurate dynamic model of the machine tool element. To simulate the dynamic characteristics of the frictional contact in a lubricated linear roller guide, which is commonly used in the machine tool positioning control system to estimate the compensating driving force, a modified approach is used to consider the contact physics of rollers and tracks and the dynamics of the lubricating film. The proposed model also includes the effects of the coupling between normal and tangential forces in the contact (Fig. 1).

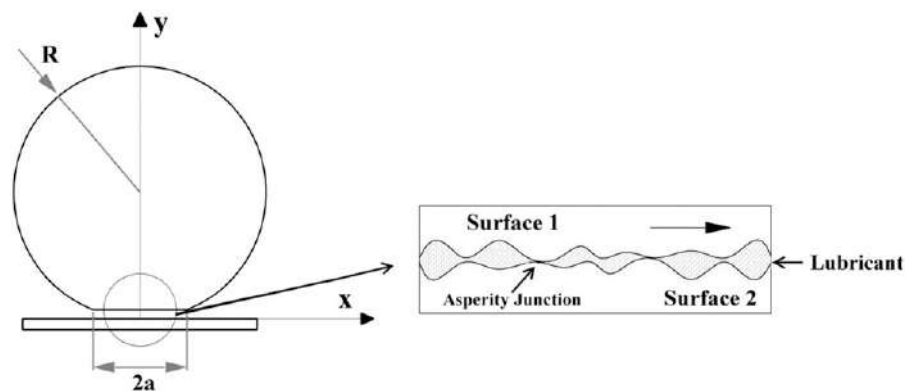


Fig. 1. Schematic representation of an elastohydrodynamic lubricating contact in a mixed lubrication mode [3]

Experimental studies were conducted on a lubricated linear roller guideway to verify the performance of the proposed modified model. The experimental observations illustrate the dynamic behavior of friction in a lubricated linear guideway. Comparison of experimentally measured data and the proposed modified samples shows that the model can accurately predict the dynamic behavior of the frictional contact.

To optimize the sliding phenomenon under low speed and high load conditions, a composite lubrication structure is used [4]. The optimal response surface design method establishes a quadratic mathematical model for the multi-stage parameters of the composite lubrication structure, including creep time and average friction coefficient. The optimal combined parameters of the multi-stage composite lubrication structures are determined. The optimal ratio of lubricant to molybdenum disulfide was identified, and a composite lubrication structure was proposed to improve the sliding phenomenon and friction efficiency of sliding guide rails under medium speed and medium load conditions. The results of these studies show that when low speed and high load are present, the creep time and friction coefficient first decrease and then increase as the width, distance, and cycle length of the sinusoidal texture and the diameter of the hexagonal pit expand. Under the circumstances of medium load and speed, the multi-stage composite lubrication structures exhibit superior friction performance. These data can guide the design of multi-stage composite lubrication structures on the surface of slideways.

In order to improve the sliding of guides [5], the design of a composite lubricating structure on the surfaces of sliding guides and the characteristics of the friction force were investigated step by step. The composite lubricating microtexture was prepared by the high temperature and high pressure mosaic method based on the laser ablation microtexture. The general scheme of the formation of structured surfaces by laser is shown in Fig. 2.

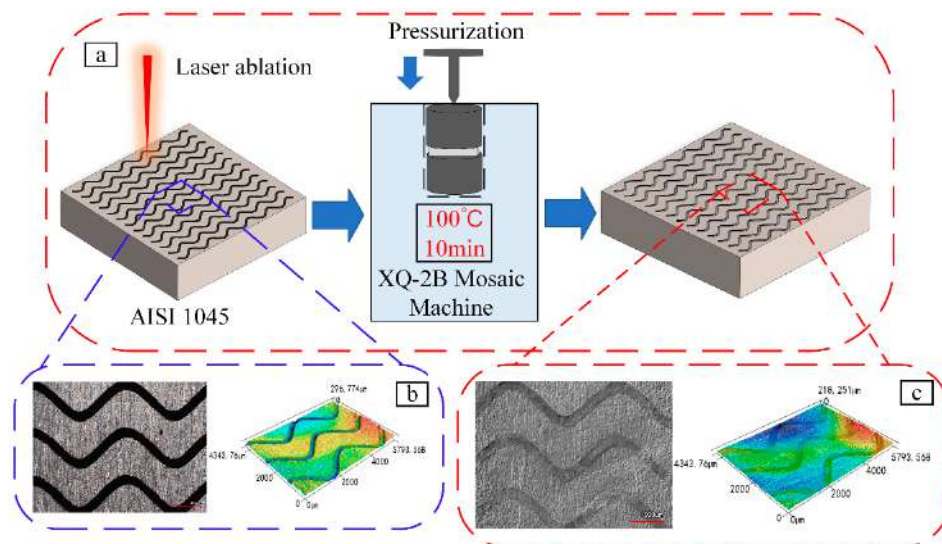


Fig.. 2. Schematic diagram of specimen preparation: (a) Laser ablation diagram. (b) Micro-texture before filling. (c) Micro-texture after filling [4]

The friction force characterization methods were proposed step by step by friction tests. The effects of different composite lubricant structures on the friction characteristic parameters of each stage were investigated. Theoretical models of composite lubricant structures for improving the creep phenomenon were established, and composite lubricant structures with the best characteristics for reducing the influence of the creep phenomenon were found. The results show that the surface microtexture only affects the sliding and rising stages of the friction force, while the composite lubricant texture has a significant effect on the entire starting stage. The multi-stage composite lubricant texture with a combination of sinusoidal grooves and hexagonal pits filled with molybdenum disulfide was the most effective in improving the surface contact conditions and suppressing the creep phenomenon (Fig. 3).

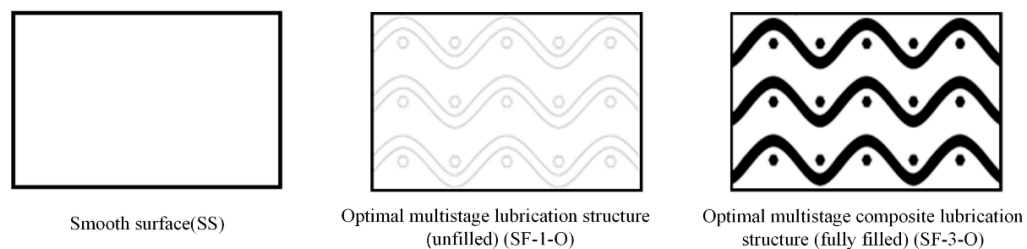


Fig. 3. Diagram of different grease textures

To study the effect of different surface treatment methods on the antifriction performance of Babbitt-Steel 45 alloy pair, hexagonal boron nitride was encapsulated in the surface texture, and composite lubricating structure surfaces were prepared [6]. The disc wear test was carried out with lubricant, and the wear process was separated by quantitative analysis. The antifriction performance of composite lubricating structure surfaces during running-in and normal wear was investigated. The results show that the composite lubricating structure surfaces have a lower friction coefficient and that the antifriction performance is better than that of the texture surface alone. Compared with the surface without texture, the average friction coefficient of the composite lubricating structure surfaces decreases by 77% during the running-in period and 68% during the normal wear period. Composite lubricating structure surfaces with larger texture pore diameter have better antifriction performance and shorter running-in period. Both textured surfaces and composite surfaces of the lubricating structure have more significant anti-friction characteristics at higher speeds. It has been found that the lower the friction coefficient of different surfaces during the break-in period, the lower the corresponding friction coefficient after entering the normal wear period.

Reducing sliding wear and friction in guide bearings can bring both economic and environmental benefits, including longer service life, lower operating costs, and higher efficiency. In a study [7], the effect of stainless steel countersurface roughness on the tribological behavior of three bearing materials used in hydropower was evaluated using linear reciprocating motion at high contact pressure and low sliding speed. Surface roughness was measured using white light interferometry. The results of this study show that surfaces that are too smooth lead to greater friction and wear of the countersurface, while rougher surfaces negatively affect polymer wear (Fig. 4).

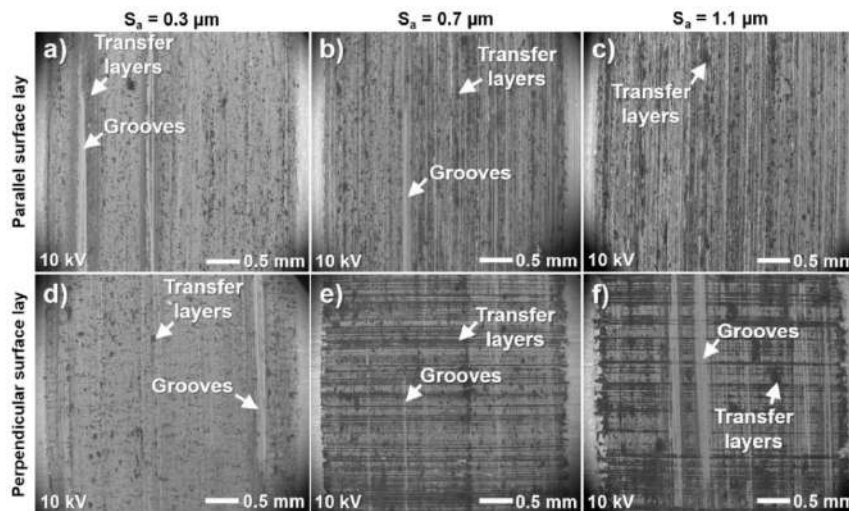


Fig. 4. SEM micrographs of transfer layers formed on polished stainless steel closer to the center of the wear track after sliding on fiber-reinforced thermoset [7]

The best surface coverage by protective transfer layers is found on steel surfaces with perpendicular stacking and is accompanied by a lower coefficient of friction compared to parallel stacking. The dominant wear mechanism of the bearing materials changes from delamination wear to abrasive wear between the lowest and intermediate roughness of the steel surfaces with parallel stacking. It is concluded that the relief of the opposing surface has a significant effect on the tribological behavior of these bearing materials and that the effect differs between self-lubricating polymer composites.

In [8-9], an experimentally validated numerical approach to the evaluation of linear guideway wear is presented, taking into account the associated vertical and horizontal movements and taking into account the lubrication starvation. The results show that the lubrication starvation has a pronounced effect on the thickness of the lubricating film, friction and the applied load at contact up to 30%. The localized pressure values can vary. The course of the starvation effect depends on the frequency. It was also found that the starvation effect can be controlled by the magnitude of the preload on the linear guide.

Based on the theory of point contact elastohydrodynamic lubrication, a model of free vibration of a contact pair is presented for qualitative analysis of the influence of vibration on film characteristics [10]. Models of film stiffness and damping coefficient under elastohydrodynamic lubrication are constructed to study the influence of operating conditions on dynamic parameters. Complete numerical solutions are obtained using multi-grid techniques. It is found that there is damping from the decay of pressure fluctuations and film thickness in a lubricated ball linear guide. In addition, high load or low speed operating conditions can lead to an increase in film stiffness at the steel ball-guide contact, but there is a tendency for the film damping coefficient to vary inversely. The study [11] studies the contact stiffness of linear rolling guides due to the effects of friction and wear during operation. The initial and final contact stiffness models were established. As a confirmation of the predicted variable stiffness, an experimental modal analysis was performed on a specialized linear guide system. The results show that the contact stiffness of linear guides decreases with the increase of the friction path, and the entire stiffness decline can be divided into two different stages depending on how the thermal effect and wear effect affect the contact deformations of the balls at different rolling distances.

The aim of [12] is to establish a simplified model of a closed hydrostatic guideway for rapid analysis of static and dynamic characteristics. In addition, the effects of compressibility and dynamic frequency are taken into account in the new dynamic model. The new model is based on the second type of Lagrange equation. In this model, a closed hydrostatic guideway is supported by 10 gaskets, and each oil gasket is equivalent to a nonlinear spring-damper system. The equivalent spring coefficient and the damper coefficient of the oil gasket are considered by three different equivalent methods. Verification experiments of the step load response and dynamic stiffness are carried out on the hydrostatic guideway.

Most studies on linear rolling bearings usually assume that the contact load between the ball and the raceway is uniform, which leads to deviations from the actual conditions. The study [13] aims to establish a load distribution model based on the Hertzian contact theory with combined ball obstacles that are transformed from the preload, the center distance error of the ball raceway. The reliability of the proposed model is verified by numerical methods for load distribution and deformation analysis. The result shows that the proposed approach is in better agreement with the experimental results compared with the preload effect alone. This work can be an important starting point for studying the friction and wear of equipment guide elements.

Hydrostatic guides have been used as an important element of precision engineering in numerous applications requiring high-precision motion and positioning with significant load capacity. Hydrostatic guides provide good operational performance, especially in terms of high rigidity and damping characteristics, but also its high load capacity combined with excellent motion accuracy. However, a comprehensive review of hydrostatic

guides has not been reported so far. The paper [14] aimed to present an informative literature review of research and engineering developments on hydrostatic guides, describing their basic operating principles and applications in precision machines, defining and characterizing hydrostatic guide concepts, briefly reviewing motion error modeling and compensation types, discussing the impact characteristics, and further discussing emerging issues of sliding guides and their engineering applications.

In [15], in order to expand the production of machine tools that use precision-machined slideways, cubic boron nitride was implemented as an alternative machining process to conventional surface grinding. While higher material removal rates can be achieved with a milling strategy, the use of a defined cutting edge results in surfaces with irregularities. These sharp peaks wear quickly during sliding contact, leading to unacceptable changes in the bearing surface of the guide. This paper investigates the use of a spindle-mounted abrasive disk tool to fabricate a functional surface. The optimal process parameters were investigated using 2D profile measurements and then compared using an analysis of ground, milled and polished surfaces. Polishing was found to reduce both the height and volume of irregularities on the milled surface, resulting in contact characteristics that were more similar to those of conventional surfaces currently used for slideways.

For economic, environmental and even technical reasons, there has been a trend for several years towards the introduction of self-lubricating materials for cylindrical slideways. This makes it possible to eliminate external lubricants, simplify the design and reduce maintenance costs. Among self-lubricating materials, the so-called engineering plastics are of increasing importance. Unfortunately, data on their friction and wear characteristics are very different, and there is often a lack of a common understanding of the physical mechanism of their action. In the article [16], some types of oil-filled engineering plastics are experimentally investigated using small-scale reciprocating tribotesting. The dependences for the coefficient of friction for such types of materials are shown in Fig. 5.

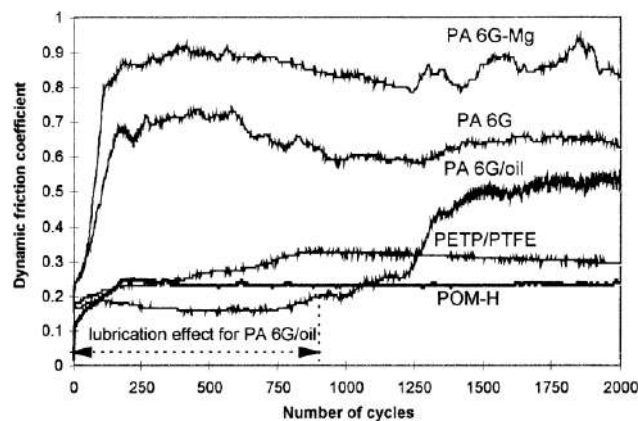


Fig. 5. Dynamic friction characteristic of polymers against smooth steel surface [16]

Tribological behavior is explained in relation to the chemical and mechanical properties of materials. The main failure processes are described for light wear conditions as well as for overload conditions.

In the article [17] a new experimental apparatus is presented, suitable for wear tests of reciprocating guides at elevated temperatures (Fig. 6).

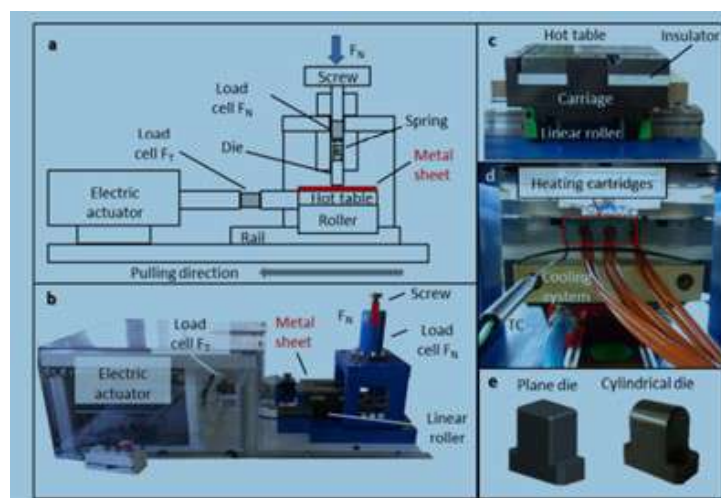


Fig. 6. (a) Schematic representation of flat strip drawing test and (b) the real version; (c) Details of the linear roller guideway; (d) Details of the hot table heating system, thermocouple to control temperature and the cooling system; (e) Plane and cylindrical die shape usable in the machine [17]

It consists of a linear slide rail connected to an electric drive and equipped with a heating plate for heating the metal sheets. The solid frame incorporates a screw device used to apply the normal load. Thermocouples placed on both the plate and the sheet sample are used to monitor the temperature during the test. The machine is also equipped with two strain gauges to record the normal and tangential loads. High-strength steel was chosen as the reference material for testing the machine. The results showed the operational capability of the new equipment and good stability of the mechanical and thermal state during the tests.

In recent years, sliding guides have been re-examined as linear motion guides for machine tools due to the demand for machines with good dynamic characteristics, which is vital in machining difficult-to-machine materials. While the traditional approach to manufacturing the sliding surface is grinding. In [18-20], an alternative manufacturing approach based on cubic boron nitride using Al and Mg additives in the cast iron material for better machinability of sliding guides was investigated. The machining results showed a significant improvement in machinability, especially in terms of tool wear under certain cutting conditions using cleaned hardened cast iron and cubonite tools. During experimental analysis, it was found that oxide films of the additives were created on the cutting edge of the tool to protect the tool from wear. By reducing tool wear, a stable surface roughness can also be achieved. The case study also demonstrated the effectiveness of a manufacturing approach based on milling slideways with cleaned cast iron and found high-speed cutting conditions.

The characteristics between the rolling balls and the raceways are key to studying the linear rolling guide. In [21-22], the contact stresses with non-standard sized balls, which include the change of contact angle, are given by the established joint model (Fig. 7).

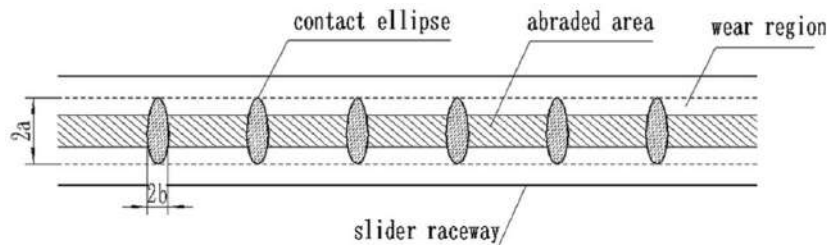


Fig. 7. Contact mechanism between the balls and the carriage raceway [22]

In addition, the influence of the location, number and degree of deviation of non-dimensional balls on the stress distribution is studied. The contact stress distribution between the ball and the raceway is analyzed for different location cases. The effectiveness of the contact stiffness and wear prediction model is verified by simulation and analysis.

In articles [23-24], favorable microdimples from the calculated results were fabricated on a guide using single-pulse process intervals with a specialized accuracy compensation method (Fig. 8).

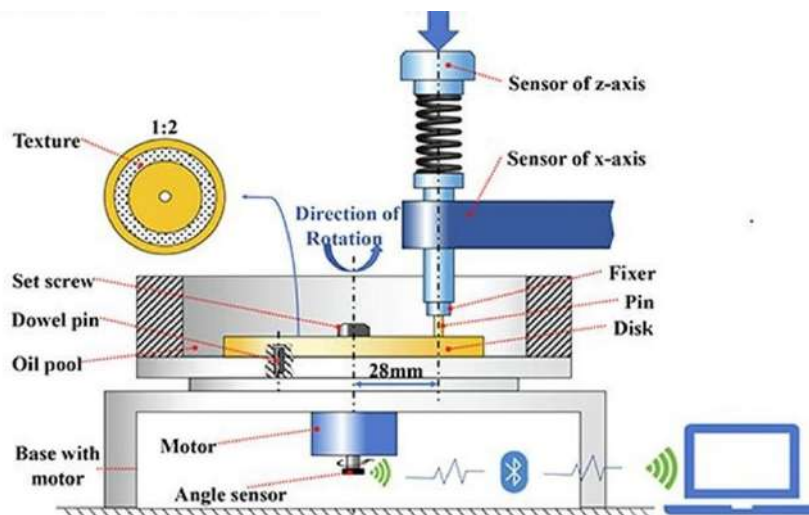


Fig. 8. Experimental setup for the formation and study of surface microprofiles [24]

Contrast tests were conducted to verify the anti-slip performance. The results showed that the favorable micro-dimple depth size could be 1-5 μm , and the area ratio was 11%~16%. The friction coefficient was reduced by 15%.

At present, the wear models and the prediction of the accuracy of the guide are established based on the elastoplastic mechanics of continuum media. These methods are limited to describing the process of accuracy

reduction using the material characteristics determined based on the conditions of the macroscopic hypothesis. In [25-26], a multi-scale method based on the principle of a quasi-continuous medium is proposed to describe the degradation process of the linear accuracy of the guide using an exponential model. According to the distribution of the wear of the guide surface with the process of micromorphology evolution, the measurement value of the linear accuracy of the guide is systematically modeled. Using the quasi-continuous medium method instead of the continuum hypothesis, an exponential model of the guide wear is established. The exponential wear model uses a wear index to describe the wear state based on the measurement of linear accuracy, rather than long-term wear products. Information about the microtopography of the guide surface is obtained. Thus, the wear condition of the guide is checked under different loading conditions, and the validity of using the method to establish an exponential guide wear model is also verified.

Solid lubricants have been widely used in many fields. In [27-28], the influence of each component in composite solid lubricants on the tribological characteristics is investigated and the antifriction effect of different types of solid lubricants is compared to solve the problem of lubrication of cylindrical sliding guides (Fig. 9). Surface textures with pits were produced on the surfaces of bearing steel by solid-state laser. Composite solid lubricants filled the micropits with heat- and pressure-supported deposition products consisting of lubricating elements. The tribological characteristics of sliding friction for different types of lubricants with different grain sizes were evaluated using a ring-on-disk tribometer.



Fig. 9. Experimental tests of solid lubricants for contact strength [28]

On this basis, an orthogonal experiment with four factors and three levels was designed to investigate the effects of different components of solid lubricants on tribological characteristics. Solid lubricants with nanoparticles can improve the antifriction ability: the friction coefficient is higher than that of micron graphite, and the friction coefficient of nano-sized molybdenum disulfide is reduced compared with that of micron-sized molybdenum disulfide. According to the experimental results, the optimal formula of composite solid lubricants was graphite nanotubes: molybdenum disulfide: polyamide: carbon.

The improvement of tribological properties by applying different textured surfaces has been reported by many researchers. In these studies, most of the surfaces used were textured by lasers. However, this texturing method has several problems, including thermal effects, accumulation formation, possible pit shapes, and lower efficiency than mechanical methods. Traditional mechanical texturing methods also have some problems. In the study [29], an alternative method was developed using vibrocutting using a diamond indenter that vibrates in the depth direction with an amplitude of tens of microns. The asperities formed around all the pits during texturing can be removed by additionally performing conventional microcutting. Dry sliding tests were performed using steel balls on surfaces textured by both the proposed and conventional methods for comparison. A series of sliding test results were analyzed using the coefficient of friction and observations of worn surfaces. As a result, the textured surface obtained with a relatively high areal density (40%) where the inclusions were completely removed showed the lowest coefficient of friction and wear. Thus, the proposed texturing method can be recommended for creating surface textures for better tribological properties.

Conclusions

1. Wear and contact fatigue are the main factors of guideway degradation, which largely depend on the friction between the contact surfaces. Optimization of roughness and tribological parameters can improve their durability.

2. Optimization of lubricating structures (using molybdenum disulfide, hexagonal boron nitride, etc.) allows to significantly reduce the coefficient of friction and improve antifriction properties, especially during running-in and normal wear.

3. The dynamic characteristics of the guideways play a key role in the accuracy and stability of the operation. The stiffness of the contact pair decreases with the increase of the friction path, and the temperature and wear affect the contact deformation.

4. Wear prediction methods based on the Archard and Hertz theories allow for optimizing load distribution between balls and raceways, which helps to increase the accuracy of friction and wear prediction.

5. New materials, such as cubic boron nitride, as well as hydrostatic guides, provide high rigidity, damping, and motion accuracy, but require further research for implementation in practical applications.

References

1. Zhao B, Zhang S, Li J, Wang P. Friction characteristics of sliding guideway material considering original surface functional parameters under hydrodynamic lubrication. *Proceedings of the Institution of Mechanical Engineers, Part J: Journal of Engineering Tribology*. 2017;231(7):813-825. doi:10.1177/1350650116681941
2. Tao, W., Zhong, Y., Feng, H., & Wang, Y. (2013). Model for wear prediction of roller linear guides. *Wear*, 305(1-2), 260-266.
3. Soleimani, P., & Ahmadian, H. (2022). Modeling friction effects in lubricated roller guideways using a modified LuGre model. *Journal of Vibration and Control*, 28(19-20), 2519-2530.
4. Bao, H., Hao, M., Du, Y., & Chen, Y. (2024). Optimal Design of Multilevel Composite Lubrication Structures on Sliding Guide Rail Surfaces. *Coatings*, 14(10), 1286.
5. Fan, Y.; Chen, Y.; Hao, M.; Wang, S.; Du, Y.; Xia, Y.; Guan, X. Study on the improvement of crawling phenomenon of sliding guideway by composite lubrication texture. *China Mech. Eng.* **2024**, 1–8
6. Huan, Z. H. A. O., Yuanka, Z. H. O. U., & Xue, Z. U. O. (2022). Anti-friction Performance of Composite Lubrication Structure Surface under Oil-lubrication. *Lubrication Engineering (0254-0150)*, 47(10).
7. Rodiouchkina, M., Berglund, K., Forsberg, F., Rodushkin, I., & Hardell, J. (2022). Influence of counter surface roughness and lay on the tribological behaviour of self-lubricating bearing materials in dry sliding conditions at high contact pressures. *Lubricants*, 10(8), 167.
8. Soleimani, P., Mohammadpour, M., & Ahmadian, H. (2021). Effect of Lubricant Starvation on the Tribo-Dynamic Behavior of Linear Roller Guideway. *Shock and Vibration*, 2021(1), 7517696.
9. Soleimani, P., Mohammadpour, M., & Ahmadian, H. (2021). Coupled tribo-dynamic modelling of linear guideways for high precision machining application. *Proceedings of the Institution of Mechanical Engineers, Part J: Journal of Engineering Tribology*, 235(4), 711-737.
10. Li, L., & Yang, J. (2018). A study of dynamic behaviors of contact pair in lubricated ball linear guide. *Industrial Lubrication and Tribology*, 70(4), 746-753.
11. Zou, H. T., & Wang, B. L. (2015). Investigation of the contact stiffness variation of linear rolling guides due to the effects of friction and wear during operation. *Tribology international*, 92, 472-484.
12. Wang, Z., Liu, Y., & Wang, F. (2017). Rapid calculation method for estimating static and dynamic performances of closed hydrostatic guideways. *Industrial Lubrication and Tribology*, 69(6), 1040-1048.
13. Liu, W., Zhang, S., Lin, J., Jiang, S., & Chen, Z. (2024). Effect of combined geometric errors on static load distribution and deformations for linear rolling guide. *Tribology International*, 191, 109079.
14. Zha, J., Cheng, K., Xue, F., Wu, D., & Liu, X. (2024). Hydrostatic guideways for precision machines: the state-of-the-art and future perspectives. *Tribology International*, 110060.
15. Raymond, N., Hill, S., & Soshi, M. (2016). Characterization of surface polishing with spindle mounted abrasive disk-type filament tool for manufacturing of machine tool sliding guideways. *The International Journal of Advanced Manufacturing Technology*, 86, 2069-2082.
16. Zsidai, L., De Baets, P., Samyn, P., Kalacska, G., Van Peteghem, A. P., & Van Parys, F. (2002). The tribological behaviour of engineering plastics during sliding friction investigated with small-scale specimens. *Wear*, 253(5-6), 673-688.
17. Ghiotti, A., Bruschi, S., Sgarabotto, F., & Medea, F. (2014). Novel wear testing apparatus to investigate the reciprocating sliding wear in sheet metal forming at elevated temperatures. *Key Engineering Materials*, 622, 1158-1165.
18. Chang, K. C. J. (2016). *Development of New Machining Method for Finish Surface of Sliding Guideways*. University of California, Davis.
19. Chang, K., & Soshi, M. (2017). Optimization of Planar Honing Process for Surface Finish of Machine Tool Sliding Guideways. *Journal of Manufacturing Science and Engineering*, 139(7), 071015.
20. Soshi, M., Ueda, E., & Mori, M. (2014). A productive and cost-effective CBN hard milling-based fabrication method of hardened sliding guideways made of refined cast iron. *The International Journal of Advanced Manufacturing Technology*, 70, 911-917.
21. Horng, T. L. (2013). The study of contact pressure analyses and prediction of dynamic fatigue life for linear guideways system. *Modern Mechanical Engineering*, 3(02), 69-76.
22. Wang, X. Y., Zhou, C. G., & Ou, Y. (2019). Experimental analysis of the wear coefficient for the rolling linear guide. *Advances in Mechanical Engineering*, 11(1), 1687814018821744.
23. He, Y., Fu, Y., Wang, H., & Yang, J. (2022). Enhancing anti-stick-slip performance by laser surface texturing on sliding guideway surface. *Journal of Manufacturing Processes*, 75, 1089-1099.
24. He, Y., Yang, J., Wang, H., Gu, Z., & Fu, Y. (2022). Micro-dimple and micro-bulge textures: Influence of surface topography types on stick-slip behavior under starved lubrication. *Applied Surface Science*, 585, 152501.
25. Cheng, Q., Qi, B., Ren, W., & Liu, Z. (2021). A new exponential wear model to analyze precision retention of guideway based on macro-micro multiscale method. *Proceedings of the Institution of Mechanical Engineers, Part J: Journal of Engineering Tribology*, 235(8), 1499-1513.
26. Horng, T. L. (2013). The study of contact pressure analyses and prediction of dynamic fatigue life for linear guideways system. *Modern Mechanical Engineering*, 3(02), 69-76.

27. Zhang, H., Lu, D., Pan, W., Rong, X., & Zhang, Y. (2024). Static and dynamic characteristics of large-span six-slider closed hydrostatic guideway considering pitch moment and yaw moment. *Industrial Lubrication and Tribology*, 76(3), 392-404.

28. Wang, H., Xie, X., Hua, X., Xu, S., Yin, B., & Qiu, B. (2020). Analysis of the lubrication process with composition of solid lubricants of laser-modified sliding surfaces. *Advances in Mechanical Engineering*, 12(4), 1687814020916078.

29. Shimizu, Jun, et al. "Friction characteristics of mechanically microtextured metal surface in dry sliding." *Tribology International* 149 (2020): 105634.

Диха О.В., Дитинюк В.О., Ковтун О.С., Фасоля В.О., Гетьман М.В. Підвищення зносостійкості напрямних: трибологічний аналіз, текстура поверхні та мастильні матеріали

У статті розглянуто основні режими руйнування напрямних, зокрема знос і контактну втому, які залежать від тертя між контактними поверхнями. Досліджено вплив трибологічних параметрів, зокрема шорсткості поверхонь і мастильних структур, на експлуатаційні характеристики лінійних напрямних. Особливу увагу приділено динамічній поведінці напрямних, яка визначає точність та стабільність роботи механічних систем. Для прогнозування зносу використано математичні моделі на основі теорії Арчарда та Герца, що дозволяють оцінювати розподіл навантаження та контактні деформації. Окремо досліджено вплив мастильних матеріалів, зокрема дисульфиду молібдену та гексагонального нітриду бору, на зменшення коефіцієнта тертя та покращення антифрикційних властивостей. Розглянуто перспективи використання новітніх матеріалів, таких як кубічний нітрид бору, для підвищення стійкості напрямних до зносу. Запропоновано методи оптимізації навантаження між елементами кочення, що сприяє підвищенню довговічності напрямних. Одержані результати можуть бути використані для вдосконалення конструкцій механічних систем та зниження експлуатаційних витрат.

Ключові слова: знос, тертя, контактна втома, жорсткість, мастильні структури, динаміка напрямних, оптимізація навантаження



Analysis of the causes of damage to centrifugal pumps during operation and methods of their elimination

I.V. Morshch

Kyiv Aviation Institute, Ukraine

2707209@stud.kai.edu.ua

Received: 25 Decemberr 2024; Revised 15 February 2025; Accept: 05 March 2025

Abstract

The paper reviews the research on improving the efficiency of operation and service life of centrifugal pumps, which are widely used in machinery for pumping various liquids. The main reasons for the failure of centrifugal pumps, as well as modern approaches to their prevention, are considered. It is established that increasing the efficiency of pump operation can be achieved by analyzing, modeling and optimizing their design. It was found that modeling the operation of smaller pump models and comparing surrogate models with the original ones is a modern, highly effective method of optimizing pump performance. The important role of protective coatings in increasing the wear resistance of parts is established, and the experience of introducing innovative coating technology at enterprises is described.

Keywords: analytics, pump shaft, centrifugal pump, mechanical seal, coating, wear resistance, adhesion.

Introduction

Today, an important technical challenge is to improve the reliability of machine parts and mechanisms that are subject to intense damage under high contact loads, elevated temperatures, aggressive media and abrasives. One of these mechanisms is centrifugal pumps, which are widely used for pumping liquids in many industries, including oil and gas.

High performance and long periods between failures or overhauls can usually be quite long as long as centrifugal pumps operate in conditions close to their design. However, it should be noted that "design" refers not only to pressures, flow rates, temperatures and other process parameters, but also to frictional torque forces, bearing and seal lubrication. Conservatively designed pumps can withstand only a certain amount of overload caused by technical processes or mechanical failure, so their components already begin to suffer damage before reaching the operating mode. Pumps should be selected for operation near the point of maximum efficiency[1].

Due to the high intensity of pump use in industrial sectors, it is important to ensure maximum durability and reliability of the equipment. One of the key factors affecting the durability and performance of pumps is the various lubrication and friction components, such as the shaft, mechanical seal, bearings, and shaft seal. This paper aims to analyze the causes of centrifugal pump failures and to study the data on the impact of shaft wear resistance and mechanical seals on pump performance and durability.

During operation, the motor or electric motor drives the rotor, converting the kinetic energy of rotation into hydrodynamic energy of the fluid flow. The fluid enters the pump axially through the casing eye, is captured by the impeller blades, where it gains speed and pressure. Then it moves tangentially and radially outward, exiting through the circumferential parts of the impeller into the diffuser part of the casing, which slows the flow and further increases the pressure.

The rotor shaft is subject to both cyclic and partial loads. Starts and stops cause voltage fluctuations with high average values. Multi-cycle fatigue analysis is often used to ensure shaft reliability. Stress analysis takes into account stress increasers due to design features such as threads, grooves, slots, and screw holes. The presence of these elements, combined with complex loads, requires finite element calculations to assess the reliability of the shaft. In addition, rotor dynamics and critical shaft speeds must be taken into account.



Article [2] notes that centrifugal pumps are subject to premature rotor shaft failures, even if all design standards are met. The causes of these failures fall into several categories: design errors or improperly selected materials of critical components, defects in manufacturing or processing, and reduced component performance due to wear. One of the main problems is the concentration of stresses due to design features, which causes excessive plastic deformation and contributes to the formation of fatigue cracks. These cracks can also occur due to internal material defects, such as non-metallic inclusions or microcavities, as well as irregularities created by machining. In addition, the authors of paper 3 note that operational wear of the working surfaces of pump parts gradually leads to degradation of the physical and mechanical properties of the material, in particular its elasticity and strength.

Other factors that can accelerate shaft failure are failure to maintain proper maintenance and errors during repairs. In the event of an equipment failure, it is important to assess the extent of damage to individual components and their impact on the functionality of the entire system. During operation, shaft damage occurs as a result of fretting corrosion and abrasive wear, which is the result of constant contact with aggressive liquids and mechanical friction. Fretting corrosion typically occurs in areas of micromovement between the shaft and surrounding parts, such as bearings or joints. This process causes rust formation and surface erosion, reducing the mechanical performance of the shaft.

Abrasive wear is often caused by solid particles from the operating environment entering the contact surfaces of the shaft and sealing elements or bearings. This results in grinding of the shaft surface, which can significantly reduce the shaft diameter at critical points, causing misalignment and increased stress on the bearings.

The pump shaft has several critical wear points, including contact points with seals, bearings and joints, as well as areas where torque is transmitted. Constant mechanical impact at these points causes microcracks, which can develop into larger damage over time. Regular shaft inspection and timely maintenance are therefore key to extending the service life of the pump.

Similar studies on shaft wear and critical damage are presented in [3]. In particular, the authors of this paper consider the consequences of an emergency due to the failure of a centrifugal pump used to pump a mixture of hydrocarbons to deliver the final petroleum product to a refinery. The shaft failure resulted in a fire of the pump and refinery pipelines within the block, with an estimated total loss of USD 48,000. The centrifugal pump was installed and commissioned about 30 years ago. There have been three major repairs of the pump due to gland leaks. The mechanical seal was installed on the threaded part of the shaft with a preload corresponding to 25-30% of the yield strength of the material. However, no abnormalities were reported on the shaft during operation and maintenance.

The typical operating cycle of a centrifugal pump consists of starting and running the pump at a nominal rotor speed of 2975 rpm for 14 hours, with a 2-hour shutdown interval. An inspection of the faulty centrifugal pump revealed catastrophic destruction of the rotor shaft surface, with the bushing remaining on the shaft.

Another basic element in a pump is a mechanical seal, designed to prevent leakage of working media, liquid or gas, at the points where the rotating shaft crosses the casing. It is used in various types of pumps, in particular centrifugal pumps, where it is necessary to ensure a tight seal between moving and stationary parts.

A mechanical seal works by the interaction of two main components: a stationary ring and a moving ring, which are pressed together by an elastic element such as a spring or bellows. The stationary ring is typically fixed in the pump casing, while the movable ring rotates with the shaft. This design minimizes friction and prevents leakage of the pumped medium, while ensuring reliable seal function under various operating conditions.

Selecting seals and sealing systems for pumps is a complex task. Cartridge seals offer significant maintenance advantages because they simplify the process of mounting and dismounting from the pump shaft. In the case of large oil seals, bellows and spring-sealed cartridges can be used. Cartridge seals are easier to replace, reducing the risk of assembly errors and damage compared to traditional mechanical seals.

The materials from which the rings are made are selected depending on the operating conditions. Fixed rings are often made of materials such as ceramics or carbon, which are highly resistant to wear. Moving rings can be made of metals or other materials that provide a snug fit and minimal friction. Their use becomes critical in conditions of high pressures, temperatures, or when dealing with aggressive media, where traditional seals such as glands may not be effective.

When selecting a sealing surface material, keep in mind that the heat generated on the sealing surface must be quickly dissipated to avoid evaporation of the liquid. High thermal conductivity and hardness make silicon carbide the preferred sealing surface material.

Many pumping systems require the mechanical seal environment to be maintained at a moderate temperature. This is sometimes achieved by external flushing. Another option for achieving moderate seal temperatures is to cool the stuffing box. In many pumps, the stuffing box cavity is remote from the sealing surfaces that require cooling.

Seals fail for two reasons: the lapped surfaces open up or one of the seal components is damaged. When the lapped surface is opened, solid particles penetrate between the lapped surfaces by the lapped surfaces. The hard particles penetrate the softer carbon/graphite surface, causing it to act like a grinding wheel. This grinding action will cause the hard surface to wear down heavily.

Article [4] states that most mechanical seal failures occur due to the destruction of the bearing and sealing surfaces for the following reasons:

- a dynamic elastomer cannot slide or move freely on a rotating shaft or sleeve. This can happen if the shaft is too large, the shaft finish is too rough;
- the product is viscous or the product crystallizes;
- the shaft is displaced, causing the seal to hit something during rotation or the rotating surface to slide off a stationary surface. This can happen if the pump is running far from its BEP; the shaft is bent; the rotor is unbalanced; the shaft deformation twists the pump seal, or due to cavitation;
- the product evaporates between the sealing surfaces of the surfaces, which leads to their rupture;
- poor quality of the end seal.

According to statistical data in [5,6], the failure rate of centrifugal pump parts is indicated, the bulk of which falls on (Fig 1):

- hydraulic wear (32%): impeller (blade wear, corrosion, cavitation), body (wear of the inner surface, corrosion);
- mechanical wear (25%): bearings (wear and tear, breakage), seals (wear and tear, loss of tightness), shaft (wear, bending, breakage);

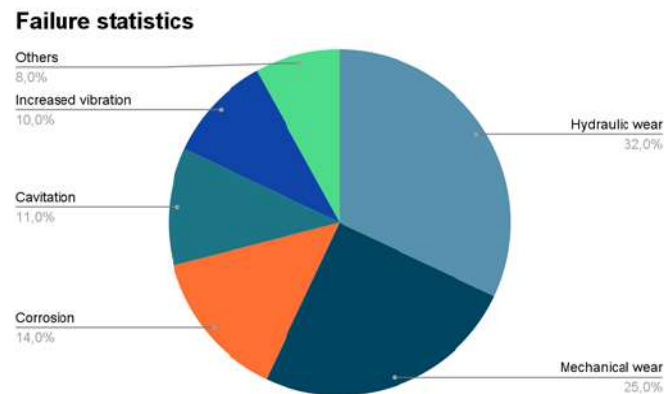


Fig 1. Statistical data on the failure of centrifugal pumps.

- corrosion (14%): all parts (corrosion can affect any part of the pump, especially in aggressive environments);
- cavitation (11%): impeller (cavitation causes the surface of the blades to be destroyed);
- increased vibration (10%): rotor imbalance, damage to the bearings, loosening of fasteners, hydraulic imbalance.
- other reasons (8%): installation errors, damage by foreign objects.

It should be noted that the data above is an average value, as each pump has its own individual performance characteristics [7].

Purpose

To analyze the dominant types of wear of centrifugal pumps of the Dickow Pumpen type and methods of increasing wear resistance through various types of hardening

Object of research

The object of the study was a Dickow Pumpen 125/320 centrifugal pump for the transportation of fuels and lubricants (Fig 2). This type of pump was used in the company's pile-lubricant warehouse.



Fig 2. Dickow Pumpen NCR 125/320 centrifugal pumps

The Dickow NCR pump is a heavy duty centrifugal pump for the oil, petrochemical and gas industries, manufactured in accordance with API 610 standards. Available in a wide range of sizes and specifications, it has a maximum flow rate of up to 700 m³/h and a maximum head of 145 m at 2900 rpm and 220 m at 3500 rpm.

Results

The pump is operated in an aggressive environment (kerosene) with an average operating time of 6 hours per day with interruptions. The total continuous service life was 3 years. The shaft, bearings, and mechanical seal are subject to the highest loads, with the mechanical seal experiencing the most significant wear (Fig 3).

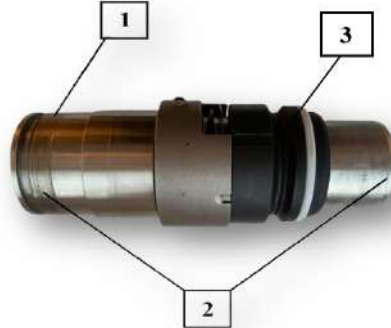


Fig 3. Dickow Pumpen mechanical seal part, operating time 6500 hours: 1 – abrasive wear of mechanical seal components; 2 – fretting corrosion due to friction and operation in aggressive environments; 3 – after abrasive wear, additional vibrations were generated on the mechanical seal part, and the graphite rings began to break down.

After 6500 hours of operation of the pump unit, significant wear of the mechanical seal was detected, which manifested itself in the form of abrasive damage and traces of fretting corrosion. These defects were caused by prolonged operation in an aggressive environment (kerosene) and constant exposure to mechanical and chemical factors. The first signs of damage were leakage of working fluid and abnormal noise during pump operation, which indicated a violation of the seal tightness. In order to prevent further malfunctions, the pump was shut down for diagnostics and inspection. As a result, it was decided to replace the damaged seal to restore normal operation of the pump. Based on the experience gained, it is now possible to implement technical solutions that will extend the mechanical seal's service life. Therefore, a lot of research is currently focused on analyzing and finding relevant solutions to improve the performance of centrifugal pumps. In particular, experimental work is carried out under unstable conditions at partial load, and the results at different operating points are compared with available experimental data, such as hydraulic performance and flow field information by measuring the particle image velocity [8,9].

It is important to note that design optimization is quite effective in improving the performance of centrifugal pumps by reducing flow recirculation and cavitation [10,11,12]. To improve pump efficiency, the design of pump impellers was optimized in [13] by numerical modeling, Latin Hypercube (LHS) sampling, a surrogate model, and a genetic algorithm (GA). The results showed that the simulated results are consistent with the experimental performance results of the original pump. Compared with the simulated efficiency of the original pump, the optimization improved the efficiency by 8.34% beyond the design point can be used to model the design of other pumps. Increasing the service life can also be achieved by increasing the performance of the centrifugal pump through independent rotation of the inductor and centrifugal impeller [14]. An inductor that provides independent rotation of both the inductor and the centrifugal impeller. Unlike conventional designs, this configuration allows for differential speeds and controlled rotation directions. In particular, the independent rotation of the inductor extends the operating range of the pump, while the rotation of the inductor and impeller in opposite directions significantly increases the pressure generation and efficiency of the pump compared to rotation in the same direction. However, along with increasing productivity, an important aspect of ensuring the durability of pumping equipment is protecting its components from wear. One of the most effective methods of improving the wear resistance of the working surfaces of pump parts is the application of protective coatings. By increasing the wear resistance, such coatings can significantly extend the service life of mechanical seal parts, shafts and bearings. The coatings can be applied by plasma or detonation spraying, laser or electric spark alloying [15]. In [16], wear-resistant WC-Co coatings were applied to pump impellers using the method of spark alloying. The resulting coatings are uniform and continuous without obvious cracks and holes, there is no clear line of separation, and a strong metallurgical bond is formed between the coating and the substrate material [17]. Coatings can also be applied to the shaft, mechanical seal, and other parts of the pump [18]. TST Coatings is a company that applies coatings to various pump parts. Their methods use gas-thermal spraying to apply tungsten carbide-based materials with 12% cobalt. These coatings have high hardness, excellent adhesion and a very dense structure. They provide excellent wear protection for several different wear mechanisms. An alternative is offered by the Ukrainian company TRIZ [19], which manufactures and improves mechanical seals and pump shafts by applying coatings that also use tungsten carbide-based materials. Currently, new wear-resistant materials and coating methods are being developed, which in the future can be used to improve the performance properties of pump working surfaces.

Conclusion

The following conclusions can be drawn from the analysis of the papers on the causes of failure of centrifugal pumps during their operation and possible methods of their elimination:

To ensure the long and trouble-free operation of centrifugal pumps, it is critical to regularly perform in-depth analysis and modeling of possible failures. This process includes not only identifying the most frequent causes of failure, but also predicting potential problems, which allows you to take preventive measures and minimize the risk of accidents.

One of the most serious problems that lead to early pump failure is the wear of the shaft and bearing running surfaces. This process can be caused by various factors such as friction, corrosion, cavitation, and vibration. To increase the wear and corrosion resistance of pump parts, an effective solution is to use protective coatings. Modern technologies make it possible to apply various materials, such as ceramics, metals or composites, to the surface of the parts, which significantly increase their service life. Another important aspect is the modernization of the design of key pump components. Replacing worn or outdated parts with more modern and reliable ones, such as the shaft, mechanical seals, seals, and bearings, can significantly increase the efficiency and durability of the pump. Optimizing flow recirculation and improving the interaction between the impeller and shaft will also help reduce wear and improve pump performance.

In further research, it is planned to study in detail the effect of different types of wear-resistant coatings on pump parts. A comparative analysis of their properties, such as hardness, wear resistance, corrosion resistance, and adhesion to the base, will be conducted. This will help determine the optimal coating option for each specific pump part, taking into account its operating conditions and requirements.

References

1. Mohammadi Z., Heidari F., Fasamanesh M. et al. Chapter Six - Centrifugal pumps. *Transporting Operations of Food Materials Within Food Factories*. 2023. P. 155-200. <https://doi.org/10.1016/B978-0-12-818585-8.00001-5>
2. Johann F. G. *Centrifugal Pumps*, 2nd edition. Springer-Verlag Berlin Heidelberg, 2010. 966 p. [English] <https://doi.org/10.1007/978-3-642-12824-0>
3. Stefanko D. B., Leishear R.A., Relationship Between Vibrations and Mechanical Seal Failures in Centrifugal Pumps, *International Mechanical Engineering Congress and Exposition*, 2008. IMECE2005-79176. P. 5-12. [English] <https://doi.org/10.1115/IMECE2005-79176>
4. Daraz A., Alabied S., Zhen D., Gu F., Ball A.D. .Detection and Diagnosis of Mechanical Seal Faults in Centrifugal Pumps Based on Acoustic Measurement. *Advances in Asset Management and Condition Monitoring*, In: Ball, A., Gelman, L., Rao, B. (eds) *Advances in Asset Management and Condition Monitoring*. Smart Innovation, Systems and Technologies, vol 166. Springer, Cham. 2020, P. 963-975. [English] https://doi.org/10.1007/978-3-030-57745-2_79
5. Ushchapiivskiy I.L., Kyrlyiv Y.B., Larin O.O. Computer modelling of vibration of a centrifugal fire pump, *Bulletin of Lviv State University of Life Safety*, 2018, P. 42-48. [English] [ISSN : 2708-1389](https://doi.org/10.1007/978-3-030-57745-2_79)
6. Liangjie Mao, Lunke Gan, Wu Li, Pengxiang Zhang, Failure analysis on weld joint of centrifugal pump diffuser for oil and gas pipeline transportation, *Engineering Failure Analysis*, 2022, Vol. 140. [English] <https://doi.org/10.1016/j.engfailanal.2022.106620>
7. K. Holmberg, A. Erdemir, Influence of tribology on global energy consumption, costs and emissions, *Friction*, 2017, Vol. 5. P. 263-284. [English] <https://doi.org/10.1007/s40544-017-0183-5>
8. T.Sahoo, Making centrifugal pumps more reliable, *World Pumps*, 2009, Issue 513, P. 32-36. [English] [https://doi.org/10.1016/S0262-1762\(09\)70219-6](https://doi.org/10.1016/S0262-1762(09)70219-6)
9. Y.Weixiang, H.Renfang, J.Zhiwu, L.Xiaojun, Z.Zuchao, L.Xianwu, Instability analysis under part-load conditions in centrifugal pump, *Journal of Mechanical Science and Technology*, 2019, Volume 33, P. 269-278, [English] <https://doi.org/10.1007/s12206-018-1226-1>
10. S. Thakkar, H. Vala, V. Patel & R. Patel, Performance improvement of the centrifugal pump through an integrated approach based on response surface methodology, multi-objective optimization and CFD, *Journal of the Brazilian Society of Mechanical Sciences and Engineering*, 2021, Volume 43. [English] <https://doi.org/10.1007/s40430-020-02753-0>
11. KM.Gulerenpp, Automatic optimization of a centrifugal pump based on impeller-diffuser interaction, *Journal of Power and Energy*, 2018, P. 1004-1018. [English] <https://doi.org/10.1177/0957650918766688>
12. S.Hyeon-Seok, K.Kwang-Yong, C.Young-Seok, Three-Objective Optimization of a Centrifugal Pump to Reduce Flow Recirculation and Cavitation, *Journal of Fluids Engineering*, 2018, P. 921-935. [English] <https://doi.org/10.1115/1.4039511>
13. W.Wenjie, P.Ji, Y.Shouqi, Z.Jinfeng, Y.Jianping, X.Changzheng, Application of different surrogate models on the optimization of centrifugal pump, *Journal of Mechanical Science and Technology*, 2016, Volume 30, P. 567-574. [English] <https://doi.org/10.1007/s12206-016-0110-0>
14. E.Dehnavi, M.Solis, A.Danlos, M.Kebdani, F.Bakir, Improving the Performance of an Innovative Centrifugal Pump through the Independent Rotation of an Inducer and Centrifugal Impeller Speeds, *Energies*, 2023, Volume 16, Issue 17. [English] <https://doi.org/10.3390/en16176321>

15. W.Huanhuan, L.Naiming, Y.Shuo, L.Zhiqi, Y.Yuan, Z.Qunfeng, F.Jianfeng, L.Dongyang, W.Yucheng, Structural improvement, material selection and surface treatment for improved tribological performance of friction pairs in axial piston pumps: A review, *Tribology International*, 2024, Volume 198. [English] <https://doi.org/10.1016/j.triboint.2024.109838>
16. S.Xiaoli, Z.Jiakai, P.Weiguo, W.Wenhuan, T.Congwei, Research Progress in Surface Strengthening Technology of Carbide-based Coating, *Journal of Alloys and Compounds*, 2022, Volume 905. [English] <https://doi.org/10.1016/j.jallcom.2022.164062>
17. Z.Ruizhu, L.Jingrui, Y.Dakao, Z.Yuanyuan, Mechanical Properties of WC-8Co Wear-Resistant Coating on Pump Impellers Surface by Electro-Spark, *Rare Metal Materials and Engineering*, 2015, Volume 44, P.1587-1590. [English] [https://doi.org/10.1016/S1875-5372\(15\)30097-7](https://doi.org/10.1016/S1875-5372(15)30097-7)
18. B. Lenling, Engineering of Coatings for Pump Components, *TST Coatings*, 2018. [English]
19. LTD.TRIZ, Floating end seals, 2024. [Ukraine]

Морщ І. В. Аналіз причин пошкоджень відцентрових насосів в процесі експлуатації та способи їх усунення

У статті здійснено огляд сучасних підходів до підвищення ефективності та довговічності відцентрових насосів, які широко використовуються для транспортування рідин. Визначено основні фактори, що впливають на зниження їх продуктивності та можливі методи покращення експлуатаційних характеристик. Аналіз причин виходу з ладу відцентрових насосів показав, що найбільш поширеними проблемами є зношення робочих поверхонь, гідравличний знос, корозія, кавітація та вібраційні навантаження. Для запобігання цим явищам доцільним є застосування сучасних рішень, зокрема використання захисних покриттів, оптимізація конструкції та впровадження інноваційних технологій у виробництво.

Одним із перспективних напрямів насосного обладнання є математичне моделювання та створення зменшених прототипів для тестування. Це дозволяє оцінити ефективність конструктивних змін без необхідності дорогих експериментів. Дослідження показують, що використання сурогатного моделювання дає змогу значно знизити витрати на розробку та підвищити точність прогнозування поведінки насосів у реальних умовах експлуатації.

Також значну увагу приділено ролі зносостійких покриттів, які можуть значно продовжити термін служби основних деталей насосів. Сучасні технології дозволяють наносити на поверхні робочих елементів захисні покриття, що підвищують їхню стійкість до механічних та хімічних впливів. Подальші дослідження у цьому напрямку спрямовані на аналіз ефективності різних типів покриттів, їх адгезії та зносостійкості залежно від умов експлуатації. Таким чином, підвищення ефективності та надійності відцентрових насосів можливе завдяки комплексному підходу, що включає оптимізацію конструкції, використання сучасних матеріалів та впровадження цифрових методів аналізу. Це дозволить значно покращити робочі характеристики насосів та зменшити витрати на їх обслуговування.

Ключові слова: аналітика, вал насоса, відцентровий насос, торцеве ущільнення, покриття, зносостійкість, адгезія



Physical and chemical processes in the application of antifriction coatings by the friction-mechanical method

A.M. Krasota, I.V. Shepelenko*, M.V. Krasota

Central Ukrainian National Technical University, Kropyvnytsky, Ukraine

**E-mail: kntucpfzk@gmail.com*

Received: 05 January 2025; Revised 20 February 2025; Accept: 08 March 2025

Abstract

A review of current models of antifriction coating formation by finishing antifriction non-abrasive treatment has shown the lack of a thorough analysis of physical and chemical processes occurring in the friction zone. From this point of view, it seems reasonable to study the process of coating formation at the stages of surface activation, deposition of antifriction components and formation of an antifriction coating. The considered characteristic structures for each of the stages of antifriction coating application and chemical reactions that occur during the formation of an antifriction coating allow us to track the processes accompanying the formation of coatings and identify ways to improve them. It is proved that the quality of coating formation directly depends on the material of the part and tool, temperature in the deposition zone, material diffusion rate, and dissociation of chemical compounds. A physical model of the process of finishing antifriction non-abrasive treatment is proposed, which determines the chemical reactions and physical processes occurring at different stages of the antifriction coating formation. The analysis of the model allows to find out and explain the characteristic phenomena in the system 'part – tool – technological environment', and, therefore, to influence the quality of the formation of an antifriction coating by the friction-mechanical method.

Key words: finishing antifriction non-abrasive treatment, physical model, antifriction coating, process medium, surface activation, tribodestruction, wear resistance

Introduction

Methods of hardening treatment and modification of working surfaces to improve the performance of friction surfaces are becoming increasingly common. The development of these methods is primarily driven by the growing demands on the durability and performance of machine parts. Wear resistance, bearing capacity, fatigue and contact strength are determined by the initial physical and mechanical state of the contacting surfaces (surface layers), and protective coatings must provide the required tribotechnical properties in a wide range under various operating conditions [1]. It should be noted that for each specific friction pair they may differ.

One of the most promising methods of applying wear-resistant coatings is the finishing antifriction non-abrasive treatment (FANT) of parts [2]. The essence of the method is that the parts are coated with thin layers of soft metals such as copper, brass, and bronze using friction [3]. Currently, there are several technological variants of FANT. In the friction-mechanical method, the antifriction coating is applied to the part by pressing a brass or copper bar in a glycerine medium and transferring the bar particles to the surface of the part. The pressing force reaches 20...70 MPa, the process is accompanied by significant heat generation, and the thickness of the applied coating is in the range of 2 to 10 μm [4].

There are other technological variants of FANT, in which the coating is applied in a liquid medium containing inorganic copper compounds and surfactants [5]. In this case, the metal coating is obtained as a result of physical and chemical processes that occur between the working medium and the workpiece during mechanical activation of the surface by the tool. The tool can be made of various materials, such as rubber, polyurethane, felt, etc.



Despite the simple kinematics and the nature of the tool-surface interaction, the FANT process is based on force and thermal effects, accompanied by a whole range of rather complex thermal, deformation, tribophysical and chemical processes.

The development of scientific foundations for increasing the durability of machine parts subjected to hardening treatment with coating by FANT methods within the framework of an integrated approach is impossible without establishing and describing the whole variety of physical phenomena accompanying this process and the parameters that determine the quality of the surface and surface layer, which determine the level of operational properties.

There are various hypotheses explaining the mechanism of coating formation in FANT. These mechanisms are described in scientific sources of information. However, due to the lack of consensus on this issue, as well as in order to improve the authors' coating technology using FANT methods, the coating formation process requires further more detailed study.

Therefore, this work is devoted to the study of physical phenomena and chemical processes occurring during the application of wear-resistant coatings by FANT methods.

Literature review

According to research [6], the formation of antifriction coatings by the FANT method is carried out in eleven stages. The author states that at the first stage, the adhesive zone is formed due to the forceful impact of the tool on the workpiece. At the second stage, the process of dispersion of irregularities and opening of juvenile surfaces takes place. The third stage is characterised by the transfer of iron atoms from the workpiece to the process medium. At the fourth stage, a chemical substitution reaction takes place on the unoxidised surface areas and more active metal ions from the process medium are deposited on the iron surface of the part. The fifth stage is caused by the chemical reactions that form pure metal compounds on the surface from individual ions. The sixth stage is the formation of a protective coating on the surface of the part from particles of dispersed metal from the process medium. The seventh stage is due to the presence in the process medium of individual wear products covered with oxide films, which also participate in the formation of the coating, packing into the overall structure of the coating, they cause the eighth stage. The ninth stage is the diffusion of the coating metal deep into the part. The tenth stage is the prevention of dislocations from reaching the surface of the part. The eleventh stage is deformation of the resulting protective coating.

In our opinion, this model is rather complicated in terms of its further development and improvement, and also does not fully take into account the chemical interaction of the components of the 'part-tool-technological environment' system.

In [7], the process of FANT is considered as three separate stages:

- surface pretreatment to strengthen and activate the surface of the base metal, obtaining a juvenile surface;
- chemical interaction of the coating components (the process of restoring the coating metal from the salts of the process fluid) formation of the diffusion layer (dislocation and grain boundary diffusion);
- coating layer growth, interaction of damping tool with the coating, strengthening of the coating and substrate.

In [8], the process of frictional material transfer is divided into two stages:

- plastic squeezing of the initial material, carried out by micro-indentations of the body on which the coating is applied, which proceeds to destruction by micro-cutting;
- adhesion of the chips formed as a result of microcutting to the surface to which the metal is transferred.

In [9], the FANT process is described in three stages. At the first stage, a surface-active medium is applied to the surface of the part, which, having good wetting properties, helps to soften and dissolve oxide films on the surface of the part. The second stage involves the contact of the workpiece with a soft counter body (tool). This stage describes the processes of tool wear due to micro-cutting by irregularities in the workpiece surface. The third stage involves increasing the thickness of the coating as a result of the adhesive forces between the coating material and the workpiece.

In our opinion, this model does not sufficiently take into account the chemical processes that occur as a result of the interaction of the components of the technological environment, as well as the tool and the workpiece.

Paper [10] describes the process of copper-containing coating formation using a gallium-indium process medium. It is shown that due to the kinematic (rotational movement) deformation load of the contact zones, chemical and thermal effects of the gallium-indium component, it is possible to carry out the process of selective dissolution of the copper alloy with the formation of a plasticised copper film on both friction surfaces. Such a structure is considered as a multicomponent - a copper frame with alloying elements of materials adsorbed on the surface, which interact.

In [11], the authors proposed a theoretical scheme of the FABO process carried out by the friction-mechanical method (Fig. 1).

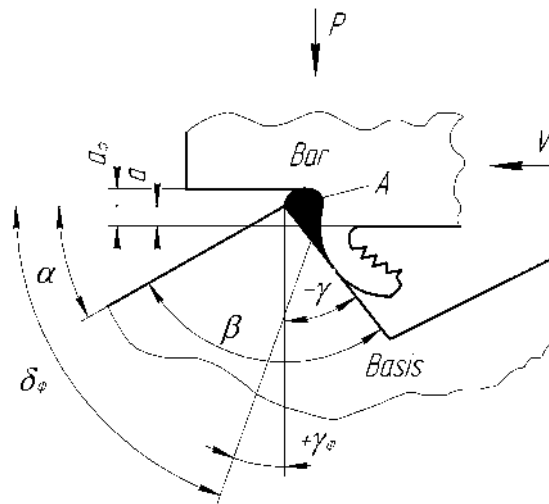


Fig. 1. The theoretical scheme of the process of microcutting during the formation of an anti-friction coating by the friction-mechanical method: P – force; V – displacement; a, a_{ϕ} – theoretical and actual thickness of the cut layer; $\alpha, \beta, \gamma, \delta$ – cutting angles [11]

The authors argue that at the initial stage of coating formation, the process of micro-cutting takes place. The paper discusses the features of filling the depressions of the microrelief of a part with an antifriction material. The coating process is divided into the following stages:

- mechanical surface preparation with the formation of a regular microrelief;
- coating application using a friction-mechanical method;
- deforming drawing.

However, this approach to considering FANT also does not fully take into account the chemical processes that occur during the formation of an antifriction coating.

Purpose

The aim of the work is to form modern ideas about the processes occurring during the application of antifriction coatings by finishing antifriction non-abrasive treatment.

Results

In our opinion, for an objective assessment of the processes occurring during the application of antifriction coatings, it is necessary to consider the initial state of the surface, as well as the physical and chemical phenomena occurring during the creation of antifriction coatings. From this point of view, it is advisable to analyse the FANT process at the stages of surface activation, deposition of antifriction components and formation of the antifriction coating.

Surface condition before FANT antifriction coating application. It should be noted that the original surface of the part before applying FANT antifriction coatings is characterised by structures that can prevent direct contact and adhesive bonding of metals during the application of the antifriction coating. In addition to moisture in the surface layer, oxides are created on the surface layer as a result of the interaction of air oxygen and the metal of the part (FeO, Fe_2O_3, Fe_3O_4), as well as chemically absorbed oxygen (Fig. 2).

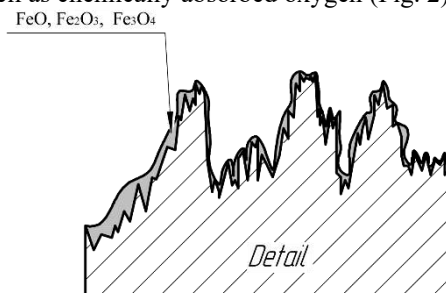


Fig. 2. Initial condition of the surface of the part before applying the antifriction coating

Activation of workpiece and tool surfaces. This stage of coating formation is characterised by the dispersion of the materials of the friction pair - tool and workpiece.

The triggering of the mechanical activation factor during friction coating occurs as a result of frictional interaction, which can partially or completely destroy the oxide layer or chemically absorbed oxygen. The brittle

oxide layer on the friction surface is subjected to significant shear deformation, which results in the destruction of the part and tool materials and removal from the contact zone.

The tops of the tool and workpiece micro-exposures are destroyed and the material is removed into the process medium. At this stage, a short-term exposure of juvenile surfaces is possible due to the presence of friction forces between the unevenness of the tool and workpiece surfaces. The activation of the contact surfaces of the workpiece and the tool promotes the formation of interatomic bonds between the coating and workpiece materials.

The duration of the atoms in the activated state is quite short, and therefore the re-formation of metal-oxygen bonds is possible. This is prevented by the surface-active components of the process medium.

This stage is characterised by high pressure on the metal surfaces of the workpiece and tool, as well as local temperature increases in the contact zone of uneven surfaces.

The tool's clamping force and the speed of its movement along the workpiece surface, as well as its own movements (rotation, oscillation, oscillation, impact, etc.) determine the value of the specific heat of friction and, consequently, the contact temperature.

As a result of the mechanical interaction of the soft tool material with the harder workpiece material, a layer of the tool material is removed due to the micro-cutting processes of the workpiece surface protrusions. This stage is characterised by high pressures and the associated penetration of the protrusions of the workpiece surface irregularities into the surface of the softer material that forms the coating.

An increase in temperature in local contact surfaces promotes the excitation of surface metal atoms involved in frictional interaction, which facilitates the destruction of metal-oxygen bonds and provides a temperature factor for the activation of the FANT process.

In this case, it is advisable to use the hypothesis of the coating formation process that occurs as a result of the transition through the activation barrier [1]. A diagram illustrating this theory is shown in Fig. 3. When the activation energy reaches a certain value (the value is determined by the chemical composition of the base material), conditions are created for the destruction of surface oxide films, which ensures the beginning of the process of chemical interaction of the process medium components with the part.

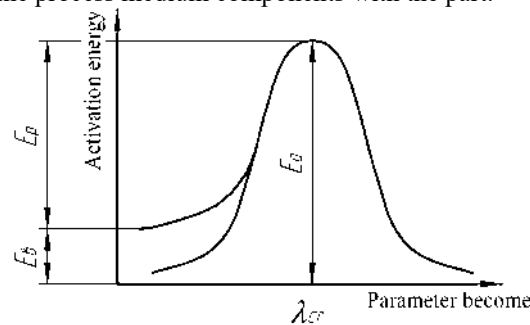


Fig. 3. Energy change during chemical interaction of the coating material and the substrate: λ_{cr} – is the parameter at which the instability of the system occurs; E_a – is the activation energy of the transition to the active state of the system; E_p – is the energy of mechanical action; E_b – is the energy of overcoming the energy barrier [1]

Under such conditions, complex chemical transformations occur in the technological environment, which is based on glycerol [12].

As a result of the interaction of the components of technological media, glycerol tribodestruction occurs, a condition for which is the provision of local temperatures in the friction zone of about 180...280 °C, which are achieved by heat generation in the friction zone of the tool and part.

Tribodestruction is the process of destruction of glycerol ($C_3H_8O_3$) molecules when it interacts with the contacting surfaces of the part-tool system to produce glycerol aldehyde ($C_3H_6O_3$), formaldehyde (CH_2O) and acrolein C_3H_4O . The scheme of glycerol tribodegradation will be as follows:



These oxidation products, in turn, actively interact with the surface of the part. They contribute to the further formation of a copper film on the surface of the steel part, which reduces the friction coefficient, increases oil capacity and wear resistance, and also participates in the restoration of metal components.

In the process medium used for FANT, one of the main components containing the cladding element is copper chloride $CuCl_2$. Copper chloride in the process medium solution dissociates with the subsequent formation of copper oxide CuO and interacts with other components of the medium.

The dissociation equation for copper chloride is:

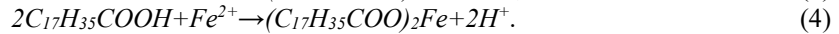
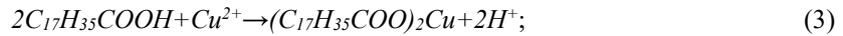


Also, at this stage, there is a chemical interaction between the surfactants present in the medium and the metal ions present.

Stearic acid is most often used as a surface active agent in the FANT of machine parts ($C_{17}H_{35}COOH$), belonging to organic fatty acids and performing the following functions: destruction of oxide films, plasticisation of surfaces, and reduction of surface tension of the process medium liquid.

The destruction of oxide films on the surfaces of parts and tools contributes to the exposure of the active juvenile metal surface of the part and tool with the subsequent formation of protective coatings from compounds formed by these metals. This is confirmed by the following works [12].

Stearic acid ($C_{17}H_{35}COOH$) reacts with the metal of the workpiece surface (Fe), and with the copper (Cu) of the process medium, thus having a positive effect on the destruction of the oxide film, while stearic acid forms complex compounds with the copper of the process medium and the iron of the workpiece, with the following reactions occurring:



As a result of reactions (3) and (4), the compounds $(C_{17}H_{35}COO)_2Cu$ – copper stearate and $(C_{17}H_{35}COO)_2Fe$ – iron stearate are formed. When they get into the microrelief of the part, the following complex compounds increase the resistance to surface wear.

The above chemical reactions and physical processes occurring at the first stage can be represented in the form of a scheme (Fig. 4).

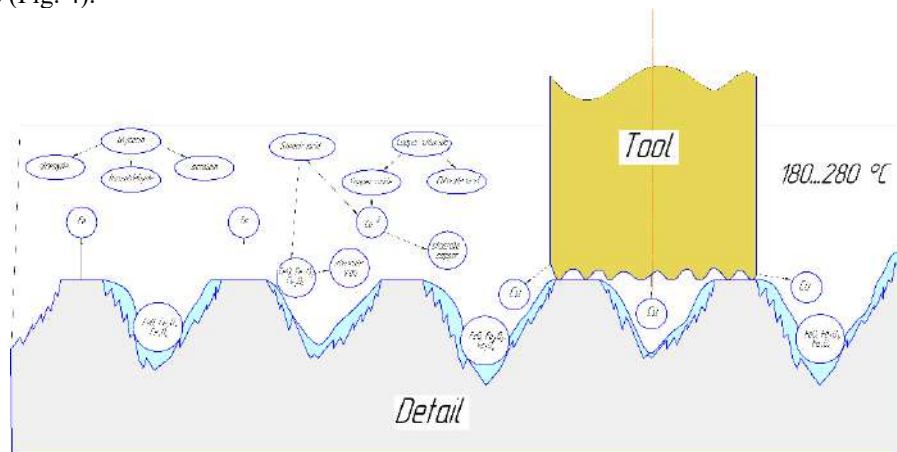


Fig. 4. Scheme of the activation stage of workpiece and tool surfaces

Deposition of anti-friction components on the surface of the part. At this stage, the process of chemical precipitation of metals from copper oxide formed from a chemical reaction (2) takes place.

As a result of tribological loads and pressures, some of the tool material particles formed as a result of cutting are pressed into the depressions between the protrusions of the part's surface profile. This results in surface smoothing, an increase in the actual contact area, and a reduction in contact pressure when the part is working with an antifriction coating. As a result of high local pressures, cohesive bonds are formed between individual particles of the coating material.

In the process medium, formaldehyde CH_2O and acrolein C_3H_4O , as products of reaction (1) of the thermal decomposition of glycerol, react with copper oxide with subsequent reduction of copper Cu on the surface of the workpiece:



As a result, more active copper ions contained in the process medium are deposited on the bare juvenile surface of the part.

The glyceric acid $C_3H_6O_4$ formed during reaction (6) interacts with the part material (Fe), improving the mechanical and tribotechnical characteristics of the applied coating, which is an important aspect for ensuring high wear resistance and long-term operation of the part under increased loads [12].

The reaction of the interaction of glyceric acid with the material of the part will be as follows:



The reaction (7) results in the formation of the complex compound $[C_3H_6O_4]_2Fe$, an iron glycerate that is involved in the formation of the coating.

In addition to copper ions from the process medium, particles of the workpiece material that were separated in the first stage are involved in the formation of the coating. These particles are coated with thin layers of antifriction material due to chemical interaction with the process medium, forming a clad material that is also deposited on the surface of the part.

The chemical reactions and physical processes that take place at this stage can be represented as follows (Fig. 5).

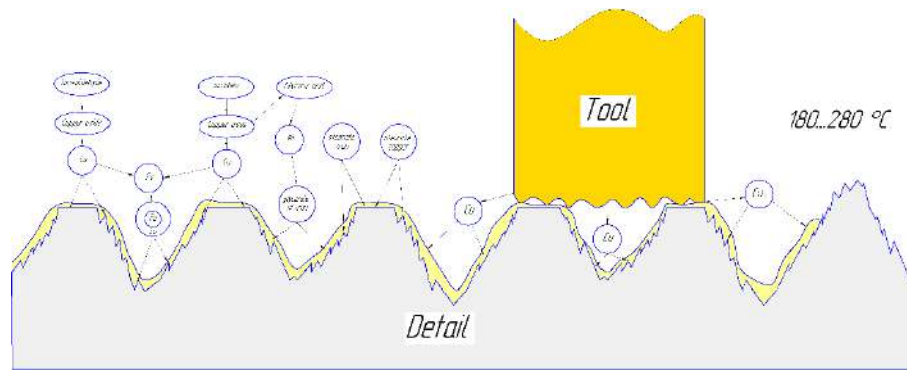


Fig. 5. Scheme of the processes that take place at the stage of deposition of anti-friction components on the surface of the part

The processes discussed above suggest that the formation of a coating depends on the material of the part, the temperature in the deposition zone, the interaction time, the rate of diffusion into the material, and the dissociation of chemical compounds.

The concentration of metal salts plays an important role in the course of chemical reactions.

Thus, the concentration of copper in the process fluid, according to [7], increases with increasing acidity *pH* (Fig. 6).

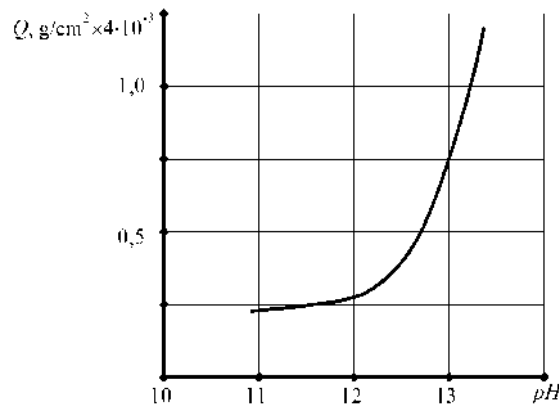


Fig. 6. Dependence of the coating deposition rate on the acidity of the *pH* of the medium [7]

Copper reduction begins at an acidity greater than 11, and the deposition rate increases with increasing acidity. The *pH* value for concentrated solutions can be as high as 11.5. Complexing agents, such as amino acetic acids and glycerol, included in the process fluid, not only increase the solubility of copper salts, but also affect the process of copper ion reduction on the deposition surface.

Reliable adhesion of the coating to the substrate can only be achieved if the coating material diffuses into the base metal.

The formation of a high-quality anti-friction coating is ensured by sufficient adhesion and is due to a reduction in the surface roughness of the part and an increase in the total contact area due to the filling of the base metal surface depressions with the coating material. Applying an anti-friction coating to a part reduces the friction forces that occur during its operation, thereby reducing its stress-strain state.

Formation of an anti-friction coating. At this stage, the transfer of tool material to the surface of the workpiece is completed (Fig. 7). The coating build-up stops as the equilibrium state is reached in terms of shear characteristics.

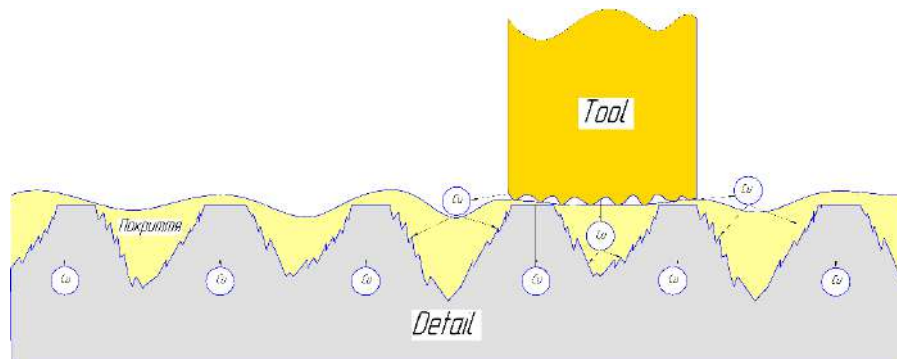


Fig. 7. Scheme of the processes involved in the formation of an anti-friction coating

The volumetric plastic flow of the tool material stops and the temperature in the friction zone decreases, which leads to inhibition of chemical reactions between the components of the process medium.

This stage is characterised by the diffusion of metal deposited on the surface deep into the surface layer of the part. Since the antifriction coatings produced by the FANT method have a certain degree of inconsistency, part of the surfactant from the process medium is adsorbed in the pores of the coating.

Conclusions

The analysis of physical and chemical processes in the contact zone ‘tool – part’ during the friction-mechanical method of applying antifriction coatings allowed to establish the following regularities:

1. For an objective assessment of the processes observed during the application of antifriction coatings, it is most appropriate to consider in detail the FANT process at the following stages: activation of the surfaces of the tool and the workpiece, deposition of antifriction components on the surface to be treated, and further formation of the antifriction coating.

2. The chemical reactions that occur during the formation of an antifriction coating allow you to track the processes of glycerol tribodestruction, copper chloride dissociation, chemical interactions of surfactants, destruction of oxide films, creation of complex compounds, etc. and identify ways to improve the quality of FANT antifriction coatings.

3. It is proved that the quality of coating formation directly depends on the material of the part and tool, temperature in the deposition zone, interaction time, material diffusion rate, and dissociation of chemical compounds.

4. The physical model of the FANT process is proposed, which illustrates chemical reactions and physical processes and allows to find out and explain the characteristic phenomena occurring at different stages of the antifriction coating creation.

References

1. Solovykh, E.K. (2012). Trends in the development of surface hardening technologies in mechanical engineering. Kirovohrad, KOD, 92 p.
2. Kosiuk, M.M., Kostiuk, S.A., Kostiuk, M.A. (2018). Technological support for the application of antifriction coating on incomplete spherical surfaces by friction-mechanical method. *Bulletin of Khmelnytsky National University*. Technical sciences. No. 4. 38-42.
3. Abdullah Rasheed A, Ihor Shepelenko, Eduard Posviatyenko (2020). Experimental quality improvement of the application of antifriction coating. First International Conference on Advances in Physical Sciences and Materials 13-14 August 2020, Coimbatore, India. *Journal of Physics: Conference Series*, Vol. 1706. 1-11. <https://iopscience.iop.org/article/10.1088/1742-6596/1706/1/012187>.
4. Gottlieb Polzer (1981). Erhöhung der Verschleißfestigkeit auf der Grundlage der selektiven Übertragung. 192 p.
5. Shepelenko, I., Nemyrovskiy, Y., Tsekhanov, Y., Mahopets, S., Bevz, O. (2020). Peculiarities of interaction of micro-roughnesses of contacting surfaces at FANT. In: Ivanov, V., Trojanowska, J., Pavlenko, I., Zajac, J., Peraković, D. (eds.) DSMIE 2020. LNME, 452-461. https://doi.org/10.1007/978-3-030-50794-7_44.
6. J. Schöfer et. al. (2001). Formation of Tribochemical Films and White Layers on Self-Mated Bearing Steel Surfaces in Boundary Lubricated Sliding Contact. Netherlands, Elsevier. 7-15.
7. Makoto Miyajima, Kazuyuki Kitamura, and Keishi Matsumoto (2017). Characterization of Tribochemical Reactions on Steel Surfaces. Nippon Steel & Sumitomo Metal Corporation. No. 114.
8. S. K. Biswas (2000). Some Mechanisms of Tribofilm Formation in Metal/Metal and Ceramic/Metal Sliding Interactions. Netherlands, Elsevier. 178-189.
9. Cherkun V.V. Increasing the wear resistance of hydraulic pump gear trunnions by finishing antifriction non-abrasive vibration treatment [Abstracts dys. ... kand. tekhn. nauk: 05.02.04]. 2011. 16 p.
10. Kubysh V.I. Increasing the wear resistance of tribo-conjugations of the crankshaft of an internal combustion engine by friction coating formation in gallium-indium medium [Abstracts dys. ... kand. tekhn. nauk: 05.02.04]. 2011. 18 p.
11. Shepelenko, I., Posviatenko, E., Cherkun, V. (2019). The mechanism of formation of anti-friction coatings by employing friction-mechanical method. *Problems of Tribology*, 24(1/91), 35-39. <https://doi.org/10.31891/2079-1372-2019-91-1-35-39>.
12. Krasota, A.M., Shepelenko, I.V., Krasota, M.V., Osin, R.A. (2024). Determination of Effectiveness and Component Classification of Technological Mediums for Finishing Antifriction Non-Abrasives Treatment of Automobile Details. *Central Ukrainian Scientific Bulletin*. Technical sciences. 10(41), II, 104-112. [https://doi.org/10.32515/2664-262X.2024.10\(41\).2.104-112](https://doi.org/10.32515/2664-262X.2024.10(41).2.104-112).

Красота А.М., Шепеленко І.В., Красота М.В. Фізичні та хімічні процеси при нанесенні антифрикційних покриттів фрикційно-механічним методом

Огляд сучасних моделей утворення антифрикційних покриттів фінішною антифрикційною безабразивною обробкою показав відсутність ґрунтового аналізу фізичних та хімічних процесів, що відбуваються в зоні тертя. З цієї точки зору доцільним виглядає дослідження процесів утворення покриття на етапах активації поверхонь, осадження антифрикційних компонентів та формування антифрикційного покриття. Розглянуті характерні структури та хімічні реакції на різних етапах створення антифрикційного покриття дозволяють відслідкувати процеси, що відбуваються в системі, та впливати на їх. Доведено, що якість формування покриття безпосередньо залежить від матеріалу деталі та інструменту, температури в зоні осадження, швидкості дифузії матеріалу, дисоціації хімічних з'єднань. Запропонована фізична модель процесу ФАБО, яка визначає хімічні реакції та фізичні процеси, що відбуваються на різних етапах формування антифрикційного покриття. Аналіз моделі дозволяє з'ясувати та пояснити характерні явища в системі «деталь – інструмент – технологічне середовище», а, отже, впливати на якість створення антифрикційного покриття фрикційно-механічним методом.

Ключові слова: фінішна антифрикційна безабразивна обробка, фізична модель, антифрикційне покриття, технологічне середовище, активація поверхні, трибодеструкція, зносостійкість



Research on thermoplastics under impact-abrasive wear

A.Gupka*, I. Yarema, I. Hevko, R. Leshchuk, V. Kobelnyk, V. Buhovets, T. Pyndus

Ternopil Ivan Puluj National Technical University, Ukraine

**E-mail: Gypkab@gmail.com*

Received: 15 January 2025; Revised 20 February 2025; Accept: 10 March 2025

Abstract

The article presents the results of research into the regularities of friction processes and impact-abrasive wear of thermoplastics under cyclic and shock loads. The conditions and modes of operation of gas transportation equipment units and the reasons for the failure of the most loaded parts are analyzed in detail. The nature of the impact of the abrasive and its characteristics on the wear resistance of the working surfaces of parts of gas transportation equipment units is revealed. The choice of thermoplastic grades for the manufacture of parts of gas transportation equipment working units that operate under cyclic shock loads is justified. The designs of existing stands for the study of surface deformation and impact-abrasive wear of thermoplastics are analyzed. The design of the experimental stand is improved and a force loading mechanism is manufactured to implement the tasks set, a comprehensive research methodology is proposed. The influence of the parameters and conditions of cyclic impact loading on the wear resistance of thermoplastics under conditions of impact-abrasive wear, as well as the features of wear of previously deformed thermoplastics, are identified and substantiated. Practical recommendations have been developed regarding the possible use of the studied thermoplastics for the manufacture of parts for gas transportation equipment assemblies.

Keywords: gas transportation equipment, thermoplastics, abrasive, friction, hydroabrasive wear, shock-cyclic loading, test bench.

Formulation of the problem

A promising direction for the development of the gas transportation industry is the replacement of traditional structural materials with polymers and composites based on them, which are used to manufacture parts of gas transportation equipment assemblies and units under conditions of impact and abrasive wear. This is due to the price factor, labor intensity and cost of manufacturing parts from polymers, which are significantly lower compared to the use of steels and alloys.

The problem of increasing the operational reliability and efficiency of gas transportation equipment assemblies and units operating under conditions of variable static and cyclic loads with impact and abrasive wear of friction surfaces is urgent. Intensive impact and abrasive wear of parts of gas transportation equipment assemblies significantly reduces its operating time, increases the costs of repair, restoration or replacement of worn parts.

To date, the problem of increasing the wear resistance of gas transportation equipment parts operating in the mode of cyclic shock loading with the specifics of contact interaction in the presence of abrasive, with varying degrees of fixation, in the environment of aggressive natural gas and gas condensate has not been solved. Corrosion, erosion and cavitation should be included among the auxiliary factors that affect the intensity of shock-abrasive wear of parts of gas transportation equipment components. When operating parts of gas transportation equipment components, it is necessary that the materials of the parts are characterized by high wear resistance under the conditions of the complex action of the working environment, abrasive, temperature, shock cyclic loads during shock-abrasive wear. The principles of selecting polymer materials (thermoplastics) for parts of heavily loaded gas transportation equipment components under the action of cyclic shock loads, the presence of abrasive, and aggressive working environment are not sufficiently developed and substantiated, there are practically no results of research into the influence of the previous cyclic shock loading on their wear resistance during shock-abrasive wear.



Analysis of recent research and publications

The study of modern trends in the production and application of polymeric materials for transport equipment is an important area of scientific research. The work considers the use and efficiency of manufacturing parts from polymeric materials for gas transportation equipment. The authors analyze the technological aspects of production and operational characteristics of such materials, which allows us to assess their potential in increasing the reliability and durability of gas transportation systems [1]. Special attention is paid to the development of modified epoxy coatings that improve the protective properties of materials.

The study proposes a method for manufacturing an epoxy coating with a filler that increases its strength and wear resistance. This study is of significant practical interest, since modified polymeric coatings can be effectively used to protect parts of vehicles and industrial equipment from corrosion and mechanical damage [2]. The work highlights the process of developing a polymer matrix with improved performance characteristics for protecting vehicle components. The research is aimed at increasing the durability and effectiveness of protective polymer materials, which is important for the automotive, gas transportation and other industries [3].

In their work [4], they determined the intensity of abrasive wear of protective polymer coatings, which made it possible to assess the durability and reliability of polymers during operation. In work [5], scientists analyzed the processes of impact-abrasive wear of the working bodies of road construction machines, focusing on materials that can withstand this type of wear, including polymer composites.

In work [6], they studied increasing the reliability of gas transportation systems through the use of new materials, including polymers that demonstrate high resistance to impact-abrasive loads. In article [7], a device for studying materials under impact-abrasive wear is presented, which is an important step in the development of testing methods for polymer materials. In study [8], the processes of abrasive wear of polymer materials are studied in detail and methods for its reduction are proposed, which is relevant for increasing the service life of polymers.

In [9], a study was conducted on the abrasive wear of antifriction materials, in particular polymers, which is important for their use under shock-abrasive loads. Thus, the analysis of literature sources demonstrates that the study of thermoplastics under shock-abrasive wear is a relevant direction that has significant scientific and practical interest, especially in the context of increasing the durability and reliability of parts and equipment.

The study of the mechanical characteristics of epoxy composites is a relevant direction in modern materials science developments. The work [10] presents the results of the study of the mechanical properties of filled epoxy composite materials. The authors analyzed the influence of various fillers on the physical and mechanical characteristics of the material, which allows optimizing its composition to improve operational characteristics.

Another study [11] considered the impact strength of epoxy coatings modified with silicate-containing additives. The work demonstrates that the use of such modifiers allows to significantly improve the impact resistance of coatings, which is critically important for increasing their durability and reliability in operation. In the article [12], an analytical analysis of stresses in furan-epoxy composite coatings during tension was performed.

The authors used fracture mechanics methods to assess the behavior of the material under load, which allows predicting its operational stability. In addition, the work [13] considered the issue of tribodiagnostics of damage to the surfaces of triboconnection materials during machine operation. The authors focus on the wear mechanisms of materials in contact under load and propose approaches to increase their wear resistance.

Thus, the analysis of recent studies indicates the active development of scientific approaches to optimizing the composition and mechanical properties of epoxy composites and coatings. The results obtained can be used for further development of effective materials with improved performance characteristics.

The purpose of the work

The purpose of this work is to find ways to increase the wear resistance, service life, and performance of parts of gas transportation equipment assemblies, and to select the most effective polymer materials. To achieve this goal, it is necessary to solve a number of practical research problems: to analyze in detail the operating conditions of parts of gas transportation equipment assemblies; to justify the choice of grades of polymer materials for their further study; to modernize the research stand with the development of research methods and criteria for assessing impact-abrasive wear of polymers under cyclic loading of test specimens; to investigate the effect of previous cyclic impact loading on the wear resistance of these thermoplastics; to develop practical recommendations for increasing the wear resistance and operational reliability of parts of gas transportation equipment assemblies made of thermoplastics under cyclic impact loading.

For a methodically correct assessment of the wear resistance of thermoplastics during impact-abrasive wear, it is necessary to analyze the characteristics of the abrasive, investigate the influence of the previous impact cyclic load on the nature of their deformation and the intensity of wear. Conduct a set of studies to determine the contact deformations and wear resistance of thermoplastics under their operating conditions and establish general patterns of wear and destruction mechanisms. Develop practical recommendations for the selection of thermoplastic grades for the manufacture of parts of heavily loaded gas transportation equipment components and criteria for assessing their performance.

Research results

To obtain objective, satisfactorily comparable results of experimental studies, it is necessary to use the same type of equipment, a single methodology for conducting research and data processing, and criteria for assessing

the performance of thermoplastics under conditions of impact-abrasive wear. When choosing grades of thermoplastics for parts of gas transportation equipment assemblies to study their wear resistance under conditions of impact-abrasive wear, the following technical characteristics were taken into account, both for the materials of the parts and for their operating conditions: impact cyclic loading on parts (impact-deformation change in the dimensions of parts); temperature; presence of abrasive; aggressive working environment; stability of geometric dimensions of parts and minimal shrinkage of the material; stability of operation under the above operating modes; relatively low cost; low friction coefficient. Taking into account the conditions and operating modes of parts of heavily loaded gas transportation equipment units, according to the results of previous studies by the authors of the article and other researchers, the most suitable thermoplastic materials are: polyamides; polycarbonates; polystyrenes. The following brands of thermoplastics were selected for the planned set of studies: glass-filled polyamides PA66-KS, PA6-210KS, PA66-PE; unfilled polyamides P-6, UMP225.

Equipment (stands) used in the study of the wear resistance of thermoplastics under conditions of impact and abrasive wear must provide periodic (cyclic) impact loading on the part under conditions of a real working environment. Objective and reliable research results can be achieved only when using special stands that reproduce the operating mode of gas transportation equipment parts under impact and abrasive wear. The most suitable for conducting experimental studies of selected materials of parts, under given operating conditions, are stands with a crank drive mechanism and additional devices, with the ability to reproduce the required range of changes in speed, frequency and impact energy in the contact zone, to simulate the nature of impact cyclic loading. Regarding parts of gas transportation equipment, a special stand has been modernized to conduct comprehensive studies of the wear resistance of selected grades of thermoplastics under conditions of impact-abrasive wear, under cyclic loading, in the presence of abrasive with varying degrees of its fixation, the general appearance of which is shown in Fig. 1, and the loading mechanism of the stand developed by the authors of the article is shown in Fig. 2.

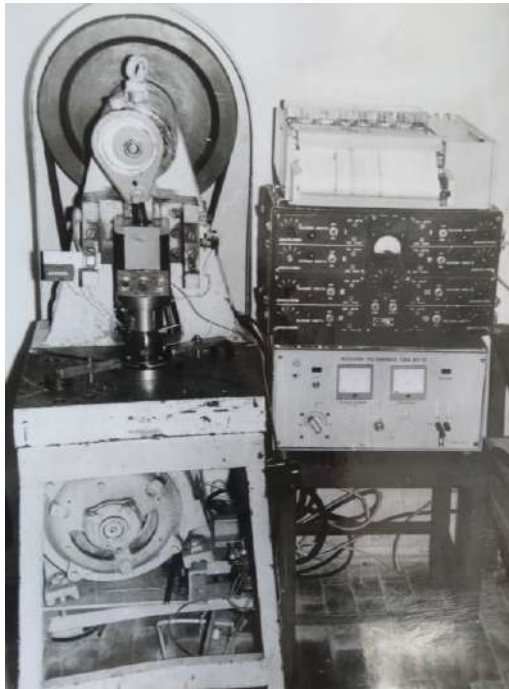


Fig. 1. General view of the stand

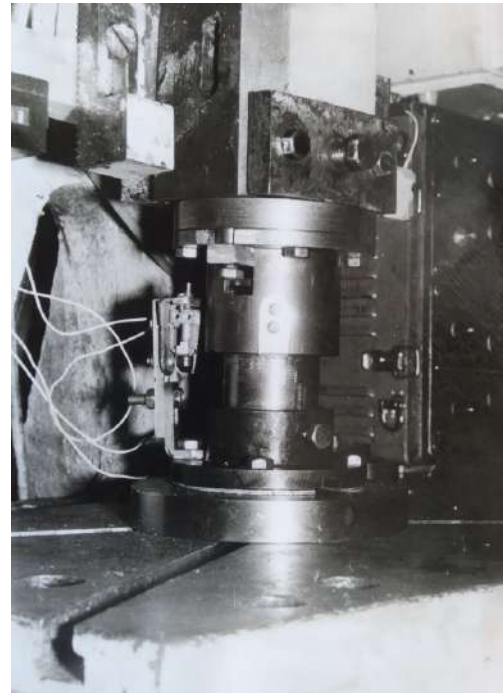


Fig. 2. Bench loading mechanism

The technical characteristics of the stand are given in Table 1.

Table 1

Technical characteristics of the stand	
Operating parameters of the stand	Value
Maximum working force, N	30000
Impact velocity, m/s	1-10
Impact frequency, Hz	1-5
Number of research cycles	1-100000
Working stroke of the slider, m	0-0,04
Working medium	Air
Condition of the abrasive	Free layer
Control parameters	Impact force
	Impact velocity
	Impact pulse length
	Deformation magnitude

The stand consists of a mechanism that performs multiple actions of the striker and the forge during the reciprocating motion of the striker slider; a control system, control and measuring equipment; replaceable auxiliary devices to expand the technological capabilities of the stand. The kinematic diagram of the stand for the study of thermoplastics under cyclic impact loading is shown in Fig. 3.

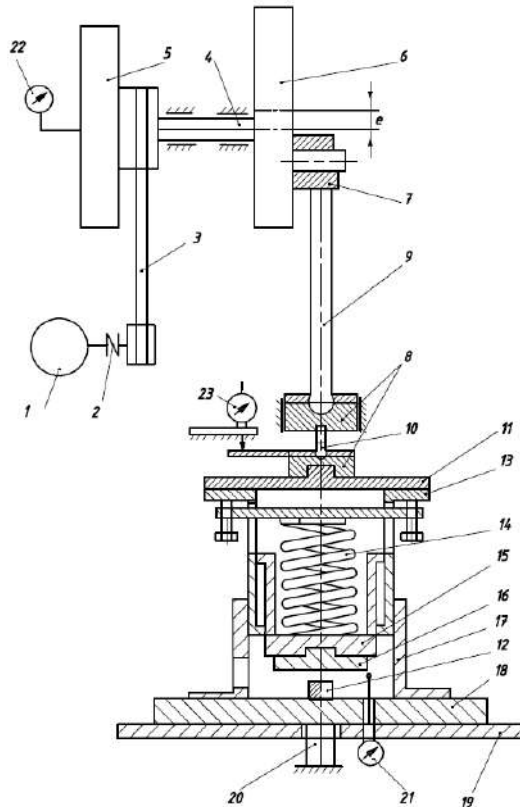


Fig. 3. Kinematic diagram of the stand for studying impact-abrasive wear of thermoplastics under impact cyclic loading conditions

Structure and principle of operation of the stand. The stand is mounted on a common frame with all working units and mechanisms placed on it. The electric motor 1 is connected to the shaft 4 through an electromagnetic clutch 2 and a V-belt transmission 3, on which a flywheel 5 is placed with a system of two mutually crossed eccentrics 6 and 7. The axis of rotation of the eccentric 6 is located at a constant distance e from the axis of the shaft 4. In the body of the eccentric of large geometric dimensions 6, an eccentric 7 is placed, with the help of which the stroke of the slider 8 is regulated. When the eccentric 7 is rotated and fixed at a certain angle relative to the initial position, the radius of rotation of the end of the rod 9 relative to the axis of rotation of the shaft 4 changes. The rod pivotally connects the eccentric 7 and the slider 8, which consist of two halves connected by an adjusting screw 10. In addition to the existing load schemes, this stand uses an elastic attachment that allows you to implement the static component of the force of interaction of the samples. The spring attachment is fixed in the seat of the lower half of the slider 8. The device consists of a shank 11, which acts through a tension beam 13 and a spring 14 on the striker 15, in which the indenter 16 is fixed. The guide cup 17 is used to center the striker and fix the samples on the anvil 18. The lower part of the device is mounted on a table 19, in which holes are provided for installing a piezo sensor 20 and a clock-type indicator 21. The torque from the electric motor through the electromagnetic clutch and V-belt transmission is transmitted to the crank mechanism, which converts the rotational motion of the drive into the reciprocating motion of the striker 15 with a given frequency and amplitude of the load on the sample 12. The given shaft rotation frequency is set using a variable drum of the V-belt transmission 3 and is controlled by a tachometer 22. The load amplitude, which determines the time of loading the sample and the time of its unloading, is set by the mutual arrangement of the eccentrics 6 and 7, i.e. by changing the radius of rotation. To create a given load force on the sample, at the initial moment, a spring 14 serves. The magnitude of this force depends on the stiffness of the spring, the magnitude of its preliminary pressing by the tensile beam 13, and the speed of contact of the indenter with the sample. The design of the striker 15 provides for the possibility of attaching indentors 16 of various shapes: flat, cylindrical, prismatic for modeling the contact interaction of parts of various configurations. The stand allows for the study of impact-abrasive and impact-fatigue wear of polymeric materials under different loading conditions, in different working environments. This paper presents the results of the study of impact-abrasive wear, which is implemented in the case of feeding the abrasive into the impact zone of the indenter 16 with the sample 12. To study samples of different thicknesses under the same power load parameters, an adjusting screw 10 is used. The difference in the height of the samples is controlled by a watch-type indicator 21 with a measurement accuracy of 0.001 mm and a bar attached to the lower moving part of the slider 8. When developing a method for measuring contact parameters in the process of impact-abrasive

wear, all the requirements that are put forward for studies of this nature were taken into account. The measuring complex of the stand includes: a system for measuring dynamic impact characteristics, a system for determining the initial static load, a system for automatically setting the number of load cycles. Fig. 4 shows a scheme for measuring dynamic impact characteristics in the study of impact-abrasive wear of thermoplastics.

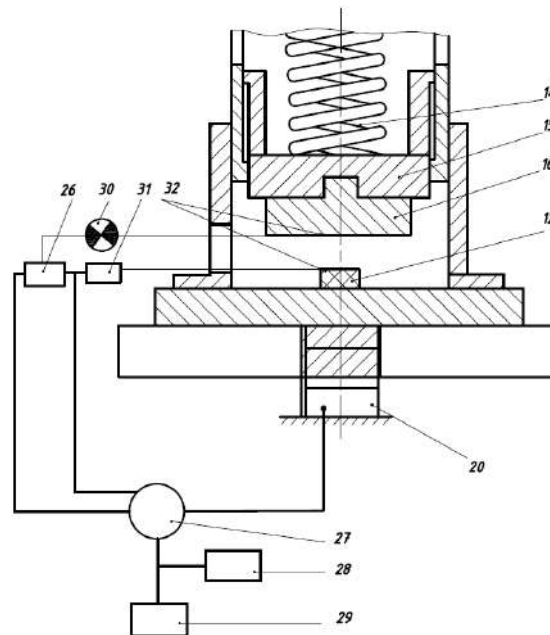


Fig. 4. Scheme of measuring dynamic impact characteristics when studying impact-abrasive wear of thermoplastics

The measuring circuit consists of a piezoelectric sensor 20, a synchronization unit 26, a universal oscilloscope 27 model S8-13, with an output to a high-speed recorder 29 model H338-6N, a digital automatic integrator 28 model I-02 and a current source 31. The initial moment of contact of the indenter 16 with the sample 12 is recorded by a light bulb 30, which is connected via a power supply to point contacts 32, which are placed on the contacting surfaces. The synchronization unit includes recording the signal on the oscilloscope 27 with its subsequent processing on a digital integrator 28 and visual reproduction by a high-speed recorder 29.

The system for setting the initial statistical parameters of the load consists in creating a preliminary force of the spring 14 on the striker 15 by pressing the strain gauge 13, on which the strain gauges are glued, with the help of two screws. The system for automatically setting the number of load cycles includes an electromechanical counter 22, which sends a signal to trigger the electromagnetic clutch of the main drive of the stand. To measure the magnitude of the deformation of the sample from the number of load cycles, a clock-type indicator 21 is fixed on the stand table 19. When studying the impact-abrasive wear of thermoplastics, cylindrical samples were used, which allow the most accurate assessment of the behavior of materials during this type of wear. A cylindrical sample with a diameter of 10 mm and a height of 18 to 30 mm was studied. The cylindrical shape of the thermoplastic sample provides higher strength compared to rectangular and triangular samples. The study of impact-abrasive wear was carried out under the action of external force factors on the samples while maintaining the specific energy of a single impact, the frequency and speed of co-impact, and the temperature. Silicon carbide with a grain size of 0.63 mm was used as an abrasive material. Impact-abrasive wear of parts of gas transportation equipment assemblies occurs mainly when they hit loose abrasive and abrasive mass contained in the gas medium being transported. In some cases, impact contact can also occur on resinous deposits of the working medium (gas) fixed on the working surfaces. The main principle schemes for the study of thermoplastics for parts of gas transportation equipment are studies on abrasive mass and loose layer of abrasive of a certain thickness, which is placed on a metal base.

Fig. 5 shows the formation of working surfaces of thermoplastics during impact and abrasive wear.

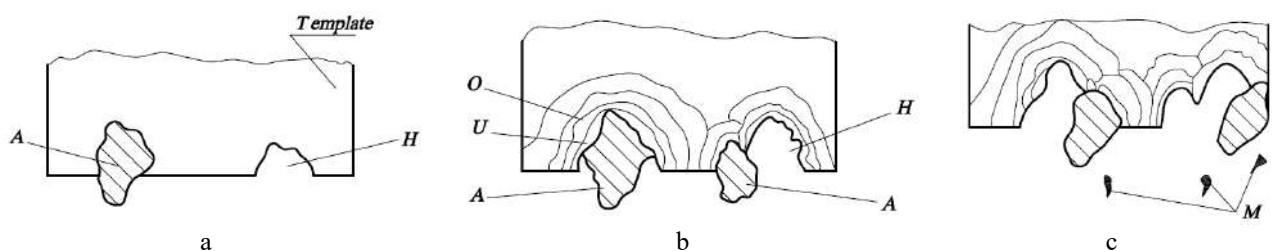


Fig. 5. Schemes of forming working surfaces of thermoplastic parts during impact-abrasive wear

When the abrasive hits, its individual grains A penetrate directly into the surface of the sample and at the first stage are wedged in the body of the sample (Fig. 5 a). Subsequent impacts of the abrasive lead to their further pressing into the sample material (Fig. 5 b) with the formation of a zone of volumetric deformation (O) and surface compaction (U) of the material under it when the wedged area expands under the action of tangential forces. The process of accumulation of the abrasive occurs in the surface layer of the sample material. Part of the abrasive, when in contact with the surface of the thermoplastic, does not wedge in it, but leaves behind characteristic holes H on the surfaces of the sample (Fig. 5 b). The subsequent impact action of the abrasive leads to repeated entry of abrasive particles into the previously formed holes on the surface of the sample and the process of removal of the sample material M from the contact zone in the form of chips or microparticles occurs (Fig. 5 c). The number of holes on the surface of the sample constantly increases, which leads to complete damage to the entire surface with the formation of wear particles. At this point, the period of running-in of the sample surface ends and the period of its stable wear begins. The dynamics of the wear mechanism of the surface of a sample made of thermoplastic PA66-KS on a layer of unbonded abrasive is presented in the photographs (Fig. 6).

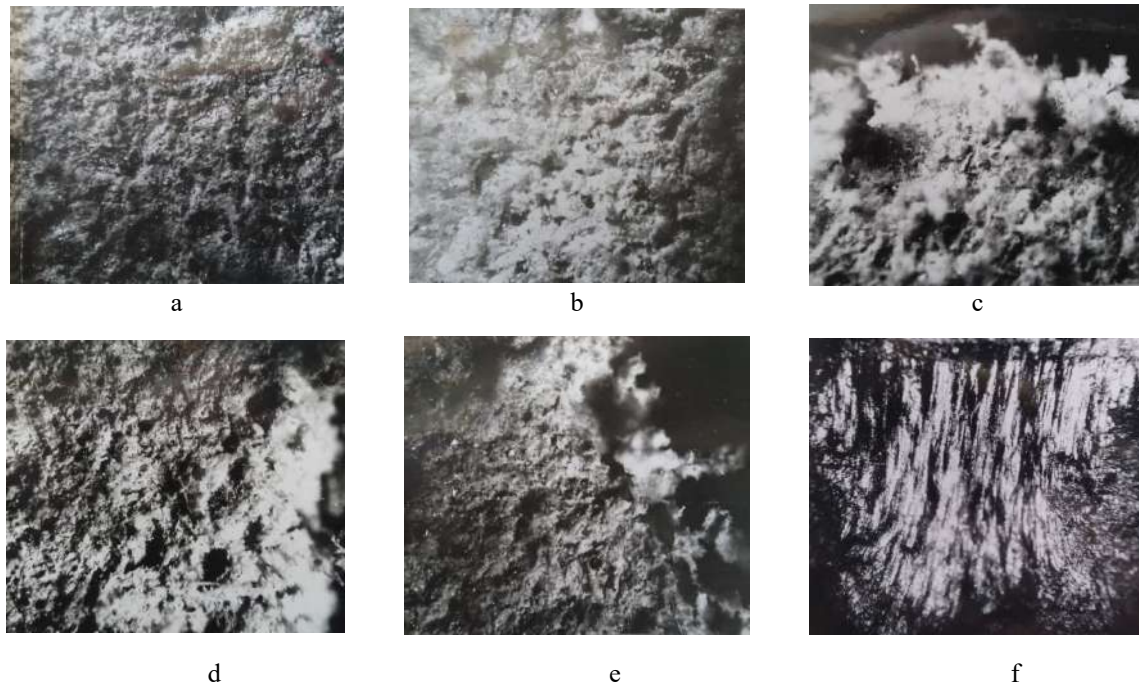


Fig. 6. The relief of the wear surface of a sample made of thermoplastic PA66-KS when hitting a layer of abrasive, depending on the number of hits: a – 50; b – 500; c – 1000; d – 1500; e – 2000; f – 3000

The parameters and conditions of the impact cyclic nature of the load on the intensity of wear of parts made of thermoplastics were studied. According to the results of the analysis of the operating conditions of parts of gas transportation equipment assemblies, it was found that most parts and assemblies are operated mainly in the range of change in the energy of a single impact from 1.3 J/cm^2 to 2.0 J/cm^2 . The frequency of mutual impacts was taken as such, which did not lead to noticeable self-heating of the materials of the parts. Fig. 7 presents graphs of the dependence of the magnitude of impact-abrasive wear of the studied thermoplastics on the number of load cycles.

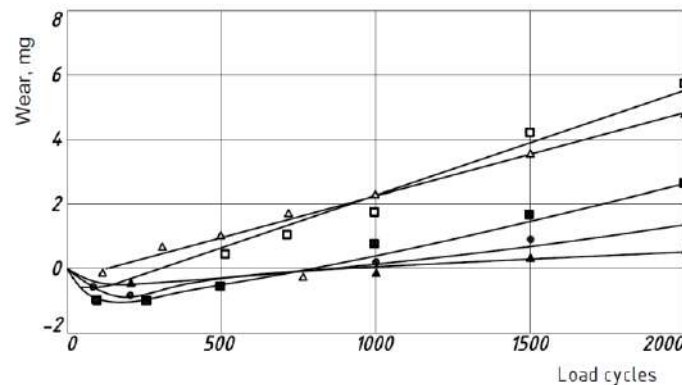


Fig. 7. Graphs of the dependence of the wear value of the studied thermoplastics on the number of loading cycles at a constant energy of a single impact: □ – PA66-PE; ● – P6; △ – PA66-KS; ▲ – P6 (secondary); ■ – PA6-210-KS

At the initial stage, in almost all thermoplastics, a relief is formed on the contacting surfaces, during which intensive penetration of abrasive particles occurs (the process of drawing), as evidenced by an increase in the

weight of the samples and the formation of a negative area on the graph. In this case, the drawing process dominates over the process of wear of the material of the parts - the running-in process. Depending on the characteristics of the material under study, the running-in period is different: in unfilled thermoplastics it is longer in comparison with glass-filled thermoplastics. The running-in process in all considered thermoplastics does not exceed 700 impacts on the abrasive.

Further, during impact-abrasive wear of thermoplastics, after the accumulation of the maximum amount of abrasive on the surfaces of the samples, determined for each material, a decrease in the weight of the sample is observed and the amount of wear becomes proportional to the number of impacts - the period of established wear, which is linear in nature. The beginning of the established nature of wear is the inflection point of the curve in the negative section of the graph. The wear rate of glass-filled thermoplastics is greater than the wear rate of unfilled thermoplastics (determined by the angle of inclination of the curve on the graph). One of the main reasons is that unfilled thermoplastics with a linear molecular structure are characterized by more developed forced elasticity. These thermoplastics are able to resist repeated deformation, and therefore impact-abrasive wear, for a longer period of time compared to glass-filled thermoplastics, which are harder and more brittle materials.

In parts made of glass-filled thermoplastics, unlike unfilled ones, a patterned layer of abrasive does not form on their surfaces, i.e. its particles do not wedge in and do not remain in the surface layer. In unfilled thermoplastics, the patterned layer counteracts the penetration of new abrasive particles into the material, taking on the initial impact load at the moment of contact of the part surface with the abrasive.

The intensive wear of glass-filled polyamides is also facilitated by the fact that glass fibers oriented in the direction of the impact force contribute to the fragmentation and damage of the original structure of the material, thus reducing its integrity and uniformity. When the energy of a single impact (A_{im}) increases to 2 J/cm^2 , a more intensive wear process of the studied thermoplastics is observed (Fig. 8).

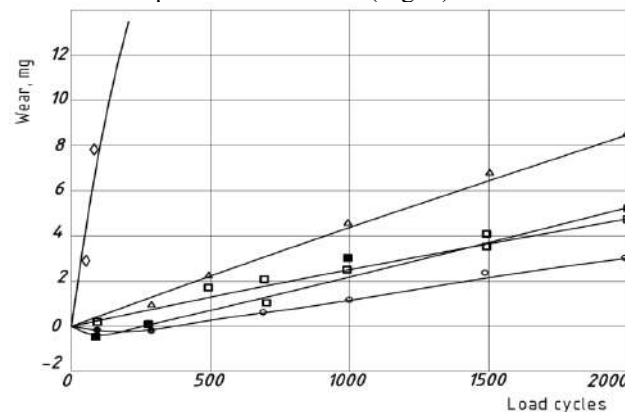


Fig. 8. Graphs of the dependence of the magnitude of impact-abrasive wear (by mass of silicon carbide) of the studied thermoplastics on the number of load cycles: $A_{im} = 2,0 \text{ J/cm}^2$; □ - PA66-PE; ● - P6; △ - PA66-KS; ◇ - P6 (secondary); ■ - PA6-210-KS

The period of the running-in process of thermoplastics decreases both in terms of the amount of wear and in terms of its length, and for glass-filled thermoplastics it is absent (PA-KS, PA66 PE) or insignificant (PA6-210KS). An increase in the energy of a single impact does not lead to a proportional increase in the amount of wear. An increase in the energy of a single impact by 35% increases the amount of wear of the PA66-KS thermoplastic by 40%, of the PA-210KS thermoplastic by 51%, of the P6 thermoplastic by 59% (Fig. 9).

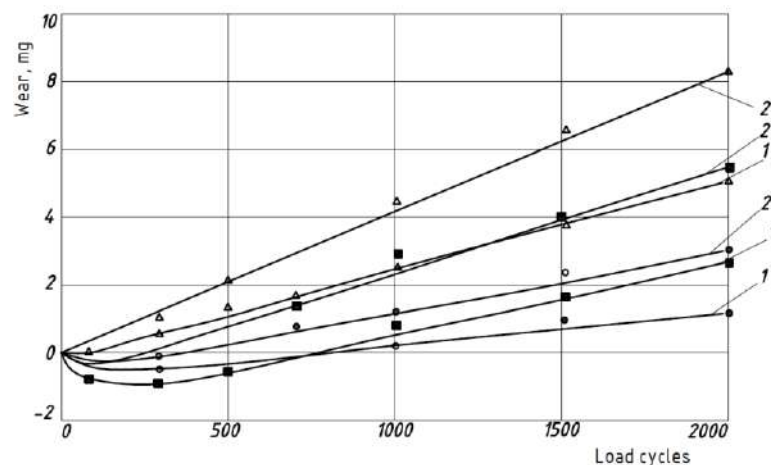


Fig. 9. Graphs of the dependence of the wear value of the studied thermoplastics on the specific impact energy (based on the abrasive mass of silicon carbide): ● - P6; △ - PA66-KS; ■ - PA6-210-KS; 1 - $A_{im} = 1,3 \text{ J/cm}^2$; 2 - $A_{im} = 2,0 \text{ J/cm}^2$

The disproportionate increase in the wear rate of thermoplastics with increasing single impact energy is mainly due to the different nature of the abrasive action on the surface of the parts. The mechanism of formation of holes and partitions during the dynamic penetration of solid particles of unfixed abrasive into the sample material is associated with the change in single impact energy. It is obvious that the abrasive particles do not wedge into the surface layer of the thermoplastic, but mechanically destroy it, while the intensity of the abrasion of these surfaces is much lower compared to low impact energies.

Under the operating conditions of gas transportation equipment components in the shock-abrasive wear mode, the surfaces of the parts wear out both in terms of the layer and the mass of the abrasive. Fig. 10 shows the graphical dependences of the wear value of glass-filled polyamide PA66-KS in the above conditions.

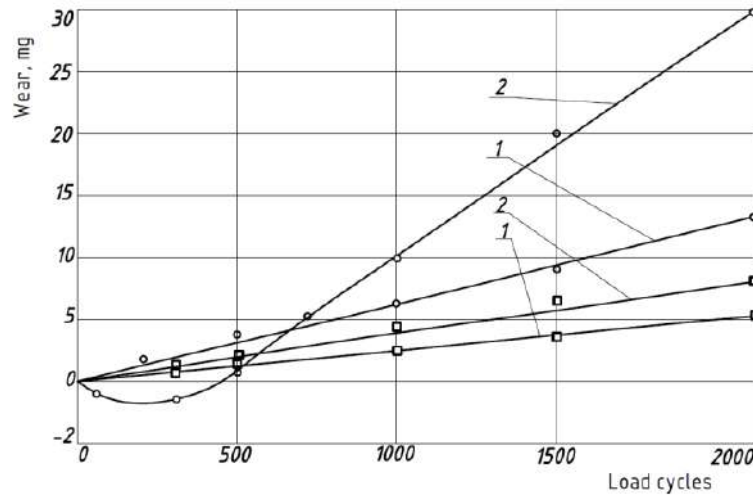


Fig. 10. Graphs of the dependence of the wear value of the PA66-KS thermoplastic on the type of abrasive and the energy of a single impact: ○ – by a layer of abrasive; □ – by mass; 1 - $A_{im} = 1,3 \text{ J/cm}^2$; 2 - $A_{im} = 2,0 \text{ J/cm}^2$

The results of the conducted studies and their analysis showed that the most dangerous type of wear for thermoplastics is the wear of working surfaces by the abrasive layer than by its mass, even at lower energies of a single impact (for PA66-KS by 2.4-3.3 times). It should also be noted that along with the thermoplastic, the metal surface on which the abrasive is placed also wears out. The characteristic relief of the surface on the forge (steel45) is shown in Fig. 11. The features of this type of wear include the formation of holes and bridges, the shape and size of which are much smaller than similar ones that form on the surfaces of thermoplastics and have a more oval shape and smoothed tops of the protrusions.



Fig. 11. Surface relief on a forge (steel 45) as a result of the action of an abrasive

When changing the characteristics of abrasive parts (hardness, dispersion, concentration), the most significant effect on the wear intensity of thermoplastics is the increase in the hardness of the abrasive. As a rule, the hardness of thermoplastics is insignificant compared to the hardness of abrasives, so the presence of any abrasive in the contact zone leads to the destruction of the surfaces of thermoplastic parts.

The final cycle was the study of the influence of the preliminary deformation of thermoplastics on the features of their wear. The contact time of the surfaces of thermoplastic parts in the presence of an abrasive is significantly shorter than when they are in contact without an abrasive. Such conditions of impact-abrasive wear are preceded by a cyclic impact interaction of the surfaces of the parts without the presence of abrasive parts in the contact zone. In this regard, it was necessary to assess the influence of the preliminary cyclic impact load on the wear resistance of thermoplastics.

During the study, the surfaces of thermoplastic samples were loaded by preliminary deformation with a given frequency and magnitude of impact energy. Fig. 12 shows graphs of the dependence of the wear value of preloaded (load cycle up to 5×10^3) unfilled polyamide P6 on the study time during impact-abrasive wear.

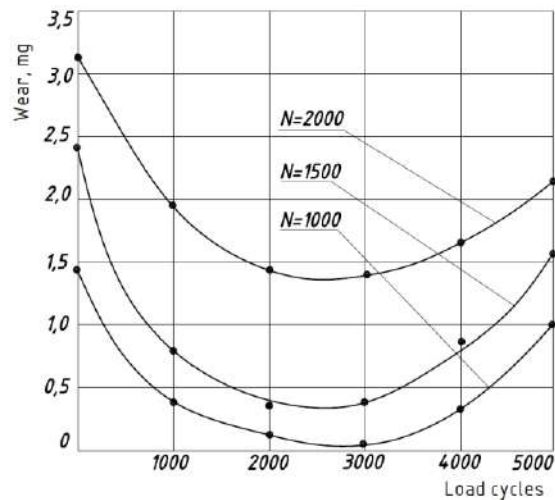


Fig. 12. Graphs of the dependence of the wear value of polyamide P6 on the number of pre-load cycles N:
 1 - $A_{im} = 1,3 \text{ J/cm}^2$; 2 - $A_{im} = 2,0 \text{ J/cm}^2$; $V = 5 \text{ Hz}$

As can be seen from the graph, the wear value of polyamide P6 decreases with increasing number of pre-load cycles only up to a certain value. This limit for the parameters of external action at a single impact energy of 5 J/cm^2 and a frequency (V) of 5 Hz for polyamide P6 is equal to 3×10^3 cycles of pre-load, which determines the appearance of the minimum value on the graph. After reaching this limit, the wear value of polyamide P6 slowly increases, however, even at 5×10^3 cycles of pre-load, the wear value of this thermoplastic is smaller in comparison with a similar material that was not subjected to pre-impact loading.

The decrease in the wear value of polyamide P6 preloaded to 3×10^3 cycles is explained by the fact that under these parameters of external action, the contact surfaces and subsurface layers are strengthened, due to the orientation and ordering of the structure.

With a further increase in the number of cycles of the pre-impact load, a gradual decrease in strength occurs, microcracks are formed and the surface layer of the part material is destroyed. The number of cycles of pre-loading on the sample can be determined by the magnitude of the relative deformation of the material. In this regard, the wear resistance of the material can be characterized as a function of the magnitude of the previous relative deformation (Fig. 13).

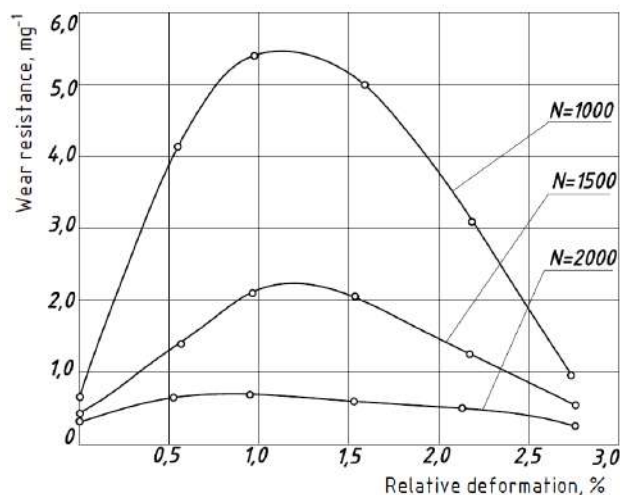


Fig. 13. Graphs of the dependence of the wear resistance of polyamide P6 on the previous relative deformation and the number of cycles of impact-abrasive wear N

According to the results of the research, it was found that preliminary deformation of polyamide P6 by 1.0-1.5% increases its wear resistance by 6-8 times. With a further increase in the time of impact-abrasive wear, its wear resistance decreases, which is explained by the gradual destruction of the upper strengthened layer of this material and the removal of destruction products from the contact zone. The insignificant difference in the value of the wear resistance of polyamide P6, which was not subjected to preliminary impact loading, is explained by the fact that during impact-abrasive wear, not only the wear of the surface layers but also the strengthening of the lower layers of the material occurs. The optimal deformation in terms of increasing the wear resistance of the surface layers for polyamide P6 is within 1.5-2.0%. The specified deformation range is achieved under conditions of cyclic shock loading on the sample with a frequency of 5 Hz , impact energy of 5 J/cm^2 and the number of cycles of 2×10^3 - 3×10^3 .

Conclusions

1. The selection of thermoplastics for parts of gas transportation equipment assemblies of a specific purpose should be carried out based on the results of research into their wear resistance during impact-abrasive wear with different characteristics of the abrasive and the degree of its fixation, the nature of the impact of the aggressive working environment, and the previous shock cyclic load.

2. The operational reliability and performance of parts of gas transportation equipment assemblies depends mainly on the selected brand of thermoplastic and its characteristics, the nature of the force load (cyclic, shock), the presence of the type of abrasive, the degree of aggressiveness of the working environment, which lead to loss of tightness of the working assembly, surface destruction of parts, and changes in their geometric dimensions as a result of shock-abrasive wear.

3. The operational (research) reliability of the developed stand for studying impact-abrasive wear of polymeric materials of different brands in wide ranges of load force parameters with obtaining objective, satisfactorily comparable and reproducible results of experimental studies has been confirmed.

4. Preliminary deformation of the surface layers of thermoplastics under the action of cyclic impact loads increases the strength characteristics of these materials (hardness, tensile strength) and wear resistance. For the studied thermoplastics, the values and ranges of preliminary deformation, the frequency of cyclic impact loading, impact energy and the number of load cycles have been determined from the point of view of increasing their wear resistance. A series of studies of glass-filled polyamides PA66-KS, PA6-210KS, PA66-PE and unfilled polyamides P-6, UMP-225 was conducted to identify the main factors that significantly affect their wear resistance during impact and abrasive wear.

5. The mechanisms of impact-abrasive wear of thermoplastics have been identified and must be taken into account when selecting materials for parts for gas transportation equipment assemblies and units in order to ensure the specified operational characteristics.

6. The peculiarities of the impact of abrasive on the processes of drawing of working surfaces of parts of gas transportation equipment assemblies made of glass-filled and unfilled thermoplastics have been identified.

7. It has been confirmed that a more intensive type of abrasive wear of the surfaces of thermoplastic parts is their wear by layer and not by mass of abrasive, even at lower energies of a single impact.

8. It has been experimentally confirmed that the main parameter that affects the intensity of impact-abrasive wear of the surfaces of thermoplastic parts is the energy of a single impact.

9. Practical recommendations have been developed for the use of thermoplastics for the manufacture of parts of working units of gas transportation equipment that operate under impact-abrasive wear conditions. Parts for gas transportation equipment units of new designs that are operated under cyclic impact loading under impact-abrasive wear conditions have been designed and manufactured (parts of spherical ball joints for the drive mechanism of the gas inlet valve of a gas motor compressor, valves of gas motor compressors, anti-pumping ball valves, seals of ball valves, seals of the rotor shaft of centrifugal gas pumping units).

References:

1. Lutsiv I., Yarema I., Kobelnyk V., Buhovets V. (2022) Using and efficiency manufacturing of polymeric materials parts for gas transportation equipment. *Scientific Journal of TNTU (Tern.)*, vol 105, no 1, pp. 80–94.
2. Method of performing modified epoxy coating with filler: pat. 148718 Ukraine / Buketov A. V., Kulinich V. G., Bezbak O. M., Kindrachuk M. V., Tisov O. V., Yarema I. T., Sotsenko V. V., Yurenin K. Yu., Smetanin S. O.; applicant and owner Kherson State Maritime Academy. – No. u202102164; appl. 23.04.2021; publ. 08.09.2021, bull. No. 36.
3. M.V. Brailo, A.V. Buketov, I.T. Yarema. Development of a polymer matrix with improved performance characteristics for the protection of vehicle elements: *Ivano-Frankivsk, journal of hydrocarbon power engineering. Oil and Gas exploration and production. Vol. 7 No. 2, 2020 p. 71-76.*
4. Ishchenko A. O., Dashko O. V. Determination of the intensity of abrasive wear of a protective polymer coating // *Bulletin of the Azov State Technical University. Series: Technical Sciences.* – 2015. – Vol. 2, No. 30. – P. 86–91.
5. Savulyak V. I., Grimashevich V. O. Analysis of the processes of impact-abrasive wear of the working bodies of road construction machines // *Scientific works of the Vinnytsia National Technical University.* – 2024. – No. 4. – P. 114–120.
6. Kopey B. V., Benmuna A., Slobodian V. I., Bellaur A., Galiy S. I. Increasing the reliability of gas transportation systems: monograph. – *Ivano-Frankivsk: Fakel, 2016.* – 200 p.
7. Shlapak L. S. Development of a device for studying materials and coatings under conditions of impact-abrasive wear // *Information on the scientific and scientific-technical activities of the Ivano-Frankivsk National Technical University of Oil and Gas for 2021.* – *Ivano-Frankivsk: IFNTUNG, 2021.* – P. 45–46
8. Budnyk A. F., Yuskayev V. B. Abrasive wear of polymeric materials and methods for its reduction // *Tribotechnical systems.* – 2018. – No. 3. – P. 45–52
9. Ivzhych O. V. Research on abrasive wear of antifriction materials based on copper and steel: master's thesis. – *Kyiv: NTUU "KPI", 2017.* – 120 p.
10. Stukhlyak P. D. Research on the mechanical characteristics of filled epoxy composites / Petro Danylovych Stukhlyak, V. O. Naumov, Roman Zakharyovych Zoloty // *Collection of abstracts of the X*

International scientific and practical conference of young scientists and students "Actual problems of modern technologies", November 24-25, 2021. — T. : FOP Palyanytsya V. A., 2021. — Volume I. — P. 21. — (New materials, strength and durability of structural elements).

11. Research on the impact strength of coatings when adding a silicate-containing modifier to the epoxy matrix / P. D. Stukhlyak, V. M. Yatsyuk, V. O. Naumov, R. Z. Zoloty // Collection of abstracts of the International Scientific and Technical Conference dedicated to the memory of Professor Bohdan Matviyovych Hevko "Problems of the theory of design and manufacturing of transport and technological machines", September 23-24, 2021. — T. : FOP Palyanytsya V. A., 2021. — P. 111. — (New materials, strength and durability of structures).

12. Dolgov, N., Stukhlyak, P., Totosko, O., Melnychenko, O., Stukhlyak, D., & Chykhira, I. (2024). Analytical stress analysis of the furan epoxy composite coatings subjected to tensile test. *Mechanics of Advanced Materials and Structures*, 31(25), 6874-6884.

13. Aulin, V., Lyashuk, O., Gupka, A., Tson, O., Дмитро, М., Sokol, M., ... & Yarema, I. (2024). Tribodiagnosis of the surface damage of tribo-coupling parts materials during machine operation. *Procedia Structural Integrity*, 59, 428-435.

Гупка А., Ярема І., Гевко І., Лещук Р., Кобельник В., Буховець В., Пиндус Т. Дослідження термопластів при ударно-абразивному зношуванні

У статті представлено результати досліджень закономірностей процесів тертя та ударно-абразивного зношування термопластів при циклічних та ударних навантаженнях. Детально проаналізовано умови та режими експлуатації вузлів газотранспортного обладнання та причини виходу з ладу найбільш навантажених деталей. Виявлено характер впливу абразиву та його характеристик на зносостійкість робочих поверхонь деталей вузлів газотранспортного обладнання. Обґрунтовано вибір марок термопластів для виготовлення деталей робочих вузлів газотранспортного обладнання, які працюють при циклічних ударних навантаженнях. Проаналізовано конструкції існуючих стендів для дослідження поверхневої деформації та ударно-абразивного зношування термопластів. Вдосконалено конструкцію дослідного стенда та виготовлено механізм силового навантаження для реалізації поставлених задач, запропонована комплексна методика проведення досліджень. Виявлено та обґрунтовано вплив параметрів та умов циклічного ударного навантаження на зносостійкість термопластів в умовах ударно-абразивного зношування, а також особливості зношування попередньо деформованих термопластів. Розроблено практичні рекомендації, щодо можливого примінення досліджуваних термопластів для виготовлення деталей вузлів газотранспортного обладнання.

Ключові слова: газотранспортне обладнання, термопласти, абразив, тертя, гідроабразивне зношування, ударно-циклічне навантаження, дослідний стенд



Tribotechnical properties of coatings based on magnesium compounds

V.V. Shchepetov¹, N.M. Fialko¹, S.S. Bys^{2*}

¹*Institute of Technical Thermophysics of the National Academy of Sciences of Ukraine*

²*Khmelnytskyi National University, Ukraine*

**E-mail : serhiibys@gmail.com*

Received: 15 January 2025; Revised 21 February 2025; Accept: 10 March 2025

Abstract

The article summarizes the results of studies of tribotechnical properties of detonation coatings based on magnesium orthosilicate under conditions of constant load in the sliding velocity field. The structural and phase composition of the coatings was studied using modern physical analysis methods. The developed and studied coatings based on magnesium orthosilicate have high and stable antifriction properties in the entire load-velocity range of tests. It is emphasized that the result of antifriction under friction conditions is the additive effect of both the carbide graphite film and dispersed surface oxide structures, the synthesis of which provides modification of the surface of the structure, which is capable of self-lubrication and at the same time limits the development of unacceptable destruction processes.

Key words: detonation coating, wear intensity, structural and phase composition, graphitization.

Introduction

Magnesium compounds, due to their exceptional properties, are widely used in innovative technologies. Without them, the functioning of technical structures from alloys and chemical current sources to fireproofing and military equipment systems is impossible [1-2]. Their use in tribotechnical materials science is associated with modern achievements in tribology. Thus, as structural components of coatings, they are used to protect machines and mechanisms from the manifestation of destructive wear processes during friction [3-4]. Widely used methods of reducing friction forces and combating wear are the use of a lubricating medium in the friction contact zone. In modern tribotechnical systems, contact interaction in the absence of lubricants is practically not carried out. The effective functioning of friction units of machines and mechanisms is ensured mainly by the use of various lubricants, which significantly reduce friction parameters, and the use of which is determined in each specific case by their lubricating properties. Thus, polymer lubricants are an effective material from room temperature to 300°C; lamellar solid lubricants extend the range to 450°C; graphite, being a layered solid material, is an exception, since it provides lubricating ability at temperatures exceeding 450°C. Stable fluorides and metal oxides are used at temperatures from 500°C to 1000°C [5-6]. Despite the positive results in achieving the quality of antifriction materials through the use of solid lubricants, the applied problems of friction and wear of machines remain the most complex technical areas of knowledge that have to be solved during the operation of modern technology. A significant need arising from current production tasks and the internal logic of scientific development requires new solutions in the study of the general material science imperative, which determines the relationship between the chemical composition and structure formation with the technology of formation and functional properties of materials. At the same time, the use of coatings containing solid lubricants is becoming increasingly necessary to ensure the long-term operation of moving joints [7]. Summing up, it can be noted that the development of powder compositions for high-quality antifriction coatings is a priority area of modern tribotechnical materials science and a relevant task related to the extension of the operational life of machine parts in industrial production conditions.

The purpose of the work is the determination, within the framework of the phenomenological approach, of the patterns of friction and wear of composite coatings based on magnesium compounds with structurally free magnesium carbide, the study of the structural and phase composition and its influence on the formation and self-organization of surface structures that have self-lubricating ability.



Materials and research methods.

Deserved attention in the field of tribotechnical materials is attracted by compounds of complex oxides and, first of all, compounds with magnesium oxide due to their high thermo mechanical properties. As a basis for self-lubricating coatings, studied in the work, magnesium orthosilicate (forsterite) with the chemical formula $2\text{MgO}\cdot\text{SiO}_2$ was purposefully used, which exists in only one modification, that is, as a material, it does not have polymorphic transformations. Doped impurities from chromium, zirconium, nickel, titanium, aluminum, silicon and carbon powders were added to magnesium orthosilicate, as a basis. The initial composition of crystalline powders of complex chemical composition for subsequent spraying was obtained by the method of mechanochemical synthesis (MCS). The use of which made it possible to obtain a nanocomposite conglomerate of micron-sized base particles and nanosized doped phases. To the powder conglomerate obtained in this way, a magnesium compound was added in the appropriate proportion, namely structurally free carbide (MgC_2), and the resulting mechanical mixture was mixed until the structural components were completely and uniformly distributed. Magnesium orthosilicate-based coatings were formed by the detonation-gas method on samples of high-strength steel type 30HGSNA. Steel 65G (HRC 62-65) was used as a counter body. The physical and mechanical properties and patterns of friction and wear of orthosilicate-based coatings were studied using the end-face scheme in the continuous sliding mode at a constant load of 14.5 MPa. At the same time, the research program provides for a comparative analysis of the friction parameters of the developed coatings with the values of coatings based on tungsten carbide type WK15 and coatings of alloyed nichrome. The adhesion strength was determined by the pin method, which for coatings based on magnesium orthosilicate was over 93 MPa with a porosity of about 0.5%, along with this, after preliminary finishing grinding, their initial roughness was R_a 0.32-0.63.

Both the wear intensity and friction coefficient, as well as the condition of the working surfaces, were used as criteria for the performance of magnesium silicate-based coatings. When studying the patterns of friction and wear, when explaining the technology-structure and structure-properties relationships, a complex of modern physicochemical methods of structural-phase analysis was used, which are capable of determining the consideration of surface layers at the macro- and microscopic levels. In this case, the complex research methodology included metallography (optical microscope "Neophot-32" with a prefix); durometric analysis (hardness tester M-40 from LECO); scanning electron microscopy (scanning electron microscope JSM-840); X-ray structural phase analyzer (diffractometer DRON-UM1).

Research results and their discussion.

The main factors on which the patterns that determine the course of friction and wear processes depend are external influences. They determine the degree and gradients of elastic-plastic deformation, temperature, activation level, a number of accompanying phenomena, and ultimately determine the leading type of wear.

The test results of the studied coatings (fig. 1) are presented in the form of graphs of functional average values of wear intensities and friction coefficients obtained in a field of monotonically increasing sliding velocities at a constant load, which corresponds to 14.5 MPa.

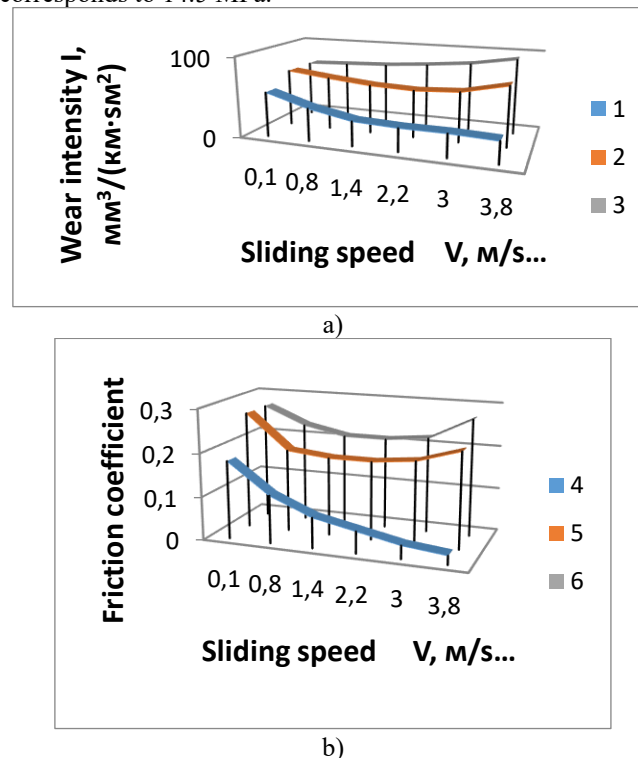


Fig. 1. Dependences of wear intensities (a) and friction coefficients (b) on the sliding speed of coatings based on magnesium compounds (1, 4), WK15(2, 5) and alloyed nichrome (3, 6) at $P=\text{const}=14.5$ MPa.

In the working range of the studies, the values of the controlled parameters for coatings based on magnesium orthosilicate compared to the control coatings are minimal and stable (curves 1 and 2, respectively), which determines normal mechanochemical wear.

The micro geometry of the working plane of silicate-based coatings in combination with the physical and mechanical properties of the surface sphere determines their operational state. The results of the studies showed that during the running-in process, the initial technological relief disappears, the chemical composition, structure of the surface layer and its geometry radically change. It is possible to determine that running-in is one of the manifestations of the self-organization process, in which the quasi-relaxation of the surface structure from the equilibrium state will pass to a stable state. At the same time, a new surface quality is formed, characterized by the formation of a balanced roughness, which is not only optimal for specific friction conditions, but also ensures stable wear in the entire test range. Thus, the initial technological roughness is transformed into an optimal operational roughness, which for silicate-based coatings corresponds to the value of Ra 2.5-1.5. At the same time, the sprayed layer is distinguished by a heterogeneous finely dispersed structure with a quasi-ordered lamellar appearance, which tightly adheres to the base and copies the surface relief, at the same time, no accumulation of films, slag inclusions and other contaminants, as well as defects in the form of micropores and micro cracks, was detected.

From the results of micro X-ray structural analysis (MRSA), it was established that the studied coatings have a multicomponent fine-grained aggregate, the basis of which consists of homogeneous hexagonal magnesium orthosilicate and an almost uniformly defined significant amount of finely dispersed inclusions of carbides, especially silicon carbide (SiC) and a fine conglomerate of strengthening compounds, which are silicides Cr₂Si₃, CrSi₂, Zr₃Si₂, TiSi, TiSi₂ and aluminides TiAl₃, TiAl, ZrAl₃, CrAl₄, as well as intermetallic formations such as ZrCr₂, ZrV₂, NiTi. In addition, the presence of high-temperature compounds of mullite Al₂SiO₄ was established, which, in our opinion, is formed with the appearance of cristobalite β-SiO₂ with a further increase in temperature, and particles of β-tialite were also found, which should have formed as a result of the interaction of solid solutions according to the reaction: Al₂O₃ + TiO₂ = Al₂TiO₅. Thus, a heterophase finely dispersed layered structure was established, which has increased physical, thermal and chemical properties both at normal and elevated temperatures. Also, the studied structure consists of small fragments of ternary compounds of transition metals in the form of Cr₂SiC, TiAlC, TiZrC, SiZrC, in addition, reflexes corresponding to magnesium aluminate (MgAl₂O₄) were found against the background of solid solutions, the crystals of which have a spinel structure and correspond to increased thermodynamic properties.

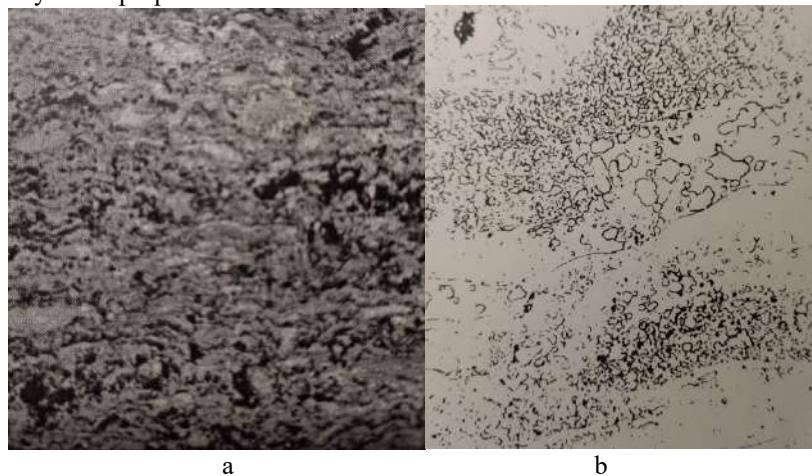


Fig. 2. Cross-sectional microstructure of coatings sprayed with composite powder based on magnesium orthosilicate (a - $\times 120$; b - $\times 5000$).

The specified structural components of coatings based on magnesium orthosilicate form solid solutions, chemical compounds and mechanical mixtures and have increased temperature resistance, significant hardness and strength, and corrosion resistance, which ensures their high wear resistance under friction conditions, especially at elevated temperatures.

The problem of coating quality is inextricably linked to the assessment of reproducibility and optimization of the spraying technological process. Changing technological modes leads to changes in the properties of coatings. Based on the cause-and-effect relationships between technological and operational factors, for the formation of high-quality coatings by optimizing the spraying mode, a comprehensive treatment of the main technological parameters was implemented, including the granulometric composition, loading depth, barrel filling degree, working gas ratio and spraying distance [8]. Thus, in the conditions of the technological process of forming the studied coatings, not only the required chemical composition was implemented, but also the predicted stable structure was obtained during spraying, which determines the set of properties that determine the stability of structural adaptability. At the same time, the possibilities of obtaining constant quality were achieved, namely, the variation of strength and plastic characteristics in samples of one batch that were sprayed was stably about 5-10%.

Studying the physical mechanisms of formation and evolution of structural-phase states of secondary structures under conditions of mechanochemical activation is one of the important tasks of controlling the surface strength of coatings based on magnesium orthosilicate while regulating their tribotechnical properties.

For comprehensive and reliable information in the study of thin surface layers in which structural-thermal activation processes occur, the secondary ion mass spectroscopy (SIMS) method was additionally applied, which analyzed the change in the microstructure and established the nature of the phases, their crystal structure, and the parameters of the elementary cells, which are necessary for identifying the composition within the regions of their homogeneity.

The obtained results allowed us to generalize that the initiation of physicochemical transformations due to elastic-plastic deformation is primarily manifested in the process of inversion of interaction with air oxygen and, as a result, the reformation of secondary surface oxide films by additional formations that form within the structure of the orthosilicate composition and, by stoichiometric composition, represent a complex in the form of oxides Al_2O_3 , SiO_2 , ZrO_2 , TiO_2 , Cr_2O_3 , MgO , which, interacting, form both solid solutions of the Cr_2O_3 - SiO_2 , ZrO_2 - Al_2O_3 type, as evidenced by the coincidence of concentration maxima (fig. 3), and spinel phases NiCrO_4 , MgAlO_4 , Zr_2SiO_4 , Al_2SiO_5 , Cr_2TiO_5 , in addition, the presence of binary compounds of the TiO - ZrO_2 , MgO - TiO_2 , MgO - ZrO_2 type was identified, also not the probability of the presence of ternary compounds such as Mg - ZrO_2 - TiO_2 , MgO - Al_2O_3 - TiO_2 is excluded. It should be noted that the secondary oxide structures that have been detected are characterized by significant strength, hardness, thermal stability and chemical inertness. In this case, the processes of formation and destruction of oxide structures are in dynamic equilibrium and automatically self-regulate, which determines the manifestation and stability of the phenomenon of structural adaptation [9]. However, due to statistical regularities, the processes of decomposition of ultra disperse secondary structures on different parts of the working surface as a result of contact discreteness do not coincide in stages. At the same time, there is an opportunity to assume that the process of their formation does not take place on the entire tribosurface, but only on separate uneven fragments of the actual working area, but their additive distribution is a stable structural-temporal state.

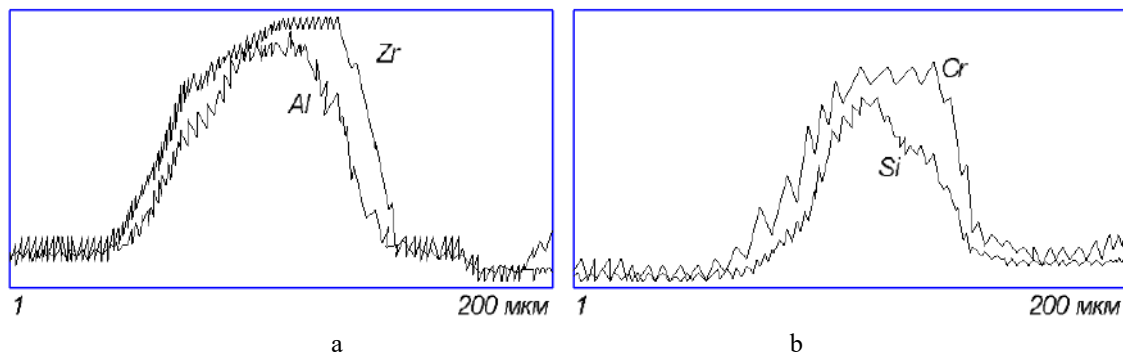


Fig. 3. Distribution of elements in the oxide film on the surface area of the orthosilicate-based coating

In order to study the state of the oxide surface layer, in which the activation processes occur during friction, electron diffraction analysis was used, performed on the EPM-100 installation (reflection recording at $U=5$ kV). Fig. 4 shows an electron diffraction pattern from the surface of the coating based on magnesium orthosilicate, which records a change in the fine structure, which indicates the presence of intensity maxima on diffusion halos. The studied thin-film layer represents an ultra disperse oriented structure. In this case, the micro hardness of the surface layer is 21.0–23.0 GPa (with an initial one of about 16.0 GPa). Thus, low and stable values of both friction coefficients and wear rates of coatings are ensured by the formation of a coherent dynamically stable conglomerate of oxide structures that screen the adhesive-molecular interaction during friction and have a finely dispersed structure and, under local contact pressures and temperatures, form dense heterogeneous heat-resistant and sufficiently plastic surface structures without cracks and chips, which contribute not only to reducing the oxidation rate and increasing heat resistance, but also play the role of solid lubricants during friction.



Fig. 4. Electron pattern from the surface of the contact ball orthosilicate-based coating at $V=1.5\text{m/s}$ and $P=14.5\text{MPa}$.

When the sliding speed increases to 0.14 m/s, the specific work of wear reaches approximately 104 kJ/mm³, which corresponds to the necessary and sufficient condition for the thermal decomposition of magnesium carbide and, as a result, fragments of structurally free α -graphite appear on the friction surface (fig. 5). The shape of the particles of the graphite structure is close to scaly, consisting of polydisperse crystallites oriented in the direction of friction. It should be noted that the strength of graphite as an antifriction material is its weak interaction between the layers. Thus, running-in, in a certain sense, can be considered as a specific type of heat treatment accompanied by graphitization.

The physical phenomenon that determines the mechanism of magnesium carbide decomposition is based on the process of structural transformation in the solid phase, which develops as a result of thermal exposure. The main factors that determine the limiting values of thermodynamic graphitization processes are, first of all, the level of dispersion of structural components, specific pressure, operating temperature, ambient environment, the presence of initiating elements (carbon, silicon, nickel, aluminum), in addition, the influence of internal factors caused by the composition, structure, presence of defects, etc.



Fig. 5. Surface topography during graphite film formation ($v=0.17$ m/s).

The elementary act of a high-temperature reaction in a unit volume of local contact, accompanied by the formation of carbide graphite, due to the exothermic effect, causes the next elementary act, thus causing the ability to self-propagate.

Self-lubrication of magnesium orthosilicate-based coatings depends on the formation of a graphite film, the dynamic equilibrium of which is maintained by the further formation of graphite. At test speeds of more than 0.21 m/s, the frictional self-lubricating surface film of graphite covers more than half of the friction area and, at the same time, is a layer of an ordered set of polydisperse graphite particles, the self-equilibrium of which is maintained by their active formation as a result of pyrolysis. At the same time, the higher the temperature, the greater the amount of carbon converted into a graphite-forming self-lubricating film, and the longer the contact areas interact, the more graphite is formed.

Thus, the means of regulating wear and ensuring self-lubrication of coatings based on magnesium orthosilicate are both the use of magnesium carbide, which, through its structure, affects the adaptation process during friction by modifying the surface layers with carbide graphite, and the joint use of stable surface oxide structures, which, with cooperative self-organization, provide an additive complex of heat-resistant surface structures that prevent direct contact of surfaces and effectively reduce the friction force, wear intensity, and prevent unacceptable destruction processes.

From the point of view of structural thermodynamics, the systemic ordering of self-adapting surface films due to changes in composition and structure can be considered as adequate elementary physicochemical processes and adaptation mechanisms in the process of structural adaptability [10].

Fig. 1 also presents the results of testing coatings of the type WK15 (curves 2, 4), sprayed with tungsten-cobalt powder. Coatings of this type, as a classic wear-resistant material, are widely used to protect against wear a significant range of different design and purpose of critical parts. As established, at sliding speeds of more than 1.9 m/s, the temperature factor has a tendency to reduce their speed against wear, which ultimately turns out to be decisive in the development of destructive processes during friction.

For coatings based on nichrome (fig. 1, curves 3, 6) doped with aluminum and boron, a monotonic increase in wear intensity with increasing speed is characteristic. The study of the phase composition showed the presence in the coating composition of both a solid solution based on nickel and dispersed compounds of nickel aluminides (NiAl , Ni_3Al), chromium borides (Cr_2B , Cr_5B_3), as well as the presence of complex borides of the type (Cr , Ni). The passive capabilities of secondary structures with increasing test speed are suppressed by the development of plastic deformation and, as a result, the dynamic equilibrium shifts towards increasing activation energy, and the type of wear changes qualitatively. According to metallographic analysis, their friction surfaces at speeds of 1.8 m/s have random local tearing, scratches, characteristic of the initial development of setting processes.

Thus, the detonation coatings based on magnesium compounds, developed by the authors, are characterized by high antifriction properties and significantly exceed the control coatings in terms of operational capabilities, in addition, they are characterized by increased adhesion strength and the ability, through their composition, to influence structural properties that are capable of self-lubrication. The conducted studies indicate the feasibility of their use in order to increase antifriction due to self-lubrication in real operating conditions. However, it can already be noted that their use will ensure reliability, increase the resource and reduce repair costs when restoring worn parts. The most appropriate application of the studied coatings is to increase the reliability of operation of friction units, for example, for moving pairs of control mechanisms, hinges of guide surfaces, cams, sliding supports, pairs with reciprocating movement, bearings, sliding guides, lever parts of high-speed and heavily loaded units, in which the use of traditional lubricants is undesirable.

It should be noted that the developed composite powder material for forming self-lubricating coatings based on magnesium compounds can be implemented by any technological methods that use powder materials. The presented work continues the cycle of research on the development of promising coatings to minimize friction coefficients and wear rates through the use of materials containing magnesium compounds.

Conclusions.

1. The developed and investigated detonation coatings based on magnesium compounds, which are characterized by stable and minimal values of friction coefficients and wear intensities under test conditions at a sliding speed of up to 4.0 m/s and a load of 14.5 MPa, have friction parameters significantly lower than those for control coatings by almost 2.5-7.0 times.

2. The creation of a powder mixture based on magnesium orthosilicate was carried out by the method of mechano-chemical synthesis, which made it possible to obtain a nanocomposite conglomerate of micron-sized base particles and nanosized alloyed phases with the subsequent addition of structurally free magnesium carbide to the powder composition.

3. A comprehensive treatment of the main technological parameters was implemented and the optimal mode of detonation-gas spraying of composite powders based on orthosilicate was worked out, while not only the planned chemical composition was reproduced, but also the predicted structure was obtained, which modernizes the friction surface and minimizes tribotechnical properties. At the same time, it was emphasized that the variation of strength and plastic properties in samples of one batch is stable and is 5-10%.

4. The structural-phase composition of coatings with magnesium orthosilicate was studied by modern means of physicochemical analysis, while the main components of the composite particles are solid solutions based on binary oxides and inclusions of chemical compounds of simple and complex carbides and intermetallics, as well as mechanical mixtures of component compounds. The determined components of the composition have increased temperature stability, significant hardness and strength and chemical inertness. In addition, there is the presence of dense and rather plastic heterogeneous oxide surface structures, which cause not only a decrease in the oxidation rate and an increase in heat resistance, but also perform an active role of solid lubricants under friction conditions.

5. The physical mechanism and main factors determining the level of thermodynamic graphitization have been determined. The nature and regularities that determine the tendency of coatings to passivation have been studied. It is noted that its implementation is carried out both due to solid-phase tribochemical reactions, which cause the formation of quasi-spherical polydisperse surface films integrated on the basis of carbide α -graphite and finely dispersed oxide compounds.

6. The developed self-lubricating antifriction coatings based on magnesium orthosilicate expand the achievements of modern tribotechnical materials science. At the same time, the studied self-lubricating coatings can be used both for strengthening and for high-quality restoration of worn parts by any technological methods using powder materials.

References

1. Hawking M. Metal and ceramic coatings: production, properties, application / M. Hawking, V. Vasantasari, p. Seeds M.: Svit, 2000 - 518 p.
2. Shchepetov V.V., Wear-resistant protective coatings / V.V. Shchepetov, O.V. Kharchenko. K.: Science. opinion; 2023. - 110 p.
3. Kovaleiro A. Nanostructured coatings/A. Covaleiro, D. Hossona M.: Technosveru, 2011. - 752 p.
4. Babak V.P., Shchepetov V.V., Kharchenko S.D. Antifriction nano component coatings containing magnesium carbide // Friction and wear, 2019, vol. 40, No. 6. - S. 783-790.
5. Tribology composite stringer, Heidelberg, 2016. ISBN: 978-3-642-3381-6.
6. Wear of composite. De Gruyter, Berlin, 2018. ISBN: 978-3-11-03529863.
7. Tribology for engineers. Wood head Elsevier. Cambridge. 2017. ISBN: 843346159.
8. Babak V.P., Shchepetov V.V., Kharchenko S.D. Mathematical modeling of the formation of detonation coatings\ Technological systems, 2020, No. 2.-p.82-88.
9. Surface strength of materials under friction\ Sub. ed. B.I. Kostetskyi. K.: Science. Opinion, 1996-296p.
10. L.I. Bershadsky. Structural thermodynamics of tribosystems. K.: Knowledge, 1990.-30 p.

Щепетов В.В., Фіалко Н.М., Бись С.С.Триботехнічні властивості покриттів на основі сполук магнію

У статті узагальнено результати досліджень триботехнічних властивостей детонаційних покриттів на основі ортосилікату магнію в умовах постійного навантаження у полі швидкостей ковзання. Методами сучасного фізичного аналізу досліджено структурно-фазовий склад покриттів. Розроблені та досліджені покриття на основі ортосилікату магнію мають високі та стабільні антифрикційні властивості у всьому навантажувально-швидкісному діапазоні випробувань. Підкреслено, що результатом антифрикційності умов тертя є адитивна дія як плівки карбідного графіту, так і дисперсних поверхневих оксидних структур, синтез яких забезпечує модифікацію поверхні структури, що спроможна до самозмащування та водночас обмеження розвитку неприпустимих процесів руйнування.

Ключові слова: детонаційне покриття, інтенсивність зношування, структурно-фазовий склад, графітизація.



Improved mathematical model of the operation of hydraulic drives of garbage truck mounted sweeping equipment with regard to the wear of a cylindrical brush

O.V. Bereziuk^{1*}, V.I. Savulyak¹, V.O. Kharzhevskiy², Ye.S. Harbuz¹

¹*Vinnitsia National Technical University, Ukraine*

²*Khmelnitskyi National University, Ukraine*

E-mail: berezyukoleg@i.ua

Received: 20 January 2025; Revised 25 February 2025; Accept: 10 March 2025

Abstract

The article is dedicated to the improvement of the mathematical model of operation of hydraulic drives of mounted sweeping equipment of a garbage truck, taking into account the wear of a cylindrical brush. An improved nonlinear mathematical model of the operation of hydraulic drives of mounted sweeping equipment of a garbage truck that takes into account the wear of a cylindrical brush, is proposed, which allowed to numerically study the dynamics of these drives during startup and determine that taking into account the wear of the cylindrical brush significantly affects such values as the pressure at the inlet of the hydraulic motor of the cylindrical brush and the angular velocities of both hydraulic motors. At the same time, the pressure at the inlet of the screw conveyor hydraulic motor after taking into account the wear of the cylindrical brush has hardly changed. The study of this mathematical model was carried out using the numerical Runge-Kutta-Felberg method of the 4th order with a variable integration step. It was also established the graphical dependencies to compare changes in the main parameters of the hydraulic drive of the garbage truck's mounted sweeping equipment during startup without taking into account the wear of the cylindrical brush and with taking into account the wear. It has been established that the creation of a linearized mathematical model of the operation of hydraulic drives of garbage truck mounted sweeping equipment, taking into account the wear of a cylindrical brush, and its analytical solution in order to obtain dependencies for an improved methodology for engineering calculations require further research.

Keywords: wear, mathematical model, rotational speed, mounted sweeping equipment, cylindrical brush, garbage truck.

Introduction

Increasing the wear resistance, durability, and reliability of machine parts is one of the key tasks of the Ukrainian machine-building industry, especially for municipal sweeping machines [1, 2]. Municipal vehicles equipped with brushing equipment are widely used to clean the road surface from contaminants. The most common is brushing equipment with cylindrical brushes, the pile of which is made of polymeric material. During operation, the bristles of a cylindrical brush wear out intensively due to interaction with the working surface containing abrasive particles. This leads to changes in its elastic properties. To maintain the optimum width of the contact patch, the force of pressing the brush against the road surface is increased. This approach ensures high quality road surface cleaning and minimizes the intensity of pile wear. An analysis of statistical data showed that the level of wear and tear of the vehicle fleet of Khmelnytskyi region's municipal enterprises decreased slightly from 63% to 59% between 2015 and 2020, despite the measures taken [3, 4]. According to the Resolution of the Cabinet of Ministers of Ukraine No. 265 [5], one of the priority tasks is to provide the country's utilities with modern and highly efficient garbage trucks, which play a key role in the processes of collection, transportation and primary processing of municipal solid waste (MSW). This task is facilitated, in particular, by expanding the functionality of the garbage truck by equipping it with mounted sweeping equipment. This approach generally helps to improve the overall reliability of utility companies' operations, while simultaneously solving a number of environmental



issues. Planning for the improvement, renewal, maintenance, and repair of municipal equipment is facilitated by improving the mathematical model of the operation of hydraulic drives of the garbage truck's mounted sweeping equipment, taking into account the wear of the cylindrical brush.

Analysis of recent research and publications

Article [6] describes measures aimed at significantly improving the efficiency of the technological process of cleaning of road's pavement. These measures are aimed at reducing the need for cleaning equipment and manual labor, as well as improving the sanitary, hygienic, aesthetic, transport and operational condition of the road surface within urban areas. It is noted that the elastic modulus of the pavement of intra-quarter passages should be at least 125 MPa, while for sidewalks and pedestrian alleys over 3 meters wide – should not exceed 85 MPa. If the moisture content of the garbage is up to 20%, it is recommended to use sweeping machines with additional moistening of the garbage to a level of less than 15%. If the moisture content of the garbage exceeds 20%, it is advisable to use water washers.

The work [7] considers the technology for maintaining the city's street and road network during the period with positive air temperatures, describes methods for planning and determining the volume of cleaning work, provides technical characteristics of sweeping machines, and presents a method for calculating their required number. The characteristics and composition of garbage on the roadway of city streets and roads are presented, including its fractional distribution, the content of dusty particles by fraction in the air above the road surface, the concentration of the main and most harmful components of road dust, seasonal changes in the composition of garbage, as well as the estimated annual accumulation of street garbage per 1 m² of road surface for cities. It was also identified the key factors that affecting the performance of street sweeping machines during the cleaning of the city's road network. The paper considers the productivity of sweeping machines, analyzes the factors that affect its level, and presents a methodology for calculating productivity. The modes (frequency) of road surface cleaning, the intensity of garbage accumulation on its surface, and the level of contamination depending on the intensity of traffic are also determined.

The paper [8] considers the results of analyzing a set of partial indicators, including fuel consumption during operation, work performance, maintenance and repair costs of brush equipment, and the cost of cleaning a certain area of roads or urban areas. These indicators make it possible to assess the efficiency of operation of municipal sweeping machines equipped with brush equipment. The study presents a functional scheme for the formation of a generalized efficiency criterion and proposes a mathematical expression for its calculation. In addition, an expression for determining a generalized criterion for the efficiency of using municipal machines based on the selected aggregation function. The paper proposes a functional scheme for the formation of a generalized efficiency criterion that provides a visual representation of the relationships between the factors that influence the partial indicators of efficiency of the use of municipal sweeping machines.

The article [9] presents a study that was carried out by modeling brushes using the finite element analysis method to develop a system for automating the road sweeping process. Taking into account the type of garbage and road conditions, it is noted that the driver of a sweeping machine needs to adjust the vertical pressure, angle of inclination, and speed of rotation of the curb brush, as well as regularly monitor the quality of sweeping. The driver's work is complicated by the need to simultaneously carefully control the machine and perform sweeping operations. Previously, achieving efficient road sweeping has been difficult, partly due to a lack of knowledge about the basic characteristics of sweeping brushes. The study uses a finite element model to analyze the deformation of metal brushes as they are pressed and rotated on the road surface. The main parameters considered include the length, width, and thickness of the teeth, the radius of their installation, the angle of installation, and the orientation of the teeth, as well as the number of teeth in a cluster, the number of clusters in a row, and the number of rows. The brush teeth were modeled as thin cantilever beams using the commercial software package FE ANSYS. This model was used to obtain the key characteristics of the brush, including the force-strain relationship, contact pattern, and torque. The effect of different tooth geometries on brush performance was also analyzed.

The research paper [10] states that the use of brush seals can increase engine performance by reducing losses. Brush seal wear models offer methods for predicting the level of wear and associated costs. However, existing models do not systematically take into account rotor eccentricity, radial deformation, and the effect of bristle hysteresis, which can lead to significant errors in certain situations. To study the effect of rotor-stator eccentricity and radial deformation on the wear process and flow characteristics of the brush seal, experimental tests were carried out. During the tests, the air leakage rate was measured under different operating conditions and at different moments in time, while the eccentricity and radial deformation were determined using eddy current sensors. The test results showed that eccentricity and radial deformation significantly affect the wear process and cost efficiency. In the theoretical study, the abrasive wear equation was used to describe the loss of pile material, while the eccentric rotor-stator motions were described using a simplified model. A wear model for the brush seal was developed taking into account the rotor-stator eccentricity and radial deformation, which especially takes into account the hysteresis effect. The developed model was verified on the basis of experimental data from brush seal tests. The results showed that when the rotor eccentricity, radial deformation, and hysteresis effect are fully taken into account, the error is 20% compared to the calculated wear losses.

The paper [11] consider the interaction of forces and temperature effects on friction and wear of the brush pile, and also determine the quantitative characteristics that affect the service life and efficiency of the sweeping process depending on the properties of the removed contaminants and operating modes. The developed and implemented on a PC simulation model of the functioning of the brush unit of a municipal sweeping machine provides forecasting of the process characteristics and identification of cause-and-effect relationships between the brush parameters and operating modes. The simulation model makes it possible to predict the service life and performance of the brush at the early stages of designing the brush body of a municipal machine, taking into account the model conditions of further use. The parametric adjustment of the simulation model was carried out by matching the calculated and experimental values of brush pile wear obtained in the experiment conditions. The criteria characterizing the intensity of brush lint wear were established. It is found out that the main factors that impede the establishment of optimal operating modes of municipal machines are the limitation of the brush rotation frequency and the heating of the contact surface of the pile, which leads to a deterioration in the mechanical properties of the pile material and an increase in the intensity of its wear.

The scientific article [12] considers the problem of improving the quality of road surface cleaning and extending the service life of brushing equipment. Improving the quality of cleaning and increasing the service life of brushing equipment will help reduce the cost of operating municipal equipment. During operation, the pile of a cylindrical brush is subject to wear, which leads to a change in its elastic properties. This makes it necessary to apply the optimal clamping force to maintain a rational width of the contact patch, which ensures high quality cleaning and minimizes pile wear. The article presents the dependence of the degree of wear of the brush pile of brush working equipment on the actual radius of the cylindrical brush. The influence of the degree of wear on the elastic properties of the brush working equipment is also analyzed. The dependence of the average stiffness coefficient on the degree of wear of the cylindrical brush bristles is given, as well as the dependence of the required clamping force on the degree of wear at different values of the width of the contact patch of the cylindrical brush. The dependence of the pressure in the hydropneumatic accumulator of the brush working body position control device on the actual free length of the cylindrical brush bristles was also determined.

Paper [13] presents a nonlinear mathematical model that describes the operation of hydraulic drives of the working bodies of the garbage truck's mounted sweeping equipment in the form of a system of differential equations, as well as the results of its numerical and analytical study. However, this mathematical model does not take into account the wear of the cylindrical brush.

Scientific publication [14] is dedicated to determining the power law of the wear of a cylindrical brush of the mounted sweeping equipment of a garbage truck depending on its rotation frequency. It has been established that for a Ukrainian-made sweeping machine of the serial model KO-713-01 that is equipped with a cylindrical brush with a rotation speed of 3200 rpm, its wear according to the obtained dependence will reach 86.5 mm. It has been also found that reducing the rotational speed of the cylindrical brush of the garbage truck's mounted sweeping equipment from 62 sec^{-1} (3700 rpm) to $26..38 \text{ sec}^{-1}$ (1550..2250 rpm) leads to a decrease in its wear by 2 orders of magnitude.

In the article [15], adequate regularities according to the Fisher criterion were established, which describe the effect of cylindrical brush wear on the performance characteristics of the garbage truck's mounted sweeping equipment. It has been established that, according to the Student's criterion, the degree of wear of a cylindrical brush has the greatest influence on the value of deformation of the brush, while the least influence has the width of the contact patch. It has been determined that the the required clamping force of a cylindrical brush is most influenced by the width of the contact patch, while the degree of its wear has the least influence. The response surfaces of the objective functions are demonstrated – the values of deformation and the required clamping force of the cylindrical brush, and their two-dimensional sections in the planes of the influence parameters, which clearly illustrate the dependence of these objective functions on individual parameters. It was determined that at a wear rate of 50%, the value of the cylindrical brush deformation increases by 1.3 times, while the required clamping force increases by 3.1-3.6 times, depending on the width of the contact patch.

However, as a result of the analysis of known publications, the authors did not find a specific mathematical model describing the operation of hydraulic drives of the working bodies of the garbage truck's mounted sweeping equipment, taking into account the wear of the cylindrical brush.

However, as a result of the analysis of known publications, the authors did not find a specific mathematical model that describes the operation of the hydraulic drives of the working bodies of the attached sweeping equipment of a garbage truck, taking into account the wear of the cylindrical brush.

Aims of the article

Improvement of the mathematical model of the operation of hydraulic drives of the mounted sweeping equipment of a garbage truck, taking into account the wear of a cylindrical brush.

Methods

Fig. 1 shows the scheme of the garbage truck operation during the sweeping operation [13], which indicates the following structural elements and parameters: GM₁, GM₂ – hydraulic motors, TR – throttle, H – hydraulic pump, SV – safety valve, F – filter, FT – working fluid tank. The scheme also shows the following basic geometric,

kinematic and power parameters: p_1, p_2, p_3, p_4 – respectively: pressures at the outlet H, at the inlet GM₁, at the inlet GM₂, at the outlet GM₂; W_1, W_2, W_3, W_4 – volumes of pipelines between H and TR, TR and GM₁, GM₁ and GM₂, GM₂ and F; Q_H – actual flow rate of H; S_{TR} – the area of inlet of TR; S_F – is the surface area of the filter element F; q_{M1}, q_{M2} – the working volumes of GM₁, GM₂; J_1, J_2 – the of inertia moments of the shafts of GM₁, GM₂; M_{T1}, M_{T2} – torques of technological load on shafts of GM₁, GM₂; ω_1, ω_2 – angular velocities of shafts GM₁, GM₂.

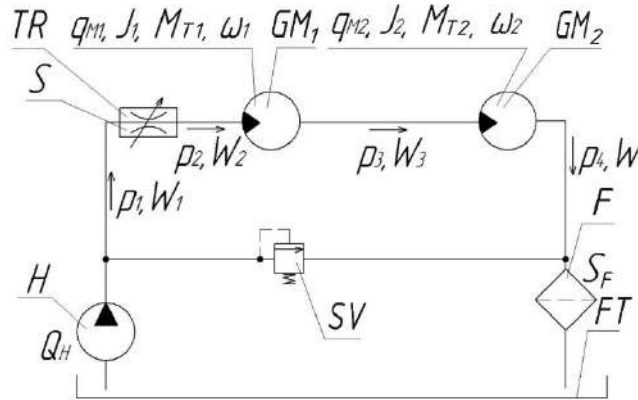


Fig. 1. Scheme of operation of a garbage truck during sweeping

The technological operation of sweeping can be described by the corresponding system of nonlinear differential equations (1-6) with the corresponding boundary conditions (7) and algebraic equation (8) [13]:

$$Q_H = \mu S_{TR} \sqrt{\frac{2(p_1 - p_2)}{\rho}} + \sigma(p_1 - p_2) + KW_1 \frac{dp_1}{dt}; \quad (1)$$

$$\mu S_{TR} \sqrt{\frac{2(p_1 - p_2)}{\rho}} = q_{MX1} \omega_1 + \sigma(p_2 - p_3) + KW_2 \frac{dp_2}{dt}; \quad (2)$$

$$q_{MX1} \omega_1 = q_{MX2} \omega_2 + \sigma(p_3 - p_4) + KW_3 \frac{dp_3}{dt}; \quad (3)$$

$$q_{MX2} \omega_2 = k_F \frac{p_4}{\mu_d} S_F + \sigma p_4 + KW_4 \frac{dp_4}{dt}; \quad (4)$$

$$q_{MX1} (p_2 - p_3) = J_1 \frac{d\omega_1}{dt} + \beta \omega_1 + \alpha q_{MX1} (p_2 + p_3) + \frac{\pi^3 r_B^3 S^6 E B_M f_B (S + R_B - h) K_R K_U \sin \gamma}{384,3 y_K^8 \eta_B}; \quad (5)$$

$$q_{MX2} (p_3 - p_4) = J_2 \frac{d\omega_2}{dt} + \beta \omega_2 + \alpha q_{MX2} (p_3 + p_4) + \frac{3,343 \pi^2 (q_m B_M v_M)^{1,4} l_K f_K^{1,2}}{[\psi(1 - \beta/50)]^{1,4} \rho_s^{0,4} [g \cdot \text{tg}(\alpha - \beta + \text{arctg} f_g)]^{0,2}}; \quad (6)$$

$$0 \leq \{p_1, p_2, p_3, p_4\} \leq p_s; \quad 0 \leq \{\omega_1, \omega_2\}; \quad (7)$$

$$q_{MX} = q_M / 2\pi, \quad (8)$$

where r_B – the radius of the cross-section of the pile bar, m; $S = 70 \dots 160$ mm – the free length of the pile, mm; E – the modulus of elasticity of the brush pile material, MPa; B_M – the width of the sweeping strip, m; f_B – the coefficient of friction of the brush pile material on the road surface; R_D – the radius drum of the cylindrical brush, mm; h – the value of brush pile deformation, mm; $K_R = 1.1$ – the coefficient of power reserve for overcoming inertial forces in an unstated mode of movement, pile deformation forces, and aerodynamic resistance; $K_U = 2 \dots 2.5$ – coefficient of unevenness of the pile arrangement on the generating surface of the brush drum; γ – pile inclination angle, deg; y_K – distance between the drum rim and the horizontal surface of the road, mm; η_B – efficiency of the drive of cylindrical brush; $q_m = 0.1$ kg/m² – amount of contamination per unit area of the road surface, kg/m²; $v_M = 0.7 \dots 6$ m/sec – operating speed of the machine during sweeping, m/sec; $\psi = 0.125$ – filling factor; β – angle of inclination of the screw conveyor, deg; l_s – length of the screw conveyor, m; f_K – friction coefficient of the particle on the conveyor casing; $\rho_s = 1.4 \cdot 10^3$ kg/m³ – density of the swept waste; $g = 9.8$ m/sec² – free fall acceleration, m/sec²; α – angle of rise of the screw line, deg; f_g – coefficient of friction of the particle on the conveyor screw.

In the paper [14] it was determined the dependence of wear of the cylindrical brush of the mounted sweeping equipment of a garbage truck depending on its rotation frequency:

$$u = 0,4593 + 1,834 \cdot 10^{-8} n^{5,6} = 0,4593 + 1,834 \cdot 10^{-8} \left(\frac{\omega_1}{2\pi} \right)^{5,6} = 0,4593 + 6,217 \cdot 10^{-13} \omega_1^{5,6} \text{ [mm]}, \quad (9)$$

where u – the wear of the cylindrical brush, mm; n – rotational speed of the cylindrical brush, sec⁻¹.

The dependence of the effect of cylindrical brush wear on the value of its deformation for different widths of the contact patch was determined in the work [15].

$$h = \Delta Y_{CB} = 0,002832 X_k - 0,04836 C_u + 6,822 \cdot 10^{-4} C_u X_k + 1,674 \cdot 10^{-4} C_u^2 + 4,297 \cdot 10^{-4} X_k^2, \quad (10)$$

where ΔY_{CB} – the deformation value of the cylindrical brush, mm; C_u – the degree of wear of the cylindrical brush, %; X_k – the width of the contact patch, mm.

To study an improved nonlinear mathematical model of the operation of hydraulic drives of garbage truck mounted sweeping equipment, taking into account the wear of a cylindrical brush in the form of a system of ordinary nonlinear differential equations with appropriate boundary conditions, the Runge-Kutta-Felberg numerical method of the 4th order was used with a variable integration step.

Results

The free length of the pile, taking into account its wear, can be determined by the following formula:

$$S = S_0 - u \text{ [mm]}, \quad (11)$$

where S_0 – the initial free length of the pile, mm.

The degree of wear of the cylindrical brush wear can be determined by the formula:

$$C_u = \frac{u}{S_0} 100\%. \quad (12)$$

After substituting formulas (9)–(12) into the equation (5), the improved nonlinear mathematical model of the operation of hydraulic drives of the garbage truck's mounted sweeping equipment, taking into account the wear of the cylindrical brush, can be written as follows:

$$\left\{ \begin{array}{l} Q_H = \mu S_{TR} \sqrt{\frac{2(p_1 - p_2)}{\rho}} + \sigma(p_1 - p_2) + KW_1 \frac{dp_1}{dt} \end{array} \right. ; \quad (13)$$

$$\mu S_{TR} \sqrt{\frac{2(p_1 - p_2)}{\rho}} = q_{MX1} \omega_1 + \sigma(p_2 - p_3) + KW_2 \frac{dp_2}{dt}; \quad (14)$$

$$q_{MX1} \omega_1 = q_{MX2} \omega_2 + \sigma(p_3 - p_4) + KW_3 \frac{dp_3}{dt}; \quad (15)$$

$$q_{MX2} \omega_2 = k_F \frac{p_4}{\mu_D} S_F + \sigma p_4 + KW_4 \frac{dp_4}{dt}; \quad (16)$$

$$\left\{ \begin{array}{l} q_{MX1} (p_2 - p_3) = J_1 \frac{d\omega_1}{dt} + \beta \omega_1 + \alpha q_{MX1} (p_2 + p_3) + \frac{(S_0 - 4,593 \cdot 10^{-4} - 6,217 \cdot 10^{-16} \omega_1^{5,6})^6}{384,3 y_K^8 \eta_B} \times \\ \times \pi^3 r_B^3 E B_M f_B K_R K_U \sin \gamma [S_0 + R_D - 2,832 \cdot 10^{-6} X_k - 4,297 \cdot 10^{-7} X_k^2 - (4,593 \cdot 10^{-4} + \\ + 6,217 \cdot 10^{-16} \omega_1^{5,6}) \left(1 + \frac{6,822 \cdot 10^{-5} X_k - 4,836 \cdot 10^{-3}}{S_0} \right) - \frac{(5,943 \cdot 10^{-4} + 8,044 \cdot 10^{-16} \omega_1^{5,6})^2}{S_0^2}]; \end{array} \right. \quad (17)$$

$$q_{MX2} (p_3 - p_4) = J_2 \frac{d\omega_2}{dt} + \beta \omega_2 + \alpha q_{MX2} (p_3 + p_4) + \frac{3,343 \pi^2 (q_m B_M v_M)^{1,4} l_B f_K^{1,2}}{[\psi(1 - \beta/50)]^{1,4} \rho_s^{0,4} [g \cdot \text{tg}(\alpha - \beta + \text{arctg} f_g)]^{0,2}}; \quad (18)$$

$$0 \leq \{p_1, p_2, p_3, p_4\} \leq p_s; \quad 0 \leq \{\omega_1, \omega_2\}; \quad (19)$$

$$q_{MX} = \frac{q_M}{2\pi}. \quad (20)$$

A comparison of the change in the main parameters of the hydraulic drive of the garbage truck's mounted sweeping equipment during startup without taking into account the wear of the cylindrical brush and with taking into account the wear is shown in the Fig. 2. The graphical dependencies shown in the Fig. 2 were obtained for the following parameters: $Q_H = 1.917 \cdot 10^{-3} \text{ m}^3/\text{sec}$; $q_{MX1} = 1.432 \cdot 10^{-5} \text{ m}^3/\text{rad}$; $q_{MX2} = 1.003 \cdot 10^{-4} \text{ m}^3/\text{rad}$; $M_{T1} = 8.3 \text{ N}\cdot\text{m}$; $M_{T2} = 261 \text{ N}\cdot\text{m}$; $J_1 = 1.98 \cdot 10^{-2} \text{ kg}\cdot\text{m}^2$; $J_2 = 3.13 \cdot 10^{-2} \text{ kg}\cdot\text{m}^2$; $W_1 = 1.48 \cdot 10^{-3} \text{ m}^3$; $W_2 = W_3 = 5 \cdot 10^{-4} \text{ m}^3$; $W_4 = 1 \cdot 10^{-3} \text{ m}^3$; $K = 10^{-9} \text{ Pa}$; $\sigma = 9.24 \cdot 10^{-11} \text{ m}^5/(\text{N}\cdot\text{sec})$; $S_{TR} = 58 \text{ mm}^2$.

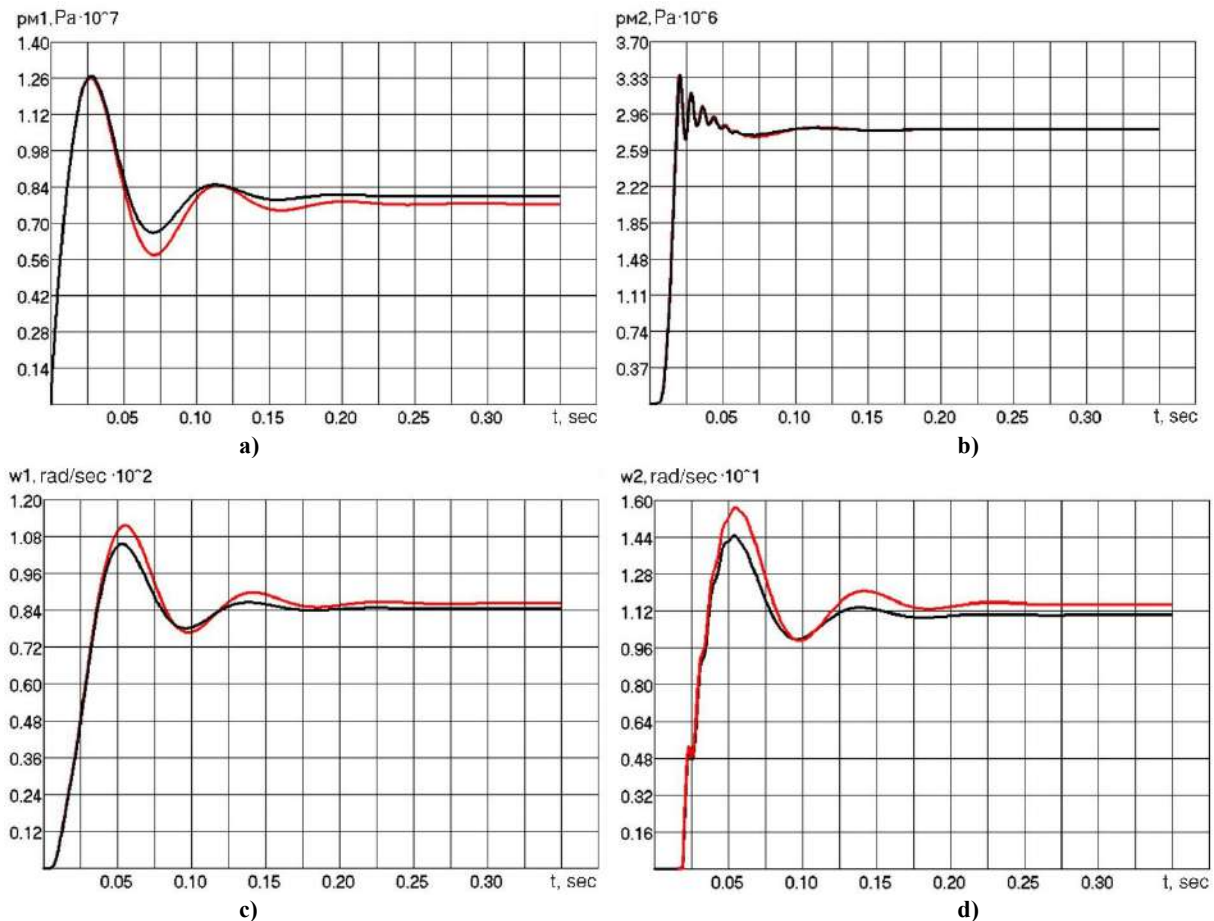


Fig. 2. Comparison of changes in parameters of the hydraulic drive of the garbage truck's sweeping equipment during startup without taking into account the wear of the cylindrical brush (—) and with wear (—): a) inlet pressure of the hydraulic motor GM₁; b) pressure of the inlet hydraulic motor GM₂; c) angular velocity of the hydraulic motor GM₁; d) angular velocity of the hydraulic motor GM₂

As it can be seen from the Fig. 2, taking into account the wear of the cylindrical brush in the improved mathematical model significantly affects on such values as the inlet pressure of the hydraulic motor GM₁ and the angular velocities of both hydraulic motors. At the same time, the inlet pressure of the hydraulic motor GM₂ after taking into account the wear of the cylindrical brush has hardly changed.

Thus, the creation of a linearized mathematical model of the operation of hydraulic drives of garbage truck mounted sweeping equipment, taking into account the wear of a cylindrical brush, and its analytical solution in order to obtain dependencies for an improved methodology of engineering calculations, require further research.

Conclusions

An improved nonlinear mathematical model of the operation of hydraulic drives of mounted sweeping equipment of a garbage truck is proposed, which takes into account the wear of a cylindrical brush and allows to numerically study the dynamics of these drives during startup. It enabled to determine that taking into account the wear of the cylindrical brush significantly affects such values as the pressure at the inlet of the hydraulic motor of the cylindrical brush and the angular velocities of both hydraulic motors. At the same time, the pressure at the inlet of the screw conveyor hydraulic motor after taking into account the wear of the cylindrical brush has hardly changed. The graphical dependencies were established to compare changes in the main parameters of the hydraulic drive of the garbage truck's mounted sweeping equipment during startup without taking into account the wear of the cylindrical brush and with taking into account the wear. It was also established that it needs further research of a linearized mathematical model's creation of hydraulic drives operation of garbage truck mounted sweeping

equipment, taking into account the wear of a cylindrical brush, and its analytical solution in order to obtain dependencies for an improved methodology for engineering calculations.

References

1. Khomenko IM, Kindrachuk MV, Kobrynets AK (2010) Hranychnodopustymy znos mashyn [Maximum permissible wear of machines]. *Problems of friction and wear*, 52, 28-37.
2. Dykha O., Sviderskyi V., Holenko K. (2024) Pidvyshchennia antyfryktsiinykh kharakterystyk porshnevnykh ushchilnen kompresora kondytsionera avtomobilia [Increasing the anti-friction characteristics of car air conditioner compressor piston seals]. *Herald of Khmelnytskyi National University. Technical sciences*, 333(2), 314-321, <https://doi.org/10.31891/2307-5732-2024-333-2-50>.
3. Ministry of Development of Communities and Territories of Ukraine (2016) Stan sfery povodzhennia z pobutovymy vidkhodamy v Ukraini za 2015 rik [The state of household waste management in Ukraine in 2015]. URL: <https://www.minregion.gov.ua/wp-content/uploads/2016/04/Zbortpv4-oblasti1.pdf>.
4. Ministry of Development of Communities and Territories of Ukraine (2021) Stan sfery povodzhennia z pobutovymy vidkhodamy v Ukraini za 2020 rik [State of household waste management in Ukraine in 2020]. URL: https://www.minregion.gov.ua/wp-content/uploads/2021/06/rozdil-4-2020_oblasti.pdf
5. The Cabinet of Ministers of Ukraine (2004) Resolution No. 265 "Pro zatverdzhennia Prohramy povodzhennia z tverdymy pobutovymy vidkhodamy" ["On Approval of the Program for Solid Waste Management"]. URL: <http://zakon1.rada.gov.ua/laws/show/265-2004-%D0%BF>.
6. Priymachenko O.V. (2008) Metody vdoskonalennia tekhnolohii ochyshchennia dorozhnogo pokryttia [Methods of improving the technology of road surface cleaning]. *Urban Planning and Spatial Planning*, 29, 265-270.
7. Ivanchenko G.M., Lyutikov A.A., Cherednichenko P.P. (2015). Utrymannia vulychno-dorozhnoi merezhi mista [Maintenance of the city street and road network]. *Urban Planning and Spatial Planning*, 55, 174-177.
8. Nalobina OO, Bundza OZ, Holotyiuk MV, Puts VS, Martyniuk VL (2022) Kontseptualne kompleksne otsiniuvannia efektyvnosti vykorystannia komunalnykh mashyn [Conceptual comprehensive assessment of the efficiency of municipal machines]. *Scientific Notes*, 73, 222-227.
9. Wahab M.A., Parker G., Wang C. (2007) Modeling rotary sweeping brushes and analyzing brush characteristic using finite element method. *Finite Elements in Analysis and Design*, 43(6-7), 521-532.
10. Xu Y., Ma T., Kong L., Zhao J., Li Y. (2023) Wear and Leakage Behaviors of Brush Seal Considering Eccentricity and Radial Deformation. *Energies*, 16(8), 3394.
11. Lepesh A.G., Lepesh G.V., Vorontsov I.I. (2011) The method of experimental determination of the durability of the brush pile and communal cleaning equipment. *Technical and technological problems of service*, 16(2), 7-19.
12. Tsekhosh S.I., Ignatov S.D., Demidenko A.I., Kvasov I.N. (2020) Increasing the life of the brush working equipment of a utility vehicle by using a device to control its position. *Journal of Physics: Conference Series. IV International Scientific and Technical Conference "Mechanical Science and Technology Update", MSTU 2020*. P. 012143.
13. Bereziuk O.V. (2021) Naukovo-tekhnichni osnovy proektuvannia pryvodiv robochykh orhaniv mashyn dlia zbyrannia ta pervynnoi pererobky tverdych pobutovykh vidkhodiv [Scientific and technical grounds of designing drives of working bodies of machines for collection and primary processing of solid household waste] *Diss. Doctor of Eng. Sciences: 05.02.02 - Mechanical Engineering, Khmelnytskyi*, 482.
14. Bereziuk O.V., Savulyak V.I., Kharzhevskyi V.O., Semichasnova N.S., Harbuz Ye.S. (2024) Establishing the regularity of wear of a cylindrical brush of the mounted sweeping equipment of a garbage truck depending on its rotation frequency. *Problems of Tribology*, 29(2/112), 31-36.
15. Bereziuk O.V., Savulyak V.I., Kharzhevskyi V.O., Harbuz Ye.S. (2023) Determination of the dependencies of the wear influence of the cylindrical brush on the operational characteristics of the garbage truck's mounted sweeping equipment. *Problems of Tribology*, 28(4/110), 22-27.

Березюк О.В., Савуляк В.І., Харжевський В.О., Гарбуз Є.С. Удосконалена математична модель роботи гідроприводів навісного підмітального обладнання сміттєвоза із урахуванням зносу циліндричної щітки.

Стаття присвячена удосконаленню математичної моделі роботи гідроприводів навісного підмітального обладнання сміттєвоза із урахуванням зносу циліндричної щітки. Запропонована удосконалена нелінійна математична модель роботи гідроприводів навісного підмітального обладнання сміттєвоза, яка враховує знос циліндричної щітки і дозволила чисельно дослідити динаміку даних приводів під час пуску та визначити, що врахування зносу циліндричної щітки суттєво впливає на такі величини, як тиск на вході гідромотора циліндричної щітки та кутові швидкості обох гідромоторів. В той же час, тиск на вході гідромотора шнекового транспортера після врахування зносу циліндричної щітки майже не змінився. Дослідження даної математичної моделі проводилось за допомогою чисельного методу Рунге-Кутта-Фельберга 4-го порядку зі змінним кроком інтегрування. Побудовано графічні залежності для порівняння зміни основних параметрів гідроприводу навісного підмітального обладнання сміттєвоза під час пуску без урахування зносу циліндричної щітки та з урахуванням зносу. Встановлено, що побудова лінеаризованої математичної моделі роботи гідроприводів навісного підмітального обладнання сміттєвоза із урахуванням зносу циліндричної щітки та її аналітичне розв'язання з метою отримання залежностей для удосконаленої методики інженерних розрахунків вимагають проведення подальших досліджень.

Ключові слова: знос, математична модель, частота обертання, навісне підмітальне обладнання, циліндрична щітка, сміттєвоз.



Research on the technological process of restoration with electrodiffusion strengthening of the working surfaces of the segments of the headers of combine harvesters

D.D. Marchenko*, K.S. Matvyeyeva

**Mykolayiv National Agrarian University, Ukraine*

E-mail: marchenkodd@mnaeu.edu.ua

Received: 22 January 2025; Revised 28 February 2025; Accept: 12 March 2025

Abstract

The paper presents a study of the technological process of restoring the working surfaces of combine harvester header segments using electrodiffusion strengthening (EDS). The EDS of restored Duracut Knife Sections was experimentally investigated. It was found that after EDS, the microhardness of the working surfaces of the Duracut Knife Sections increased 1.03 - 2.09 times to a depth of 200 - 500 microns. With a current density range from 0.022 - 0.095 A/cm², the ratio between the hardness of the front and rear surfaces of the blade was observed to range from 1.26 - 1.30, ensuring a self-sharpening effect. The relative wear resistance of the restored segments with EDS hardening was on average 1.3 times higher than that of new segments. Quantitative microanalysis of the chemical composition across the cross-section of the EDS-treated segments revealed an increase in the concentration of alloy-forming components in the hardened surface by 1.1 - 2.4 times compared to the core. As a result of diffusion segregation, the concentration of elements increased in the following ranges: carbon 1.6 - 1.8 times, chromium 2.2 - 2.4 times, silicon 1.7 - 2.1 times, and manganese 1.1 - 1.3 times. Larger values were observed on the rear surface of the restored segment's blade. A technological process for restoring the working surfaces of the Duracut Knife Sections of the John Deere 900 combine harvester header using EDS has been developed. The proposed technology allows for the restoration and strengthening of the working surfaces of segments in grain harvesting and forage harvesting combines, as well as mowers. Comparative operational tests on the John Deere 900 combine harvester during wheat harvesting showed that after processing with EDS, the wear resistance of the Duracut Knife Sections increased to 1.43 - 1.65 ha/mm after 90 hectares of use, which is 1.5 - 1.9 times higher than the standard segments restored without hardening. For the EDS-hardened segments, the blade thickness were maintained after the operational tests, indicating the presence of the self-sharpening effect. The resource of the Duracut Knife Sections restored with EDS was 1.7 - 2.4 times higher than that of standard segments restored without hardening.

Key words: wear resistance, friction coefficient, electrodiffusion strengthening, header segment, durability.

Introduction

Segments are mass-produced for equipping new agricultural machinery but are primarily used to replace worn-out parts. The highest failure rate in grain harvesters occurs in the harvesting unit, with approximately one-third of these failures due to the breakdown of cutter bar segments. Operational experience shows that standard segments, both domestic and foreign, have a relatively low service life. This leads to forced downtime of agricultural equipment due to the replacement of worn parts.

During operation, cutter bar segments in grain and forage harvesters, as well as in mower cutting mechanisms, undergo abrasive wear. As the cutting edges dull, agricultural requirements and deadlines are compromised, crop losses increase, and energy consumption rises, ultimately raising production costs and reducing the competitiveness of agricultural enterprises.

Therefore, extending the service life of harvester cutter bar segments is a highly relevant issue. To achieve this, it is necessary to selectively form reinforced layers with different properties on the working surfaces of segments during restoration. Unfortunately, existing strengthening technologies and methods cannot fully provide



the desired results. In our view, the most promising approach involves restoration and reinforcement techniques based on electrical treatment.

Literature review

Restoring and strengthening components allow agricultural machinery to regain its operational lifespan and, in some cases, extend it by up to 2.5 times. This is especially crucial when it comes to repairing imported components. To enhance the durability of harvester header components, it is necessary to create coatings with high physical and mechanical properties or apply a reinforced layer to the wearing cutting surfaces [1].

Standard cutting mechanism segments are typically made from tool-grade carbon steels such as U8, U9, and U10. During production, these components undergo hardening to a hardness level of HRC 50–55 through high-frequency induction hardening (HFH) along the cutting edge of the segment [2]. These tool-grade carbon steels exhibit high hardness and reduced brittleness [3]. However, field operation experience with segments made from U8, U9, and U10 steels shows that, despite heat treatment, they lack sufficient wear resistance, wear down quickly to their minimal limit, and have a short service life.

Recently, manufacturers have increasingly used steels such as 65 and 65G for segment production. These segments undergo edge hardening with tempering to the specified hardness [4], penetrating up to 1 mm deep. However, practical field experience indicates that such segments also suffer from poor wear resistance and degrade rapidly. The primary causes of standard segment failure include rapid dulling, which increases the energy consumption of the cutting process and negatively impacts both the cut quality and overall harvesting efficiency.

Methods for increasing the service life of harvester cutting mechanism components by altering material composition or design have well-documented drawbacks [5]. Therefore, preference is given to methods that enhance the durability of components. Existing methods for extending the service life of cutting mechanism components are primarily implemented by increasing the wear resistance of cutting surfaces.

A review of the literature indicates that the dulling of standard segment blades results from rounding, abrasion, deformation, and chipping of the cutting edge. This occurs because standard segment processing leads to either excessively high or insufficient surface hardness [6]. The following technological methods provide high surface hardness: electrolytic hardening, high-speed induction boriding, nitriding, thermodiffusion chromizing, and plasma metallization. However, boriding has disadvantages, such as increased brittleness of borides and high internal stresses in the treated part. Unfortunately, plasma metallization involves complex equipment, the release of harmful compounds, ultraviolet radiation, and high noise levels. Thermodiffusion chromizing significantly affects the thermal state of the part and contributes to air pollution, gas contamination, and workplace dust. Nitriding is associated with high internal stresses, long processing times, and complex equipment. Using welding for cutting elements is impractical because it requires extensive machining to achieve the required segment geometry.

The authors of [4] suggest extending the lifespan of harvester segment blades by electrolytic chrome plating. However, when the coating thickness exceeds 32 μm , excessive cracking occurs, leading to coating delamination. Additionally, the application of electrolytic coatings, including electrolytic chrome plating, is characterized by high labor costs, low environmental friendliness, and relatively low efficiency.

Among the most promising [6] and effective methods for restoring worn surfaces, the following are considered the most justified.

The most promising and effective methods for restoring worn surfaces reasonably include electrocontact techniques. The advantages of electrocontact welding include high hardness and wear resistance of the coating, minimal heating of the part, low machining allowance, no burnout of alloying elements, favorable working conditions, and more. However, after electrocontact welding of a steel strip, it is necessary to perform chemical-thermal or thermomechanical treatment, or surface hardening, to achieve a uniform microstructure in the heat-affected zone.

In the cutting units of harvesting machines, the primary challenge in addressing segment wear and durability lies in ensuring their self-sharpening during plant cutting. This should help maintain the segment's initial optimal profile while significantly reducing the pressure of the cut plant stems on the cutting edge.

In agricultural and engineering sciences, the theoretical models of Goryachkin V.P. and Reznik N.E. have found widespread application in describing the interaction between a blade and the material being cut. Meanwhile, the self-sharpening effect of a reinforced blade is explained by the phenomenological model of Tkachev V.N. [7]. Some authors use original approaches and integrate the aforementioned models.

By controlling the wear rate of different blade surfaces, self-sharpening can be achieved [6]. The blade surfaces must resist wear differently, ensuring equal wear rates for both the more and less loaded areas while maintaining a constant blade profile.

When determining the required parameters of cutting blades in harvesting machinery, it is necessary to consider their operating conditions. The wear pattern of blade segments depends on their interaction with the cut mass and abrasive particles [8]. At high movement speeds of cutting components, intensive wear can occur even in the absence of abrasive particles in organic matter.

Studies on segment wear during operation show that the wear intensity on the rear side is significantly higher than on the front side [9]. As a result, the blade's microgeometry changes, reducing its cutting ability. This necessitates the subsequent restoration of the required working surface parameters of the segments.

The essence of the self-sharpening phenomenon lies in the selective wear of the blade, which preserves its necessary shape and cutting properties.

The authors of [10] have established that to ensure the self-sharpening effect of grain harvester segments, the hardness ratio between the rear and front surfaces of the blade should be within the range of $HV_2/HV_1 = 1.26-1.30$.

Based on information about the wear characteristics of the cutting elements under consideration, it can be concluded that increasing their durability through self-sharpening during operation may be achieved by applying hard and wear-resistant coatings of the required thickness to the working surfaces [9].

The longevity of thin-bladed cutting components made of steel that has undergone hardening and tempering is relatively low, reducing the reliability and, consequently, the productivity of agricultural machinery [10].

Chromium plating the segments on the rear side results in less wear compared to chromium plating on the front side [7]. Extending the lifespan of segments is possible by forming coatings on the working surface that provide high hardness without increasing the brittleness of the metal from which the segment is made.

Foreign researchers suggest achieving a self-sharpening effect by strengthening the front and rear surfaces of the blade segments with a laser beam to an approximate depth of 254–1016 μm [8]. The preferred thickness of the hardened layer on the rear and front surfaces of the segment is 508 μm .

Research on the wear resistance of structures with hard inclusions is of great interest, as these inclusions can significantly influence the scratch formation mechanism during friction against a metallic surface [10].

Many researchers assert that the wear resistance of alloys increases with a higher concentration of carbides in the structure and their greater hardness [11]. This viewpoint is difficult to dispute.

Thus, to reduce wear on cutting components of agricultural machinery, it is necessary to develop strengthening methods that not only enhance the wear resistance of steel but also provide a self-sharpening effect for the blades [6].

In recent years, significant attention has been given to utilizing the self-sharpening effect in cutting mechanisms. One of the promising methods for improving the wear resistance of blade tools in this direction is gas-flame spraying [7]. This treatment results in a hardened layer thickness of up to 1000 μm , with the restored surface achieving a hardness of HRC65.

Another promising method for increasing wear resistance is the application of hardening coatings to the surfaces of cutting unit segments in grain harvesters. One such method is electro-spark treatment (EST), which can be applied both during manufacturing and repair processes [8]. As a result of low-voltage EST, a layer with a modified microstructure and a thickness of 10–30 μm forms on the surface of the part [9]. The application of electro-spark coatings to the cutting surface of the harvester finger increases its wear resistance by 1.7 to 2.2 times compared to standard versions and extends its service life by up to 2 times [10].

The advantages of electro-spark deposition (ESD) include the simplicity of technological operations, low energy consumption, and minimal heating of parts, even those with complex geometries. However, increasing the thickness of electro-spark coatings with high contact density remains a challenge [11].

A unique method that combines mechanical and thermal effects on a restored part is electromechanical processing (EMP) [12]. Among EMP techniques aimed at improving wear resistance [13], electromechanical restoration has been tested as a method for enhancing part dimensions while improving their physical and mechanical properties. The hardened layer depth after electromechanical surface hardening can reach up to 2 mm, with surface hardness ranging from 42 to 68 HRC. However, the maximum hardness is observed at a depth of 0.10 to 0.15 mm from the treated surface. Therefore, EMP requires an additional allowance for final surface finishing.

Overall, most existing hardening methods are unsuitable for the cutting segment components of harvesting machinery [12]. The current situation in the agricultural sector necessitates comprehensive scientific research.

Purpose

The purpose of the research is to increase the service life of the segments of grain harvester combines by developing a restoration technology with strengthening through electrodiffusion strengthening (EDS).

Research methodology

The research program included the following objectives: to conduct theoretical and experimental studies on the EDS segments of grain harvesting combine headers, to study the patterns of hardened layer formation on the working surfaces of EDS segments, to carry out comparative operational tests of the hardened combine segments, and to develop a technology for restoring segments using electrode diffusion hardening.

The theoretical research was based on the laws of upward diffusion in steels. Standard methods were used for the experimental research, including: experimental design planning, microhardness measurement, metallographic analysis, scanning electron microscopy, X-ray fluorescence analysis, energy-dispersive spectroscopy, X-ray diffraction phase analysis, and wear resistance testing. The results of the studies were processed using standard methods of mathematical statistics.

In accordance with the set goals and objectives of the dissertation, a selection of agricultural machinery components was made. For the research, worn-out serial segments Duracut Knife Sections (Canada) with a large upper notch were chosen. These segments are installed on grain harvesters for various crops.

The choice of electrolyte for the EDS process was based on its performance at processing temperatures of 800–850 °C, weakly oxidative properties, availability, environmental cleanliness, safety for humans, and low cost.

To evaluate the microstructure of the segments, a metallographic method according to ISO 643:2019 was used. Some of the segments strengthened by EDS were cut. Subsequently, microsections were made from the obtained fragments for research [13].

The microhardness of the segments was determined using the Vickers restored indentation method (6361-4:2014) on a PMT-3M microhardness tester (3-3.1377) with a load on the diamond tip of 1.962 N.

To determine the chemical composition of the segment material, the X-ray fluorescence method was used. Primary X-rays irradiate the analyzed alloy and cause secondary X-ray radiation. The resulting spectrum depends on the elemental composition of the material. The element was determined based on the dependence of the radiation intensity on its mass fraction in the alloy.

Operating experience shows that during operation, the segments of grain harvester headers are subject to abrasive wear, with their back side wearing out more. In this regard, a method for testing segments for wear resistance during friction against loosely fixed abrasive particles according to (23.208-79) was chosen for laboratory studies. The tests were carried out on a friction machine SMC-2 using the "roller – plate" scheme.

Research results

In EDS with a current density of 0.120 A/cm², the microhardness of the blade's front surface increases significantly, leading to a reduction in the analyzed ratio. In contrast, at a current density of 0.011 A/cm², surface hardening is minimal, resulting in a negligible difference between the microhardness of the blade's front and rear surfaces. Consequently, the ratio between these values approaches unity.

According to the research plan and methodology, wear resistance tests of restored and new segments were conducted using the SMTs-2 friction testing machine, with friction against loosely fixed abrasive particles [14].

For some segments after EDS, a quantitative microanalysis of element concentrations across the cross-section was performed using energy-dispersive spectroscopy. Fig. 1, a shows the spectral analysis areas with marked points on the image obtained from a scanning electron microscope (SEM). Fig. 1, b presents the corresponding distribution of alloying element concentrations by depth on the hardened front surface of the segment blade after EDS at a current density of 0.070 A/cm².

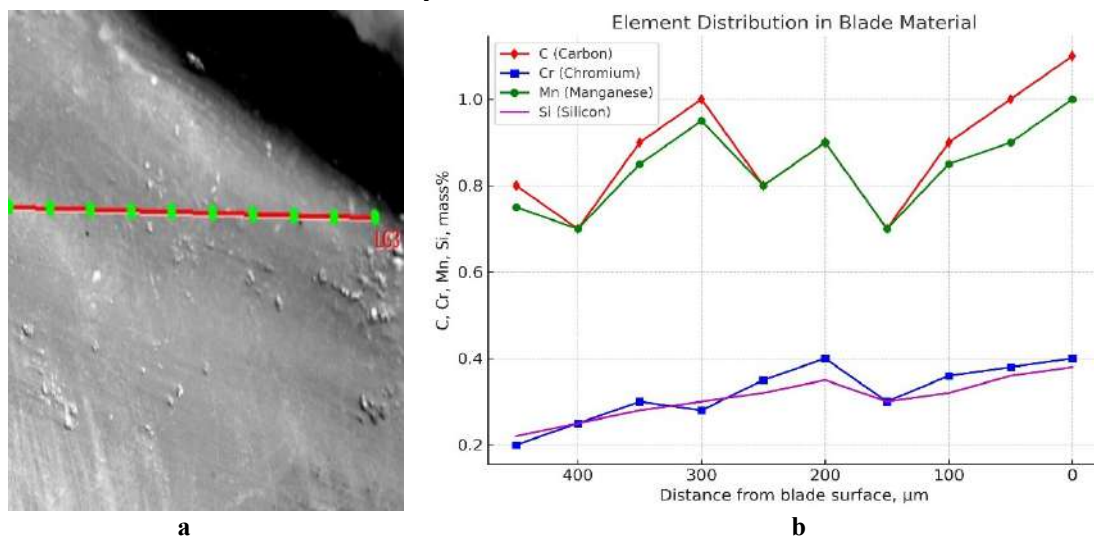


Fig. 1. Distribution of alloying elements by depth on the reinforced front surface of the segment blade after EDS: a - spectral analysis areas (SEM ×250); b - element concentration

In segments subjected to EDS, an increased concentration of carbon and alloying elements was detected in the hardened layer to a depth of up to 400 μm. Due to diffusion segregation during EDS, the concentration of carbon in the working surfaces of the segments increased by 1.6-1.8 times, chromium by 2.2-2.4 times, silicon by 1.7-2.1 times, and manganese by 1.1-1.3 times [15]. Notably, after electro-diffusion hardening, the concentration of alloying components on the rear surface of the segment blade was higher than on the front surface, specifically: carbon by 0.07 wt.%, chromium by 0.12 wt.%, silicon, and manganese by 0.02 wt.%. The microstructure of the Duracut Knife Sections segment after EDS at a current density of 0.095 A/cm² consists of medium- and coarse-needle martensite [16]. On the front and rear surfaces of the segment blade after EDS, the precipitation of strengthening phases is observed, appearing as small, irregularly shaped light inclusions (Fig. 2). The strengthening phases are locally concentrated on the working surfaces of the segment as separate inclusions. The average size of the inclusions is 1.9 μm. Pearlite is present in the form of isolated small-area regions.

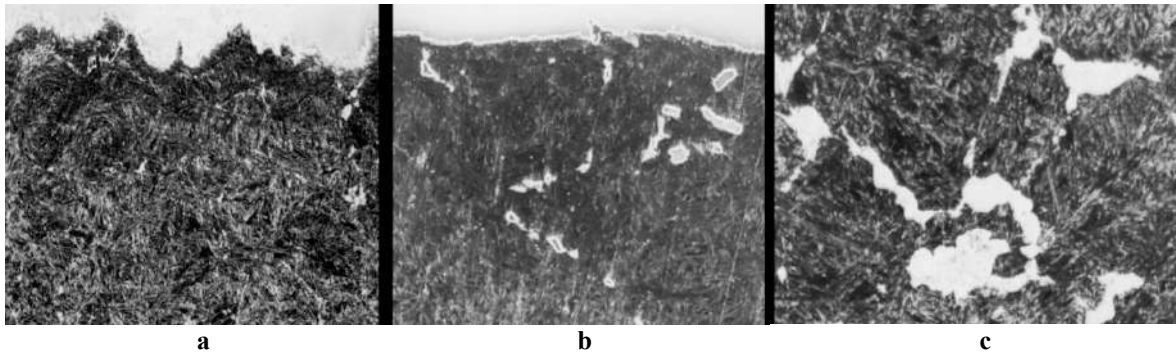


Fig. 2. Microstructure of the Duracut Knife Sections segment after EDM with a current density of 0.095 A/cm²: a - surface layer; b - surface layer with highlighted strengthening phases; c - core (×500)

Fig. 3 shows the comparison graphs of experimental and theoretical microhardness values of the working surface of the segment as a function of current density and voltage during EDM

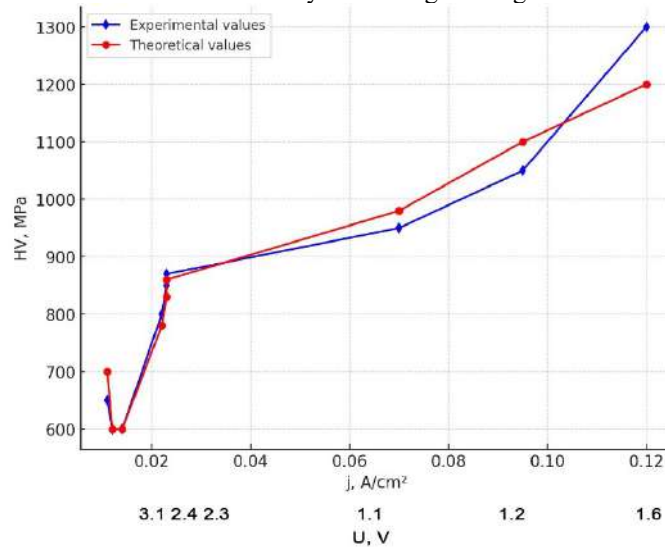


Fig. 3. Comparison of experimental and theoretical values of microhardness of the working surface of the segment as a function of EDS modes

The difference between the theoretical and experimental values of microhardness for the working surface of the segment, depending on the EDS modes, ranges from 0.5% to 9.8%, with an average difference of 5.5% [17]. Overall, comparative operational tests showed that after the combine harvester had processed 90 hectares, the wear resistance of the segments Duracut Knife Sections, restored with strengthening through electrode diffusion treatment, was 1.43-1.65 hectares/mm, which is 1.5-1.9 times higher than that of the standard segments (0.85-0.93 hectares/mm), restored without strengthening (Fig. 4). During the tests, no failures or downtime due to the loss of operational condition of the tested parts were observed [18].

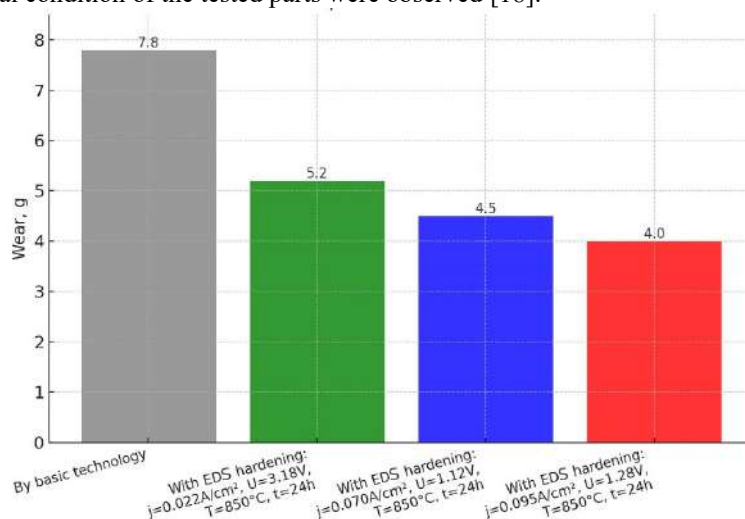


Fig. 4. Wear diagram of the refurbished segments Duracut Knife Sections after testing with 90 hectares of use

Based on the test results, the lifespan of the Duracut Knife Sections segments restored with EDS hardening [19] ranged from 3.0 to 4.4 ha per unit, which is 1.7 to 2.4 times higher than that of standard segments (1.8 ha per unit) restored without hardening (Fig. 5).

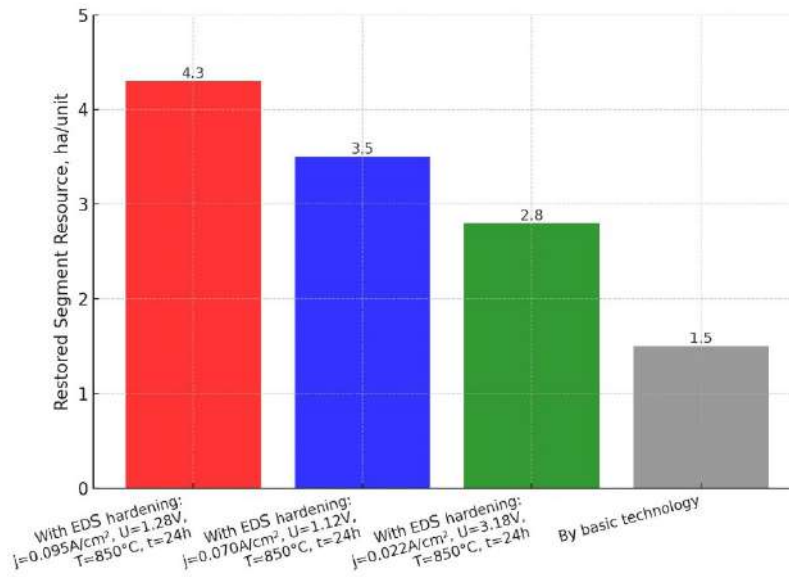


Fig. 5. The resource of restored segments Duracut Knife Sections

Thus, the use of electro-diffusion hardening increases the wear resistance and service life of the restored segments Duracut Knife Sections of the cutting unit of the John Deere 900 grain harvester.

Conclusions

1. Increasing the service life of grain harvester header segments during restoration is ensured by electrodiffusion treatment with selective formation of hardened layers with different characteristics.

2. A mathematical model of EDS of segments has been developed that describes the upward diffusion of carbon from the core to the front and back surfaces of the segment blade and allows determining its concentration in the hardened layer. Experimental studies have established that after EDS the microhardness of the working surfaces of Duracut Knife Sections segments increases by 1.03-2.09 times to a depth of 200-500 μm . As a result of diffusion segregation during EDS, the concentration of carbon in the working surfaces of the segments increased by 1.6-1.8 times, chromium by 2.2-2.4 times, silicon by 1.7-2.1 times, and manganese by 1.1-1.3 times. The formation of hardening phases in the working surfaces of the restored segments after EDS has been established. The segments restored with EDS hardening have a relative wear resistance 1.3 times greater than that of new segments. 3. A method for electrodiffusion hardening of the working surfaces of segment knives and an installation for its implementation have been developed, allowing for a selective increase in the microhardness and wear resistance of restored parts. An installation has been assembled that provides for the simultaneous hardening of 64 segments in a crucible with an internal diameter of 120 mm, a height of 230 mm and an electrolyte volume of 1.8 dm^3 .

3. The optimal parameters for hardening the segments with a self-sharpening effect are achieved by using sodium tetraborate as the electrolyte and the following EDS modes: voltage 1.12-3.18V, current density 0.022-0.095 A/cm^2 , electrolyte temperature 850°C , and processing duration of 2 hours. The greatest influence on the surface hardening and microhardness of the working surfaces of the segment is exerted by the current density during EDS.

4. Comparative operational tests have shown an increase in the lifespan of segments restored with EDS hardening by 1.7-2.4 times compared to the standard segments restored without hardening.

References

1. Merbach, L. Systematic analysis of the influences on the wear of cutting knives / L. Merbach, F. Beneke, C. Walther, S. Hartwig, M. Haseney, H. Siebald, // Proc. 73th Int. Tagung Land. Technik. – 2015. – P. 395–404.
2. Nutu, G. Experimental Determination of the Wear Resistance of Devices used for cutting the Stalks of Agricultural Plants / G. Nutu, P. Cârlescu, I. Tenu, V. Carlescu // Lucr. Stiintifice. – 2017. – №60. – P. 73–76.

3. Chernoiyanov, V.I. Features of wear of agricultural machinery components strengthened by Fe_n B-Fe-B composite boride coatings / V.I. Chernoiyanov, V.P. Ljaljakin, V.F. Aulov, A.V. Ishkov, N.T. Krivochurov, V.V. Ivanajsky, D.V. Koval, A.V. Sokolov // *Journal of Friction and Wear*. – 2015. – Vol. 36. – №2. – P. 132–137.
4. Gabitov, I.I. Distribution of temperature on the depth of restorable details at electrocontact welding of a steel tape / I.I. Gabitov, R. Saifullin, M.N. Farkhshatov, N. Yunusbayev, A.P. Pavlov, I. Gaskarov, A. Fayurshin, A. Kunafin, L. Islamov, R. Masyagutov // *International Journal of Civil Engineering and Technology*. – 2019. – Vol. 10. – №1. – P. 2496–2511.
5. Wilkey R. L. «Reciprocating cutting blade having laser-hardened cutting edges and a method for making the same with a laser» / R.L. Wilkey, D.L. Turner // U.S. Patent No. 6857255. 22 Feb. 2005.
6. Kanatnikov N. Strengthening of Low-Alloyed Steels by Carbides During Carbon-Black-Gas Carburizer Cementation / N. Kanatnikov, O. Ivanova, G. Harlamov // *International Conference on Industrial Engineering*. – Springer, Cham, 2018. – P. 1639–1645.
7. Shchegolev A.V. Modification of wear-resistant coatings of the Fe- Cr-C system with spherical tungsten carbide WC-W₂C / A.V. Shchegolev, A.V. Ishkov, V.V. Ivanayskiy // *IOP Conference Series: Materials Science and Engineering*. – IOP Publishing, 2020. – Vol. 939. – №. 1. – P. 12–71.
8. Darken L. S. Diffusion of carbon in austenite with a discontinuity in composition / L.S. Darken // *Trans. AIME*. – 1949. – Vol. 180. – P. 430–438.
9. Liu, Y. Atomic mobilities, uphill diffusion and proeutectic ferrite growth in Fe-Mn-C alloys / Y. Liu, L. Zhang, Y. Du, D. Yu, D. Liang // *Calphad*. – 2009. – Vol. 33. – №. 3. – P. 614–623.
10. Vu, B.D. Dynamics of Negative Diffusivity and Uphill Diffusion in Ternary and Single systems / B.D. Vu, B.T. Tong // *EPJ Web of Conferences*. – EDP Sciences, 2019. – Vol. 206. – P. 9–15.
11. Durand, A., Peng, L., Laplanche, G., Morris, J. R., George, E. P., Eggeler, G. Interdiffusion in Cr–Fe–Co–Ni medium-entropy alloys // *Intermetallics*. – 2020. – T. 122. – P. 106789.
12. Nishibata, T. Kinetic Analysis of Uphill Diffusion of Carbon in Austenite Phase of Low-Carbon Steels / T. Nishibata, T. Kohtake, M. Kajihara // *Materials transactions*. – 2020. – P. MT-M2019255.
13. O. Lymar, D. Marchenko, “Prospects for the Application of Restoring Electric Arc Coatings in the Repair of Machines and Mechanisms”, *Proceedings of the 2022 IEEE 4th International Conference on Modern Electrical and Energy System, MEES 2022*. <https://doi.org/10.1109/MEES58014.2022.10005709>.
14. Marchenko, D., Matvyeyeva, K. (2022). Increasing warning resistance of engine valves by gas nitrogenization method. *Problems of Tribology*, 27(2/104), 20–27. <https://doi.org/10.31891/2079-1372-2022-104-2-20-27>.
15. Marchenko, D., Matvyeyeva, K. (2022). Study of the Stress-Strain State of the Surface Layer During the Strengthening Treatment of Parts. *Problems of Tribology*, 27(3/105), 82–88. <https://doi.org/10.31891/2079-1372-2022-105-3-82-88>.
16. Marchenko, D., Matvyeyeva, K. (2023). Increasing the Wear Resistance of Restored Car Parts by Using Electrospark Coatings. *Problems of Tribology*, 28(1/107), 65–72. <https://doi.org/10.31891/2079-1372-2023-107-1-65-72>.
17. Marchenko, D., Matvyeyeva, K. (2023). Research of Increase of the Wear Resistance of Machine Parts and Tools by Surface Alloying. *Problems of Tribology*, 28(3/109), 32–40. <https://doi.org/10.31891/2079-1372-2023-109-3-32-40>.
18. Marchenko, D., Matvyeyeva, K., Kurepin, V. (2024). Increasing the wear resistance of plunger pairs of high-pressure fuel pumps using extreme pressure additives. *Problems of Tribology*, 29(4/114), 24–31. <https://doi.org/10.31891/2079-1372-2024-114-4-24-31>
19. Marchenko, D., Matvyeyeva, K. (2024). Study of Wear Resistance of Cylindrical Parts by Electromechanical Surface Hardening. *Problems of Tribology*, 29(1/111), 25–31. <https://doi.org/10.31891/2079-1372-2024-111-1-25-31>

Марченко Д.Д., Матвєєва К.С. Дослідження технологічного процесу відновлення із електродифузійним зміцненням робочих поверхонь сегментів жаток зернозбиральних комбайнів

У роботі наведено дослідження технологічного процесу відновлення із електродифузійним зміцненням (ЕДЗ) робочих поверхонь сегментів жаток зернозбиральних комбайнів. Досліджено експериментально ЕДЗ відновлених сегментів Duracut Knife Sections. Встановлено, що після ЕДЗ спостерігається підвищення мікротвердості робочих поверхонь сегментів Duracut Knife Sections у 1,03 - 2,09 рази на глибину 200 - 500 мкм. При ЕДЗ з щільністю струму від 0,022 до 0,095 А/см² спостерігається співвідношення між твердостю задньої та передньої поверхонь леза від 1,26 до 1,30 разів, що забезпечує ефект самозаточування. Відносна зносостійкість відновлених сегментів зі зміцненням ЕДЗ в середньому в 1,3 рази більша, ніж у нових сегментів. Кількісний мікроаналіз хімічного складу по поперечному перерізу відновлених сегментів, підданих ЕДЗ, виявив підвищення в зміцненій поверхні концентрації сплавоутворювальних компонентів у 1,1 - 2,4 рази порівняно з осердям. Внаслідок дифузійної сегрегації концентрація елементів підвищилась у таких діапазонах: вуглецю в 1,6 - 1,8 рази, хрому в 2,2 - 2,4 рази, кремнію в 1,7 - 2,1 рази, марганцю в 1,1 - 1,3 рази. При цьому більші величини спостерігаються на задній поверхні леза відновленого сегмента. Розроблений технологічний процес відновлення з ЕДЗ робочих поверхонь сегмента Duracut Knife Sections жниварки зернозбирального комбайна John Deere 900. Запропонована технологія дозволяє відновлювати та зміцнювати робочі поверхні сегментів жаток зернозбиральних і кормозбиральних комбайнів, а також косилок. Порівняльні експлуатаційні випробування на зернозбиральному комбайні John Deere 900 під час збирання пшениці показали, що при наробітку 90 га зносостійкість сегментів Duracut Knife Sections відновлених з ЕДЗ обробкою становила 1,43 - 1,65 га/мм, що в 1,5 - 1,9 рази вище, ніж у серійних сегментів 0,85 - 0,93 га/мм, відновлених без зміцнення. Протягом випробувань відмов та простоїв через втрату працездатного стану випробуваних деталей не спостерігалось. У сегментів, зміцнених ЕДЗ, після експлуатаційних випробувань зберігалася товщина лез і кут заточування 22 ... 23°, що свідчить про наявність ефекту самозаточування. Ресурс сегментів Duracut Knife Sections, відновлених зі ЕДЗ, вище в 1,7 - 2,4 рази, ніж у серійних сегментів, відновлених без зміцнення.

Ключові слова: зносостійкість, коефіцієнт тертя, електродифузійне зміцнення, сегмент жаток, довговічність.



Selection of informative acoustic emission parameters for determining the wear rate of woodworking equipment in transient modes

A.V. Voitov*, V.I. D'yakonov, Y.O. Gradiskiy

State Biotechnological University, Kharkiv, Ukraine

**E-mail: K1kavoitov@gmail.com*

Received: 30 January 2025; Revised 28 February 2025; Accept: 15 March 2025

Abstract

The directions of application of the acoustic emission (AE) method for the study of transient processes in tribosystems are considered. Woodworking equipment during running-in. The use of this method will allow obtaining information about the condition of friction surfaces and the wear rate during transient processes (running-in) in online mode. To justify choice informative AE parameters analyzed the type of AE - signal frames captured during the transition process at characteristic points. It is shown that when evaluating speed wear in transient modes is best use acoustic emission power radiation. After completion transitional process (steady state of operation), the AE signal frame takes the form that much different from transitional regime. Experimental research presented in the form of experimental dependencies that reflect average value power of AE signals, where along the axis *X* placed experimental value power signals acoustic emissions from the zone friction, unit measurement – mB^2/s . Along the axis *Y* postponed relevant calculated value speed works dissipation in tribosystems, unit measurement - J/s . Dependence allows for the measured in the process experiment calculate AE power value speed wear in the tribosystem woodworking equipment in real time. To determine maximum values speed wear during the transient process the AE method and the informative parameter - power are justified AE signals. It has been experimentally established that AE power correlates from speed wear woodworking equipment, coefficient correlation $R = 0.98$ and adequately reflects process Earnings. Received dependencies allow determine speed works dissipation in tribosystems woodworking equipment during the transition process by values power signals acoustic emissions, which allowed us to develop a calculation methodology quantities speed wear in woodworking equipment during training in any point transitional process.

Keywords: tribosystem; speeds wear and tear; acoustic emission; power acoustic radiation; transient processes; woodworking equipment; working out.

Introduction

Modern understanding the nature of friction and wear indicate that this the process is not stationary. Acoustic friction vibration initiated by impact interaction microprotrusions and elastic-plastic deformation surfaces that rub, processes destruction friction connections and structural-phase rearrangement materials, formation and development microcracks in the surface layers of interacting bodies, departments particles wear and tear. Registration acoustic signals allows with high accuracy determine the time of events that are happening, which include elastic interaction microprotrusions connected surfaces, formation and destruction adhesive connections, the emergence microcracks and separation particles wear and tear.

Acoustic emission (AE), as a way diagnostic for mechanical tests, has been widely used since the early 1980s as effective method of obtaining information about the change in the state of the material in the process load. The use of this method will allow to obtain information about the condition of surfaces friction during the transition processes (training) in online mode.



Literature review

Review literary sources, which performed in [1], allows make conclusion that research on acoustic emission diagnosing mechanisms mostly based on the use of signs that come from related industries techniques. Above all it signs discrete emissions: account (number pulses registered during the entire test period); activity (number of pulses per unit time) [2]. What concerns continuous emissions (when individual impulses to distinguish impossible), then it's characterized by parameters widely used in vibration diagnostics – mean square value, peak factor, and oscillation spectrum [3]. In addition, they use hourly parameters (pulse rise and fall duration) [3], parameters distribution pulses by amplitude and apply wavelet transform [4].

Based on analysis works western scientists [5-11], the author of the work [11] concludes that promising direction research is the justification of acoustic emission signs defects bearings rolling, invariant to the scaling of the signal in amplitude. Due to it because fluctuations attenuation emissions, differences amplitude-frequency characteristics of sensors emissions and others factors that affect the measurement result energy parameters emissions, such as energy, root mean square value, spectrum and wavelet transform result. Listed factors affect the parameters acoustic emissions, when calculating whose is carried out comparing the signal with some threshold level. According to the authors of [11, 14], the procedure for selecting such a level is often not enough formalized or is based on factors that are themselves variable (e.g., the amplifier's own noise or background level emissions). Therefore, when measuring hourly parameters acoustic emissions expedient threshold level choose in accordance to the order of the quantile of the distribution amplitudes that is determined from the condition minimum probabilities errors diagnosing.

Summarizing result analysis completed research by choice informative AE parameters for diagnosing tribosystem woodworking equipment can make conclusion that for registration speed wear in transient modes (during running -in), most informative and invariant parameter can speak AE signal power generated surfaces friction, which are in contact and mutual moving. Power AE signals correlate with the magnitude of the registered amplitudes for a certain time period (level quantization).

Purpose

One of tasks this research is the development of a method and methodology for determining speed wear woodworking equipment in non-stationary modes during online running-in, which will give possibility study transitional processes in different structures tribosystem.

Methods

To justify choice informative AE parameters during control processes wear woodworking equipment we will consider change speed wear tribosystems in process running-in, Fig. 1 and the type of AE - signal frames taken during the transition process (running-in) of the tribosystem at characteristic points, Fig. 2. From the presented signal frames it is clear that The amplitude of AE, hereinafter $A(t)$, can be given as a function valid variable t .

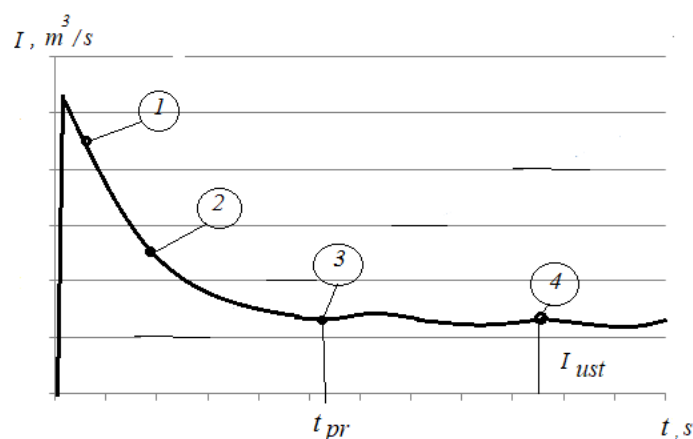


Fig. 1. Nature of change speed wear tribosystems in process running-in: t_{pr} - running-in time; I_{ust} - speed wear after completion running-in: 1-2-3-4 - typical running-in points

After completion transitional process (steady state of operation), the AE signal frame receives view presented in Fig. 2, point 3 and point 4. Study structures of the AE signals presented in Fig. 2 gives foundation to claim that on a permanent basis mode process friction and wear has oscillations.

For selection AE signals from noise most often used frequency filtering and amplitude discrimination [12]. In this work was used amplitude discrimination AE signals, which was carried out by introducing a threshold device into the equipment, which lets out only those signals, amplitude whose exceeds some given level - level

discrimination.

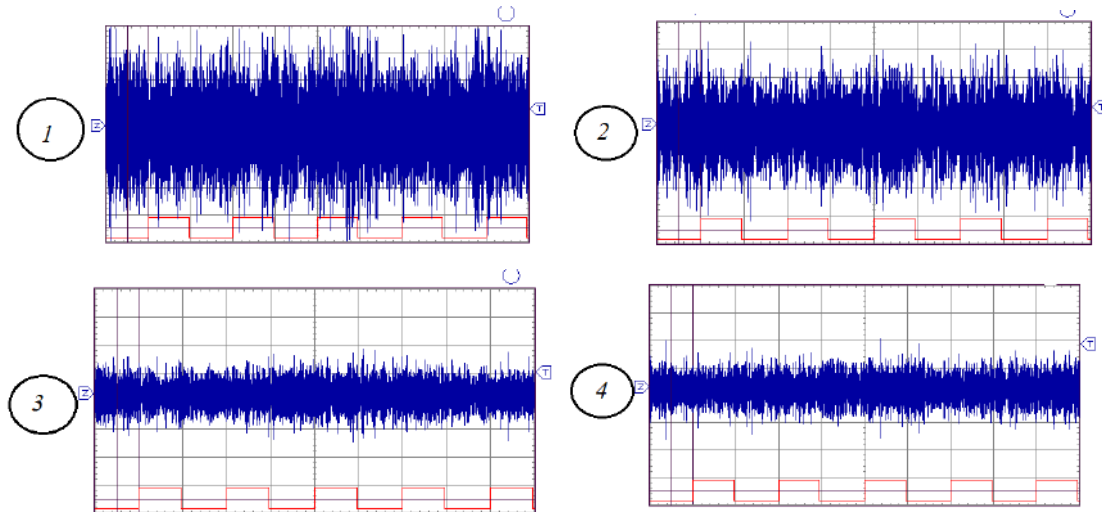


Fig. 2. Frames AE signals at characteristic points on the curve working out according to Fig. 1

Justification equal discrimination was carried out experimentally and is important condition receiving reliable results.

Non-stationary process characteristic because has certain trend development over time and characteristics of such a process depend from the beginning of the countdown and from duration registration. However, for each non-stationary process exist time intervals within which, with a known approximation, this process maybe to be considered stationary and ergodic.

Thus, changing interval integration (assigning enough small interval) when changing frames AE signals, possibly study processes superficial destruction (speeds wear and tear and damage limits) at the stage working out tribosystem.

Random function $A(t)$ maybe to be considered by definition stationary, at a certain time interval t , if all its probabilistic characteristics do not change under any displacement arguments, from which they depend on the axis t . However, one of the main conditions that must be satisfied stationary random function is condition sustainability dispersion.

Therefore, when analyzing transitional processes time interval t of amplitude registration AE signals should be chosen so that provided condition sustainability dispersion. This interval in the work is determined experimentally.

Many conducted analyses experiments process working out tribosystems showed that when evaluating speed wear in transient modes is best use acoustic emission power radiation, which was determined by the expression:

$$W_{AE} = \frac{A_{\Sigma}^2}{t_p}, \quad (1)$$

where A_{Σ}^2 is the total value of the square of the amplitudes all AE pulses, mV^2 during registration t_p ; t_p is the registration time, s.

Experimental research were carried out in two stages and aimed to determine correlational connection between speed wear – I_v , m^3/h and power signals:

$$W_{AE} = \frac{mB^2}{s_e}.$$

First stage experimental research aimed to definition functional communication between the listed parameters during the transition process.

Second stage aimed to definition correlation communication between listed above parameters on a constant mode works tribosystems, i.e. after completion transitional process (working in).

Completion working out can determine by stabilization the following parameters transitional process: friction moment M_f , $N\cdot m$; temperatures elements tribosystems T , $^{\circ}C$; minimum dispersion of AE radiation from zones friction - D , mB^2 . In this work during the experimental research completion time transitional process was determined by all listed above parameters.

Results

Experimental research were carried out by car friction according to the kinematic scheme "ring-ring", with such combinations materials.

First tribosystem: mobile triboelement steel 40X (45 ... 47 HRC), fixed triboelement Br.AZH 9-4 (90 ... 110 HB).

Second tribosystem: mobile triboelement steel 40X (45 ... 47 HRC), fixed SCM triboelement (293 HB).

Third tribosystem: mobile triboelement steel 40X (45 ... 47 HRC), fixed triboelement steel 40X (45 ... 47 HRC).

For everyone three tribosystem lubricating environment was selected engine oil M-10G_{2k} ($E_y = 3.6 \cdot 10^{14} \text{ J/m}^3$).

Experimental flow chart recording and processing equipment AE signals are presented in Fig. 3.

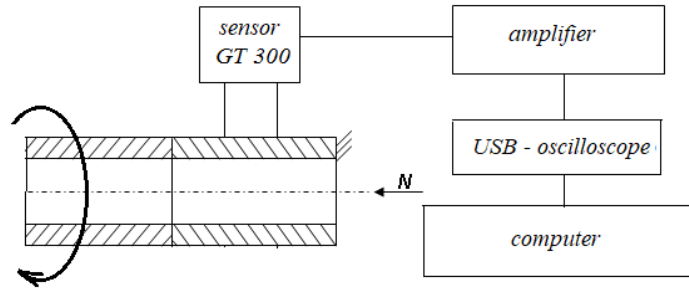


Fig.3. Experimental block diagram recording and processing equipment AE signals

Acoustic signal emissions that generates tribosystem, perceived from a stationary triboelement broadband acoustic sensor emission GT300 (100.. 800 kHz) and enters the amplifier, and from the output amplifier - to the USB oscilloscope PV6501 and then to the computer.

Amplifier consists of an input stage, a three-pole filter high frequencies and an amplifier with adjustable coefficient transmission (1 - 100). General coefficient strengthening reaches 1000. The lower limit of the band transmission amplifier selected equal to 50 kHz, which corresponds low-frequency acoustic sensors emissions that are produced, for example, by the company GlobalTest. Upper band limit transmission selected equal to 1.5 MHz, which surpasses the corresponding serial limit high-frequency sensors acoustic emissions. This restriction related also from increase attenuation elastic waves in metal with increasing frequency.

Strip transmission of the used USB oscilloscope is 20 MHz, which repeatedly exceeds upper limit of the bands sensor and amplifier throughput acoustic emissions. Filter high frequencies are intended for highlighting signals acoustic emissions that have much smaller intensity than AE signals. By weakening the passage AE signals to the USB oscilloscope input 300 times using filter high frequencies and proportionally increasing coefficient reinforcement, it became possible to isolate the acoustic signal emissions with a predominant frequency of 70-600 kHz.

Oscillograph worked in mode wait, scan start threshold marked with the symbol "T" in Fig. 2. Duration previous samples was installed equal to 100 μs , which allows watch the value of the signal that precede exceeding the threshold level. Results acoustic signal measurements emissions with a USB oscilloscope stored in a computer, data that contained in these files are processed programs statistical analysis with definition dispersion of the square of the amplitudes - D_A and the total value of the square of the amplitudes during the registration time - . Having data value according to formula (1) was determined W_{AE} . Registration time t_p was determined experimentally by reproducibility results with equivalent repetitions. When checking homogeneity dispersions aggregates AE signal results at constant mode that equivalently confirmation their reproducibility, under conditions for small sample sizes, ISO 5725 recommends using criterion Cochran.

Criterion Cochran allows compare homogeneity dispersions results analysis amplitude AE signals at different points of the transition process.

Test statistic of the criterion Cochran S_r is determined expression:

$$S_r = \frac{D_{Amax}}{\sum_{i=1}^n D_{Ai}}, \quad (2)$$

where D_{Amax} is the largest value dispersion amplitude during the transition process;

n is the number measurements;

D_{Ai} is the current value variances on the i -th experiment.

According to ISO 5725, the hypothesis Homogeneity (reproducibility) is checked according to the following expression:

$$C_p < C_m, \quad (3)$$

where C_p is the calculated value criterion Cochran, formula (2); C_m is the tabular value criterion for a given equal significance [13].

If condition (3) is fulfilled, then it is accepted hypothesis about statistical homogeneity results measurements.

Experimental research were carried out under the following friction modes: load $N = 300 \dots 1200$ N; speed sliding 0.5 m/s.

In progress experiments using recorders machinery friction recorded in time change in friction torque, temperature, and with the help of computer calculated dispersion and power AE signals.

Results experimental research presented in the form of experimental dependencies in Fig. 4, which reflect average value power AE signals for three with the same type of repetitions and three tribosystems with different combination materials, where along the axis X placed experimental value power signals acoustic emissions from the zone friction, W_{AE} , formula (1), unit measurement – mB^2/s . Value W_{AE} obtained for different combinations materials in the tribosystem, different loads and speeds sliding. Along the axis Y postponed relevant calculated value speed works dissipation in tribosystems W_{tr} , which equal algebraic sum speeds works dissipation in moving and stationary triboelements, unit measurement - J/s . Formulas for calculation W_{tr} presented in [14]:

speed works dissipation in the moving triboelements;

$$W_{mov} = \sigma_{acs} \cdot \dot{\epsilon}_{mov} \cdot V_{dmov} \cdot J / s. \quad (4)$$

speed works dissipation in a stationary triboelements;

$$W_{stat} = \sigma_{stat} \cdot \dot{\epsilon}_{stat} \cdot V_{dstat} \cdot J / s. \quad (5)$$

Speed works dissipation in the tribosystem:

$$W_{tr} = W_{mov} + W_{stat} \cdot J / s. \quad (6)$$

In formulas (4) and (5) we assume next designation:

σ_{acs} is the stress on the actual contact spots, Pa;

$\dot{\epsilon}_{mov}, \dot{\epsilon}_{stat}$ is the speed deformations in movable and stationary triboelements, $1/s$;

V_{dmov}, V_{dstat} is the volume material movable and stationary triboelements, which participates in deformation in the process friction, m^3 .

Received dependence, Fig. 4, establishes linear relationship between measured in the process experiment power AE signals, formula (1) and speed works dissipation in the tribosystem, formula (6). Using the method of least squares squares was received regressive equation:

$$W_{tr} = 0.033 \cdot W_{AE} \quad (7)$$

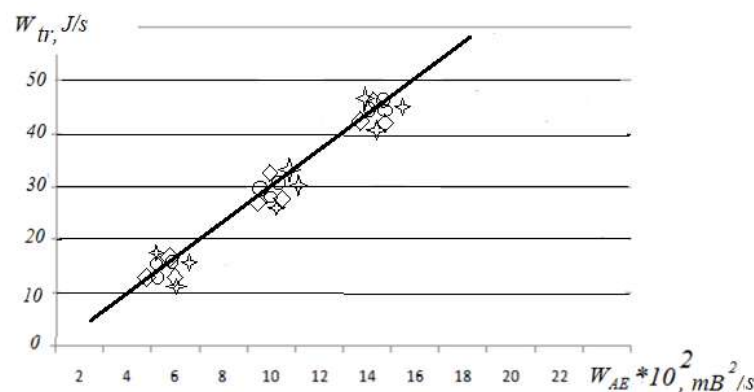


Fig. 4. Dependence changes speed works dissipation in different tribosystems W_{tr} from power signals acoustic emissions from the zone friction W_{AE}

Dependence (7) allows for the measured in the process experiment power AE - W_{AE} , calculate value speed works dissipation in the tribosystem W_{tr} . Using received value W_{tr} and the formula obtained in [13] can be calculate speed wear in the tribosystem in real time:

$$I_v = 6 \cdot 10^{-10} \exp \left(0.795 \cdot 10^{16} \cdot \frac{1}{E_y} \sqrt{\frac{\pi}{\delta_{mov} \cdot \delta_{stat}}} W_{tr} \right), m^3 / h, \quad (8)$$

where I_V is the volumetric speed wear, m^3/h in real time;

δ_{mov} and δ_{stat} are coefficients that take into account rheological properties structures material from moving and stationary triboelements.

The second stage experimental research began to determine functional relationship between speed wear I_V and parameters AE - W_{AE} for the specified above tribosystem when changing load on the node friction from 300 N to 1200 N on a stationary mode works tribosystems, i.e. after completion transitional process (running in). Change load leads to change speed works dissipation in tribosystems - W_{tr} .

The purpose of the research is to show that by the value of W_{AE} , mB^2/s , it is possible determine the speed wear I_V , m^3/h .

Research were carried out in stationary friction modes, i.e. depreciation for running-in was not taken into account. For this after completion working in (after stabilization parameters) on the surface friction wells were applied for measurement wear and tear and after carrying out tests for two hours by the method of artificial bases was determined linear wear and tear, which converted into volumetric.

Speed wear was determined by the formula:

$$I_v = \frac{\Delta b \cdot A_H}{t_e}, m^3 / h, \tag{9}$$

where Δb is the value of the linear wear, m;
 A_H is the area friction triboelement, m^2 ;
 t_e is the time of execution experiment, hours.

Results experimental research are presented in Fig. 5.

We will do it assessment reproducibility results measurements signals acoustic emissions using criterion Cochren, formula (2). Parameters signals acoustic emissions at different values speed works dissipation for dispersion amplitudes and dispersions AE power specified above tribosystem are presented in Table 1.

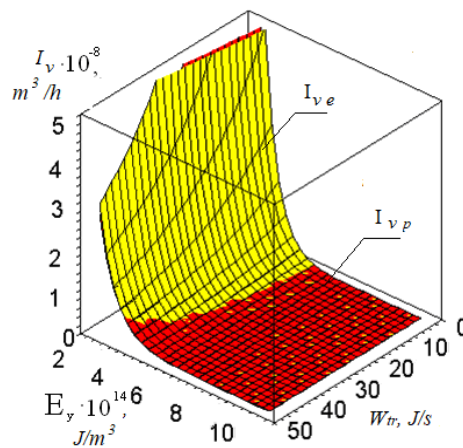


Fig. 5. Estimated I_{Vp} and experimental I_{Ve} surface feedback volumetric speed wear and tear when changing tribological properties lubricating environment E_y and speed works dissipation W_{tr} in tribosystem steel 40X + Br.AJ 9-4

Table 1

Parameters signals acoustic emissions at different values speed works dissipation in tribosystems

$W_{tr}, J/s$	D_{Amax}	ΣD_{Ai}	S_r	D_{wmax}	ΣD_{wi}	S_r	S_t
10	47.1	60.41	0.764	309.35	461.22	0.695	0.853
20	57.3	70.75	0.764	315.30	460.08	0.715	0.853
30	70.5	91.30	0.785	430.25	572.67	0.720	0.853
40	113.6	144.76	0.795	613.33	822,14	0,755	0,853

Analysis calculated values criterion Cochran - C_p and tabular values - C_t at a given levels significance level 0.95 (number of evaluated parameters - 2, number repetitions - 10), allows make conclusion that condition (3) is fulfilled, i.e. results measurements homogeneous and reproducible.

For the subjects tribosystem coefficient correlations between dependencies I_V and D_A has R value = 0.96, and for dependencies I_V and W_{AE} has R value = 0.98.

From the analysis presented values in Table 1 it follows that dispersion amplitude and power AE signals adequately reflect process wear and tear and are in functional condition interconnection from speed wear and tear. This allows to put forward assumption that the magnitude of the AE power can be to judge the magnitude of the speed wear at any time during work tribosystems, i.e. in transient regimes.

Practical recommendations: determination method values speed wear during the transition process boils down to the following operations.

1. Conducted trial specific tribosystems and in the process transitional process are registering AE parameters and according to formulas (1) are calculated value power acoustic emissions - W_{AE} .

2. According to the known values W_{AE} , according to expression (7), is calculated value speed works dissipation in the tribosystem at a given time - W_r .

3. Numerical value volumetric speed wear at a given time - I_V is determined by formula (8).

Conclusions

To determine maximum values speed wear during the transition process the AE method and the informative parameter - power are justified AE signals. It has been experimentally established that AE power correlates from speed wear and tear, coefficient correlation $R = 0.98$ and adequately reflects process working out.

Received dependencies that allow determine speed works dissipation in tribosystems of woodworking equipment during the transition process by values power signals acoustic emissions, which allowed the development of calculation method quantities speed wear during training in any point transitional process.

References

1. Shevchenko S.A. Classification and justification requirements for acoustic emission signs friction pair defects mechanisms, Bulletin Kharkiv national technical university rural farms named after P. Vasylenko, 2012, issue 121, pp. 159-163.
2. Abdullah M., D. Al-Ghamd, Zhechkov, D. Mba. A comparative experimental study on the use of Acoustic Emission and vibration analysis for bearing defect identification and estimation of defect size, Mechanical System and Signal Processing, 2006, No.7, pp.1537-1571.
3. Mazal P., V.Koula, F.Hort, F.Vlasic. Applications of continuous sampling of AE signal for detection of fatigue damage, NDT in Progress, 2009, No.4. -8 p.
4. Yanhui Feng. Discrete wavelet-based thresholding study on acoustic emission signals to detect bearing defect on a rotating machine, The Thirteen International Congress of Sound and Vibration. Vienna, Austria, 2-6 July, 2006. -8 p.
5. Faris Elasha., Matthew Greaves, David Mba, Abdulmajid Addali. Application of Acoustic Emission in Diagnostic of Bearing Faults within a Helicopter gearbox, The Fourth International Conference on Through-life Engineering Services. Procedia CIRP, 2015, Vol.38, pp. 30-36.
6. Seyed A. Niknam, Tomcy Thomas, J. Wesley Hines, Rapinder Sawhney. Analysis of Acoustic Emission Data for Bearings subject to Unbalance, International Journal of Prognostics and Health Management, 2013, Vol. 15, pp. 1-10.
7. Badgujar M.P., Patil A.V. Fault Diagnosis of Roller Bearing Using Acoustic Emission Technique and Fuzzy Logic, International Journal of Latest Trends in Engineering and Technology, 2014, Vol. 3, Issue 4, pp.170-175.
8. Rao V.V., Ratnam Ch. A Comparative Experimental Study on Identification of Defect Severity in Rolling Element Bearings using Acoustic Emission and Vibration Analysis, Tribology in Industry, 2015, Vol. 37, No. 2, pp.176-185.
9. Zahari Taha., Indro Pranoto. Acoustic Emission - Research and Applications. Chapter 4 - Acoustic Emission Application for Monitoring Bearing Defects, InTech. 2013, pp.71-90. <http://dx.doi.org/10.5772/55434>
10. Nienhaus K., Boos F.D., Garate K., Baltes R. Development of Acoustic Emission (AE) based defect parameters for slow rotating roller bearings, Journal of Physics: Conference Series. 364. 2012. 012034. 1-10. doi:10.1088/1742-6596/364/1/012034
11. Yongyong He., Xinming Zhang, Michael I. Friswell. Defect Diagnosis for Rolling Element Bearings Using Acoustic Emission, Journal of Vibration and Acoustics, 2009, Vol. 131 / 061012.
12. Victor Vojtov, Katherine Fenenko, Anton Voitov, Andriy Hryniv, Oleg Lyashuk, Yuriy Vovk. Methodical Approach to Using Acoustic Emission Method for Tribosystem Monitoring. Tribology in Industry, Vol. 44, No. 3, pp. 470-481, 2022. DOI: 10.24874/ti.1298.05.22.08
13. V. A. Vojtov, K. A. Fenenko, A. V. Voitov Methodology for diagnosing various tribosystem designs using the acoustic emission method // Problems of friction and wear. 2021. - No. 2 (91). - P. 18-26. DOI: 10.18372/0370-2197.2(91).15525
14. V. A. Vojtov, K. A. Fenenko, A. V. Voitov Substantiation of informative amplitudes during registration of acoustic emission signals from the friction zone of tribosystems // Problems of Tribology, V. 26, No 1/99 - 2021, 6-12. <https://doi.org/10.31891/2079-1372-2021-99-1-6-12>

Войтов А.В., Д'яконов В.І., Градиський Ю.О. Вибір інформативних параметрів акустичної емісії для визначення інтенсивності зносу деревообробного обладнання в перехідних режимах

Розглянуто напрями застосування методу акустичної емісії (АЕ) для дослідження перехідних процесів у трибосистемах. деревообробного обладнання під час обкатки. Використання даного методу дозволить отримувати інформацію про стан поверхонь тертя та швидкість зношування під час перехідних процесів (обкатки) в режимі онлайн. Для обґрунтування вибору інформативних параметрів АЕ проаналізовано тип АЕ – сигнальні кадри, захоплені в процесі переходу в характерних точках. Показано, що при оцінці швидкісного зносу в перехідних режимах найкраще використовувати потужність випромінювання акустичної емісії. Після завершення перехідного процесу (стаціонарний режим роботи) кадр сигналу АЕ набуває форми, яка сильно відрізняється від перехідного режиму. Експериментальні дослідження представлені у вигляді експериментальних залежностей, що відображають середнє значення потужності сигналів АЕ, де по осі X розміщено експериментальне значення потужності сигналів акустичної емісії із зони тертя, одиниці вимірювання – $\text{mB}^2/\text{с}$. По осі Y відкладене відповідне розрахункове значення швидкості роботи розсіювання в трибосистемах, одиниця вимірювання - Дж/с. Залежність дозволяє за виміряним у технологічному експерименті розрахувати значення потужності АЕ швидкості зносу в трибосистемі деревообробного обладнання в режимі реального часу. Для визначення максимальних значень швидкості зношування під час перехідного процесу обґрунтованими сигналами АЕ є метод АЕ та інформативний параметр – потужність. Експериментально встановлено, що потужність АЕ корелює зі швидкістю зносу деревообробного обладнання, коефіцієнтом кореляції $R = 0,98$ і адекватно відображає прибуток процесу. Отримані залежності дозволяють визначити швидкість роботи дисипації в трибосистемах деревообробного обладнання під час перехідного процесу за значеннями потужності сигналів акустичної емісії, що дозволило розробити методику розрахунку величин швидкості зносу деревообробного обладнання під час тренування в будь-якій точці перехідного процесу.

Ключові слова: трибосистема; знос; акустична емісія; потужність акустичного випромінювання; перехідні процеси; деревообробне обладнання; розробка.



Strengthening of tribocoupling parts of transport and agricultural machines with fullerene materials

V.V. Aulin^{1*}, A.A. Tykhyi¹, O.D. Derkach², S.V. Lysenko¹, D.O. Makarenko²

¹*Central Ukrainian National Technical University, Ukraine*

²*Dnipro State Agrarian And Economic University, Ukraine*

**E-mail: AulinVV@gmail.com*

Received: 30 January 2025; Revised 28 February 2025; Accept: 20 March 2025

Abstract

The aim of this work is a comparative study of tribological properties and tribotechnical characteristics of polymer nanocomposites based on polyamide 6, modified with nanosized fillers. The work investigates polyamide 6 as a matrix modified with the following fillers: fulleroid materials (carbon fibers), microsized fillers containing nanoparticles (fullerene carbon black), nanoparticle fillers (fullerene C60). The influence of fulleroid modifiers and carbon fibers on the tribological properties of samples and parts made of polymer nanocomposites based on thermoplastic (polyamide 6) polymer matrices was studied. It was shown that the introduction of fulleroid modifiers allows to significantly reduce the friction coefficient of polymer compositions while increasing their mechanical characteristics. It was found that the use of carbon fibers for modification of polyamide 6 with an increase in mechanical characteristics during operation leads to an increase in the friction coefficient of the conjugated steel sample by more than two times compared to the original polymer matrix.

Key words : transport vehicles, agricultural machinery, parts, fulleroid modifiers, polymer matrix.

Introduction

The durability of parts, assemblies, systems and units of transport and agricultural machines is largely determined by the phenomena of friction and wear. The use of new progressive structural materials ensures the creation of tribocoupling of machine parts with a high level of specified operational characteristics. An important place among these materials has recently been occupied by polymer nanocomposites. The main advantage of polymer nanocomposites as materials for tribocoupling of parts is their increased strength characteristics and tribotechnical indicators. This is due to the peculiarities of the interaction in the system "polymer matrix-filler nanoparticle" [1-3].

Literature review

Increasing the strength of polymeric materials leads to a decrease in the coefficient of friction and wear in triboconjugates of samples and parts [4,7,8]. At the same time, this pattern is not observed for polymer composites filled with micro-sized fillers in the form of fibers [5,6]. This can be explained by the fact that during the wear process, micro-sized fillers are torn out of the polymer matrix, which leads to an increase in the abrasive properties of the conjugated surfaces [9,11,14]. This causes an increase in the coefficient of friction [10,12]. This problem can be solved using polymer nanocomposites [13]. In such materials, nanoparticles are more firmly held in the matrix, and their detachment does not lead to a change in the properties of the microsurface [15].

Purpose

The aim of this work is a comparative study of the tribological properties and tribotechnical characteristics of polymer nanocomposites based on polyamide 6 (PA-6) modified with nanoscale particles.



Results

The work investigates polyamide PA-6 as a matrix modified with the following fillers: fulleroid materials (carbon fibers), micro-sized fillers containing nanoparticles (fullerene carbon black), and nanoparticle fillers (fullerene C60).

Polymer nanocomposites were obtained by polymerization in situ according to the method [2] after mixing the filler and monomer, and mixing the finished PA-6 with the filler in an extruder. C60 fullerenes (purity 99.0%) and fulleroid carbon black (fullerene content 10.5%; 68% C60 fullerene, 30% C70 fullerene by weight, the sum of higher fullerenes about 2%) were used as fillers. Fulleroid carbon black is an ultrafine carbon - a product of burning graphite electrodes in an arc in an inert gas atmosphere with an average particle size of 0.5...2.0 microns. Fulleroid carbon black is the main raw material for producing fullerenes. Fractionated chopped viscose carbon fiber (average length 400 μm) was used as a filler. Tests on the MTY-01 friction machine were carried out according to the "roller-plate" scheme. The roller with a diameter of $D = 19$ mm is made of 40X steel, heat-treated to a hardness of approximately 58 HRC. The roller rotated at a frequency of $n = 60$ rpm. This corresponded to a linear sliding velocity of 0.06 m/s. The roller was pressed against a plate measuring $40 \times 40 \times 5$ mm with a force of 400 N. Young's modulus and tensile strength were determined on a UTS 10 tensile testing machine (UTStestsysteme, Germany) during compression for samples in the form of a half-cylinder with a diameter of 8...9 mm and a height of 9...12 mm in the load range from 0.001 N to 10 kN. In this case, the range of deformation rates of the samples was from 1 $\mu\text{m}/\text{min}$ to 1 m/min. All measurements were performed for series of samples of at least five obtained by different methods of forming nanocomposites.

As already noted, PA-6 was chosen as the thermoplastic matrix as a polymer that is widely used for the manufacture of sliding bearings of transport and agricultural machines. It is known that the optimal method for obtaining nanocomposites is polymerization in situ [6]. All other methods of their production are associated with problems of aggregation of filler particles. In which they are difficult to overcome. This problem complicates the uniform distribution of filler particles in the polymer matrix. Mixing the finished polymer with a filler in an extruder is the most common method of preparing polymer composites. In this work, both methods of obtaining polymer composites were considered. The PA-6 matrix material is obtained by anionic polymerization using metallic sodium as an initiator and toluene diisocyanate as a cocatalyst. Fullerene C60 is chemically unstable under these conditions. Therefore, polymer composites obtained by polymerization in situ are chemically modified. In them, nanoparticles are chemically bound to a polymer matrix. In addition, the comparative nature of the tribological properties of composites obtained by different methods is interesting. Introduction of fullerene C60, at a filling level of 0.01...0.1 wt.%, into the PA-6 matrix during synthesis by polymerization in situ, the Young's modulus and strength increase by approximately 18...20%. Nanocomposite samples obtained by mixing the polymer melt with other components in an extruder were tested [7,8]. The test data are given in Table 1. As can be seen from the data presented, the melt mixing method does not lead to a significant increase in the strength characteristics of PA-6 at a fullerene C60 content of 0.01 wt.% (an increase of 3%). The introduction of both fullerene C60 and fullerene carbon black in amounts of 1 wt.% leads to a decrease in mechanical properties. The sharp drop in the mechanical characteristics of PA-6 filled with 1 wt.% fullerene C60 is due to the fact that the insufficiently uniform distribution of fullerene C60 in the polymer matrix necessitates the introduction of a co-solvent (Erucamide 0.05 wt.%), which simultaneously acts as a plasticizer and prevents crystallization of PA-6, which leads to a decrease in mechanical characteristics. The decrease in the mechanical properties of nanocomposites at high filling degrees is due to the uneven distribution of the filler in the polymer matrix.

Table 1 – Mechanical properties and characteristics of nanocomposites based on PA-6 obtained by extrusion

Modifier content	Young's modulus E , MPa	Destructive force σ_u MPa	Elongation ε , %	Friction coefficient f_{fr}
PA-6 without additives	673 ± 15	64 ± 1	285 ± 5	0.26...0.30
C60 – 0.01 wt. %	702 ± 12	66 ± 1	302 ± 5	0.187...0.19
C60 – 1 wt.%; Erucamide 0.05 wt. %	258 ± 14	12 ± 1	289 ± 5	0.28...0.30
Fullerene carbon black – 1 wt. %	618 ± 15	63 ± 1	276 ± 5	0.29...0.30

In this work, the tribotechnical characteristics of polymer nanocomposites were investigated (Fig. 1–3). For the PA-6 nanocomposite 0.01 wt.% fullerene C60, obtained by polymerization in situ, a significant decrease in the friction coefficient (from 0.28 ± 0.02 to 0.18 ± 0.05) is observed compared to pure PA-6. This can be justified by the increase in the mechanical strength of the polymer nanocomposite. At the same time, for the PA-6 polymer matrix filled with 10 wt.% carbon fiber, an increase in the friction coefficient (up to 0.52 ± 0.05) is observed. To

explain the obtained result, we studied the materialography of wear spots on the material of the samples and parts (Fig. 4).

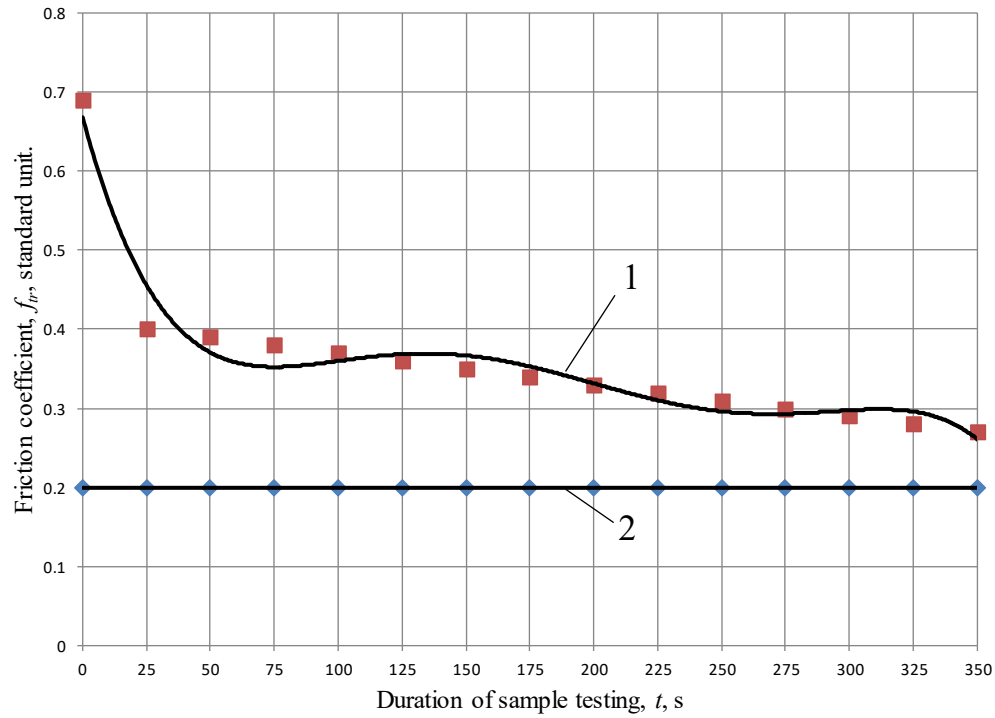


Fig. 1. Dynamics of changes in the friction coefficient for samples of PA-6 (1) and PA-6 with 0.01 wt.% of C60 fullerenes (2), obtained by the polymerization method in situ

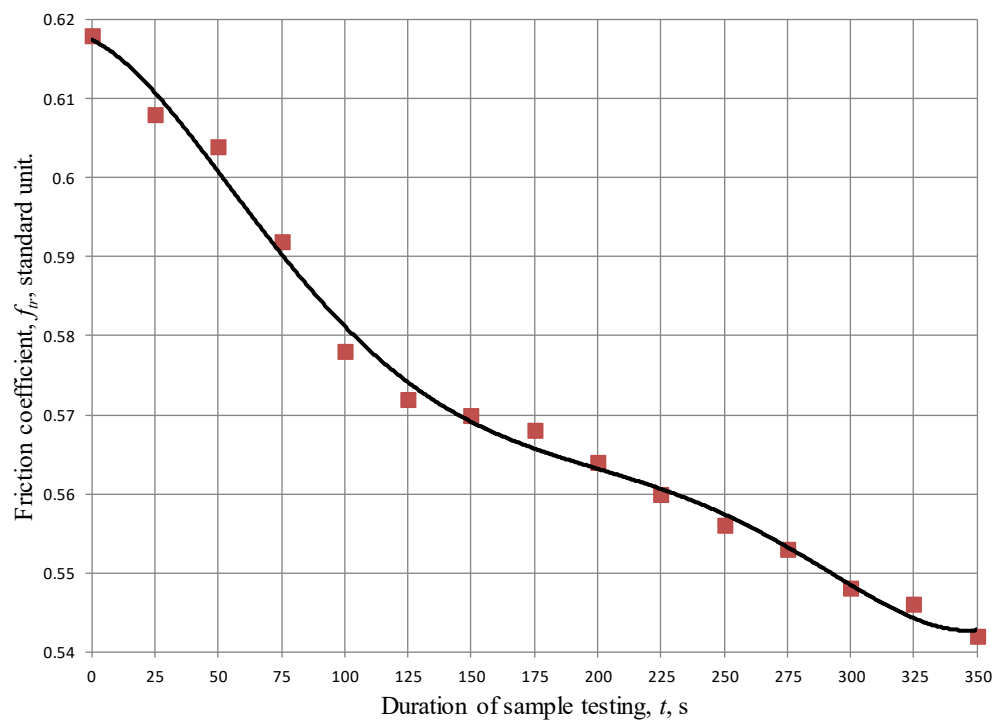


Fig. 2. Dynamics of changes in the coefficient of friction for samples of composite material: PA-6 filled with 10 wt.% carbon fibers, obtained by polymerization in situ

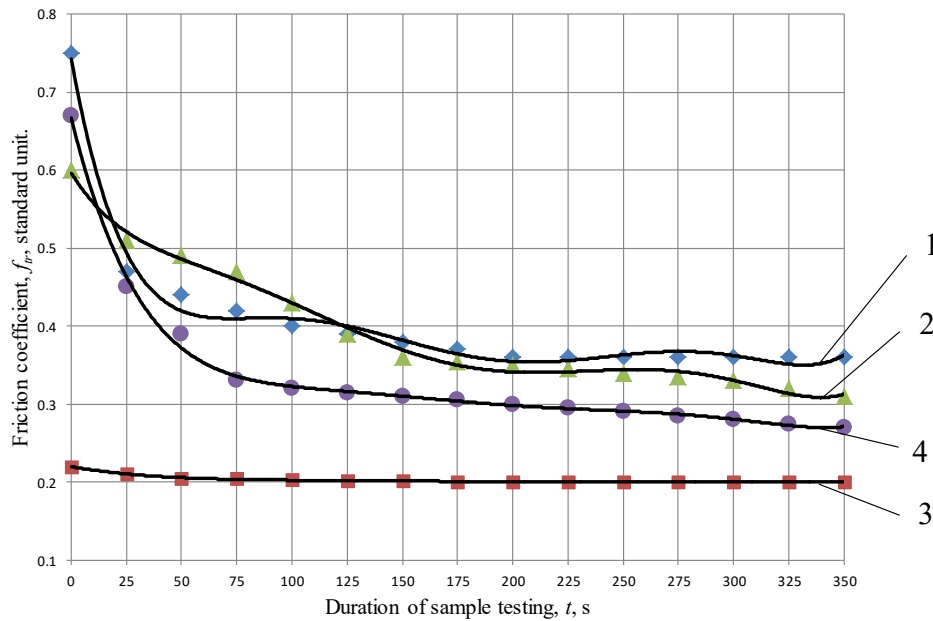


Fig. 4. Dynamics of changes in the friction coefficient for pure PA-6 (1) and polymer nanocomposites obtained by extrusion and containing: 1 wt.% C60 fullerenes and 0.05 wt.% Erucamide (2); 0.01 wt.% C60 fullerenes (3); 1 wt.% fullerene carbon black (4)

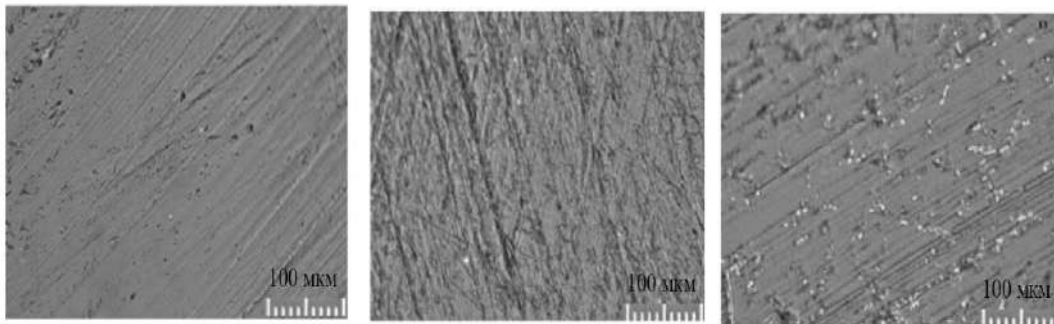


Fig. 4. General view of friction surfaces for pure PA-6 (a), PA-6 with 0.01 wt.% C60 fullerenes (b) and for PA-6 with 10 wt.% carbon fibers (c), obtained by polymerization in situ, x400

The study of the surfaces of the samples after testing (Fig. 4, a, b) shows that chemically incorporated fullerene C60 does not change the sliding properties of the surface compared to pure PA-6. It was found that in samples reinforced with carbon fibers, fiber particles break away from the polymer matrix and become burrs, which worsen the sliding properties of the surface. Such an effect of fibers in polymer compositions is observed in [9]. For nanocomposites obtained by extrusion (Fig. 3), a decrease in the friction coefficient is also observed. In this case, the value of the friction coefficient is lower than for the polymer synthesized by polymerization in situ with the introduction of 0.01 wt.% fullerene C60. The friction coefficient changes from 0.30 ± 0.2 to 0.25 ± 0.02 . It was found that the most effective modification of PA-6 is 1 wt.% fullerene carbon black. In this case, the friction coefficient decreases to 0.20 ± 0.01 . The increase in the friction coefficient for the nanocomposite filled with 1 wt.% fullerene C60 in the presence of Erucamide 0.33 ± 0.02 is associated with an increase in the viscosity of the composite during friction. This is due to the fact that the surface heats up and the glass transition temperature decreases in the presence of the additive. This is confirmed by the study of friction spots (Fig. 5).

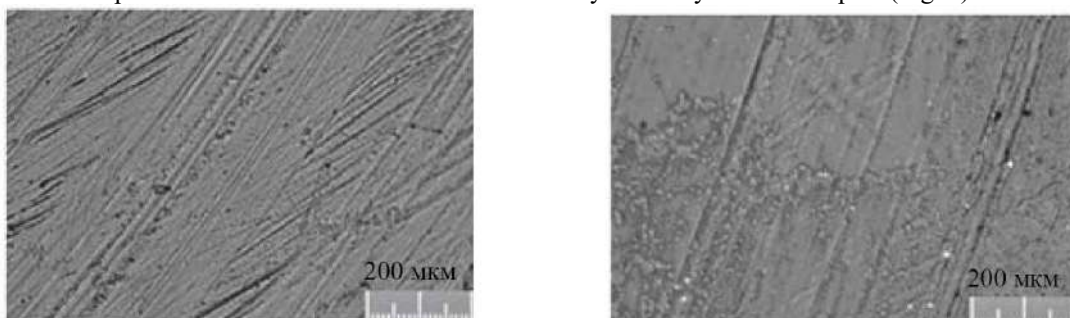


Fig. 5. Photographs of friction surfaces of polymer nanocomposites obtained by extrusion and containing 0.01 wt.% of C60 fullerenes (a); 1 wt.% C60 fullerenes and 0.05 wt.% Erucamide (b), x200

It was found that for a nanocomposite filled with 1 wt.% fullerene C60 in the presence of Erucamide, leakage is clearly visible.

Conclusions

1. As a result of the research, the possibility of creating polymer nanocomposites based on polyamide 6 matrices modified with fullerene materials has been shown.
2. It has been shown that the introduction of fullerene materials significantly (by half) reduces the friction coefficient of nanocomposites compared to pure polyamide 6.
3. The decrease in the friction coefficient of polymer nanocomposites can be justified by the increase in the mechanical strength of the composites in the absence of the removal of nanoparticle aggregates to the conjugate surfaces of the samples being lapped.

References

1. Treacy, M. M. J., Ebesen, T. W., & Gibson, J. M. (1996). Nanoparticles as reinforced agents. *Nature (London)*, *381*, 678–680. <http://dx.doi.org/10.1038/381678a0>
2. Mai, Y.-W., & Yu, Z.-Z. (2006). *Polymer nanocomposites*. CRC Press.
3. Naffakh, M., Diez-Pascual, A. M., Marco, C., Ellis, G. J., & Gomez-Fatou, M. A. (2013). Opportunities and challenges in the use of inorganic fullerene-like nanoparticles to produce advanced polymer nanocomposites. *Progress in Polymer Science*, *38*, 1163–1231. <http://dx.doi.org/10.1016/j.progpolymsci.2013.04.001>
4. Aulin, V., Lysenko, S., Hrynkiv, A., & Pashynskiy, M. (2022). Improvement of tribological characteristics of coupling parts "shaft-sleeve" with polymer and polymer-composite materials. *Problems of Tribology*, *27*(3/105), 96–107.
5. Berladir, Kh. V., Budnyk, O. A., Dyadiura, K. O., et al. (2017). *Scientific foundations for the development of polymer composite materials for tribotechnical purposes based on polytetrafluoroethylene* (K. O. Dyadiura, Ed.). Sumy State University.
6. Schaefer, D. W., & Justice, R. S. (2007). How nano are nanocomposites? *Macromolecules*, *40*(24), 8501–8517. <http://dx.doi.org/10.1021/ma070356w>
7. Aulin, V., Lysenko, S., Hrynkiv, A., Tykhyi, A., Kuzyk, O., & Livitskiy, O. (2023). The regularity of the change in the coefficient of friction of the coupling of "shaft-sleeve" parts using polymeric materials. *Problems of Tribology*, *28*(1/107), 81–91.
8. Aulin, V., Lysenko, S., Hrynkiv, A., Derkach, O., & Makarenko, D. (2022). Influence of high-modulus filler content on critical load on tribocouples made of microheterophase polymer composite materials. *Problems of Tribology*, *27*(2/104), 71–79.
9. Bijwe, J., Logani, C. M., & Tewari, U. S. (1990). Influence of fillers and fiber reinforcement on abrasive wear resistance of some polymeric composites. *Wear*, *138*(1), 77–92. [http://dx.doi.org/10.1016/0043-1648\(90\)90169-b](http://dx.doi.org/10.1016/0043-1648(90)90169-b)
10. Buketov, A. V., et al. (2018). *Restoration of transport means using fullerene-containing epoxy composites* (Text). Kherson State Maritime Academy.
11. Tomina, A.-M., Burya, O., Lytvynova, Y., & Gavrish, V. (2020). The research on the influence of titanium-tantalum-tungsten-cobalt hard alloy on the tribological properties of phenylone C-2. *Problems of Tribology*, *25*(2/96), 42–48.
12. Tarnavskiy, A. (2018). Changes in thermophysical properties of polyamide-6 under the influence of functionally active polymer. *Bulletin of Lviv State University of Life Safety*, *8*, 184–189.
13. Friedrich, K. (2018). Polymer composites for tribological applications. *Advanced Industrial and Engineering Polymer Research*, *148*, 3–39. <http://dx.doi.org/10.1016/j.aiepr.2018.05.001>
14. Hosseini, M., & Makhlof, A. S. H. (2016). *Industrial applications for intelligent polymers and coatings*. Springer International Publishing.
15. Pan, B. L., Zhao, J., Zhang, Y. Q., & Zhang, Y. Z. (2012). Wear performance and mechanisms of polyphenylene sulfide/polytetrafluoroethylene wax composite coatings reinforced by graphene. *Journal of Macromolecular Science, Part B*, *51*(6), 1218–1227. <http://dx.doi.org/10.1080/00222348.2011.627821>

Аулін В.В., Тихий А.А., Деркач О.Д., Лисенко С.В., Макаренко Д.О. Зміцнення трибоспряження деталей транспортних і сільськогосподарських машин фулероїдними матеріалами.

Метою даної роботи є порівняльне дослідження трибологічних властивостей і триботехнічних характеристик полімерних нанокомпозитів на основі поліаміду 6, модифікованих нанорозмірних. В роботі досліджуються поліамід 6 як матриця, модифікована наступними наповнювачами: фулероїдними матеріалами (вуглецеві волокна), мікророзмірними наповнювачами, що містять наночастинки (фулеренова сажа), наночастинками-наповнювачами (фулерен C60). Досліджено вплив фулероїдних модифікаторів та вуглецевих волокон на трибологічні властивості зразків і деталей з полімерних нанокомпозитів на основі термопластичних (поліамід 6) полімерних матриць. Показано, що введення фулероїдних модифікаторів дозволяє значно знизити коефіцієнт тертя полімерних композицій при підвищенні їх механічних характеристик. Виявлено, що використання вуглецевих волокон для модифікації поліаміду 6 при зростанні механічних характеристик в процесі експлуатації призводить до зростання коефіцієнта тертя спряженого сталевого зразка більш ніж удвічі порівняно з вихідною полімерною матрицею.

Keywords: транспортні машини, сільськогосподарські машини, деталі, фуллероїдні модифікатори, полімерна матриця.